**Anatomy of the Chicken Hippocampus:**

**Investigating its Role in Stress Regulation**

by

Karina Santiago Gonzalez

A thesis submitted for obtaining the degree of

Doctor of Philosophy (PhD)

Institute of Biosciences

Faculty of Medical Sciences

Newcastle Upon Tyne, UK

April, 2024

# Abstract

The avian hippocampus, an evolutionarily ancient brain structure, plays a crucial role in both memory and emotional regulation. Its complex internal organization, characterized by diverse subdivisions and a functional longitudinal arrangement, poses a unique challenge in comparative neurobiology. This thesis investigates the role of the avian hippocampus in stress regulation through an integrative approach involving immunohistochemistry, gene expression analysis, and tract-tracing experiments in chickens. Contrary to the mammalian hippocampal functional dichotomy, our study reveals significant activation in the rostral avian hippocampus in response to acute stress, accompanied by intricate activation patterns across the ventral, dorsomedial, and dorsolateral hippocampal subdivisions. These findings suggest a more comprehensive involvement of the hippocampus in stress modulation than previously acknowledged. By advancing our understanding of avian neurobiology and stress mechanisms, this research highlights the need for further research into the anatomical and functional complexity of the avian hippocampus. Moreover, it opens new avenues for investigating the evolutionary conservation of hippocampal functions across vertebrates.

# Acknowledgements

First of all, I would like to thank my supervisors Tom Smulders and Tim Boswell for their continuous support and guidance throughout my PhD. This thesis would not have been possible without your advice and constant encouragement. I feel very fortunate to have worked with such excellent people whose research and love for science inspired me to do my best work and to become a better scientist.

I also owe special gratitude to Loreta Medina, Ester Desfilis, and Alessandra Pross from the IRBLleida whose expertise and and assistance were instrumental in the completion of Chapter 4. I also extend my heartfelt appreciation to Ellisa Foulkes and Lei Huag for their invaluable support and time, and for always being a source of positive attitude. I am deeply thankful for their contributions to this work.

I would also like to thank the CBC staff for their diligent care of my chickens and for their prompt assistance whenever needed.

A special thanks to Anna Gray for her continuous support, humour, and friendship. You made me feel welcome in Newcastle and I cannot imagine this journey without you.

To my friends in Mexico, your support and encouragement have been a constant source of strength throughout my academic career. Your presence, whether near or far, has made all the difference, and I am always grateful for having you in my life.

I would like to thank my family for their love, patience, and understanding. Mamá and Papá, words cannot express how grateful I am for your endless support and unconditional love. You are the driving force behind all my big dreams and my commitment to always strive for excellence. Your support continues to help me through good and bad times, even more than you realize.

Finally, to my biggest cheerleader, Wietse Nouws, thank you for keeping me sane for the past four years. You have lived every high and low of this PhD with me and supported me with the utmost patience, love, and care. I feel incredibly lucky to have you by my side. Thank you for being my rock throughout this journey and for embarking on this adventure with me.

**Table of Contents**

## List of Tables

## List of Figures

## List of abbreviations

| | | | |
|---|---|---|---|
| A | adrenaline | LC | locus coeruleus |
| | | lfb | lateral forebrain bundle |
| AAV | adeno-associated virus | LHy | lateral hypothalamic area |
| Ac | anterior commissure | LS | lateral septal nucleus |
| ACSF | artificial cerebrospinal fluid | LSt | lateral striatum |
| ACTH | adrenocorticotropic hormone | LTer | lamina terminalis |
| ah | amygdalohypothalamic tract | lv | lateral ventricle |
| AH | anterior hypothalamic area | MCs | mineralocorticoids |
| AIH | alar hypothalamic nucleus | MEA | medial extended amygdala |

| | | | |
|---|---|---|---|
| AL | nucleus of the ansa lenticularis | ML | mediolateral |
| ANS | autonomic nervous system | MPA | medial preoptic area |
| AP | anteroposterior | MRs | mineralocorticoid receptors |
| APH | area parahippocampalis | MSt | medial striatum |
| APit | anterior pituitary | MV | mesopallium, ventral part |
| Au | auditory area, nidopallium | MVPe | periventricular region of the MV |
| AVP | arginine vasopressin | NA | noradrenaline |
| AVT | arginine vasotocin | NAcc | nucleus accumbens |
| B | basal nucleus | NC | nidopallium |
| BSA | bovine serum albumin | NDB | nucleus of the diagonal band |
| BST | bed nucleus of the stria terminalis | NHpC | nucleus of the hippocampal commissure |
| BSTL | lateral BST | ns | nigrostriatal tract |
| BSTM | medial BST | OCT | optimal cutting temperature |
| C | caudal | OD | optical density |
| CA | cornu ammonis | OF | open field |
| CEA | central extended amygdala | PalE | ectopic part of pallidum |
| CeC | capsular amygdala | PalSe | pallidoseptal transition area |
| chp | choroid plexus | PalV | ventral part of pallidum |
| CM | caudal-most | PaMC | magnocellular part of the PVN |
| CNS | central nervous system | PaPC | parvicellular part of the PVN |
| CORT | corticosterone | PBS | phosphate buffer saline |
| CRH | corticotropin-releasing hormone | Pe | periventricular stratum |
| CRHR1 | CRH type receptor 1 | PEI | polyethyleneimine |
| CRHR2 | CRH type receptor 2 | PFA | paraformaldehyde |
| csm | corticoseptomesencephalic tract | PHAL | phaseolus vulgaris leucoagglutinin |
| CTB | cholera toxin b subunit | PNS | parasympathetic nervous system |
| DAB | 1,31- diaminobenzidine | POMC | proopiomelanocortin |
| DAPI | 4', 6-diamidino-2-phenylindole | PVM | nucleus periventricularis magnocellularis |
| DG | dentate gyrus | PVN | hypothalamic paraventricular nucleus |
| DL | dorsolateral | PVNc | core region of the pvn |
| DM | dorsomedial | R | rostral |
| DMEM | Dulbecco's modified eagle's medium | RM | rostral-most |

| | | | |
|---|---|---|---|
| DREADD | designer receptors exclusively activated designer drugs | ROI | regions of interest |
| DV | dorsoventral | Rt | reticular nucleus |
| EA | extended amygdala | RT | room temperature |
| FBS | fetal bovine serum | SAM | sympathoadrenomedullary |
| fi | fimbria of the hippocampus | SCE | stratum cellulare externum |
| FR | fluoro-ruby | SCI | stratum cellulare internum |
| GAPDH | glyceraldehyde 3-phosphate dehydrogenase | Se | septum |
| GAS | general adaptation syndrome | SFi | septofimbrial nucleus |
| GCs | glucocorticoids | Shi | septohippocampal nucleus |
| GEE | generalized estimating equations | SM | medial septal nucleus |
| GFP | green fluorescent protein | sm | stria medullaris |
| GLM | generalized linear model | SMS | submedial septal nucleus |
| GRs | glucocorticoid receptors | SPa | subparaventricular nucleus |
| HDB | nucleus of the horizonal limb of the diagonal band | StAm | strioamygdaloid transition area |
| HF | hippocampal formation | StPal | striopallidal area |
| Hi | hippocampus | Ta | nucleus taeniae in the amygdala |
| Hp | hippocampus proper | TR | Texas red |
| HPA | hypothalamic-pituitary-adrenal | V | ventral |
| HRP | horseradish peroxidase | VDB | nucleus of the vertical limb of the diagonal band |
| IEG | immediate early gene | VLT | ventrolateral thalamic nucleus |

# 1. Chapter 1. Introduction

## 1.1. Principles of Brain Evolution

### 1.1.1. Conservation, homology, and convergence

The origin of the vertebrate brain traces back more than 500 million years to shared evolutionary ancestors. At the core of brain evolution lies the process of conservation, a scenario of minimum transformation that preserves certain features and functions across time. This principle suggests that certain elements of the brain's architecture are so fundamental to survival and adaptation that they have remained relatively unchanged. For instance, all vertebrates possess a suprachiasmatic nucleus that lies in the hypothalamus, receives retinal inputs, and plays a crucial role in controlling circadian rhythms (Striedter, 2005).

Through the course of evolution, however, brain areas have changed either by the multiplication of existing neuronal classes, and/or the loss and addition of new ones, or by changes in differential gene regulation including mutations in developmental regulatory genes (Carroll, 2008). Simultaneously, small changes in neural pathways can lead to dramatic changes in an organism's abilities, and novel levels of organisation emerge through the loss of connections and the incorporation of new areas. All these changes are governed by a set of interacting principles, which entail the loss, reduction, or modification of ancestral neural structures throughout a species' ontogeny. To understand these evolutionary dynamics, researchers employ two conceptual frameworks: homology and convergence.

To explain how evolutionary changes occur it is necessary to compare diverse brain components across species. As brains do not fossilize, formulating phylogenetic sequences requires the identification of patterns of observed variations in homologous characters within extant species. This challenge is exacerbated by the question of what constitutes the vertebrate brain archetype and the substantial diversification of brain structures across different vertebrate classes, along with different neurochemical, connectional, anatomical, embryological, and molecular criteria contributing to the discussions of which of these features should be considered decisive in determining homologies (Aboitiz, 2011; Northcutt, 1984; Striedter, 2005).

Striedter (2005) suggests that evolution has consistently resulted in diverse methods to construct similar structures and repurpose existing materials. Therefore, recognizing at least three levels of comparison becomes essential: one for brain regions, another for cell types, and a third for molecules. Moreover, it is crucial to acknowledge that the patterns observed in embryonic brains may differ from those for mature brains, as homologies observed during embryonic development may not necessarily align with those seen in adults.

Central to this debate is the challenge of defining the concept of homology. Formulated by Owen (1843) as 'The same organ in different animals under every variety of form and function', homologous characters were then differentiated from analogous characters, those superficially similar performing similar functions. This definition changed with the emergence of the evolutionary theory to imply a hypothesis of common ancestry between two traits, as proposed by Lankester (1870). Lankester also suggested a replacement for Owen's usage of the term homology with the term homogeny, and the term analogy with homoplasy. However, even though the evolutionary experts adopted Lankester's homogeny definition, they continued to use the term homology. On the other hand, homoplasy was embraced as a simpler concept compared to analogy, which requires evidence for an adaptive cause of the similarity (Amundson, 2001).

Over time, Lankester's definition encountered certain limitations as it did not exclude instances of divergent evolution, where homologous characters might exhibit significant dissimilarity, and cases of parallelism, where a feature is present in closely related organisms but not present continuously in all members of the lineage (Hall, 2003, 2013; Striedter & Northcutt, 1991).

Expanding on these complexities, ancestral characters may persist in two or more descendant taxa without undergoing any transformation, a phenomenon known as static homology. Conversely, the ancestral character might be retained exclusively in one of the descendant taxa, undergoing a distinct transformation and resulting in a different character in the other taxon, a scenario termed transformational homology. Wiley (1981) distinguished between these scenarios and proposed that a character is homologous in two or more taxa if it is present in the common ancestor of these taxa, or, two characters are homologous if one directly derives from the other (Northcutt, 1984; Striedter & Northcutt, 1991).

While homology explores the similarities among species resulting from shared evolutionary ancestry, convergence is the term used when similar features evolve in distantly related organisms in response to similar environmental selection pressures. Examples of convergence abound in the evolution of nervous systems, including the evolution of electric organs and electric communication in gymnotiform and mormyriform fishes (Bullock *et al.*, 1975; Kawasaki,1993); the evolution of a variety of cerebellum-like structures among vertebrates (Bell, 2002) and even the evolution of intelligence between corvids and apes (Emery & Clayton, 2004). Gould (2002) and Hall (2003) contributed to the discussion on convergence by proposing a distinction between convergence and parallelism, identifying convergence as a specific class of homoplasy, and recognizing parallelism as a type of homology (Hall, 2013). According to Gould (2002), the distinction between convergence and parallelism lies in the fact that parallelism involves the independent evolution of identical structures from two closely related species, while convergence refers to the evolution of similar parts from species that are not closely related.

Two essential considerations deserve attention. It is crucial to note that homology at a specific level within the biological hierarchy does not necessarily confirm, negate, or contradict homology at other levels. In addition, the identification of non-homologous novel features, like turtle shells, tetrapod digits, and the origination of the neural crest in early vertebrates, has shifted the evolutionary discourse, making 'novelty' a new category of evolutionary change (Hall, 2013).

The principles delineated here contribute to the analysis of the adaptive influences shaping the evolution of the brain. Moving beyond the recognition of similarities based on topology, contemporary approaches explore similarities through the lens of comparative developmental genetics and advances in systematics. As we continue to unravel the unique relationships between different structural components across vertebrate brains and explore the neural populations and connections characterizing distinct regions, more answers to the question of how vertebrate brains have evolved will emerge.

This thesis aims to contribute to this ongoing exploration by providing valuable insights into the broader context of stress regulation in birds and a deeper understanding of the evolutionary changes in the avian brain, with a specific emphasis on the role of the avian hippocampus in stress regulation.

## 1.2. Neurobiology of Stress

### 1.2.1. The concept of stress

Before delving into the analysis of stress in avian brains, it is crucial to define the concept of stress. The definition of stress can vary across different research fields and may take on different meanings depending on the specific conditions being studied, here I specifically define the concept of physiological stress.

Over time, the concept of stress has undergone significant evolution from its initial definition by Hans Selye in 1936 describing stress as a non-specific response of the body to any demand. Currently, stress is defined as a real or perceived threat to an individual's physiological or psychological well-being, which triggers physiological and/or behavioural responses, as proposed by McEwen (2000).

To understand this definition, we first need to refer to the concept of homeostasis. Coined by Cannon (1939), homeostasis represents a state of equilibrium of several physiological variables in an organism, ensuring the survival and optimal function of essential physiological systems. Thus, the stress response involves behavioural and physiological changes whose objective is to regain homeostasis back to pre-stress levels (De Kloet *et al.*, 1998; Jacobson & Sapolsky, 1991).

Cannon, also coined the term 'fight-or-flight' to describe how animals respond to perceived threats. According to the concept of 'fight-or-flight', which is also known as an acute

stress response, animals react to perceived threats by triggering a chain of rapidly occurring reactions inside the body which prepare the animal to either fight or flee (Cannon, 1915). Later, this response would be identified as the first stage of the General Adaptation Syndrome (GAS), which was proposed by Hans Selye as a universal stress response among vertebrates and other organisms (Fink, 2016).

Selye's concept of the GAS is a framework that explains how the body responds to stress. According to Selye, when exposed to stress, the body undergoes three distinct stages: alarm, resistance, and exhaustion. During the alarm stage, the body responds to the stressor by internal changes that prepare it for action. In the resistance stage, the body attempts to adapt to the stressor and maintain normal functioning. However, if the stressor persists for an extended period, the body enters the exhaustion stage, where it can no longer cope with the stressor and experiences a decline in function, which can ultimately lead to death. This prolonged exposure to stress can lead to what Selye called "diseases of adaptation," which are health problems that arise due to the body's attempts to adapt to chronic stress (Selye, 1946).

In addition, in his book Stress in Health and Disease (1976a), Selye argued that stress can arise from a wide range of situations, such as physical trauma, emotional stress, fatigue, pain, fear, and various other demands of daily life. Yet, the stress response is a stereotyped pattern of biochemical, functional, and structural changes. Furthermore, he emphasized that stressors do not make a distinction between positive and negative situations and that stress can be divided into two categories: "eustress," which refers to constructive stress, and "distress," which defines harmful stress (Selye, 1976b).

Stressors can be physical (e.g. cold, heat, radiation, noise, and pain) or psychological (e.g. anxiety, fear, and frustration) (Lu *et al*., 2021). Stimuli that are considered stressors from one individual´s point of view or the human point of view may not necessarily be stressors to another individual or a non-human animal. Moreover, an individual's response to stress and susceptibility to stress-related disorders is influenced by multiple factors such as genetics, sex, age, environmental conditions, and early life experiences. For instance, a study in domestic chicken (*Gallus gallus*) demonstrated that exposure to intermittent social isolation early in life has a lasting impact on the physiological stress response of the affected birds and their male offspring resulting in a dampened corticosterone (CORT) response to restraint stress (Goerlich *et al*., 2012).

In terms of duration, stressors may be either acute (single, intermittent, time-limited exposure) or chronic (continuous long-term prolonged exposure, intermittent long-term exposure) (Nostramo & Sabban, 2015). While the response to acute stress allows an organism to survive and restore homeostasis, after prolonged or repeated exposure the stress response is hindered and can become maladaptive leading to numerous negative health outcomes (De Kloet *et al*., 2005; Nostramo & Sabban, 2015). These alterations can accumulate, contributing to an increased workload for the organism, particularly when multiple changes happen simultaneously

or persist over an extended period, requiring intensified efforts from the organism to uphold stability. A persistent condition of imbalance can lead to insufficient or prolonged adaptive response where individuals manage to survive but experience negative outcomes (Charmandari *et al.*, 2005; McEwen & Wingfield, 2003). This condition is commonly referred to as allostatic load or allostatic overload, and I will delve deeper into its explanation in the following section.

### *1.2.2. Allostasis model*

The concept of allostasis provides a complementary perspective to understanding how organisms adapt to continually changing life conditions. Allostasis is defined as the process of maintaining stability through change (Sterling & Eyer, 1988). The term refers to the process of maintaining homeostasis, and it recognizes that invariant set points may change in response to a spectrum of stimuli, ranging from external factors like weather and pollution to internal factors such as disease, encompassing daily and seasonal physiological adaptations referred to as allostatic states.

Allostatic states play a vital role in maintaining key physiological parameters, e.g. glucose levels, within critical life-sustaining ranges because while physiological variables are kept constant, the primary mediators of these variables, e.g. insulin secretion, vary to ensure overall stability. However, over time, allostatic states can also produce wear and tear on the regulatory systems in the brain and body, leading to what is known as allostatic load. This cumulative result of an allostatic state can predispose an individual to disease (McEwen, 2005, 2016, 2017; McEwen & Wingfield, 2003; Ramsay & Woods 2014; Romero *et al.*, 2009).

Thus, the distinction lies in the terminology: homeostasis refers to the constancy of physiological parameters, while allostasis refers to the physiological parameters and the physiological mechanisms orchestrating that homeostasis through allostatic mediators. This is important because while homeostasis's primary focus is on those processes crucial for the immediate survival of the organism, overlooking vital functions such as reproduction or migration that may not be immediately imperative but are essential for the overall life cycle of an organism, the allostasis model provides a more comprehensive perspective by integrating these vital processes (McEwen & Wingfield, 2003).

The concepts of allostasis, allostatic states, and allostatic load, provide a framework for comprehending the long-term effects of stress. Sustained activation of allostatic effectors in conditions of allostatic imbalance can result in allostatic overload potentially worsening pathophysiologic processes. McEwen and Wingfield (2003) have identified two types of allostatic overload. Allostatic overload Type I occurs when the animal's energy demand for maintaining homeostasis exceeds the energy the animal can obtain from its environment prompting the animal to adjust its behaviour and physiology to alleviate the strain. Allostatic Overload Type II occurs when the overall allostatic load remains excessively high for an extended duration, leading to the

emergence of pathological problems within the physiological systems responsible for maintaining allostasis. Even with sufficient energy available, the extended activation of these systems contributes to detrimental health effects. For example, chronic activation of the Hypothalamic-Pituitary-Adrenal (HPA) axis and the release of endogenous excitatory amino acids in the brain reduce hippocampal volume impairing cognitive function and potentially contributing to psychiatric conditions such as major depression (Belleau *et al.*, 2019; Goldstein & McEwen, 2002).

Despite advancing the definition of stress by extending the concept of homeostasis, the descriptions above highlight a fundamental challenge of the allostasis model which is its heavy reliance on the ability to measure energy input and expenditure. This task is inherently intricate due to several factors such as the time frame of the measurements, different life-history stages, the thermoregulation strategies of animals, and the contextual nuances such as measurements in fasting versus fed states. In addition, due to the nature of the sympathetic and behavioural responses, moderate psychological stressors and rapid changes may not always manifest in measurable changes in energy expenditure, for example, behavioural and cognitive processes that cost little energy (Romero *et al.*, 2009).

Moreover, as highlighted by Day (2005), the allostasis model does not contribute to our understanding of how the brain distinguishes stressful from non-stressful stimuli and lacks a comprehensive framework for identifying the specific neural circuits that underlie the stress response.

### 1.2.3. Reactive Scope Model

The Reactive Scope Model (Romero *et al.*, 2009) refines the allostasis model and traditional concepts of stress while addressing many of the criticisms. Central to this model is the presence of a physiological mediator (homeostatic mediator), operating within four distinct ranges, each contributing to a comprehensive understanding of an individual's physiological responses.

The first is the range of Predictive Homeostasis, which involves responses initiated in anticipation of predictably timed challenges. Comparable to the concept of allostasis, this range encompasses normal circadian and seasonal variations, such as those influenced by photoperiod, but also extends its scope to life-history changes like pregnancy (Romero *et al.*, 2009).

The second range, Reactive Homeostasis, consists of increases above the normal circadian range designed to return the body to homeostasis. Originating from the traditional concept of stress, this range embodies the stress response. The combination of Predictive and Reactive Homeostasis ranges establishes the normal reactive scope, essentially defining the physiological constraints of a healthy individual. It is worth noting the normal reactive scope can vary between individuals and even within a single individual in response to specific stimuli (Romero *et al.*, 2009).

The third range, Homeostatic Overload, is characterized by increases surpassing the normal reactive scope. In this scenario, the physiological mediator itself becomes a problem and the animal enters a pathological state. An example is the prolonged cardiovascular responses to stressors contributing to cardiovascular disease (Sapolsky, 2010; Romero *et al*., 2009).

Finally, the fourth range, Homeostatic Failure, manifests when a physiological mediator cannot be maintained within the normal reactive scope, often leading to mortality. For example, death following the inability to maintain blood pressure due to hypertension (Darlington *et al*., 1990; Romero *et al*., 2009).

In introducing these different types of ranges, the model improves the categorisation of how individual animals respond to stressors, facilitating its predictability, and allowing for modifications tailored to the species, the individual, or the disease under investigation. Importantly, this model extends its applicability by shifting the focus from humans and presenting a valuable framework for comprehending stress dynamics in other animals (Romero *et al*., 2009).

Collectively, the refinements made to the concept of stress helped bridge the gap between human and animal stress experiences. The way researchers conceptualize and define stress profoundly influences their approach to the exploration of the molecular and structural components underlying the stress response in the brain, a subject that I will examine in the next section.

### 1.2.4. The ANS and HPA systems

The basic components and organization of the neuroendocrine stress axis arose early in evolution and are highly conserved across vertebrates (Denver, 2009). The response to stressors is dependent on the activation of two key pathways: the HPA axis and the autonomic nervous system (ANS). These two systems act together and exert control over each other's activity.

#### 1.2.4.1. Activation of the ANS

The ANS plays a crucial role in the immediate response to stressors and consists of two divisions, the sympathetic nervous system (SNS) and the parasympathetic nervous system (PNS). The principal neurotransmitters of the ANS are norepinephrine (NE), epinephrine (E) and acetylcholine (ACh) (Won & Kim, 2016).

Acute stress promptly activates a small number of cells located in the locus coeruleus (LC) and across the medulla and the pons in the brainstem resulting in the release of NE in its downstream targets, including the VTA, prefrontal cortex (PFC), amygdala, and hippocampus. Activation of the LC is followed by activation of the peripheral sympatho-adrenomedullary system (SAM) system, causing medullary cells in the adrenal medulla to release E and, to a lesser extent, NE into the bloodstream initiating the body's "fight or flight" response. In addition, E further increases NE release through ascending vagal projections to the nucleus of the solitary tract (NTS)

(Chrousos & Gold, 1992; Godoy *et al.*, 2018; Hermans *et al.*, 2014; Smith & Vale, 2006: Won & Kim, 2016).

Overall, sympathetic activity is enhanced via the activation of adrenoceptors, a superfamily of guanosine triphosphate-binding protein (G protein)-coupled receptors (GPCRs) activated by NE and E. Activation of these receptors facilitates the rapid transfer of signals to downstream effectors, resulting in swift changes in neuronal function in those cells that express these receptors. Consequently, the increase in catecholamine levels leads to immediate alterations in neuronal activity (Joëls & Baram, 2009; Lewis & Coote, 1990; Unnerstall *et al.*, 1984; Won & Kim, 2016; Zhang *et al.*, 2022).

The adrenoceptor superfamily can be further classified into three subfamilies: the alpha1-, alpha2-, and beta-adrenoceptor subfamilies. The beta-adrenoceptor subfamily comprises the beta-1, beta-2, and beta-3 subtypes. Adrenoceptors are widely distributed in the nervous and non-nervous systems, playing critical roles in various physiological processes. In cardiac tissue, they are essential for regulating heart function and the cardiovascular response. In the central nervous system, these receptors influence symptoms of mental disorders like depression and anxiety. They are also present in smooth muscles, including those in the bronchi, veins, and gastrointestinal tract, mediating responses such as bronchodilation and vascular tone. In adipose tissue, adrenoceptors regulate lipolysis, contributing to fat metabolism. Additionally, they are located in the gallbladder and urinary bladder, facilitating smooth muscle relaxation, and in skeletal muscle, where they assist in thermogenesis and muscle relaxation (Zhang *et al.*, 2022).

Beyond these physiological responses, SAM activation enhances overall arousal, alertness, vigilance, cognition, attention, and analgesia (Ulrich-Lai & Ryan, 2014). Moreover, activation of the ANS significantly influences immune response and inflammation. For example, research has demonstrated that NE enhances the production of tumor necrosis factor (TNF), and stimulates the release of interleukin (IL)-6 from both immune and peripheral cells while enhancing macrophage activity and tumoricidal functions (Chrosus, 200: Won & Kim, 2016).

Once stress subsides, the activation of the PNS triggers the release of ACh, which helps restore balance by counteracting the SNS and maintaining physiological homeostasis. However, during prolonged stress, the SNS remains overactive resulting in elevated catecholamine levels and reduced acetylcholine (ACh). ACh takes on an inhibitory role, reducing the release of pro-inflammatory cytokines like TNF, IL-1, IL-6, and IL-18 (Chrosus, 200: Won & Kim, 2016).

Nevertheless, this initial response is short-lived, and within a matter of minutes, hormonal mechanisms activate the HPA axis resulting in a long-lasting secretory response.

### 1.2.4.2.  *Activation of the HPA system*

Compared to the SAM activation, HPA axis induction occurs relatively slowly and results in a prolonged and intensified hormonal secretion. Activation of the HPA axis begins in the

parvocellular neurons located in the paraventricular nucleus (PVN) of the hypothalamus (Jiang *et al.*, 2019).

Corticotropin-releasing hormone (CRH), also known as corticotropin-releasing factor (CRF), containing neurons are expressed throughout the central nervous system (CNS) and in peripheral tissues of mammals (Smith & Vale, 2006), such as the adrenal glands (Bruhn *et al.*, 1987) and testes (Audhya *et al.*, 1989). These neurons secrete CRH, a 41-amino acid peptide (Vale, 1981), which exerts its activity through two different G protein-coupled receptor subtypes, the CRH type receptor 1 (CRHR1) and the CRH type receptor 2 (CRHR2) distributed in the central and peripheral nervous systems (Denver, 2009; Smith & Vale, 2006). In birds, CRH-containing neurons are found through the nucleus accumbens (NAcc), lateral bed nucleus of the stria *terminalis* (BSTL), nucleus taeniae of the amygdala (Ta) in the subpallium, the PVN, and the lateral hypothalamic area in the hypothalamus; with the PVN being the major site of CRH neurons (Kuenzel & Jurkevich, 2010).

In mammals, arginine vasopressin (AVP), together with CRH, induces the release of adrenocorticotropic hormone (ACTH) when binding to pituitary corticotropes. ACTH is a small peptide hormone derived by proteolytic processing of the precursor protein proopiomelanocortin (POMC). In non-stressful situations, both CRH and AVP are released into the hypophyseal portal system in a circadian fashion paralleling the activity cycle, e.g. with early morning secretory bursts in diurnal species (Dallman *et al.*, 1987; Krieger, 1975). Alone, AVP has limited ACTH secretagogue activity but, together, AVP amplifies the effect of CRH (Smith & Vale, 2006). During stress, the relative proportion of the subset of neurons that secrete both CRH and AVP increases significantly (Tsigos *et al.*, 2020).

When released into the systemic circulation, adrenocorticotropic hormone (ACTH) stimulates corticosteroid biosynthesis in the adrenal cortex after binding to ACTH receptors (Denver, 2009). Corticosteroid hormones are categorized into two main groups: glucocorticoids (GCs) and mineralocorticoids (MCs). They are capable of crossing the blood-brain barrier, allowing them to potentially access all regions of the brain and play integral roles in behavioural, metabolic, cardiovascular, and immune processes, binding to glucocorticoid receptors (GRs) and mineralocorticoid receptors (MRs) present ubiquitously in nearly all tissues and organs (Kino & Chrousos, 2001). In most mammals and fish, cortisol serves as the primary glucocorticoid, while in rodents, birds, reptiles, and amphibians, corticosterone (CORT) assumes this role (Hermans *et al.*, 2014; Kadhim *et al.*, 2019).

In birds, the overall effect of stressors resembles that in mammals. The regulation of the stress response involves the activity of two major neuropeptides: CRH and arginine vasotocin (AVT). AVT differs from AVP by a single amino acid residue substitution, specifically isoleucine at position 3 instead of phenylalanine (Acher *et al.*, 1970; Cornett *et al.*, 2013) and plays an important

role in various physiological processes, including osmoregulation, blood pressure regulation, and oviposition (Baeyens & Cornett, 2006).

A unique feature of the avian stress regulatory system, however, involves the engagement of an additional neural structure known as the nucleus of the hippocampal commissure (NHpC). Positioned within the septum, the NHpC shares similarities with the PVN. Like the PVN, the NHpC contains CRH-producing neurons responsible for the synthesis of CRH. Notably, these CRH-producing neurons within the NHpC seem to be involved in the avian acute response to stress even preceding the activity of the PVN (Nagarajan *et al.*, 2017) (Figure 1.1).



**Figure 1. 1.** Schematic representation of the avian HPA axis system. In birds, both the nucleus of the hippocampal commissure (NHpC) and the paraventricular nucleus (PVN) in the hypothalamus appear to be critical for the activation of stress responses. PVN uses both CRH and AVT to trigger the release of ACTH from the anterior pituitary gland, while NHpC only makes CRH. The connection from NHpC to the anterior pituitary gland is not known yet. Reproduced from Nagarajan *et al.* (2017) with permission from Elsevier LTD under license number 1540086.

### 1.2.5. Termination of the stress response

Across vertebrates, feedback inhibition from circulating glucocorticoids modulates the HPA axis within minutes (Dallman, 2005). Like the circadian rhythm observed in plasma corticosteroid levels, the feedback sensitivity of the entire axis also displays a circadian pattern. This implies that, during the peak of the rhythm, elevated plasma steroid levels are necessary to effectively inhibit ACTH (Jacobson & Sapolsky, 1991).

Glucocorticoids inhibit HPA axis activity by rapidly shutting off hypothalamic and pituitary responses through both direct and indirect modulation of CRH neuronal activity. The direct process involves the GCs direct action on hypothalamic CRH neurons and on corticotropes in the anterior pituitary gland to decrease hormone synthesis and secretion. Indirectly, GCs modulate the activity of CRH neurons in the PVN via descending pathways from the hippocampus, amygdala, and the bed nucleus of the stria *terminalis* (BST) or via pathways originating in the brain stem (Denver, 2009; Uchoa *et al.*, 2014).

A distinguishing feature that sets the hippocampus apart from other components of the feedback regulation of the stress response is the presence of both corticosteroid receptor types. Notably, the highest concentration of receptor sites for glucocorticoids in the brain is found in the hippocampus (De Kloet *et al.*, 1998; Jacobson & Sapolsky, 1991; Reul & Kloet, 1985). Like in mammals, both GR and MR are present in the avian hippocampal formation (HF) (Senft *et al.*, 2016).

The regulation of the HPA axis through negative glucocorticoid feedback is crucial to prevent adverse consequences. Conditions such as anxiety, depression, and chronic inflammatory processes, along with the impairment of the cognitive function affecting memory, attention, and learning in both human and animal models, have been associated with hippocampal atrophy and dysregulation of the stress response (McEwen, 1999; Tsigos & Chrousos, 2002).

While the hippocampus is recognized for its pivotal role in suppressing the activity of the HPA axis, the mechanisms underlying this function and the anatomical and functional variations of this structure across species are still not fully understood. The upcoming section will focus on key aspects of the morphology of this structure.

## 1.3. Comparative Neuroanatomy of the Hippocampal Formation

### 1.3.1. Brain structures involved in stress

The regulation of the HPA axis is differentially influenced by the structural properties and functional roles of three key brain regions: the hippocampus, amygdala, and PFC. These regions interact with each other, impacting one another through direct and indirect neural connections (McEwen, 2007). At the same time, stress affects each of these regions in unique ways leading to distinct behavioral outcomes (Figure 1.2).

Anatomical studies suggest that hypothalamic inputs from the hippocampus/PFC and amygdala influence the HPA axis differently and can be either excitatory or inhibitory. Specifically, input from the hippocampus and prefrontal cortex is typically excitatory, enhancing GABAergic tone, while input from the amygdala is generally inhibitory, reducing GABAergic tone (Herman & Cullinan, 1997; Herman *et al.*, 2002; Jacobson & Sapolsky, 1991). In other words, increased input

from the hippocampus or prefrontal cortex suppresses the HPA axis, whereas increased input from the amygdala has the opposite effect, activating the HPA axis as demonstrated in electrical stimulation studies (Mandell *et al.*, 1963).

Behavioural studies highlight another key difference between these regions: chronic stress affects learning and memory processes differently depending on whether they are hippocampus- or amygdala-dependent (Chattarij *et al.*, 2015). In rodents, severe stress enhances fear conditioning and anxiety-like behaviours but impairs spatial memory. For example, while repeated stress leads to dendritic atrophy in the hippocampal CA3 region, disrupting hippocampal-dependent learning, the basolateral amygdala (BLA) undergoes hypertrophy, with increased dendritic arborization of spiny neurons facilitating stress-induced aversive learning (Conrad *et al.*, 1996, 1999; Luine *et al.*, 1994; McGaugh & Roozendaal, 2002; Vyas *et al.*, 2004).

These region-specific stress effects set the stage for a detailed examination of each of this brain regions. Consequently, as it is the purpose of this thesis, the next sections will delve into the role of the hippocampal formation in stress regulation offering a comprehensive analysis of its structure and function.
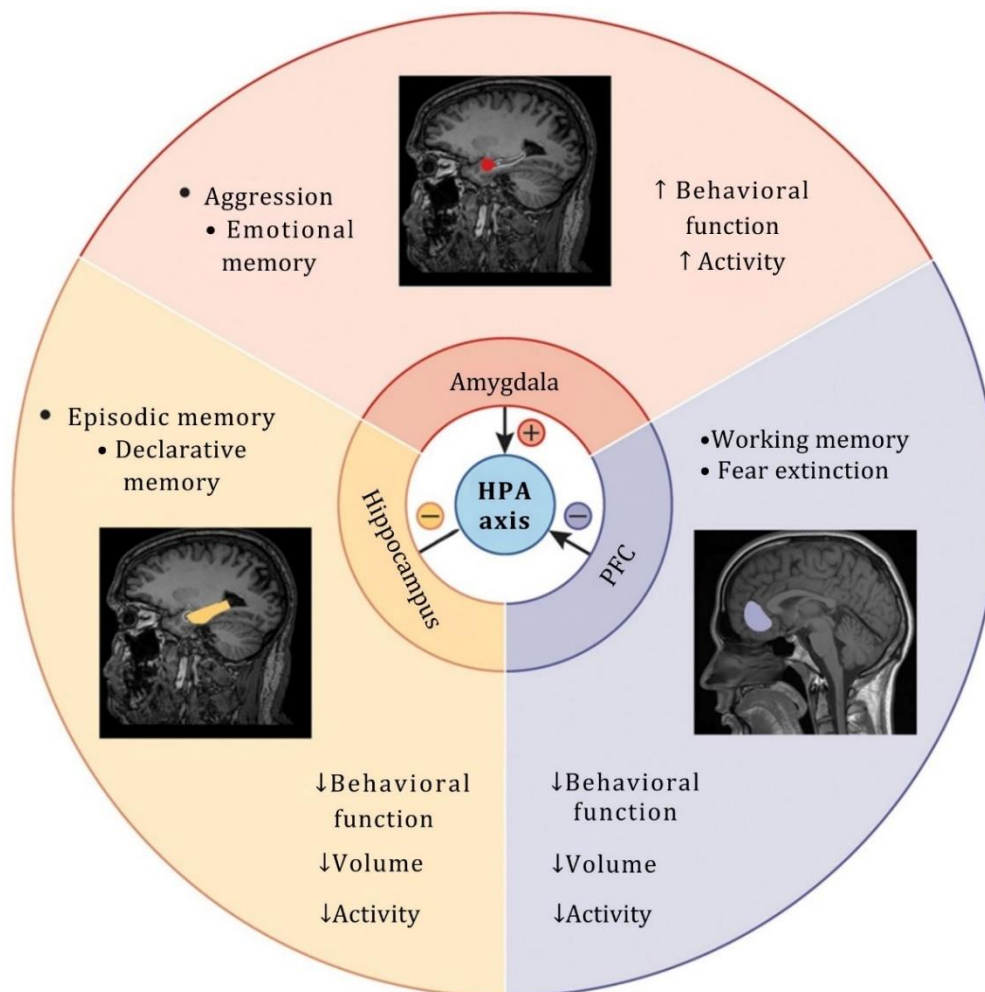


**Figure 1. 2.** Brain structures involved in regulating the stress response in humans. Activity in the amygdala stimulates the HPA axis, while activity in the hippocampus and PFC inhibit HPA axis activity. Reproduced from Chattarij *et al.* (2015) with permission from Nature Neuroscience under license number 1540063.

### 1.3.2. Anatomy of the mammalian and avian hippocampal formation

#### 1.3.2.1. Subdivisions

The hippocampus originates in the telencephalic pallium, from the distal, anterior portion of the embryonic telencephalic alar plate. It is considered an evolutionarily conserved region across all the vertebrate lineages (Bingman *et al.*, 2009; Striedter, 2016).

In mammals, it occurs as a three-layered, bilateral, oblong structure located in the forebrain resembling two interlocking "C"-shaped segments, and comprising three distinct anatomical regions: the subiculum, the dentate gyrus, and the *cornu ammonis* (CA) designated as CAl- CA4 in the direction from the subiculum to the dentate gyrus (DG) (Jacobson & Sapolsky, 1991) (Figure 1.3). The three subdivisions are cytoarchitectonically distinct. The dentate gyrus can be further subdivided into the molecular layer, the granule cell layer, and the polymorphic layer. Positioned as the outermost layer, the molecular layer is distinguished by its relatively sparse cell population. In contrast, the granule cell layer, or principal layer, is packed with granule cells and encloses the cellular polymorphic layer, also known as the hilus (Witter, 2012).
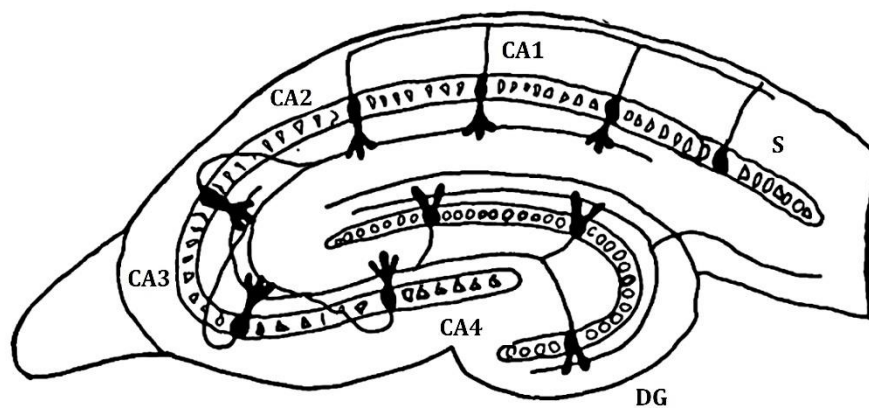


**Figure 1. 3.** Anatomical regions of the mammalian hippocampus. The dentate gyrus (DG), subiculum (S), and Ammon's horn CAl- CA4 fields are represented in a transverse section in the image. Reproduced from Jacobson & Sapolsky (1991) with permission from Oxford University Press under license number 5875330137031.

The cytological composition and topographic position of the avian HF have undergone changes during the avian and mammalian evolutionary trajectories, mainly due to the intensive development of the mammalian neocortex and corpus callosum, which displaced the HF. As a result, the avian hippocampus is structurally different from the mammalian hippocampus (El-Falougy & Benuska, 2006).

When compared to the mammalian hippocampus, the avian HF possesses a less apparent structural organization and it is essentially non-laminated (Medina & Abellán, 2009; Striedter, 2016). It also lacks a distinct Ammon's horn, an identifiable DG, a hilar region, and a postcommissural fornix (Colombo & Broadbent, 2000). Moreover, the avian hippocampus is not covered by more laterally derived parts of the telencephalon (i.e. cortex), and therefore it is located on the surface of the brain instead of lying inside the telencephalon's caudal pole as the rodent's hippocampus (Atoji & Wild, 2006, Striedter, 2016) (Figure 1.4).
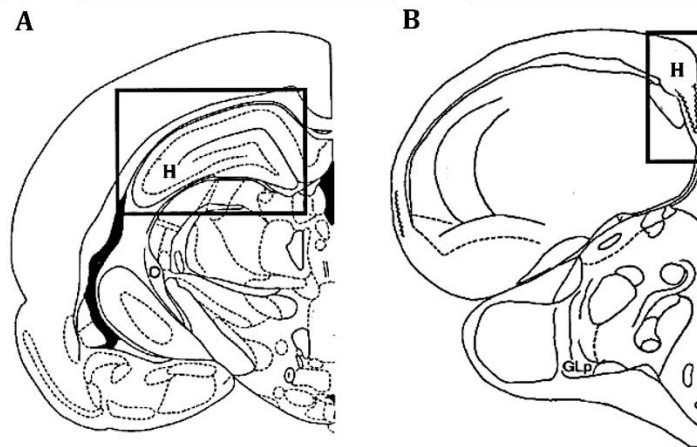


**Figure 1. 4.** Comparison of the telencephalic position of the hippocampus in coronal sections of rat and pigeon brains. The avian hippocampus (B) is located on the surface while the mammalian one (A) is covered by derived parts of the telencephalon. Modified from Colombo & Broadbent, (2000) with permission from Oxford University Press under license number 587534038990.

This less-defined structural arrangement has sparked various speculations regarding its internal organization, subdivisions, and boundary delineations. Different proposals have emerged based on different lines of evidence. For instance, Erichsen and colleagues (1991) identified six hippocampal subdivisions using a variety of immunohistochemical markers in pigeons: a medial fibre tract (Area1), a V-shaped area (Area 2), a ventromedial region between the arms of the V-shaped area (Area 3), a DM region defined by the presence of vasoactive intestinal polypeptide-positive cells (Area 4), a DM area (Area 5), and a lateral area (Area 6). Alternatively, when considering Nissl and zinc stainings, five subdivisions were identified in the zebra finch by Montagnese *et al.* (1996) encompassing the area parahippocampalis (APH), lateral and medial hippocampal layers, central field of the parahippocampus, and a crescent field.

Over time, subdivisional schemes have evolved to incorporate evidence from connectivity patterns and the descriptions not only of the HF of pigeons (Atoji & Wild, 2004; Herold *et al.*, 2014; Hough *et al.*, 2002; Kahn *et al.*, 2003), but also of domestic chickens (Fujita *et al.*, 2022; Gupta *et al.*, 2012; Puelles *et al.*, 2007; Suarez *et al.*, 2006), and songbirds (Montagnese *et al.*, 1996; Székely, 1999). For instance, based on fibre connectivity, the HF of the zebra finch was divided by Székely & Krebs (1996) into three main subdivisions, namely the dorsolateral (DL), dorsomedial (DM),

and ventral (V). As reviewed in Székely and Krebs (1996) the region recognized as the DL subdivision aligns with the lateral aspect of the APH described by Karten and Hodos (1967), and by Montagnese *et al.* (1996). Additionally, it corresponds to Area 6 along with the lateral portion of Area 3 according to Erichsen *et al.* (1991). The subdivision named DM is synonymous with Area 5 and also encompasses the dorsomedial part of Area 4 as described by Erichsen *et al.* (1991). Meanwhile, the V subdivision corresponds to the area designated as the hippocampus proper (Hp) by Karten and Hodos (1967) and occupies a position consistent with areas 1, 2, and the medial aspect of area 3 as delineated by Erichsen *et al.* (1991).

The use of evoked field potentials offered another perspective, leading to the recognition of five subdivisions, as outlined by Kahn *et al.* (2003): DM, DL, ventral core, ventrolateral and ventromedial areas of the V-shaped layer. But, perhaps one of the most influential subdivisional schemes comes from combined evidence obtained by tract-tracing and Nissl staining techniques. In 2004, Atoji and Wild proposed seven subdivisions in the pigeon HF with each subdivision containing different types of cells. The DL division segregates into dorsal (DLd) and ventral (DLv) portions, while the ventral, named the V-shaped layer complex, is subdivided into lateral (ll) and medial (ml) layers. Positioned along the dorsomedial corner of the HF, the magnocellular (Ma), parvocellular (Pa), and cell-poor (Po) regions are relatively small. The Ma region predominantly comprises large multipolar neurons, the Pa region consists of medium- or small-sized neurons densely packed compared to Ma and Po regions, and the Po region is characterized by an abundance of neuropil. Notably, the DL and DM regions are limited by a shallow sulcus designated as the parahippocampal sulcus. (Figure 1.5).
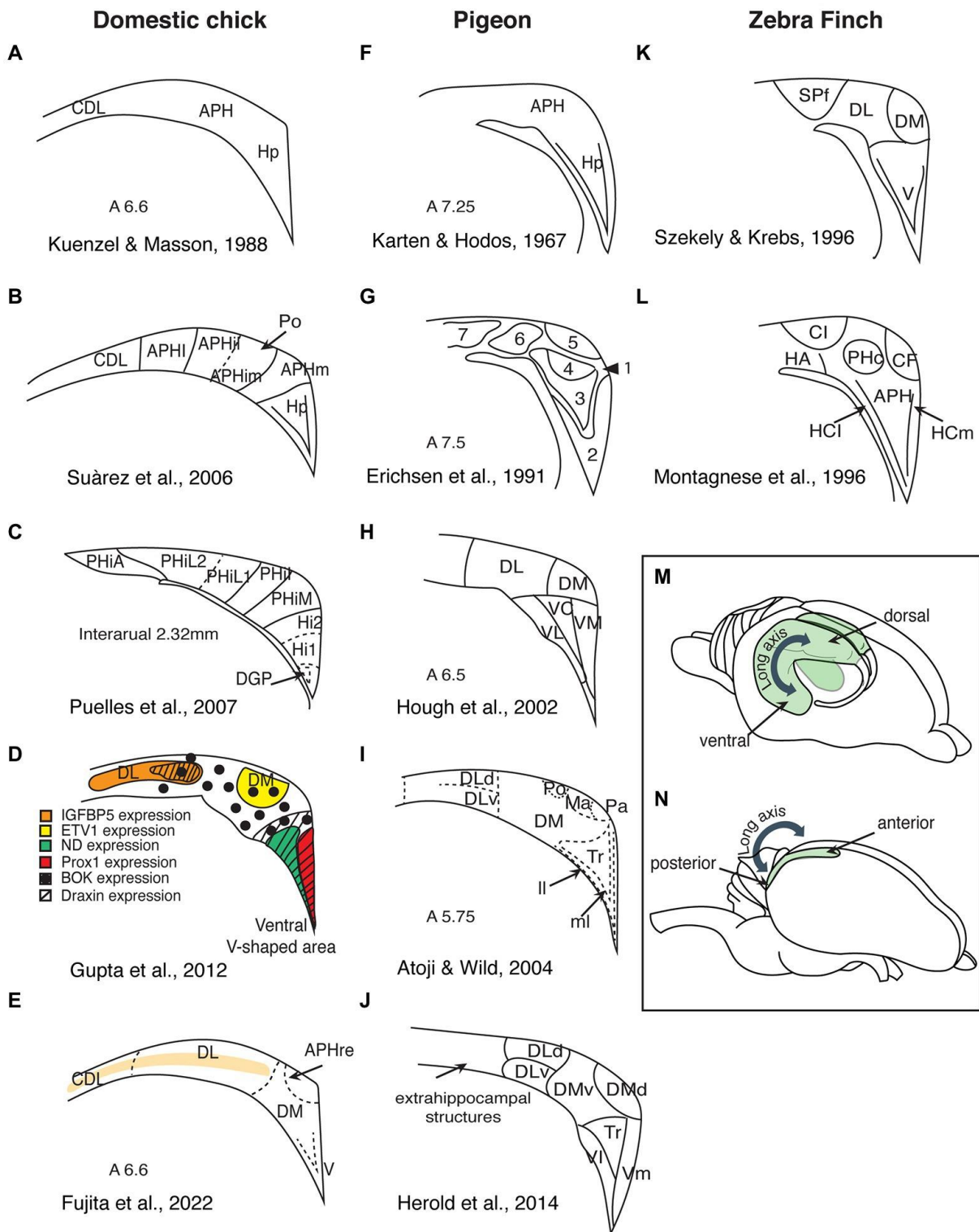
**Figure 1. 5.** Overview of different structural subdivisions proposed for the hippocampal formation of birds including domestic chicks (A–E), pigeons (F–J), and zebra finches (K, L). For comparison, panel (M) shows the hippocampal formation along the dorsoventral axis of a rodent brain, and panel (N) depicts the corresponding anteroposterior organisation in an avian brain. This figure is reproduced from Morandi-Raikova & Mayer (2022).

The diversity in internal structure and subdivisions prompts intriguing questions regarding the conservation of hippocampal function throughout evolution and the homologies between mammalian and avian subdivisions. It is still unclear which regions of the avian HF

correspond to the better-described mammalian hippocampus as different evidence suggests different relationships. For instance, based on the immunoreactivity distribution of different neuropeptides, Erichsen *et al.* proposed (1991) that the V-complex corresponds to the Ammon's horn, the DM hippocampus to the DG, and the DL area (area 6) to the subiculum. Other tract tracing studies, such as those conducted by Kahn *et al.* (2003) in homing pigeons and by Székely and Krebs (1996) in the zebra finch would also support Erichsen *et al.*'s conclusions.

By contrast, based on connectivity data and kainic acid lesions, Atoji and Wild (2004) proposed a different homology for the mammalian DG comparing it to the V subregion of the avian hippocampus, whereas an Ammon's horn-like subdivision is found in DM, and the mammalian entorhinal cortex seemed comparable to the DL hippocampus. These relationships have been further supported by more recent findings involving the distribution of neurotransmitters in pigeons (Herold *et al.*, 2014), physiological studies in food-caching songbirds (Applegate *et al.*, 2023) and the expression of developmental regulatory genes in chickens. These studies have shown that the ventral edge of the avian hippocampus expresses a similar set of genes (*Lef1* and *Prox1*) as the DG during embryonic development (Gupta *et al.*, 2012; Puelles *et al.*, 2007). Moreover, in mice, the highest expression of the developmental regulatory gene, *Lmo4,* is observed in the CA1 region, whereas *Lmo3* exhibits its strongest expression in the subiculum. Similarly, in chickens, the most pronounced *Lmo4* expression is observed in the DM, while the highest expression of *Lmo3* is seen in the DL subdivision (Abellán *et al.*, 2014).

It is interesting to note that while earlier studies acknowledged the uncertainty surrounding a DG-like structure in the avian hippocampal formation, as there was a lack of evidence for a mossy fibre system characteristic of mammals (Erichsen *et al.*, 1991; Montagnese *et al.*, 1993), this debate continues with more recent authors still arguing that the DG might be a unique mammalian acquisition (Papp *et al.*, 2007) and despite fibre-like projections have been identified in pigeons (Herold *et al.*, 2014) these appear less organized than in the mammalian DG.

Another intriguing aspect lies in understanding how neuronal networks have adapted amidst the structural variation across taxa. The next sections describe the connectivity of the HF. Through the text, distinctions at the level of subdivisions will focus on the main DL, DM, and V subdivisions recognized by Atoji & Wild (2004), delving deeper into their unique characteristics when possible.

### 1.3.2.2. *Connectivity*

The primary source of input to the mammalian hippocampus arrives from the entorhinal cortex via the perforant pathway (Witter & Amaral, 2004). Intrinsic connections within the mammalian HF are typically characterized by a unidirectional pattern referred to as the trisynaptic circuit. Specifically, the granular cells of the dentate gyrus establish one-way connections, projecting to the CA3 field of the hippocampus. In turn, CA3 cells project to the CA1

field, and subsequently, cells within the CA1 field project to the subiculum. However, information may also be processed through inputs from a variety of sources in CA3, from here axons of pyramidal cells spread information through the hippocampus projecting in the opposite direction of the trisynaptic circuit (Scharfman, 2007) (Figure 1.7).

The subiculum stands out as a crucial output region within the HF, subicular fibres innervate several cortical and subcortical regions, including the hypothalamus (Witter & Amaral, 2004).

While there is a possibility of some unidirectional circuits within the smaller subdivisions of the avian hippocampus (Kahn *et al.*, 2003), connections between the DL, DM, and the V-shaped area appear to be primarily reciprocal, implying a bidirectional flow of information suggesting that intrahippocampal circuits became increasingly unidirectional in birds and mammals (Rook *et al.*, 2023; Striedter, 2016).

In recent years, at least two additional distinct pathways have been identified within the avian hippocampal formation of the homing pigeon: a more dorsomedial (superficial) pathway and a more ventrolateral (deep) pathway. In the superficial pathway, the dorsal DL (DLd) sends projections to the dorsal DM (DMd) and the medial Tr, with some connectivity to the medial V-shaped layer (Vm). The DMd subsequently projects back to both Vm and medial Tr, and also has reciprocal connections with the ventral part of the DM (DMvd). Vm further sends projections to the lateral V (Vl) and the Tr (Rook *et al.*, 2023).

In contrast, the deep pathway is primarily characterised by projections from the ventral DL (DLv) to the ventral part of the ventral DM (DMvv), which also shows weak connections to Vl. Efferents from DMvv extend to Vl and lateral Tr, with Vl projecting back to DMvv and Tr. Additionally, DMd and DMvv receive inputs from the medial and lateral portions of Tr, respectively. Importantly, the superficial and deep pathways are interconnected within the dorsal lateral (DL) and dorsomedial (DM) areas, as well as in the V-shaped region via connections between the lateral and medial Tr (Rook *et al.*, 2023) (Figure 1.6).
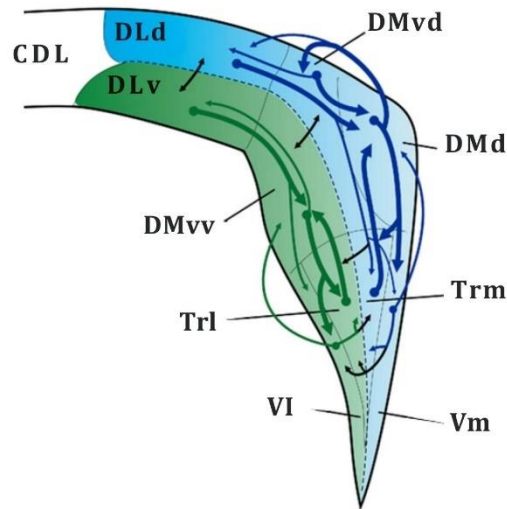
**Figure 1. 6.** Deep and superficial intrahippocampal pathways in the homing pigeon. In short, the superficial pathway (blue) connects the dorsal portion of the dorsolateral region (DLd) to the dorsal portion of the dorsomedial region (DMd) and the triangular subdivision (Tr), with further connections extending to the ventral region (Vm). In the deep pathway (green), the ventral DL (DLv) links primarily to the medial portion of the ventral DM (DMvv), in turn, the DMvv sends signals to Vl and lateral Tr. Both pathways interconnect. Modified from Rook *et al.* (2023) with permission from John Wiley & Sons under license number 1540094.

Fibre connections in the avian HF have been identified by immunohistochemical and tract-tracing studies. Telencephalic inputs to the avian hippocampus originate mainly from the hyperpallium (Reiner *et al.*, 2004) which provides multimodal sensory information, but also from the nidopallium that processes somatosensory and auditory information, as well as from the dorsolateral corticoid area, which receives inputs from the primary olfactory cortex. Extra-telencephalic inputs derive mainly from the dorsal thalamus and the supramammillary region of the hypothalamus (Atoji & Wild, 2004, 2005; Berk & Hawkin, 1985) (Figure 1.7).

The efferent projections from the avian hippocampus primarily originate from the DM and DL subdivisions, with the DM exhibiting significant projections to the septum, with weaker septal projections originating from the DL and V subdivisions (Figure 1.7). Notably, the DM division also directly projects to the lateral hypothalamus (Atoji & Wild, 2004).
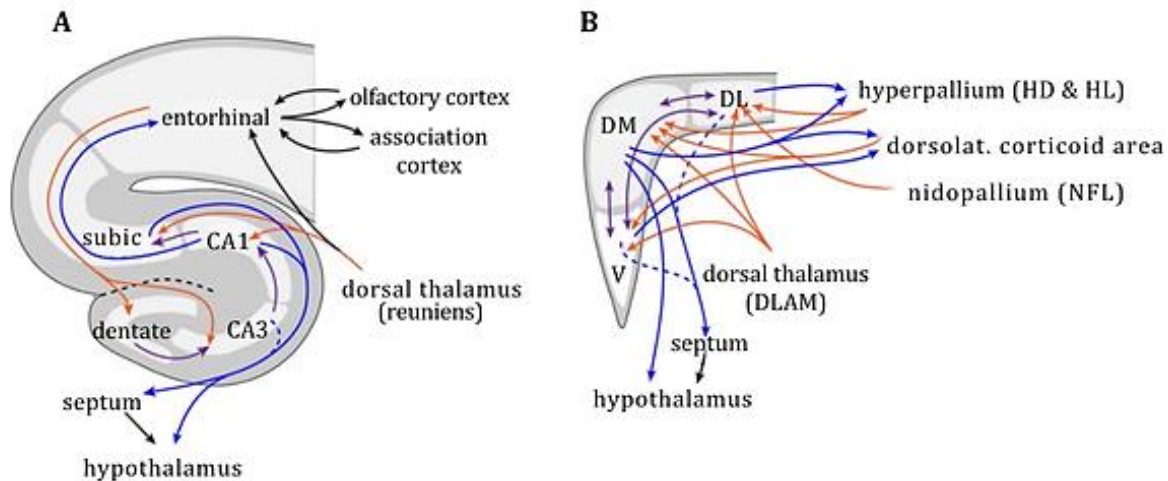
**Figure 1. 7.** Principal connections of the mammalian (A) and avian (B) hippocampal formation. The dentate gyrus (DG), subiculum (subic), and cornu ammonis CAl to CA4 fields are represented in the mammalian hippocampus (A) while ventral (V), dorsomedial (DM), and dorsolateral (DL) subregions are shown in the avian hippocampus (B). Modified from Striedter, (2016) with permission from John Wiley & Sons under license number 1529861.

Despite the overall similarity of functional networks, recent studies have observed notable species differences in functional connectivity. For example, while analysing the hippocampus of as an unfolded cortical surface, Eichert *et al*. (2024) observed a marked reconfiguration of the macroscale functional networks between humans and macaques with increased neuronal integration and connectivity characterising the human lineage.

The coexistence of both unique features and apparent homologies of the hippocampus raises the question of the extent of conservation of the hippocampal function across lineages. The next section describes the main functions of the mammalian hippocampus and provides an overview of the available comparative data on the functions of the avian hippocampus.

### 1.3.3.  Function of the Hippocampal Formation

#### 1.3.3.1.    Episodic memory and spatial navigation

For years, most of the interest in the hippocampus has centred on its role in spatial navigation and episodic memory. Research shows that damage to the hippocampus in humans does not typically affect vocabulary or factual knowledge, but it does impair the recalling of recent events (Bird & Burgess, 2008). Additionally, damage to the hippocampus can result in global amnesia, affecting both spatial and non-spatial domains in both humans and animals (Eichenbaum *et al.,* 1999). Evidence in rats also shows that damage to the hippocampus impairs place learning (Morris *et al*., 1982).

Furthermore, in conditions like Alzheimer's disease, characteristic memory impairment and topographic disorientation are linked to degeneration of the hippocampus. The neuropathological abnormality in this disease includes neuronal loss and gliosis in the hippocampus (Ball *et al.* 1985).

In 1971, O'Keefe and Dostrovsky published the first report on the presence of place cells in the hippocampus of freely behaving rats. These specialized hippocampal neurons are found in the DG and the CA, they activate when an individual is in a particular spatial location, creating a neural representation or 'place field' for that specific area. As an organism moves through its environment, different place cells become active, forming a pattern of activity that corresponds to the individual's physical location in the brain, the basis of spatial navigation (Poulter *et al.*, 2018: Takashi, 2018).

The hippocampus influences navigation through two distinct mechanisms: firstly, by the formation of spatial maps to facilitate navigation, and secondly, by guiding exploration to enable map-building. For example, in rats, previous research has found that place cells exhibit pre-activation before navigation begins, coding for locations ahead of the rat on the path to intended destinations (Pfeiffer & Foster, 2013). Rats employ behaviours such as rearing on hind legs and head scans to gather information about distal cues. Research shows that injection of cholinergic agonists into the medial septum or hippocampus increases rearing in rats. Additionally, during the initial exposure to a new environment, rearing frequency is highly positively correlated with hippocampal acetylcholine (Lever *et al.*, 2006).

The hippocampus also allows social animals to know the spatial positions of conspecifics. Research in bats has shown that a distinct subpopulation of neurons in the hippocampal septal-CA1 region exhibits the position of another bat in allocentric coordinates. Notably, approximately half of these neurons, termed 'social place cells', also represent the observer's own position, thereby functioning as place cells (Omer *et al.*, 2018).

In birds, most of the studies about the hippocampal formation have focused on relatively few species that rely on their food-caching and navigation abilities (e.g., jays, chickadees, and pigeons) (De Morais Magalhães *et al.*, 2017; Pravosudov *et al.*, 2006; Rehkämper *et al.*, 1988; Smulders & DeVoogd, 2000; Striedter, 2016). These investigations focus on the remarkable bird migratory navigation and memory capabilities of scatter-hoarding species. Particularly intriguing is the ability of these birds to remember numerous locations for long periods of time.

Pigeons learn the location of their home loft by employing diverse spatial cues, including distant visual landmarks, the earth's magnetic field, wind-induced infrasound, and wind-borne odorants (Able, 2000; Hagstrum, 2013; Holland, 2014; Phillips & Jorge, 2014; Wallraff, 2014 in Striedter, 2016). Bilateral lesions of the hippocampus impair their ability to return to their home loft from both unfamiliar and familiar sites (Bingman *et al.*, 1984) even when the pigeons with hippocampal lesions are released very close to home (Bingman *et al.*, 1985).

Early research exploring the circuit mechanisms involved in bird navigation suggested that some neurons in the pigeon hippocampus fire preferentially in specific locations. However, it was concluded that the degree of spatial specificity is lower than what is observed in mammals, as the cells in the hippocampal formation of pigeons may code for unspecified behavioural, motivational, or environmental factors in addition to a pigeon's momentary location (Siegel *et al.*, 2005). Nevertheless, more recent studies have shown that the hippocampal circuit mechanisms are more similar to mammals than previously thought with mammalian-like neural activity found in the hippocampus of a food-catching bird, the tufted titmouse. The findings showed localized spatial neural activity, sharp-wave ripples, and anatomically organized place cells, with the rostral -anterior- segment of the hippocampus having the highest density of place cells (Payne *et al.*, 2021).

Furthermore, birds employ distant landmarks to locate their food caches. For instance, Clark's nutcrackers (*Nucifraga columbiana*) can remember thousands of cache sites, with a memory of some of them for at least 9 months (Kamil *et al.*, 2001). Research has shown a correlation between the larger relative size of the HF in these birds concerning both body and total brain size. This greater hippocampal volume is associated with superior performance in laboratory tests of spatial memory and with stronger dependence on food stores in the wild (Basil *et al.*, 1996; Kamil *et al.*, 2001).

Therefore, lesioning the hippocampus can impair the ability of these birds to retrieve food. In a study with black-capped chickadees, bilateral hippocampal aspiration reduced the accuracy of cache recovery (Sherry & Vaccarino, 1989), while excitotoxic lesions in the DM hippocampus of zebra finches impaired their ability to remember the location of seeds only when the goal location was not marked with a colour cue (Patel *et al.*, 1997).

Taken together, these findings show that similar patterns emerge when examining the effects of damage to the hippocampus on the performance of comparable tasks between birds and mammals, suggesting that shared functions -at least when it comes to spatial navigation and memory tasks- may accompany the structural homology between the avian and mammalian hippocampi.

### 1.3.3.2. Stress regulation

Despite the focus on the cognitive properties of the hippocampus in both mammalian and avian species, literature also shows that a crucial link between the hippocampus and stress exists. For instance, Madison and colleagues (2024) conducted a comprehensive review of the role of the avian hippocampus in spatial cognition and stress responses, highlighting the potential functional significance and shared anatomy between the avian and mammalian hippocampi.

Evidence of the susceptibility of the hippocampus to stress comes from early physiological evidence in mammals with the observation of selective retention of cortisol in the hippocampus

of adrenalectomized rats (McEwen *et al.*, 1968). Today, we know that the mammalian hippocampus participates in all three aspects of the HPA activity: the stress response, the circadian rhythm control, and the corticosteroid feedback inhibition, primarily by mediating the sensitivity to corticosteroid inhibition.

In addition to harbouring a substantial concentration of GRs and MRs, the hippocampal MRs, in particular, are crucial contributors to the glucocorticoid-mediated feedback control of the HPA axis. Specifically, hippocampal MRs play a crucial role in mediating proactive feedback, influencing the maintenance of basal HPA activity, particularly during the nadir of the circadian rhythm. Upon the termination of a stressor, the hippocampus assumes a regulatory role, termed reactive feedback, modulating glucocorticoid concentrations. This regulatory mechanism comes into play as high concentrations of corticosteroids gradually saturate GRs, leading to a slow reduction and restoration of glucocorticoid levels to pre-stress levels (Dallman *et al.*, 1989; Jacobson & Sapolsky, 1991).

Studies have found that stimulation of the hippocampus can lower plasma corticosteroid levels in both mammals (Mandell *et al.*, 1963; Jacobson & Sapolsky 1991; Slusher & Hyde, 1961) and birds (Bouillé & Baylé, 1973). Conversely, in mammals, research has shown that damage to the hippocampus and complete hippocampectomy can potentially elevate CRH mRNA expression (Herman *et al.*, 1989) and plasma levels of corticosteroids (Magariños *et al.*, 1987; Sapolsky *et al.*, 1984) delaying the termination of the stress response (Knigge, 1961; Sapolsky *et al.*, 1984). Also in birds, hippocampal lesions have been observed to affect the circadian rhythm in CORT titres, with the titres remaining continuously at the highest level of the normal circadian rhythm (Bouillé & Baylé, 1973). Reciprocally, increased levels of stress hormones contribute to hippocampal dysfunction in both humans and rodents impairing various hippocampal-dependant memory tasks (Johnson *et al.*, 2022; Kim *et al.*, 2015).

While there is a considerable body of evidence supporting the role of the hippocampus in stress regulation, the complex mechanisms governing this association are still not fully understood, underscoring the need for additional exploration.

### *1.3.3.3.    Functional organization of the hippocampus*

The existence of both specialized functions in the hippocampus has been explained by the postulation of distinct functional domains along the longitudinal axis of the hippocampus where different parts of the hippocampus are responsible for different functions.

The long axis of the hippocampal formation, known as the septotemporal axis, extends from the septal nuclei of the basal forebrain to the temporal regions of the brain. Under this framework, the hippocampus comprises a dorsal region, identified as the posterior hippocampus in primates, which corresponds to the first 50% of the hippocampal volume from the septal pole; and a ventral region, recognized as the anterior hippocampus in primates, constituting the initial

50% of the hippocampal volume from the temporal pole (Bannerman *et al.*, 2004; Zhang *et al.*, 2004) (Figure 1.8).
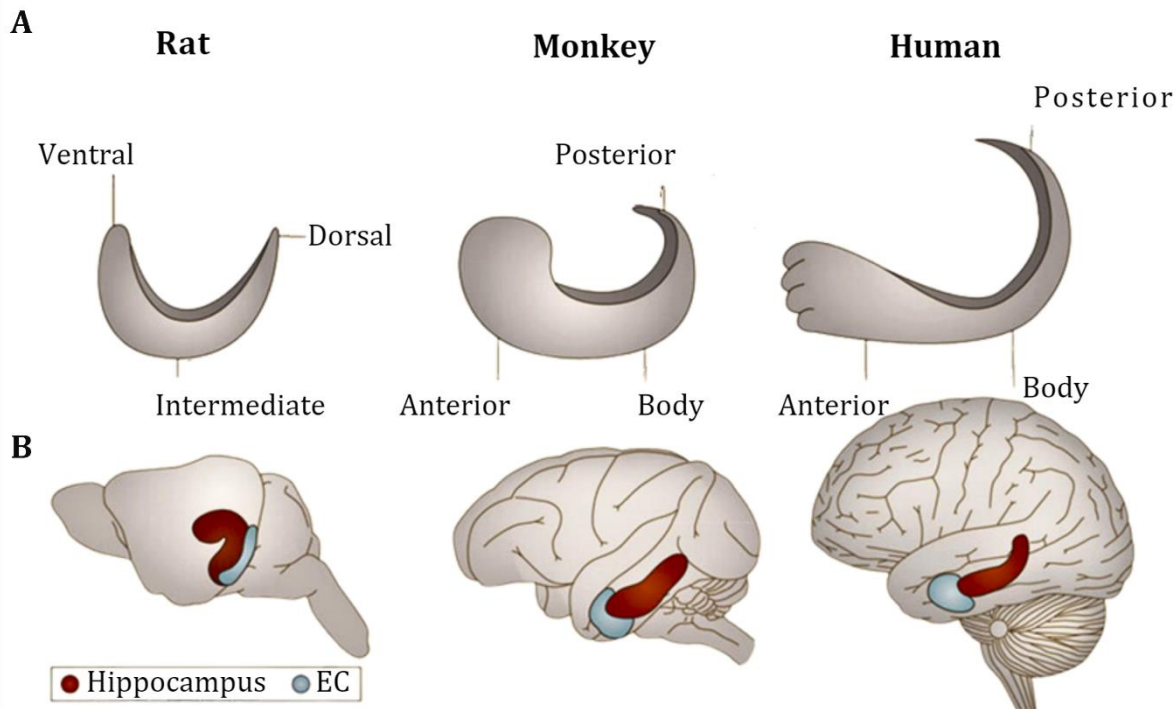


**Figure 1. 8.** (A) Schematic illustrations of the orientation of the hippocampal longitudinal axis in mammals including rats, macaque monkeys, and humans. In rodents, the orientation is described as septotemporal, while in primates, including humans and macaque monkeys, it is termed anteroposterior (alternatively referred to as rostrocaudal in non-human primates). (B) The position of the hippocampus is highlighted in red and the entorhinal cortex (EC), crucial for hippocampal function, is depicted in blue. Modified from Strange *et al.* (2014) with permission from Springer Nature under license number 1529882.

In this context, the hippocampus can be viewed as a composite structure with a separate septal/dorsal/posterior zone responsible for cognitive functions and another temporal/ventral/anterior zone associated with emotional aspects. This segmentation finds support through evidence from gene expression, behavioural studies, and connectivity analyses.

In the DG, the expression of two genes, *Lct* and *Trhr* genes, exhibits preferential localization. Specifically, *Lct* is predominantly expressed in the septal one-third, while *Trhr* is preferentially expressed in the temporal one-third of the DG (Fanselow & Dong, 2010). Multiple segregated molecular subdomains, each containing a unique complement of expressed genes, have been proposed by other studies suggesting that the longitudinal axis of the hippocampus may not be simplified into only two distinct portions (Strange *et al.*, 2014).

Anatomical investigations also suggest that the input and output connections of the septal hippocampus and temporal hippocampus exhibit distinct patterns. In rats, most prominent projections of the septal CA1 and the septal parts of the subicular complex project to the retrosplenial and anterior cingulated cortices, areas that mediate cognitive processes such as

learning, memory, navigation, and exploration; while the temporal hippocampus is in an ideal situation to regulate the impact of emotional experiences and to control general affective states exhibiting bidirectional connectivity with the infralimbic, prelimbic, and agranular insular cortices including the medial and central amygdalar nuclei, and BST (Fanselow & Dong, 2010).

 Additionally, studies by Moser and colleagues (1995) indicated that spatial memory is more reliant on the septal hippocampus rather than the temporal hippocampus with lesions affecting as little as 25% of the septal hippocampus resulting in an impaired acquisition of spatial memory in tasks such as the water maze. Interestingly, additional damage to the temporal region does not exacerbate the deficit. Similar findings have been replicated in comparable studies, consistently supporting the notion that spatial memory is primarily associated with the septal hippocampus (Ferbinteanu & McDonald, 2001; Pothuizen *et al.*, 2004).

However, the impact of manipulations of the temporal hippocampus on the regulation of emotional responses may be somewhat less straightforward, with fewer behavioural studies directly supporting its crucial role in stress responses over cognition, some examples do exist. Notably, in Henke's research (1990), compelling evidence was presented. According to this study, lesions specifically targeted at the temporal hippocampus, in contrast to the septal hippocampus, had a significant impact on stress responses and emotional behaviour enhancing cold/restraint stress ulcers.

Thus, the evolutionary conservation of the hippocampus supports the existence of a similar functional differentiation in the avian HF with distinct subregions contributing to spatial cognition and emotional processing (Smulders, 2017). In fact, some studies in birds have demonstrated increased neuronal activation in the caudal HF in response to both acute and chronic stress, as measured by FOS immunoreactivity and markers of long-term neuronal activation such as Δ*FosB* (Zanette *et al.*, 2019). However, the precise functional mechanisms and anatomical hippocampal subregions implicated in this response remain unknown.

### 1.3.4. *Hippocampal plasticity*

Stress has been found to impact both the structure and function of the hippocampus (Dranovsky & Hen, 2006). One particular aspect of this influence is neurogenesis, a multistep process involving the proliferation, migration, and differentiation of new neurons (Barnea & Pravosudov, 2011). While neurogenesis naturally decreases regularly and gradually as individuals transition into adulthood (He & Crews, 2007), stress-induced suppression of cell proliferation appears to occur throughout most of the postnatal life affecting the early postnatal period and adulthood in similar intensity (Mirescu & Gould, 2006).

Research conducted on rats has shown that prolonged exposure to chronic restraint stress leads to a decrease in hippocampal volume compared to its size prior to the stressor (Lee *et al.*, 2009). This reduction is associated with a decline in the number of dendritic spines and branches

of pyramidal neurons in the CA3 region (Conrad *et al.*, 1999), and a suppression in the generation of new granule neurons in the DG (Schoenfeld & Gould, 2012). These structural alterations are accompanied by impairments in spatial navigation and episodic memory, as evidenced by deficits observed in various studies (Kim & Diamond, 2002; Vyas *et al.*, 2002).

Furthermore, in humans, decreased hippocampal volumes and hippocampal dysfunction are associated with psychological disorders such as post-traumatic stress disorder, bipolar disorder, and depression (Bonne *et al.*, 2008, Frey *et al.*, 2007). Notably, pharmacological treatments addressing these disorders often target hippocampal function and physiology for their effectiveness. For instance, antidepressant treatment increases cell proliferation in the mammalian temporal DG (Banasr *et al.*, 2006).

The impact of stressors on hippocampal neurogenesis is not restricted to mammals. Previous research shows that environmental stressors such as captivity affect hippocampal neurogenesis in wild-caught birds such as mountain chickadees (*Poecile gambeli*) (LaDage *et al.*, 2009) and adult black-capped chickadees (*Poecile atricapilla*) (Tarr *et al.*, 2009). Social subordination, associated with social stress, also reduces hippocampal cell proliferation in food-caching mountain chickadees (Pravosudov & Omanska, 2004) and social isolation reduces the recruitment of new neurons in the HF of zebra finches when compared to communally housed birds (Barnea *et al.*, 2006).

Likewise, chronic exposure to unpredictable mild stressors (e.g., temperature, chasing, wind, wet litter, and nest box removal) reduces adult hippocampal neurogenesis in layer hens, particularly in the caudal pole of the HF (Gualtieri *et al.*, 2019), while chronic food restriction reduces the number of newly generated neurons in the hippocampus in broiler breeder chickens, as evidenced by a lower density of cells expressing proliferation markers (Robertson *et al.*, 2017). And yet, few investigations have focused on whether changes in neurogenesis and the regulation of the stress response are associated with regional specialization of the hippocampus in birds.

For this reason, additional research on the avian HF in animal models of stress is necessary before a consensus about the caudal pole and other subregional specializations of this structure are reached and the homologies between mammalian and avian HF are clarified.

## 1.4. Project's Rationale

As reviewed here, the avian hippocampus has a unique neuroanatomy, sharing distinct functional and connectional properties with the mammalian hippocampus. One of these properties is their involvement in the regulation of the stress response. Therefore, it is important to investigate the rostrocaudal and subdivisional distribution of involvement in the stress response as well as the complex neural circuits involved in the communication between the HF and the PVN. By understanding the neural mechanisms underlying stress regulation in the avian brain, we can gain insights into the general principles governing the evolution of the hippocampus

26

and the conservation of its functions across vertebrates. In addition, this research can advance our understanding of the neurobiology of stress regulation in birds.

For this reason, this study aims to extend the understanding of the avian HPA axis functioning and to shed light on the role of the hippocampus in the regulation of stress in birds. Broadly speaking, there are two major research enquiries 1) What is the hippocampal region participating in the regulation of the stress response in birds? and 2) How does the avian HF communicate with the PVN?

Specifically, it aims to identify which hippocampal subdivision is involved in the feedback regulation of the HPA axis through the mapping of the expression of the immediate early gene (IEG) FOS in response to acute stress. Chapter 2 describes an exploratory study employing immunohistochemical methods to detect protein FOS expression and map the subdivisions of the HF activated by acute stress, and Chapter 3 addresses the issues encountered in Chapter 2 while incorporating the measurement of *FOS* gene expression. Finally, Chapter 4 explores the configuration of the fibre connections between the hippocampal formation and the hypothalamic PVN contributing to the negative feedback control over the HPA axis.

# Chapter 2. Immunohistochemical Analysis of FOS Induction and HPA-Axis Activation in Adult Hens Under Restraint Stress

## 2.1. Introduction

Stress can lead to significant physiological and behavioural changes in animals. Acute exposure to stress leads to activation of the Hypothalamic-Pituitary-Adrenal (HPA) axis leading to the release of glucocorticoids, which play a vital role in regulating the stress response through a negative feedback system (Chrousos, 2009; De Kloet *et al.*, 2005; Keller-Wood, 2011; Vandenborne *et al.*, 2005).

Immediate-early genes (IEGs) have been used to study transiently induced changes in the central nervous system (CNS) in response to a wide variety of transsynaptic stimuli by regulating initial genetic events that eventually lead to long-term functional changes. This family of genes includes *FOS, FRA-1*, *FRA-2*, *FOS-B* (Long), *FOS-B* (Short), *C-JUN*, *JUN-B*, *JUN-D*, *KROX-20*, and *KROX-24* (also known as *ZIF 268*, *NGFI-A*, *EGR-1*, or *ZENK*) (Sheng & Greenberg, 1990; Morgan & Curran, 1991; Sadananda & Bischof, 2004).

Various forms of stress lead to increased expression of lEGs within the brain (Ceccatelli *et al.*, 1989). The IEG FOS is a well-established marker of neuronal activation, normally, basal FOS levels in naive animals are low (Herdegen & Leah, 1998). In response to stress, mapping its activation can provide valuable insights into the brain regions involved in the stress response.

Stress-related studies have identified a stressor-associated increase in IEG expression within several brain regions in both mammals (Coveñas *et al.*, 1993; Honkaniemi, 1992) and birds (Jaccoby *et al.*, 1999; Løtvedt *et al.*, 2017). For example, in rats, FOS expression is upregulated after forced swim and restraint stress treatments in the hippocampal formation (HF), the hypothalamus, and within the medial and cortical nuclei of the amygdaloid complex (Cullinan *et al.*, 1995).

While the induction of *FOS* gene expression in the hippocampus has been well-documented in numerous acute stress induction studies involving mammals (Chowdhury *et al.*, 2000; Hansson *et al.*, 2003; Melia *et al.*, 1994; Ryabinin *et al.*, 1999), this phenomenon remains relatively unexplored in birds.

Unlike the mammalian hippocampus, the avian hippocampal formation (HF) is characterized by poorly defined boundaries making it difficult to establish a clear subdivisional nomenclature. As anatomical approaches and techniques have evolved, so has our understanding of the anatomy and nomenclature of the avian hippocampus. Early attempts to establish subdivisional homologies in the avian hippocampus relied primarily on immunohistochemical studies using cytoarchitecture or the distribution of neurochemical markers as landmarks (Erichsen *et al.*, 1991; Karten & Hodos, 1967; Krebs *et al.*, 1991).

Although several studies have attempted to identify avian hippocampal subdivisions, no clear consensus has been reached. The avian HF was first proposed to be subdivided into two major subdivisions, a hippocampus proper (Hp) and an area parahippocampalis (APH) (previously referred to as the accessory hyperstriatum in Karten & Hodos, 1967). This scheme heavily influenced early studies on the connectivity and functional properties of the avian hippocampus including research into the role of the avian hippocampus in stress regulation (Benowitz & Karten, 1976; Bouillé & Baylé 1973, 1976; Bouillé *et al.*, 1977; Krayniak & Siegel, 1978).

Currently, the most influential subdivisional scheme subdivides the avian hippocampus into three main subdivisions: dorsolateral (DL), dorsomedial (DM), and ventral (V). For Atoji and Wild, these three main subdivisions can be further subdivided. Within the ventral region or the V-complex lies a triangular area (Tr) bounded by adjacent ventromedial (Vm) and ventrolateral (Vl) dense cell layers. The DL is further divided into a dorsal (DLd) and ventral (DLv) portion, while the DM is divided into a dorsal (DMd) and ventral (DMv) portion (see Figure 1.3, Atoji & Wild, 2004, 2006). This subdivisional framework has received support from more recent findings analysing the distribution of several (11) neurotransmitter receptors (Herold *et al.*, 2014).

Evidence suggests that different parts of the hippocampus have different functions. Notably, in response to social stress, the DL subdivision of the HF of chicks exhibits robust activation, as evidenced by the extensive FOS immunoreactivity spanning from the rostral to the caudal HF (Takeuchi *et al.*, 1996).

In mammals, the septal hippocampus (posterior in primates) appears to be more involved in cognitive functions such as spatial memory. In contrast, the temporal hippocampus (anterior in primates) appears more related to regulating emotion, including the stress response (Fanselow & Dong, 2010). Recent literature suggests that the rostral portion of the avian hippocampus is equivalent to the septal hippocampus in rodents, while the caudal portion of the avian hippocampus is equivalent to the temporal hippocampus in rodents, if so, these regions in avian species may perform similar functions to their mammalian counterparts (Smulders, 2017, Smulders, 2021).

Beyond hippocampal activation, previous research has demonstrated an upregulation in the expression of FOS in the paraventricular nucleus (PVN) of the hypothalamus in response to stressors (Pace *et al.*, 2005). As already reviewed in the previous chapter, in response to stress, the HPA axis becomes activated culminating in the release of glucocorticoids that modulate various physiological processes. In both birds and mammals, the PVN is recognized for its role in orchestrating the glucocorticoid activity of the stress response as a pivotal component of the HPA axis. The PVN synthesizes two critical adrenocorticotropic hormone (ACTH) releasing factors, corticotrophin-releasing hormone (CRH), and arginine vasopressin (AVP) or arginine vasotocin (AVT) in birds, which play a fundamental role in the stress response (Cornett *et al.*, 2013).

Recently, another structure, the nucleus of the hippocampal commissure (NHpC) has emerged as a distinctive and significant player in the regulation of stress responses in birds. This nucleus, housing CRH neurons, has been implicated in the early stages of the avian stress response. For example, nutritional stress in birds results in CRH gene expression in the NHpC and in the PVN suggesting a role of the NHpC in the regulation of the anterior pituitary proopiomelanocortin (POMC) and the subsequent production of corticosterone (CORT) (Kadhim *et al.*, 2019). Notably, the temporal activation of the NHpC precedes that of the PVN suggesting a crucial role in initiating the stress response cascade, possibly influencing downstream components (Nagarajan *et al.*, 2017a; Kadhim *et al.*, 2019).

In addition, the avian amygdala, like its mammalian counterpart, is involved in the regulation of emotional responses. The bed nucleus of the stria *terminalis* (BST) is recognized as a key component of the extended amygdala, and its lateral (BSTL) and medial (BSTM) divisions exhibit distinct functional roles. The BSTM is part of the medial extended amygdala (MEA) and is implicated in social behaviour and sexual motivation, while the BSTL is considered part of the central extended amygdala (CEA) and is primarily associated with the regulation of anticipatory stress responses (Goodson, 2008; Martínez-García *et al.*, 2008; Medina *et al.*, 2017).

Moreover, previous findings underscore the crucial role of the molecular responses in the pituitary gland during stress in birds. For instance, in response to immobilization stress, chickens exhibit significant changes in pituitary POMC heteronuclear RNA. The cleavage of the POMC prohormone protein results in the production of ACTH, which activates adrenal production of the stress hormone CORT (Jayanthi *et al.*, 2014; Kuenzel *et al.*, 2013; Selvam *et al.*, 2013).

The aim of this study is a better understanding of the anatomical organization of hippocampal functions, in particular its role in the regulation of the stress response. By investigating FOS protein induction and HPA-axis activation in adult hens subjected to restraint stress, the goal is to observe the activation of stress-related areas such as the PVN, BSTL, and NHpC, and to pinpoint the anatomical region responsible for negative feedback regulation of stress within the hippocampus at two levels: subdivision and rostrocaudal axis. The hypothesis is that, in response to acute stress, there will be an increase in FOS activation, particularly discernible within the caudal hippocampus, specifically targeting the DL subdivision.

## 2.2.    Methods

### 2.2.1.  *Animals and housing*

A total of 44 Dekalb White hens aged between 36-38 weeks were provided by The Lakes Free Range Egg Company (Penrith, UK). The initial group of birds, collected on January 14th, 2020, consisted of 34 birds, while a subsequent batch of 10 hens was collected on February 2nd, 2020. Among these, 4 birds were euthanized between January 14th and 24th due to health concerns: 2

birds exhibited head swelling, one had a severe wound in the foot with exposed bone, and the last one displayed immobility. An additional 2 birds were euthanized between February 7th and 8th; one had a prolapsed vent, and the other was flat and immobile without apparent signs of trauma. On March 3rd, an extra bird was euthanized due to comb wounds caused by pecking and repeated attacks by the other chickens. To address the issue of immobility in hens without trauma-related signs, dietary changes were introduced on March 2nd, 2020. These changes involved the addition of Layer Mash (Dodson & Horrell) and Layers Pellets (Farmgate) into the original diet (Poultry Grower from Special Diet Services) to reduce possible neurological problems related to nutrient imbalance, in particular calcium.

The birds were housed at the Comparative Biology Centre Animal Unit at Newcastle University in accordance with the Home Office code of practice. They were provided *ad libitum* food and water, as well as environmental enrichment materials such as nest boxes. Starting under the light/dark cycle conditions from the provider (14L: 10D cycle, with lights on at 06:00), animals gradually adjusted to their new environment. The adjustment period entailed daily shifts, commencing the day after their arrival and continuing until the 7th of February, during which the timing was shifted by 30 minutes each day. This culminated in a final dark phase starting at 13:00, while maintaining the same light-dark (L:D) ratio as before. The provider assisted with the shifting of the L: D cycle of the second batch of animals so they could integrate into the housing conditions of the first batch without imposing a sudden change in their conditions.

In the week preceding the initiation of the experimental phase, animals were familiarised with handling through positive reinforcement with mealworms (Livefoods Direct™, regular). Positive reinforcement was achieved by capturing and gently holding the birds followed by providing mealworms after placing them on the floor. By the end of the week, animals were actively approaching the experimenter, facilitating the process of handling them.

### *2.2.2. Environmental conditions*

To prevent the potential masking of the stress response due to natural daily fluctuations, all experiments were conducted during the dark phase of the circadian cycle. This approach was chosen because the circadian elevation in CORT secretion occurs before the activity (awake) period begins (Girotti et al., 2007). Experimental procedures started at 14:00 and were carried out under red light illumination.

The animal unit consisted of 4 rooms. Just prior to commencing the procedures, animals were evenly distributed across 2 rooms where they remained until the experiment's conclusion. The remaining 2 rooms were designated as follows: one for the stress induction and the other used for the dissection of the animals. All rooms were equipped with red light bulbs, however, the corridor connecting the rooms was not. Instead, the corridor lights were turned off each morning

before the start of the experimental procedures, and the safety lights were covered with translucent red acetate.

The stress induction room was equipped with a table. Pillowcases, used for restraining the birds, were positioned at opposite sides of the table, connected with a rope, and suspended with metal hooks. The rope was secured to the table with tape and the pillowcases were detachable from the hook. A string inside of the pillowcase facilitated its opening and closing.

The dissection room was used for the euthanasia and the dissection of the animals. It was equipped with the necessary materials to perform the UK Home Office Schedule 1 procedure. In all cases, the Schedule 1 method involved an overdose of sodium pentobarbital (Euthatal, approx. 2 ml per bird) administered intravenously in the brachial vein following intramuscular (*pectoralis* muscle) injection of anaesthesia with a combination of Ketamine (40 mg/Kg) /Xylazine (8 mg/Kg), in accordance with the dosage guidelines provided by the veterinarian.

Control over the lighting conditions both inside and outside of the rooms allowed for the easy transfer of the animals between rooms. Consequently, no boxes or additional equipment were used to transport the animals between the different rooms.

### 2.2.3. Stress induction

In the stress induction experiment, two distinct outcome measures were analysed: first, the identification of FOS expression within brain regions of interest through tissue dissections, and second, the assessment of temporal variations in the circulating CORT levels through blood sampling.

For this, the experiment involved a total of 32 animals. These animals were chosen randomly and allocated into 4 treatment groups (Figure 2.1), as follows:

Group A (n= 8) - The bird was taken from the pen and transferred to the stress induction room where a blood sample was taken. After this, the animal was immediately weighed and euthanized (around 16:00) using the Schedule 1 method mentioned above.

Group B (n= 8) - The bird was taken from the pen and transferred to the stress induction room where a blood sample was taken. Then, the bird was put inside one pillowcase and left hanging for 30 minutes to induce the stress response. After the completion of the stress period, a second blood sample was collected. The animal was temporarily identified by attaching a small piece of electrical tape to its back before returning to the flock. After 60 minutes, the bird was transferred back to the stress room where the last blood sample was taken. Finally, the animal was euthanized in the dissection room using the Schedule 1 method mentioned above.

Group C (n= 8) - The bird was taken from the pen and transferred to the stress induction room where a blood sample was taken. Then, the bird was put inside the pillowcase and left hanging for 30 minutes to induce the stress response. After the completion of the stress period, a second blood sample was collected. The animal was temporarily identified by attaching a small

piece of electrical tape to its back before returning to the flock. After 30 minutes, the marked bird was transferred back to the stress room where the last blood sample was taken.  Finally, the electrical tape was removed, and the animal was marked in the back feathers with a commercial dark non-toxic marker, weighed, and transferred back to the pen where it was left undisturbed until rehoming.

Group D (n= 8) - The bird was taken from the pen and transferred to the stress induction room where a blood sample was taken. Then, the bird was put inside the pillowcase and left to hang in there for 30 minutes to induce the stress response. After the completion of the stress period, a second blood sample was collected. The animal was temporarily identified by attaching a small piece of electrical tape to its back before returning to the flock. After 90 minutes, the marked bird was transferred back to the stress room where the last blood sample was taken. Finally, the electrical tape was removed, and the animal was marked in the back feathers with a commercial dark non-toxic marker, weighed, and transferred back to the pen where it was left undisturbed until rehoming.
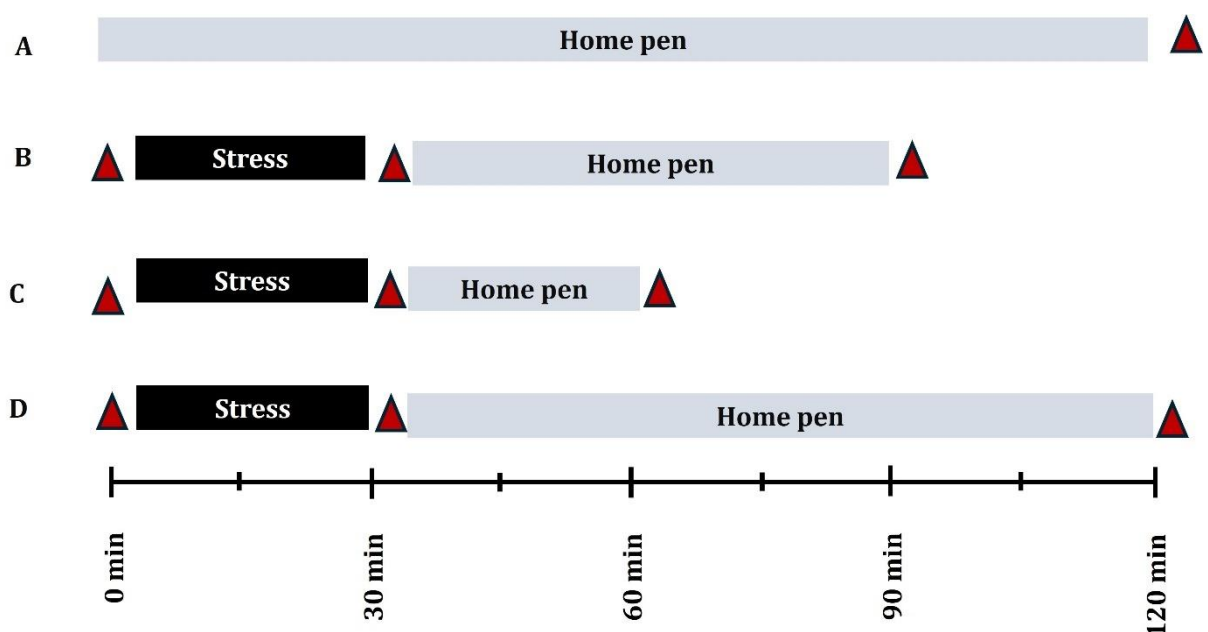


**Figure 2. 1**. Overview of the experimental groups. Timelines for each group and blood sampling (red triangles) times are shown in the figure. Birds in Group A (n=8) had a blood sample taken, were weighed, and immediately euthanized. Group B (n=8) birds had a blood sample taken and 30 minutes of stress followed by a second sample, then a final sample after 60 minutes before euthanasia. Group C (n=8) followed the same steps, with the final sample after 30 minutes, then marked, weighed, and returned to the home pen. Group D (n=8) had the final sample at 90 minutes, then marked, weighed, and returned to the home pen.

### 2.2.4.   Tissue sample collection

Birds from groups A and B were euthanized following the previously described methods. Subsequently, the brain was removed from the skull and immediately preserved by embedding it

in an Optimal Cutting Temperature (OCT) compound and dry ice. The frozen brains were stored at -80 ˚C until use for FOS staining.

Pituitary glands were also dissected. These were placed in 2 ml vials containing 1 ml of RNAlater (Sigma Life Science). Samples were left at -4 ˚C overnight and up to 48h to allow the RNAlater to thoroughly penetrate the tissue before storing at -80 ˚C until used for gene expression analysis.

### 2.2.5. Blood sampling

Blood samples were obtained within 3 min of entering the housing room. The samples were extracted from the medial metatarsal (leg) vein using capillary tubes with a maximum volume of 200 μl. Approximately 2 to 3 heparinized capillary tubes measuring 75mm (Hawksley) were used. The vein was punctured using a small sterile needle (23 G LUER 6% needles, Agani™). When compared to the brachial wing vein, blood collection from the medial metatarsal vein has less risk of hematoma formation.

The collected blood was transferred into 1.5 ml Eppendorf tubes and placed on wet ice until centrifugation. The samples were centrifuged for 15 min at 3000 rpm to separate plasma from blood cells.

The plasma, once separated, was collected and stored at -80 ˚C until use for ELISA CORT analysis.

### 2.2.6. ELISA on plasma CORT levels

Plasma CORT levels were determined using the Corticosterone ELISA kit from Enzo Life Sciences (ADI-900-097-96 well kit) following the protocol outlined in Gualtieri *et al.* (2019).

Plasma samples were thawed, and a five-point standard curve was generated using the supplied CORT (200,000 pg/ml), with the following concentrations: 20000, 4000, 800, 160, and 32 pg/ml. Samples were prepared by adding 10 μl of the sample (1:40 dilution), 10 μl of 1:100 steroid displacement reagent (SDR), and 380 μl of ELISA assay buffer.

In the initial incubation, the plate was left at room temperature (RT) for 2 hours in a microplate shaker at 500 rpm. This step involved the alkaline phosphatase conjugated with corticosterone and sheep polyclonal antibody to corticosterone. Following this incubation, the contents of the plate were emptied, and the wells were washed 3 times.

For the subsequent incubation with p-Npp substrate solution, the plate was incubated at RT for 1 hour without agitation. After the addition of the stop solution, the optical density was immediately measured with an Infinite® 200PRO plate reader (TECAN) at 405 nm, with correction between 570 and 590 nm according to the manufacturer's instructions. Values for each plate were then analysed with My Assays software (Brighton, UK), employing a ready-to-use Excel macro designed for the specific ELISA assay.

To ensure consistency and mitigate plate-to-plate variability affecting within-bird comparisons, three samples from the same animal were simultaneously processed on a single 96-well plate. Additionally, samples from different groups of animals (treatments) were evenly distributed across 3 plates and measured in duplicates. Furthermore, samples from various animals (n=5) were combined into pooled samples of high and low CORT responders (HR and LR, respectively), which were used across plates to standardize the data and account for any plate-specific variations. The values obtained from the pooled samples were averaged and a correction factor was obtained by calculating the ratio of the mean value of the pooled samples between plates. The correction factor obtained was 1.73 and it was applied uniformly to all data points from Plate 3 which were considerably higher than values in Plate 1 and 2. This measure was applied accounting for any variations due to the handling of the samples across plates and mitigating plate-specific effects.

### 2.2.7. *Quantitative real-time PCR*

The following procedures (RNA extraction, retro transcription, and qPCR) were carried out by Dr Timothy Boswell who prepared the samples and collected the data. RNA was extracted from the entire pituitary gland tissue obtained during the tissue sample collection. RNA extraction was performed using TRIsure reagent (Meridian Bioscience) and a Precellys Evolution homogenizer (Cambridge instruments) with Zymo Research Bashing Beads and a Zymo Direct-zol kit with in-column DNAse treatment (Cambridge Bioscience). Reverse transcription was carried out using 1µg RNA and a Tetro cDNA synthesis kit (Meridian Bioscience) as per the manufacturer's guidelines. The generated cDNA was subsequently diluted 1.7 x before use in qPCR.

Quantification of mRNA levels was performed through qPCR, employing primers for the target genes: Proopiomelanocortin (*POMC*) Forward: 5- ATTTTACGCTTCCATTTCGC; Reverse: 5-AATGGCTCATCACGTACTTGC; vasotocin 2 receptor (*VT2R*) now renamed vasopressor receptor 1B (*AVPR1B*)  Forward: 5-CTTCAGCATGCAGATGTGGT; Reverse: 5-AACATGTAGATGCAGGGGTTG; vasotocin 4 receptor (*VT4R*) now renamed vasopressor receptor 1A (*AVPR1A*) Forward: 5-GGTTGCAGTGTTTTCAGAGTCG; Reverse: 5-CAAGATCCGCACCGTCAAG; corticotrophin-releasing hormone receptor 1 (*CRHR1*) Forward: 5-CCCTGCCCCGAGTATTTCTA; Reverse: 5-CTTGCTCCTCTTCTCCTCACTG and corticotrophin-releasing hormone receptor 2 (*CRHR2*) Forward: 5- GCAGTCTTTTCAGGGTTTCTTTG; Reverse: 5-CGGTGCCATCTTTTCCTGG (Kuenzel *et al.*, 2013).

A reference gene, Lamin B receptor (*LBR*), was used for normalisation. It was amplified by forward primer 5′-GGTGTGGGTTCCATTTGTCTACA and reverse primer 5′-CTGCAACCGGCCAAGAAA (Dunn *et al.*, 2013).

DNA standards were produced for absolute quantification through end-point PCR on pituitary cDNA for each gene. The resulting products were purified from a gel using the QiaQuick

gel extraction kit (QIAGEN) in accordance with the manufacturer's protocol. Standard concentrations were determined using a NanoDrop spectrophotometer (Thermo Fisher Scientific). Serial dilutions of the standards were produced beginning with a 1:100 dilution followed by 5-fold dilutions.

Real-time qPCR was run using the MIC qPCR cycler (Biomolecular Systems, UK) with an initial step of 95°C for 5 min, followed by 40 cycles of 95°C for 5 seconds, 60°C for 20 seconds and 72°C for 10 seconds. Reactions mixtures included 4μl cDNA, 5μl SYBR mix (No-ROX kit, Bioline, London, UK), and 0.5μl of 10 μM of each forward and reverse primer, making a final volume of 10μl and a final primer concentration of 500 nM. For the no-template control, 4μl of cDNA was substituted for sterile water. Both the standard curve and samples were run in singlicates within an assay run. A melting curve analysis was performed to verify reaction specificity.

The results were evaluated as the ratio of the target gene expression to that of the reference gene *LBR* in the same individual samples.

### 2.2.8. Immunohistochemistry

The extracted brains (n=16) were sectioned (12 μm thick) using the cryostat at -20 ˚C. These sections were then placed onto positively charged slides (Thermo Scientific™ SuperFrost Plus™ Adhesion slides) in sets of 10 series, with each slide containing 3 to 4 sections. Sets of slides were stored in a -80 ˚C freezer until use for immunohistochemical staining.

To detect FOS, tissue sections from one set of slides underwent a brief fixation using 4% paraformaldehyde (PFA)/0.1 M phosphate buffer saline (PBS) for 10 min. Following fixation, the slides were treated with 1% hydrogen peroxidase for 30 min to inhibit endogenous peroxidase activity. Subsequently, they were rinsed twice for 5 minutes each with 0.1 M PBS.

Next, the slides were placed in bovine serum albumin (BSA)-blocking solution containing 0.1 PBS/0.3% Triton X-100 mix (PBSx) and 2% goat serum for 60 min. After the incubation period, the blocking solution was removed by gently tapping the slides on a paper towel. The slides were then rinsed 3 times for 5 min each with 0.1 M PBS. As a last step on the first day of the procedure, the slides were incubated overnight at RT with the primary antibody solution (FOS mouse monoclonal IgG Santa Cruz Biotechnology-166940) that was diluted at 1:250.

On the following day, slides were rinsed 2 times for 5 min each with 0.1 M PBS and incubated for 120 min at RT with the secondary antibody (Biotinylated Antimouse raised in goat-9200 Vector labs) at a dilution of 1:200. Afterwards, slides were rinsed 2 times for 5 min each with 0.1 M PBS before undergoing enzyme-conjugation with horseradish streptavidin (Vector Labs, SA-5004) at a 1:250 dilution using PBSx for 60 min at RT. The peroxidase reaction was visualized after a 5 min incubation in the chromogen 1,3[1]- Diaminobenzidine (Sigmafast tablets: 1 silver tablet (0.7 mg/ml DAB) + 1 golden tablet (0.67 mg/ml Urea Hydrogen Peroxide) in 30 ml ultrapure

H$_2$O). Finally, slides were rinsed by 3 consecutive distilled water immersions of 1 min each and left to dry overnight.

Following immersion in Histoclear I and II for five minutes each, slides were mounted using EUKITT® mounting medium (Orsatec, USA) and left to dry overnight before being ready for observation under the microscope (Figure 2.2).
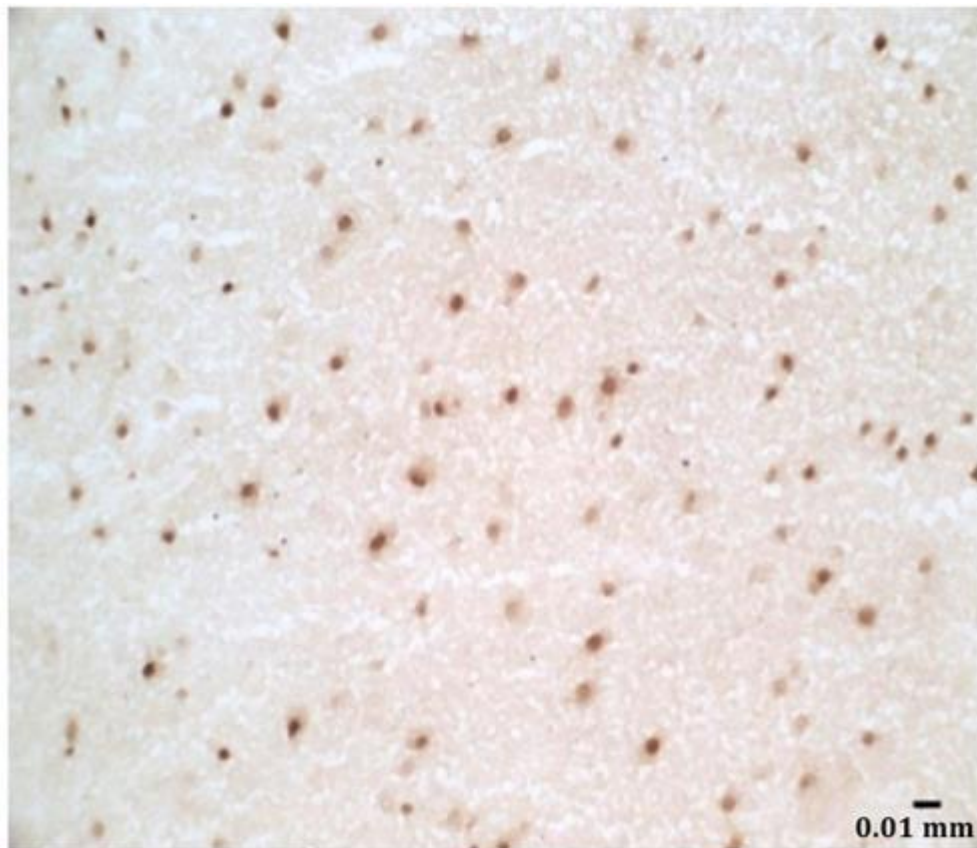


**Figure 2. 2**. (A) Example of immunohistochemical (IHC) FOS staining of avian hippocampal tissue. DAB staining results in dark FOS-positive nuclei (20x magnification).

### 2.2.9.  Image processing

Images from the designated regions of interest (ROI) were captured with the researcher blind to the subject's conditions. The analysed ROI comprised the V, DM, and DL subdivisions of the avian hippocampus at 4 different rostrocaudal levels (caudal-most=CM, caudal=C, rostral=R, and rostral-most=RM), the BSTL, the PVN, and the NHpC (Figure 2.3).
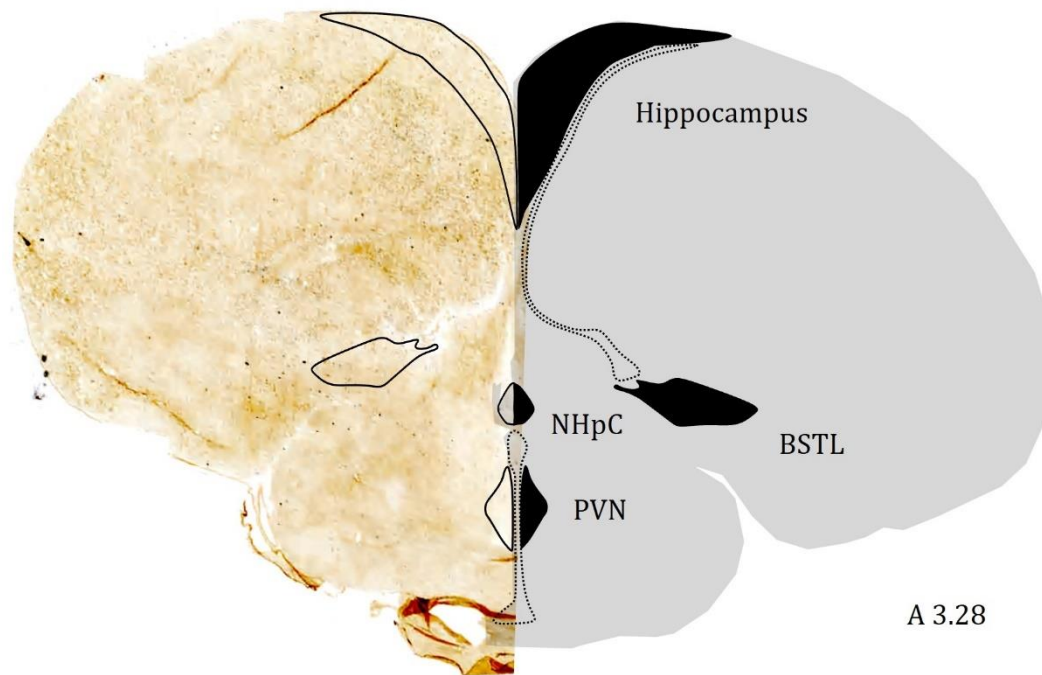
**Figure 2. 3**. Overview of the regions of interest. The approximate location of the hippocampus, bed nucleus stria *terminalis lateralis* (BSTL), the paraventricular nucleus of the hypothalamus (PVN), and the nucleus of the hippocampal commissure (NHpC) are shown. A indicates the approximate anteroposterior position described in the chick brain atlas by Puelles *et al*. (2007).

After staining, images from the slides containing the hippocampal ROI were captured using a Leica microscope with an objective magnification of 40× which was linked to a digital camera (Optronics, MicroFire™) and a computer installed with Stereo Investigator software (version 2019, MBF Bioscience, USA). To ensure unbiased sampling, captured frames were randomly positioned within the regions of interest, maintaining a minimum distance of 712.5 µm to the frame's borders. Only one section per ROI (CM, C, R, and RM) was photographed from each of the left and right brain hemispheres. The images were captured by delineating the HF into three subregions: V, DM, and DL, based on their shape and anatomical landmarks (Figure 2.4). Each of these subregions' images was assessed individually.
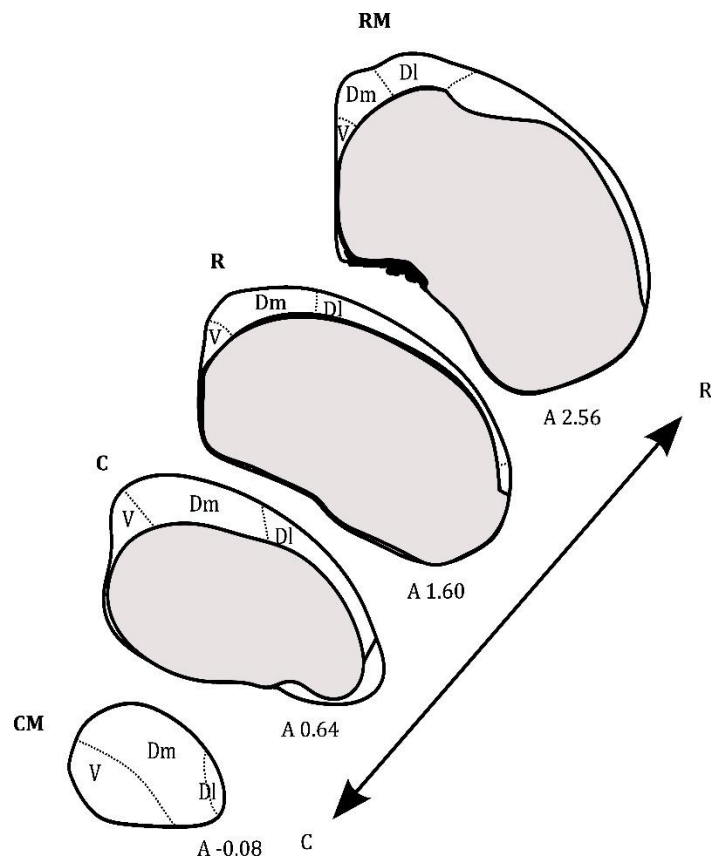
**Figure 2. 4**. Hippocampal regions of interest. The image shows the selection of the coronal sections along the longitudinal axis, sections belonging to either caudal-most (CM), caudal(C), rostral (R), or rostral-most (RM) levels. Sections were portioned into ventral (V), dorsomedial (Dm) and dorsolateral (Dl) regions of interest. A indicates the approximate anteroposterior position described in the chick brain atlas by Puelles *et al.* (2007).

Furthermore, whole tissue images were obtained by slide scanning in the ZEISS Axioscan 7 with a 10x magnification and the BSTL, NHpC and PVN were directly analysed from these scans.

The analysis of PVN and BSTL was like that of the hippocampus and involved the capture of images from both hemispheres using the Leica microscope. Due to its compact size and position, the NHpC analysis omitted interhemispheric differences and was conducted directly from the whole tissue scanned images.

### 2.2.10. Cell quantification

The quantification of FOS-ir cells was performed using QuPath version 0.3.2 (University of Edinburgh, UK). Cell identification was executed using the cell detection command with optical density (OD) sum analysis of nuclear staining (accessed via Analyse ‣ Cell analysis ‣ Positive cell detection ‣ Detection image ‣ Optical density sum). After detection, an intensity threshold was determined using the measurements for the Nucleus: DAB OD mean histogram.

Fine adjustments were made to prevent the inclusion of fragmented nuclei and tissue debris. The minimum area was adjusted to 250 $px^2$, while sigma values were augmented from 1px to 4px (Figure 2.5).

39
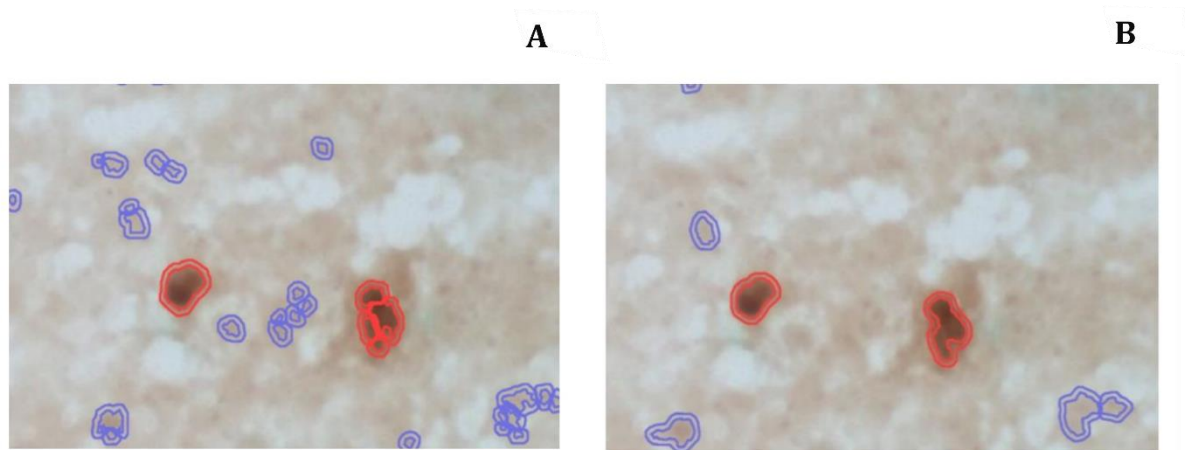
**Figure 2. 5**. Cell detection parameters. The image shows an example of a fragmented nucleus after cell detection (A) and an example of cell detection after the sigma nucleus parameter is increased from 1px to 4px (B).

Once detection was adequate, these same values were consistently applied across the entire analysis of the 16 brains. To streamline the process, images were processed in a batch using the workflow function (accessible through the Workflow tab ‣ Create workflow ‣ Create script).

Following the identification of positive cells, results tables were generated (via Measure ‣ Show annotation measurements), and the collected data was saved using Microsoft Excel.

### 2.2.10.1. Area measurements

Images acquired through the Leica microscope were processed using Image J (NIH, USA). The measurement of areas was executed using the measure function (accessed through Analyse ‣ Measure ‣ Area) after outlining the ROI via the wand (tracing) tool with the scale set to 4.027 pixels/microns for all ImageJ area measurements. After determining the area values for each individual image, the areas were aggregated to obtain the total area values for each subregion (V, DM, and DL) within each rostrocaudal section of the hippocampus per hemisphere.

For the NHpC, BSTL, and PVN, area values were directly extracted from the scanned tissue images using QuPath. The area value can be observed in the annotation details as $\mu m^2$ after selecting the region of interest using one of the area selection tools.

### 2.2.10.2. Density maps

Further analysis of the hippocampus involved the identification of high-density areas in whole-tissue sections using density maps. These density maps were generated through the cell detection command in QuPath version 0.3.2 (University of Edinburgh, UK), employing the same methodology as detailed earlier. Once positive cells were identified, local densities were computed using a Gaussian-weighed sum (accessed via Analyse ‣ Density maps ‣ Create density map) with a density radius of 300 µm.

Throughout the image analysis, consistency was maintained in terms of density radius and density type used.

### *2.2.10.3. Density analysis*

The FOS immunoreactive (FOS-ir) cell density is the outcome parameter generated to evaluate the occurrence of FOS-ir cells within selected tissue samples. This density is derived by the relation of 1) the sum of quantified FOS-ir cells within the ROI and 2) the cumulative area of the sampled tissue converted from square micrometres ($\mu m^2$) to square millimetres ($mm^2$).

$$\text{FOS density} = \frac{\sum \text{\# FOS} - \text{ir cells}}{\sum \dfrac{\text{Area in } \mu m^2}{1{,}000{,}000}}$$

### *2.2.11. Statistical analysis*

Prior to statistical analyses, the homogeneity of variances was assessed using Levene's test while a careful examination of the distribution of the normalised data was conducted using graphical methods, including histograms. These steps were crucial in validating the appropriateness of the chosen statistical analyses and ensuring the reliability of the results.

Normalisation of CORT concentration values was carried out by applying a logarithmic transformation (base 10) to the data after the correction factor application, as explained before. A paired-samples t-test was used as an initial analysis comparing baseline to just after stress induction to evaluate the effect of the stress induction treatment, and then a Two-way repeated measures ANOVA was employed to analyse the log-transformed data across different time points. For the Two-way repeated measures ANOVA, time was employed as the within-subjects factor.

For the analysis of the gene expression (qPCR) data, ratios obtained by dividing the expression level of each target gene by the expression level of the reference gene (*LBR*) were normalised using logarithmic transformation base 10. An independent-sample t-test was employed for the statistical analysis of the data. Original Ct values are provided in Annex 1.

$$Gene\ expression\ ratio = \log10\ (\frac{\text{Ct target gene}}{\text{Ct reference gene}})$$

The relationship between hippocampal longitudinal levels, subregions, hemispheres, and treatment in relation to the cell density was assessed using a Generalized Estimating Equations (GEE) model. The significance of the relationship was determined using P values derived from Wald's $\chi^2$ test statistics, while parameter estimates were obtained by a maximum likelihood approach. The analysis included one between-subject factor (treatment with 2 levels: stressed and

unstressed) and 3 within-subject factors (rostrocaudal position with 4 levels: CM, C, R, and RM; hemisphere with 2 levels: left and right; subregion with 3 levels: V, DM, and DL).

The analysis of the BSTL and PVN also involved a GEE model. This analysis included one between-subject factor (treatment with 2 levels: stressed and unstressed) and 1 within-subject factor (hemisphere with 2 levels: left and right). In the case of the NHpC, differences in activation between treatments were assessed using an independent-sample t-test.

All analyses were performed using IBM SPSS Statistics version 28.0 for Windows (IBM Corp., Armonk, N.Y., USA). For all tests conducted, statistical significance was accepted at $p < 0.05$.

## 2.3.  Results

### 2.3.1.  Corticosterone analysis

As an initial step, a paired samples t-test was conducted on log-transformed (base 10) data to determine the effect of the stress treatment. The results indicated a non-significant difference between the initial CORT levels before the stress treatment (M=0.813; SD=0.616), and the average CORT plasma concentration after 30 min of restraint stress (M=0.912; SD=0.662); $t_{(21)}$ = -1.620, p= 0.060, suggesting no effect of the stress treatment on CORT levels.

The main effect of time was further analysed by comparing CORT levels from plasma samples obtained at 30, 60 and 90 min after stress termination. The analysis of the log-transformed data indicated no statistical significance, $F_{(2, 18)}$ = 1.309, p=0.205. The interaction between the effects of time and treatment indicated that the fluctuation in means among the treatment groups remained consistent irrespective of time, $F_{(4, 36)}$ = 1.482, p=0.228.

Although the mean CORT concentration appeared to increase 30 min after the termination of the restraining treatment and to decrease after 60 and 90 min, the average CORT values between the groups were not statistically significant. The levels of plasma CORT showed no significant variance between 30 min and 60 min after stress termination (p=0.972), as well as between 30 and 90 min after stress termination (p=1). Similarly, the average CORT concentration exhibited no significant changes over time. Baseline CORT levels did not significantly differ from CORT concentrations after the stress treatment (p=0.375), or in the recovery phase after stress induction (p=1).

To understand the individual variations in CORT plasma concentrations, raw values were normalised by setting the baseline individual data to 100%. Following exposure to stress, most but not all the animals increased CORT plasma levels, for example, while case B.3 showed a substantial increase from baseline 100% to 383.91%, case B.4 showed a decrease from baseline 100% to 85.77%.  The variable response between individuals is observed also during recovery after stress induction, while some individuals exhibit a decline from the peak stress values (e.g., B.3: 383.91% to 60 minutes: 98.77%), others display further increases (e.g., B.2: 112.67% to 60

minutes: 123.08%). This variability highlights the individual responses to stress and recovery (Figure 2.6).
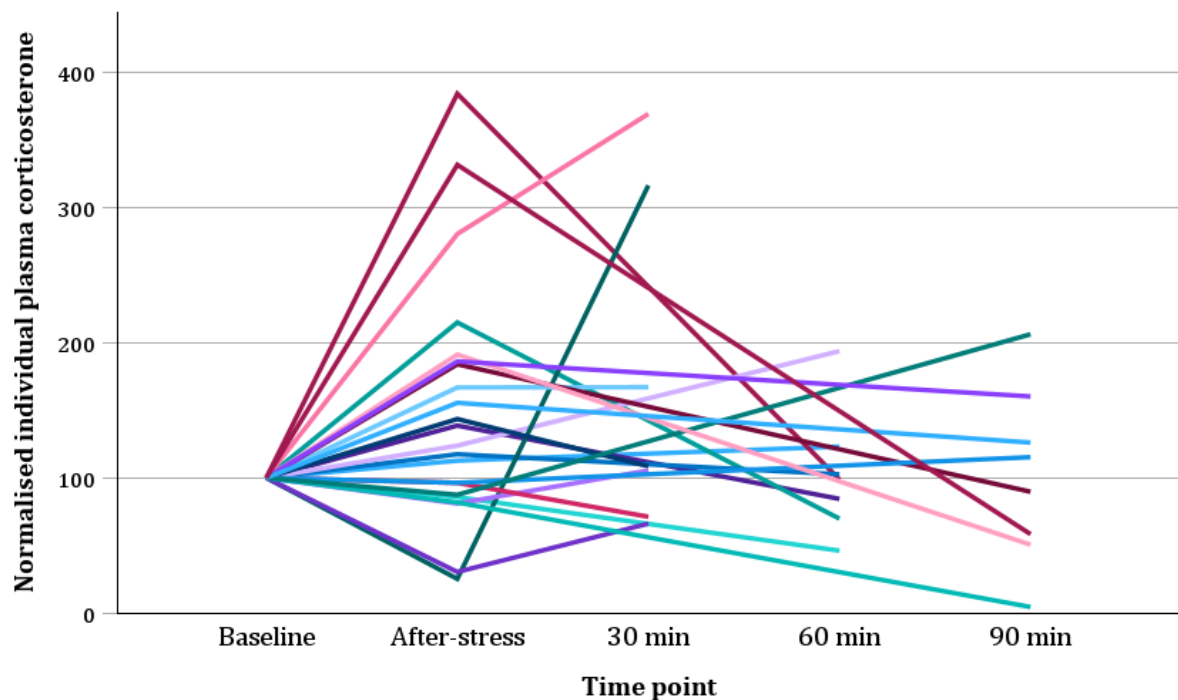


**Figure 2. 6**. Individual variations in corticosterone plasma levels. Corticosterone (CORT) values were normalised to a baseline of 100%, indicating diverse individual responses to stress. Each line in the graph represents the change in CORT levels for individual animals from baseline to measurements taken immediately after stress induction and at 30, 60, and 90 minutes post-induction. For each animal, CORT titers are expressed as a percentage of the baseline titer.

### 2.3.2. *Pituitary gene expression after acute stress*

The independent-samples t-test analysis of the log-transformed ratios obtained from the gene expression of the selected genes of interest (*POMC, CRHR1, CRHR2, AVPR1B*, and *AVPR1A*) between stressed and unstressed birds, revealed that the restraint treatment did not induce any changes in the expression levels of *POMC* ($t_{(14)}$= -0.960, p=0.353), *CRHR1* ($t_{(14)}$= 0.998, p=0.335), *CRHR2* ($t_{(14)}$= 0.599, p=0.559), *AVPR1B* ($t_{(14)}$= 0.981, p=0.343), or *AVPR1A* ($t_{(14)}$= 0.767, p=0.456) measured 90 min after stress induction in stressed birds and compared to unstressed birds (Figure 2.7).
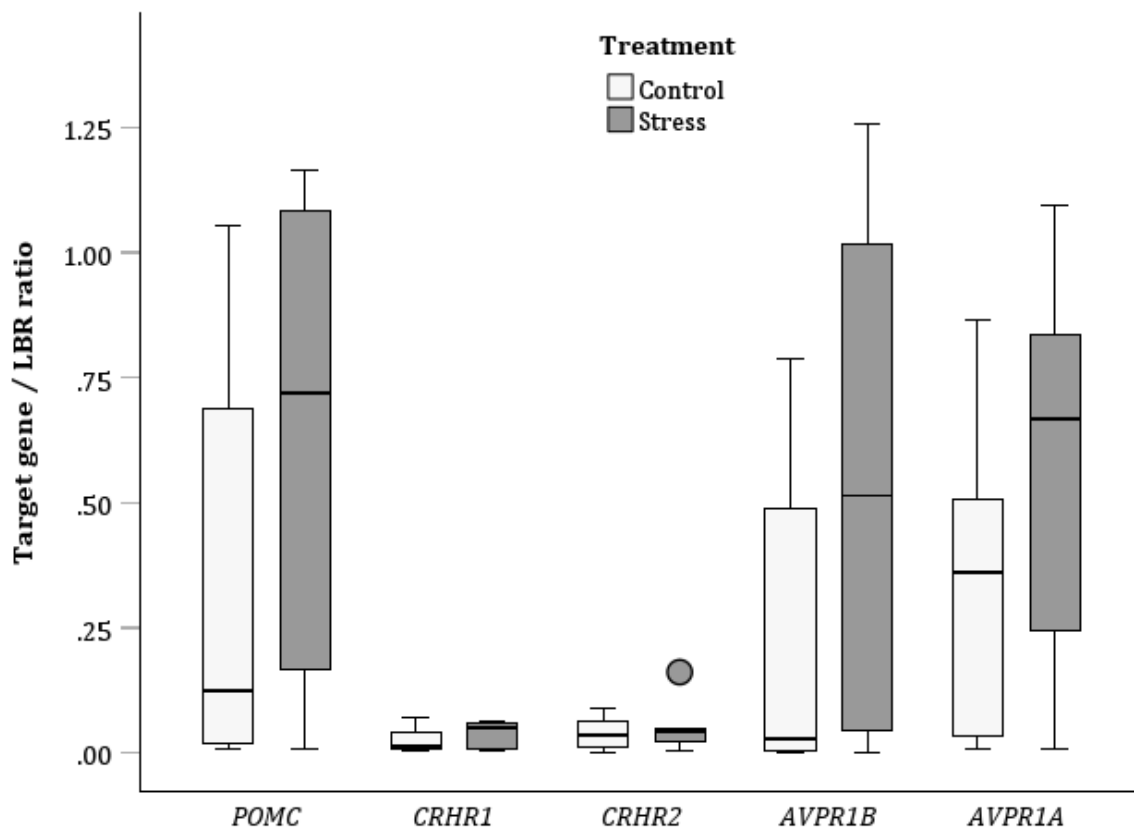
**Figure 2. 7**. Expression levels of selected genes in the chicken pituitary. The genes shown are *POMC*, *CRHR1*, *CRHR2*, *AVPR1A* and *AVPR1B*. The box plot showcases the taget gene ratios in relation to the reference gene LBR, with the central box indicating the interquartile range (IQR) and the horizontal line inside the box representing the median value. The whiskers extend to the minimum and maximum values within 1.5 times the IQR from the first and third quartiles, respectively. The point represents an outlier (more than 1.5 times the IQR). Values in the figure are not log-transformed ratios but rather represent the obtained ratios of the target gene's expression. No significant differences were observed between treatments.

### 2.3.3. Overview of FOS densities

The collected brains (n=16) were processed for the staining and density quantification of FOS immunoreactive (-ir) cells within specific regions of interest. In certain cases, particular brain subregions were excluded from the analysis due to the absence of an appropriate tissue section representing those subregions. The summarized densities are presented in Table 2.1 below.

**Table 2. 1. Summary of FOS-ir cell densities (cells/ mm$^2$) in brain regions of interest between control and stressed groups.**
**(V-Ventral, DM-Dorsomedial, DL- Dorsolateral; Mean Densities ± SEM, rounded to the nearest whole number; Size refers to Sample Size)**

| Area of interest | | | Control | | | | Stressed | | | |
|---|---|---|---|---|---|---|---|---|---|---|
| | | | Left | Size | Right | Size | Left | Size | Right | Size |
| Hippocampus | DL | Caudal-most | 9 ± 4 | 8 | 21 ± 10 | 7 | 28 ± 26 | 8 | 18 ± 14 | 8 |
| | DM | Caudal-most | 10 ± 4 | 8 | 13 ± 4 | 7 | 16 ±10 | 8 | 14 ± 4 | 8 |
| | V | Caudal-most | 7 ± 5 | 8 | 3 ± 2 | 7 | 7 ± 1 | 8 | 6 ± 2 | 8 |
| | DL | Caudal | 37 ± 12 | 8 | 38 ± 14 | 7 | 52 ± 16 | 8 | 65 ± 20 | 8 |
| | DM | Caudal | 19 ± 7 | 8 | 11 ± 4 | 7 | 28 ± 9 | 8 | 40 ± 16 | 8 |
| | V | Caudal | 17 ± 5 | 8 | 8 ± 4 | 7 | 28 ± 7 | 8 | 19 ± 7 | 7 |
| | DL | Rostral | 38 ± 8 | 8 | 48 ± 9 | 8 | 80 ± 16 | 8 | 102 ± 21 | 8 |
| | DM | Rostral | 20 ± 7 | 8 | 14 ± 5 | 8 | 33 ± 5 | 8 | 39 ± 12 | 8 |
| | V | Rostral | 15 ± 6 | 8 | 25 ± 9 | 8 | 58 ± 15 | 8 | 39 ± 12 | 8 |
| | DL | Rostral-most | 59 ± 11 | 8 | 58 ± 14 | 8 | 72 ±10 | 8 | 71 ± 16 | 8 |
| | DM | Rostral-most | 30 ± 5 | 8 | 27 ± 8 | 8 | 26 ± 6 | 8 | 22 ± 5 | 8 |
| | V | Rostral-most | 69 ± 17 | 8 | 66 ± 18 | 8 | 52 ± 15 | 8 | 43 ± 15 | 8 |
| BSTL | | | 80 ± 13 | 8 | 105 ± 21 | 8 | 73 ± 15 | 8 | 83 ± 29 | 7 |
| PVN | | | 14 ± 4 | 8 | 12 ± 4 | 8 | 22 ± 5 | 8 | 23 ± 6 | 8 |
| NHpC | | | 17 ± 9 | | 8 | | 24 ± 7 | | | 8 |

The GEE analysis focused on super-regions, which encompass the hippocampal aggregated values for the subregion (V, DM, and DL) and rostrocaudal location (rostral-most, rostral, caudal-most, and caudal hippocampus) combined. It is also worth noting that this approach encompasses hemispheric-specific data and as such incorporates the BSTL and PVN super-regions but excludes the NHpC. The results of the GEE analysis revealed significant main effects due to the super-region location ($X^2_{(13)}$ = 12274.623, p<0.001) but not for hemisphere ($X^2_{(1)}$ =0.001, p=0.970) or treatment ($X^2_{(1)=}$2.615, p=0.106).

The analysis of interactions indicated an impact of the interaction between hemisphere and super-region ($X^2_{(13)}$ = 40.640, p<0.001), while no significant interaction between hemisphere and treatment was observed ($X^2_{(1)}$ = 0.017, p=0.896). However, there were interactions between super-region and treatment ($X^2_{(13)}$ = 1824.857, p<0.001), as well as between hemisphere, super-region, and treatment ($X^2_{(13)}$ = 103.223, p<0.001).

To identify more specific differences the regions of interest were analysed separately. For the hippocampus analysis at the subregional level, the data from the hippocampal super-regions were subdivided, and the rostrocaudal locations and subregions were analysed as distinct factors.

### 2.3.4. BSTL, PVN, and NHPC

#### 2.3.4.1. Bed Nucleus of the Stria Terminalis Lateralis FOS densities

The GEE analysis revealed that no effects can be attributed to interhemispheric differences ($X^2_{(1)}$ = 1.144, p=0.285) or differences between stressed and control treatments ($X^2_{(1)}$ = 0.418, p=0.518). The interaction involving treatment and hemisphere ($X^2_{(1)}$ = 0.194, p=0.660), similarly, did not show statistical significance (Figure 2.8).
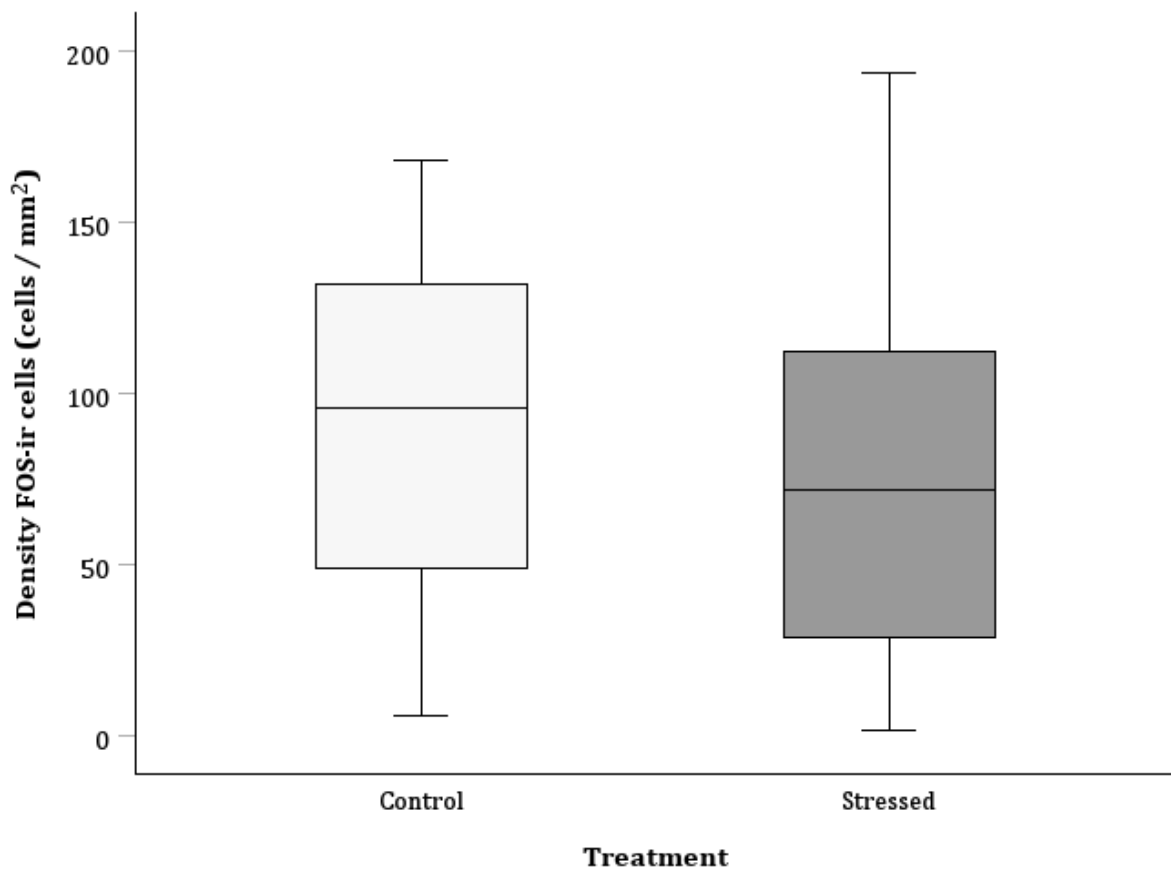


**Figure 2. 8**. Neuronal activation in the BSTL of adult hens under acute stress. The box plot illustrates neuronal activation in the BSTL of adult hens subjected to acute stress, as indicated by the densities of FOS-immunoreactive (FOS-ir) cells per mm² on the Y-axis, with the central box indicating the interquartile range (IQR) and the horizontal line inside the box representing the median value. The whiskers extend to the minimum and maximum values within 1.5 times the IQR from the first and third quartiles, respectively. No differences were observed between treatments.

#### 2.3.4.2. Paraventricular Nucleus FOS densities

Likewise, the GEE analysis revealed that there was no effect due to interhemispheric differences ($X^2_{(1)}$ = 0.001, p=0.980) or differences between stressed and control treatments ($X^2_{(1)}$

= 3.003, p=0.083) nor for the interaction of treatment and hemisphere ($X^2_{(1)}$ = 0.213, p=0.644) (Figure 2.9).
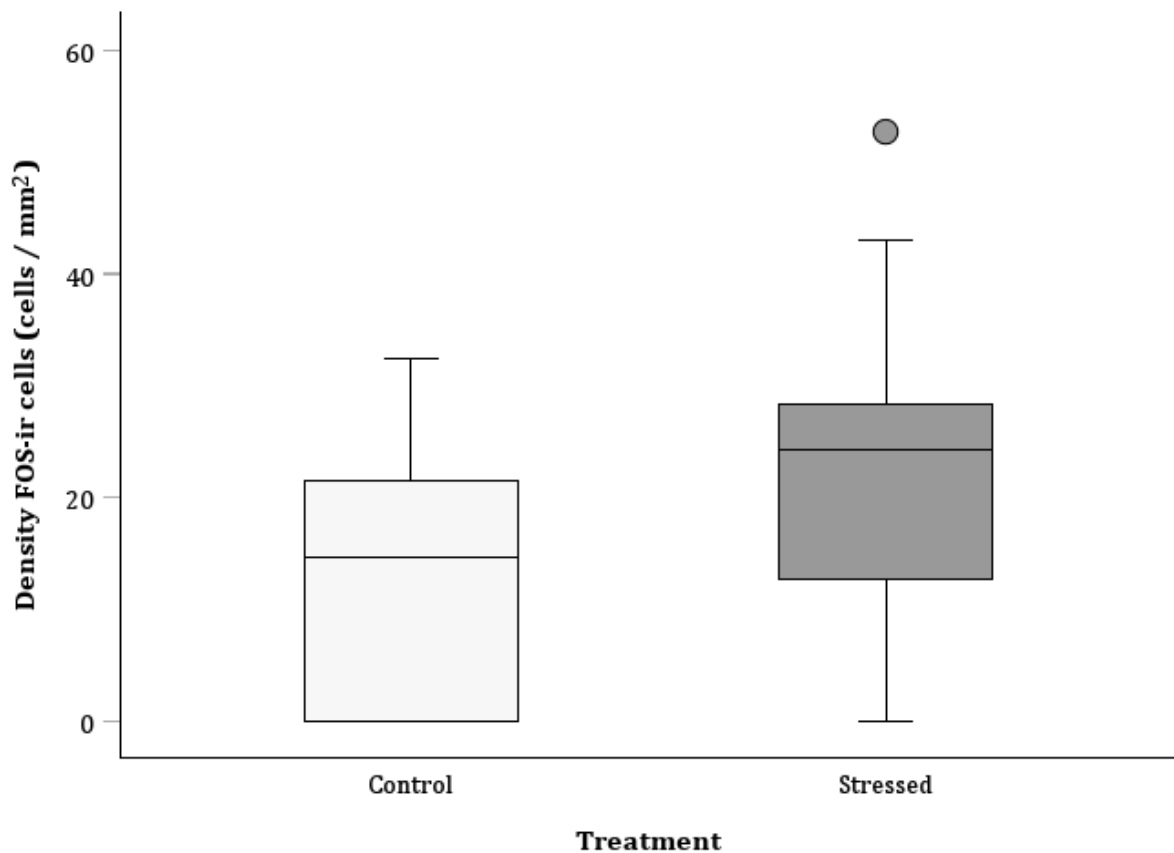


**Figure 2. 9**. Neuronal activation in the PVN of adult hens under acute stress. The box plot illustrates neuronal activation in the PVN of adult hens subjected to acute stress, as indicated by the densities of FOS-immunoreactive (FOS-ir) cells per mm² on the Y-axis, with the central box indicating the interquartile range (IQR) and the horizontal line inside the box representing the median value. The whiskers extend to the minimum and maximum values within 1.5 times the IQR from the first and third quartiles, respectively. The point represents an outlier (more than 1.5 times the IQR). No differences were observed between treatments.

### 2.3.4.3. Nucleus of the Hippocampal Commissure FOS densities

The results derived from the independent-sample t-test indicate that the density of FOS-ir cells remained unchanged in response to the acute stress treatment used (t $_{(14)}$ = 0.620, p=0.273) (Figure 2.10).
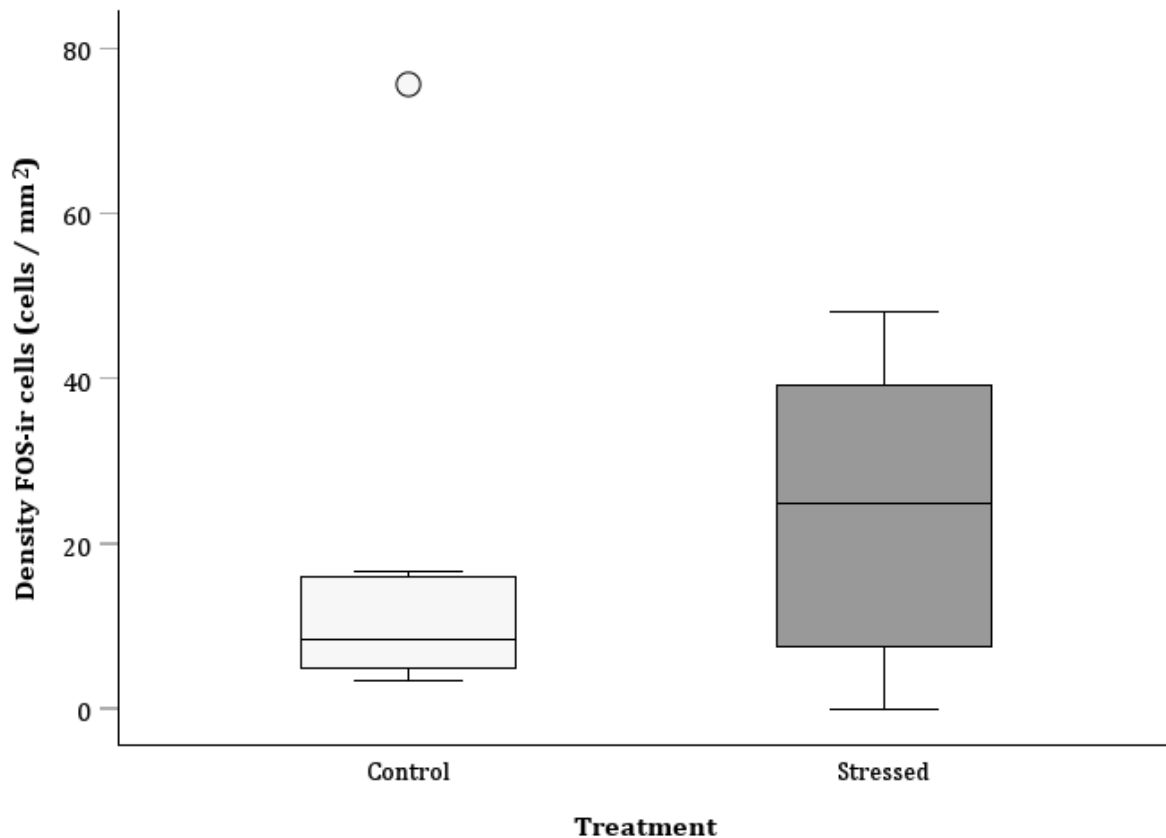
**Figure 2. 10**. Neuronal activation in the NHpC of adult hens under acute stress. The box plot illustrates neuronal activation in the bed nucleus of the NHpC of adult hens subjected to acute stress, as indicated by the densities of FOS-immunoreactive (FOS-ir) cells per mm² on the Y-axis, with the central box indicating the interquartile range (IQR) and the horizontal line inside the box representing the median value. The whiskers extend to the minimum and maximum values within 1.5 times the IQR from the first and third quartiles, respectively. The point represents an outlier (more than 1.5 times the IQR). No differences were observed between treatments.

### 2.3.5. Hippocampus

#### 2.3.5.1. Distribution of FOS-ir cells

Density maps were generated to investigate the distribution of FOS-positive cells in the examined brain sections. Unfortunately, certain sections were excluded from the analysis as density maps could not be generated due to tissue damage. The missing sections correspond to both the left and right hemispheres of brain A.11, along with the right hemisphere of brain A.15 at the same caudal-most level and brain C.8 at the rostral level.

##### 2.3.5.1.1. Caudal-most hippocampus

The visual analysis of whole-tissue images from caudal-most sections revealed FOS activation predominantly distributed across the DM and V subregions in stressed animal brains.

Specifically, in cases such as A.1, A.2, A.3, A.5, A.6, A.7, and A.8, with activation in the DL subregion restricted to the right hemisphere in A.2, the left hemisphere of brain A.4, and both hemispheres of cases A.3, A.5, and A.8 (Figure 2.11).

In unstressed brains, high-density areas appeared within the DM subregion (A.9, A.10, A.12, A.14, A.15, and A.16) and in the DL subregion (A.9, A.10, A.13, A.14, and A.16), observed in either both hemispheres or exclusively in one with no apparent preference. Notably, only brain A.14 exhibited activation in the V subregion (Figure 2.11).
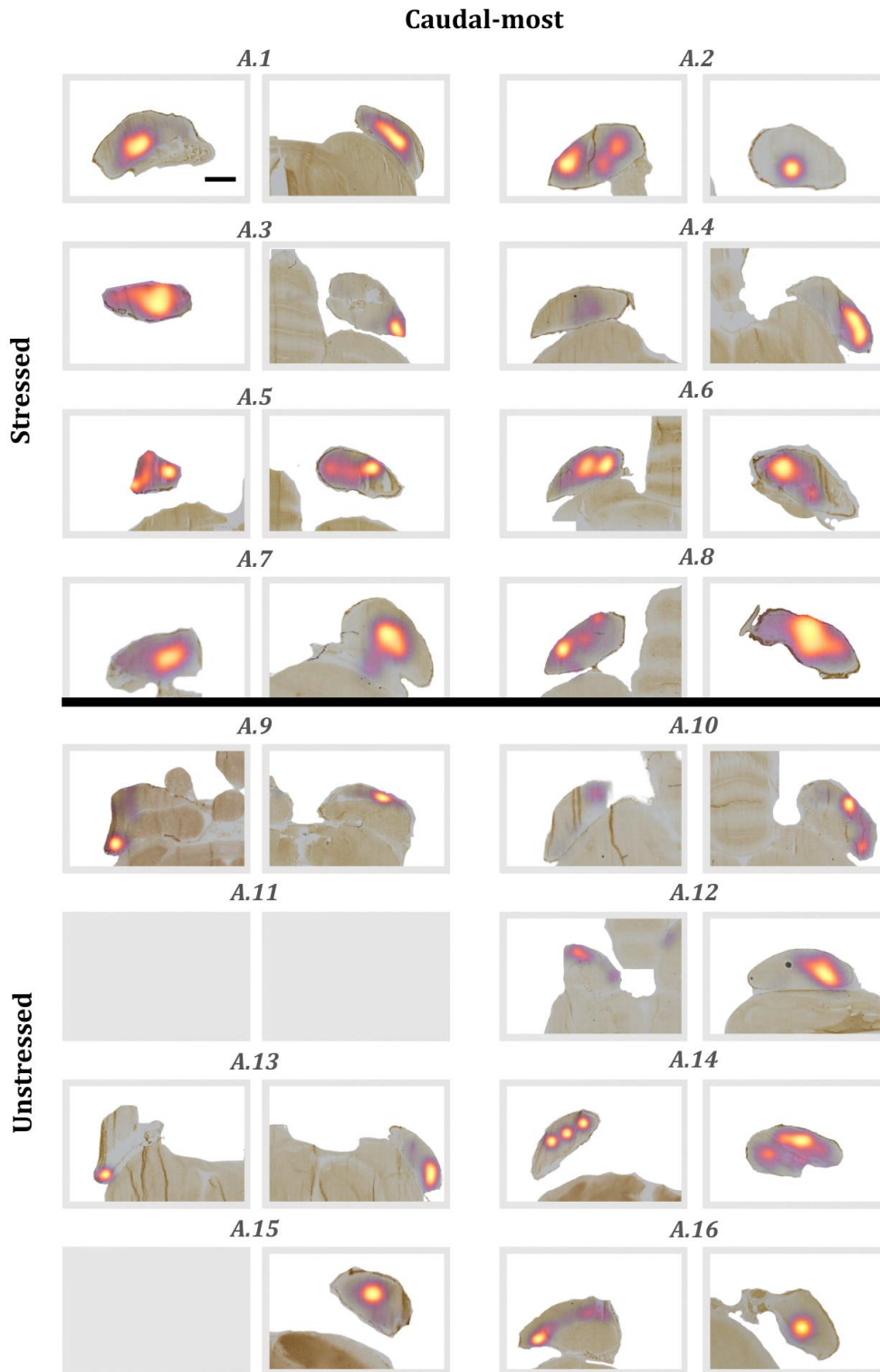
**Caudal-most**



**Figure 2. 11**. Density maps of caudal-most hippocampus coronal sections. Density maps from both stressed and unstressed birds highlight areas of high cell density through colour variations. Due to the cryostat-mounted nature of these sections, the right hemisphere is located on the left side in each image, while the left hemisphere is on the right side. The scale bar in the first image represents 800 μm. This scale applies to each image individually.

### 2.3.5.1.2. Caudal hippocampus

The caudal sections of stressed animals showed a distribution of FOS-positive cells predominantly in the DM and DL subregions of the hippocampus. These high-density areas span the entire DM and DL subregion in cases B.3, B.4, B.7, and B.8 (Figure 2.12).

In sections from unstressed animals on the same level, the highest cell density is found consistently across the DM subregion (Figure 2.12).
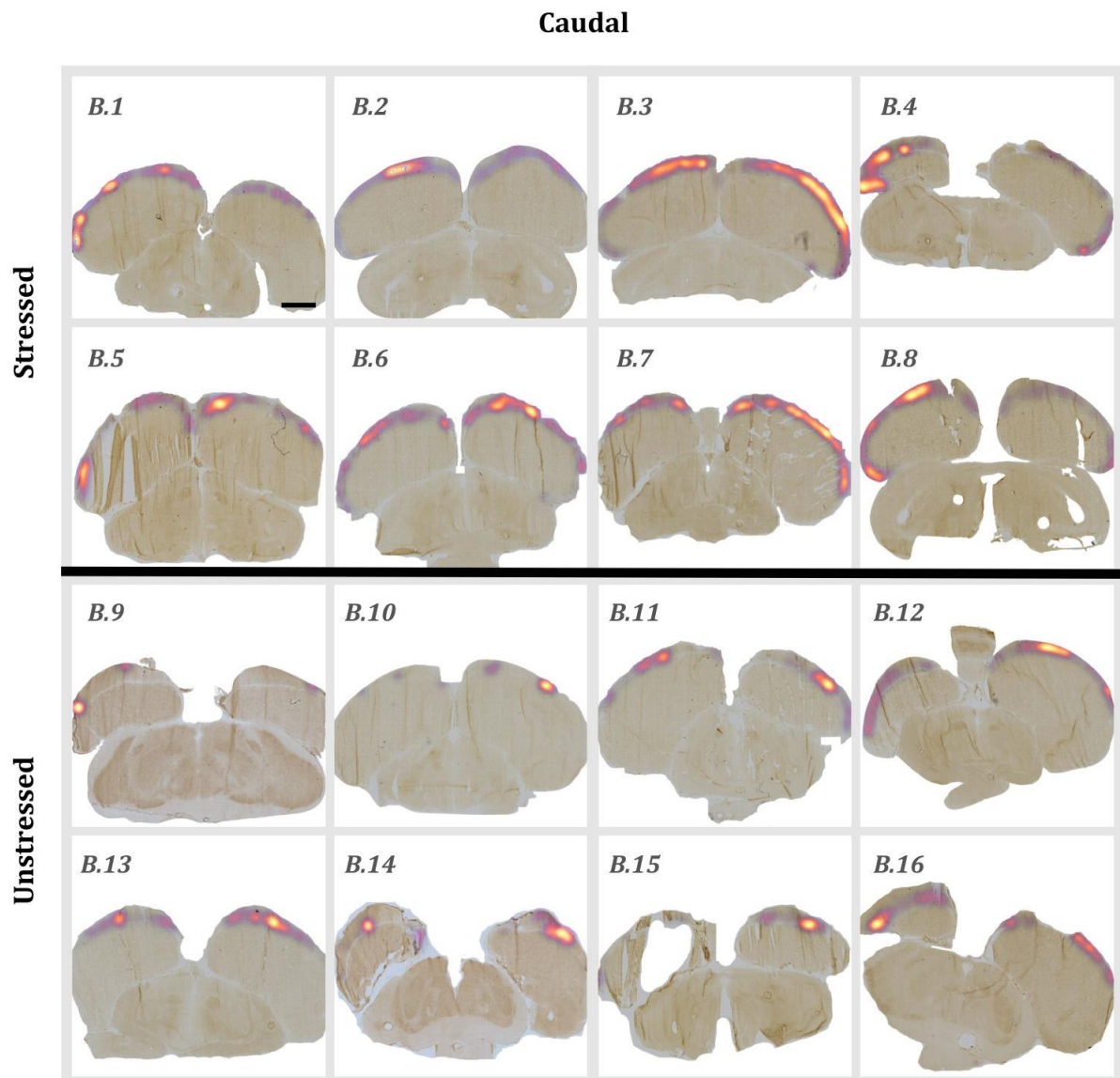
**Caudal**



**Figure 2. 12**. Density maps of caudal hippocampus coronal sections. Density maps from both stressed and unstressed birds highlight areas of high cell density through colour variations. Due to the cryostat-mounted nature of these sections, the right hemisphere is located on the left side in each image, while the left hemisphere is on the right side. The scale bar in the first image represents 2 mm. This scale applies to each image individually.

### 2.3.5.1.3. Rostral hippocampus

In the rostral sections, the highest densities are concentrated in the DM subregion in both stressed and unstressed animals, as evidenced by observations in cases C.1, C.2, C.6, C.7, C.12, C.13,

and C.16. However, certain sections also exhibit elevated densities in the V subregion, exemplified by cases C.4, C.5, C.6, C.10, and C.13 (Figure 2.13).
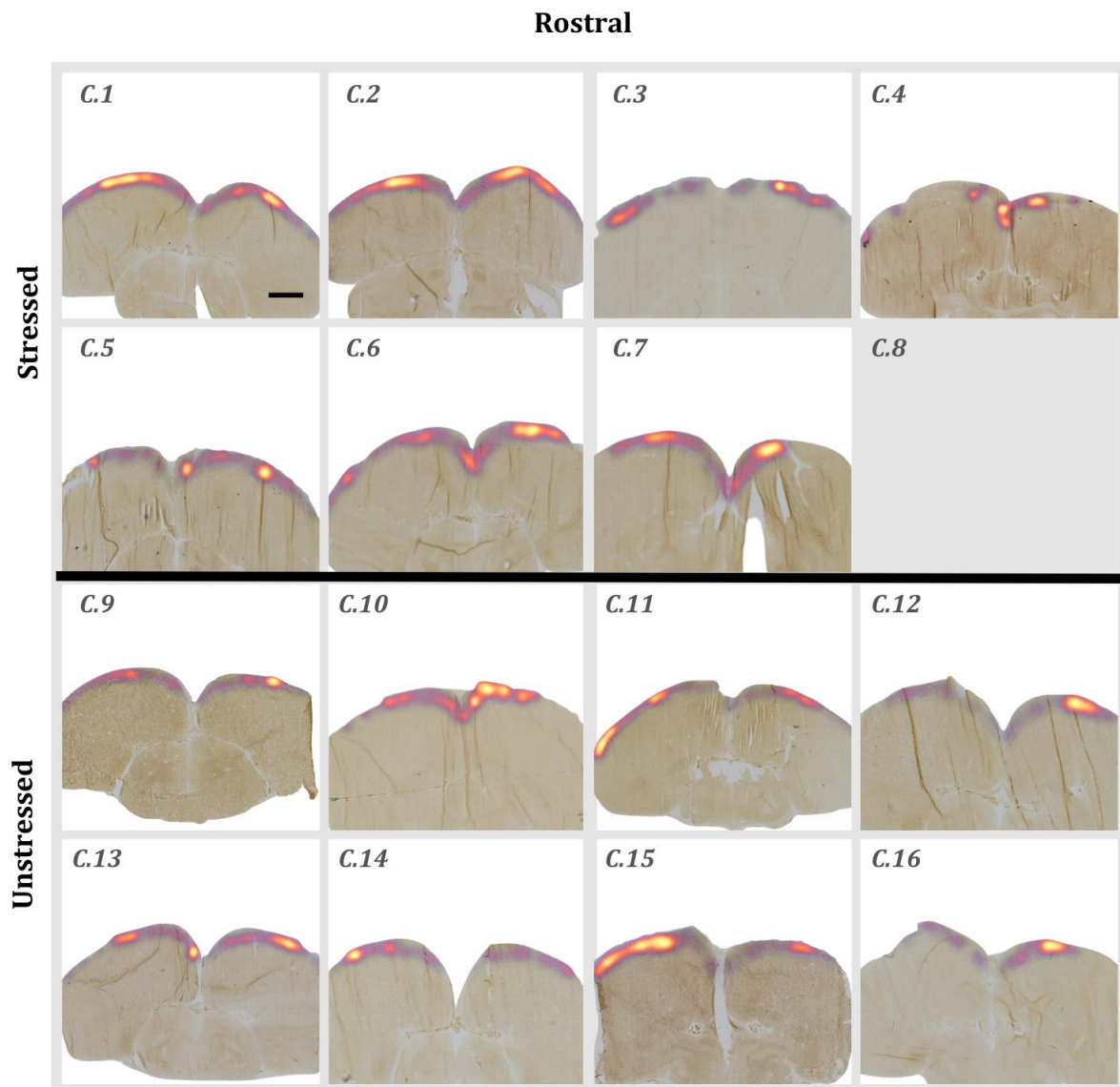
**Rostral**



**Figure 2. 13**. Density maps of rostral hippocampus coronal sections. Density maps from both stressed and unstressed birds highlight areas of high cell density through colour variations. Due to the cryostat-mounted nature of these sections, the right hemisphere is located on the left side in each image, while the left hemisphere is on the right side. The scale bar in the first image represents 2 mm. This scale applies to each image individually.

### 2.3.5.1.4. Rostral-most hippocampus

In the rostral-most sections of stressed animals, there was a distinct pattern of FOS activation in the DL subregion across all cases. Noteworthy exceptions include three cases with activation in the V subregion (C.1, D.7, and D.8) and two cases with activation in the DM subregion (D.1 and D.7). Conversely, in unstressed animals, the activation pattern is more varied, ranging from widespread activation throughout the entire hippocampus (D.9, D.10, D.12, D.13, and D.14)

to focal activation in specific areas, such as the DL (D.11 and D.15) or the V (D.16) subregions (Figure 2.14).
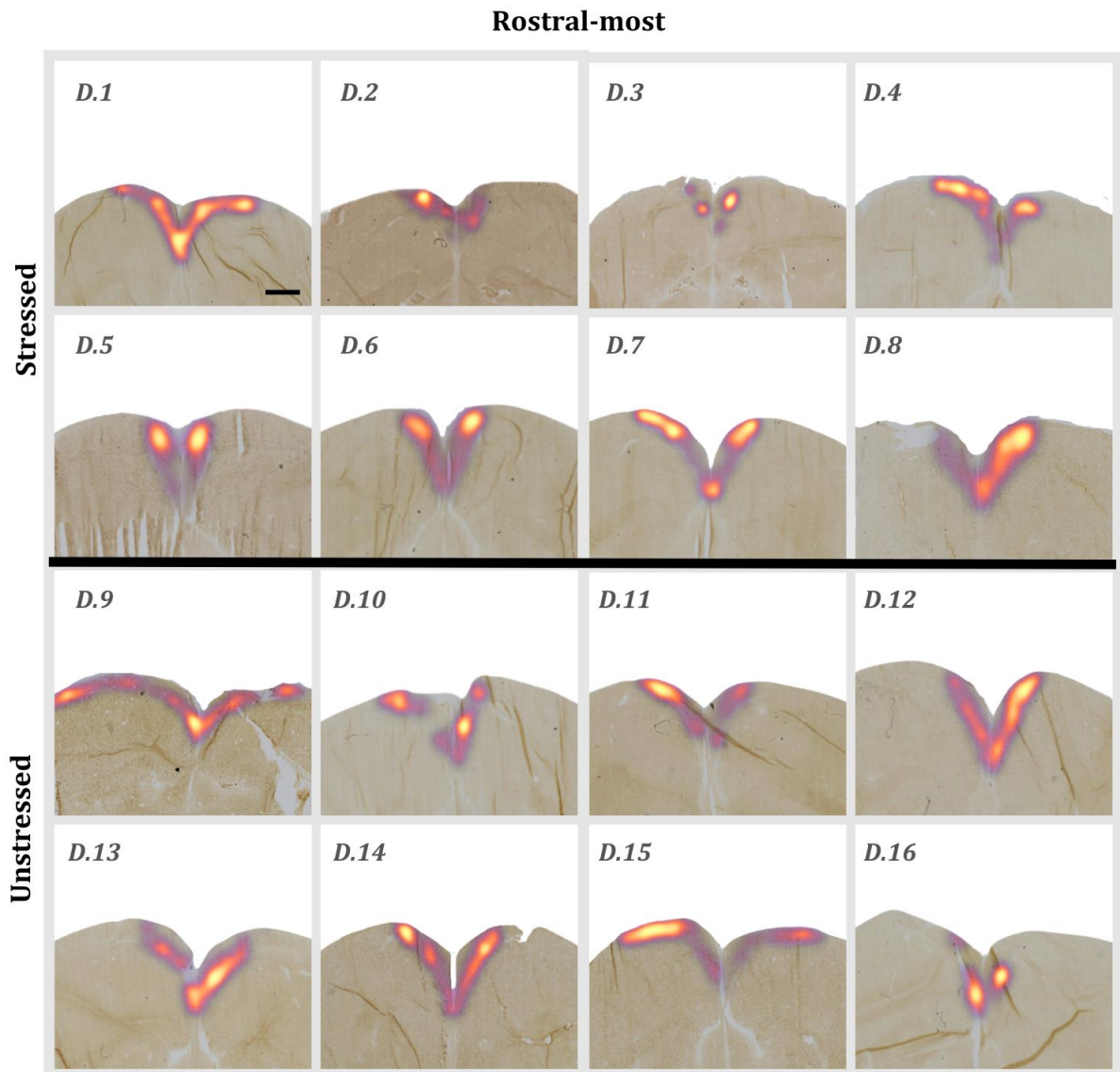
**Rostral-most**



**Figure 2. 14**. Density maps of rostral-most hippocampus coronal sections. Density maps from both stressed and unstressed birds highlight areas of high cell density through colour variations. Due to the cryostat-mounted nature of these sections, the right hemisphere is located on the left side in each image, while the left hemisphere is on the right side. Scale bar in the first image represents 1mm. This scale applies to each image individually.

Furthermore, it is important to highlight that variations in density were present between the left and right hemispheres across most cases. Despite this, no pattern was observed where one hemisphere consistently exhibited higher density than the other. Importantly, this lack of discernible bilateral asymmetry was further supported by the statistical analysis of FOS cell counts discussed next.

### 2.3.5.2. *Hippocampal FOS densities*

In the hippocampus, the stressed condition corresponded to higher densities across various subregions and locations, compared to the control condition. The analysis of the hippocampus data demonstrated an absence of an overall effect due to interhemispheric differences ($X^2_{(1)}$ = 0.101, p=0.750) or treatment groups ($X^2_{(1)}$ = 2.741, p=0.098). However, significant effects were observed involving subregions ($X^2_{(2)}$ = 77.496, p<0.001) and the rostrocaudal position ($X^2_{(3)}$ = 0.017, p<0.001).

The interactions between hemisphere and treatment ($X^2_{(1)}$ = 0.118, p=0.732), subregion ($X^2_{(2)}$ = 2.537, p=0.281), or rostrocaudal position ($X^2_{(3)}$ = 2.728, p=0.435) were not statistically significant. Similarly, the interaction between treatment and subregion was not found to be significant ($X^2_{(2)}$ = 4.901, p=0.086). However, significant interactions were found between subregion and rostrocaudal position ($X^2_{(6)}$ = 60.758, p<0.001) and between treatment and rostrocaudal position ($X^2_{(3)}$ = 14.089, p=0.003). This effect is mainly due to a substantial difference between stressed and unstressed animals within the rostral region of the hippocampal formation (p<0.001) (Figure 2.15).

While positive cells appeared to increase in the rostral hippocampus of stressed birds, for the DL, DM, and V subregions, and the density of FOS-ir cells similarly appeared to increase in the caudal hippocampus of stressed birds, specifically for the V subregion, the analysis of various three-way interactions revealed no statistical interactions. Lastly, the results revealed no interaction between hemisphere, treatment, subregion, and rostrocaudal position ($X^2_{(6)}$ = 5.512, p= 0.480) revealing the lack of complex interactions involving the combination of these factors in the present study.
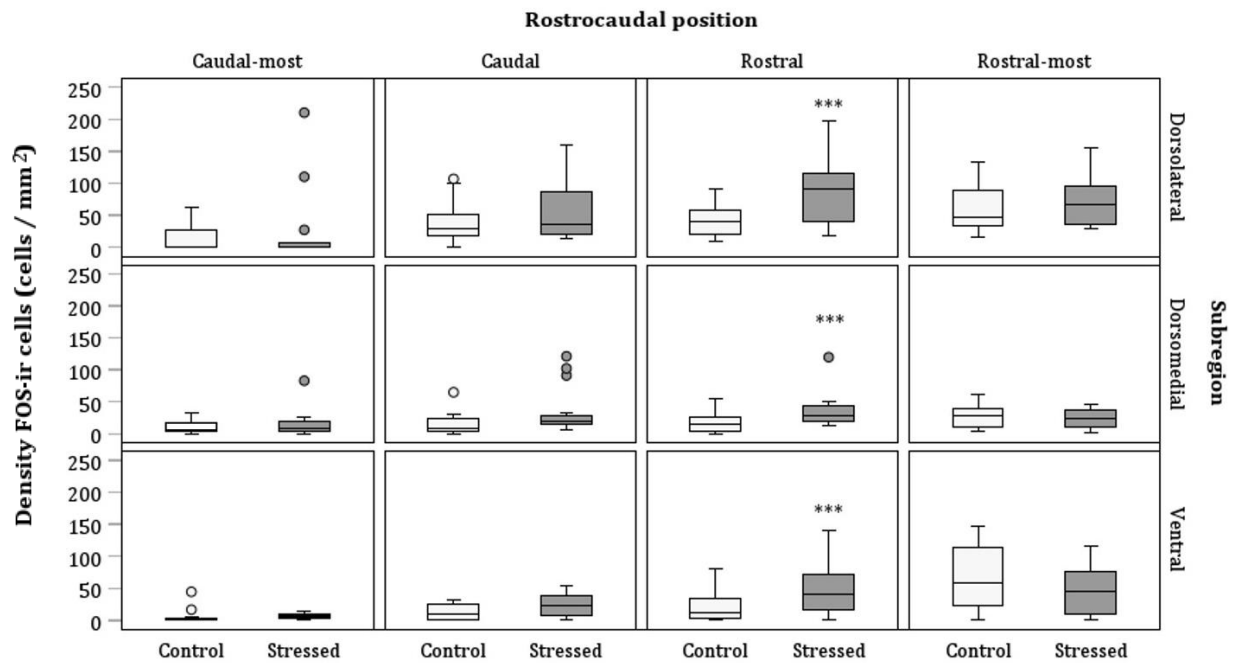
**Figure 2. 15.** Neural activation in hippocampal formation (HF) under acute stress. Densities of FOS-ir cells are represented across three subregions: dorsomedial, dorsolateral, and ventral, as well as across four rostrocaudal divisions: caudal, caudal-most, rostral, and rostral-most. The box plots showcase the cell densities, with the box indicating the interquartile range (IQR) and the horizontal line inside the box representing the median value. The whiskers extend to the minimum and maximum values within 1.5 times the IQR from the first and third quartiles, respectively. Points represent outliers (more than 1.5 times the IQR). Asterisks indicate significant differences between the two treatment groups (***p<0.001).

## 2.4. Discussion

### 2.4.1. Summary

The primary objective of this study was to investigate the involvement of different subdivisions within the avian hippocampal formation in the feedback regulation of the HPA axis. I hypothesized that, in response to acute stress, hens would demonstrate FOS activation in the caudal hippocampus, contrasting with the rostral portion. This conceptualization parallels the well-established mammalian hippocampus, where distinct regions are associated with cognitive and emotional regulatory functions along its longitudinal axis. In terms of which hippocampal subdivision activates in response to stress the literature is scarce but based on the observations by Takeuchi *et al.* (1996) I expected the DL subdivision to show increased activation in response to stress induction when compared to the V and DM subdivisions.

The research methodology included not only the analyses of FOS activation due to the acute stress induction treatment but also analyses of CORT levels and gene expression in the pituitary gland. These measures were undertaken to comprehensively evaluate the impact of the stress-inducing treatment on the overall activation of the HPA axis. For the assessment of CORT

plasma levels, I observed high variability in the individual response to the stress treatment, resulting in an overall lack of differences between the baseline levels, those after stress induction, and during stress recovery. Moreover, the analysis of gene expression of *POMC, CRHR1, CRHR2, AVPR1B*, and *AVPR1A*, selected based on insights from prior studies indicating an upregulation in response to stress (see Cornett *et al.*, 2003; Kuenzel & Jurkevich, 2010; Selvam *et al.*, 2013), did not reveal significant differences between stressed and unstressed animals in this study.

In addition, contrary to the initial expectations, significantly increased FOS immunoreactivity was observed in stressed hens in the V, DM, and DL subregions of the rostral hippocampus when compared with their unstressed counterparts. This increase in FOS density in the rostral hippocampus, however, did not coincide with an increase in FOS activity in any of the other brain areas examined, nor was it supported by an increment in CORT levels or a heightened expression of stress-related genes in the pituitary.

Therefore, before interpreting these unexpected results, it is crucial to consider various potential factors that may have contributed to these findings. In particular, it is crucial to address the fundamental question of whether the birds were indeed stressed during the experimental procedures.

### 2.4.2. *Were the birds stressed?*

To better evaluate the effectiveness of the stress induction treatment employed in this study, it is essential to discuss whether the stress induction treatment effectively elicited a robust stress response.

The most prominent finding from this study is the observed activation specifically within the rostral hippocampus, contrasting with the lack of activation in the caudal region. As outlined in Chapter 1, the septal hippocampus in mammals, proposed as the equivalent to the avian rostral hippocampus, is known to be involved in spatial cognition. Conversely, the temporal hippocampus, which would correspond to the avian caudal hippocampus, is primarily associated with emotional processing (see Smulders, 2017). Given this, a plausible explanation is that the activation of the rostral hippocampus is driven by input related to the processing of spatial information, while the lack of activation in the caudal hippocampus may be attributed to the insufficient stressfulness of the induction treatment.

This explanation is reinforced by the absence of activation seen in other brain regions implicated in the stress response. Prior studies have suggested that comparable levels of FOS expression may occur in brain regions involved in activating the HPA axis. For instance, Nagarajan *et al.* (2014) documented heightened FOS immunoreactivity in various brain areas, including the lateral hypothalamic area (LHy), ventrolateral thalamic nucleus (VLT), lateral septum (LS), BSTL, NHpC, and the core region of the paraventricular nucleus (PVNc) in response to psychological stress in birds, however, in the present study I did not observe a similar increase in FOS expression

levels when the same regions were examined (NHpC, BSTL, and PVN). This suggests that factors beyond the immediate stressor itself, such as the spatial cues present during the experimental conditions, may have exerted a more influential role in modulating neuronal activation patterns.

Previous studies investigating IEG induction in the hippocampus have faced similar challenges in disentangling the stress-inducing aspects of an experience from the influence of spatial cues. For instance, research conducted in rats examined HPA axis activity and hippocampal FOS expression following exposure to four distinct novel environments (empty housing tub, circular arena, elevated pedestal, and restraint tube) (Pace *et al.*, 2005). The study revealed a reduction in hippocampal FOS induction in the only environment that prevented active exploration; the restraint tube environment, thus indicating that hippocampal FOS levels were primarily associated with the extent of exploration in each environment rather than the perceived stressfulness of the experience.

As an additional validation of my experimental approach, I examined relative levels of pituitary gene expression of *POMC, CRHR1, CRHR2, AVPR1B*, and *AVPR1A* with no statistically significant differences observed in stressed animals when compared to their unstressed counterparts, further reinforcing the possibility of an absence of robust stressful stimuli. However, this absence of discernible responses in both FOS activation and pituitary gene expression cannot be solely attributed to a lack of stress activation. The cascade of events in the stress response involves various brain regions and hormonal signalling pathways, each with its own temporal dynamics. For instance, a study by Hakeem *et al.* (2021) revealed the temporal dynamics of gene expression in response to immobilization stress in chicks, focusing on the NHpC, PVN, and anterior pituitary (APit). The findings revealed that while in the NHpC *CRH* mRNA levels surged rapidly, reaching a significant peak at 15 minutes post-stress induction, and returning to baseline at 60 min, the PVN displayed a more gradual increase, peaking at 90 min and declining by 120 min. Meanwhile, in the APit, *POMC* gene expression mirrored the NHpC with a significant upregulation at 15 min, followed by notable downregulation at 30 and 60 min. These temporal dynamics offer valuable insights that could clarify the absence of significant results in the gene expression study conducted 90 minutes post-stress induction.

Considering that, in the context of HPA axis activation, *CRH* mRNA activation in the PVN peaks at 90 minutes, it is plausible that protein activation at the time of sampling might have occurred slightly earlier. In contrast, the NHpC and pituitary, which appear to activate in a coordinated manner, demonstrate an early peak in mRNA levels at 15 minutes, making the 90-minute time point of the current study relatively late for capturing their peak activation contributing to the lack of observable FOS immunoreactivity and pituitary gene expression changes.

Regarding the absence of changes in plasma CORT concentration, it is notable that despite previous studies in birds indicating that plasma CORT levels typically peak 30 minutes after stress

induction and subsequently decline within an additional 30-minute interval (Hakeem *et al.*, 2021), aligning with the same timing employed in this investigation, my analysis did not uncover significant changes in CORT levels at the 30-minute mark. Moreover, there was no evident return to baseline levels after 30-, 60-, or 90-minutes following stress termination. Again, these findings support the possibility that the stress induction might not have been effective enough to elicit a robust stress response.

So, what factors may have contributed to the reduced stressfulness of the experience? As mentioned in the methods, all experiments were conducted during the dark phase of the circadian cycle to prevent the potential masking of the stress response due to natural daily fluctuations, as I was aiming for a low baseline CORT level and the circadian elevation in CORT secretion in egg-laying hens typically occurs before the activity period begins and reaches its minimum at the beginning of the dark phase (Beuving & Vonder, 1977). However, this precautionary measure may have inadvertently reduced the impact of the stressor.

While the specific impact of stress-induced changes in the activation of the avian HPA axis based on the time of day of stressor presentation remains largely unknown due to the lack of reporting on this aspect in studies related to stress induction in birds, studies in mammals have provided insights into the role of both circadian phase and sex in shaping behavioural responses to stress, particularly in rats. For example, it has been observed that female rats, even at rest, exhibit higher baseline CORT levels than their male counterparts, with this distinction being more pronounced during the dark phase, and overall plasma CORT levels in the dark phase being significantly higher than the light phase for both males and females. Additionally, when subjected to behavioural tests, females tend to display more "despair" behaviour (immobility) in the dark, while males demonstrate higher levels of anxiety than females on the elevated plus maze, specifically in the light phase (Van Reeth *et al.*, 1991). Applying these findings to chickens, which are diurnal animals, may offer a framework for understanding potential differences in stress responses. In this study's context, I would expect CORT levels in chickens to be significantly lower during the dark phase compared to the light phase. Additionally, hens may demonstrate lower levels of anxiety in response to novel or aversive stimuli during the dark phase compared to their male counterparts. This could potentially manifest as a dampened response to stress-inducing stimuli, offering a plausible explanation for the observed lack of response to the restraint treatment.

Character in birds also plays a crucial role in determining their CORT responses, while some individuals may exhibit rapid and robust hormonal responses, others may exhibit more subtle or delayed reactions to stressors. As reported in other studies, birds with proactive traits demonstrate active behavioural reactions accompanied by relatively lower levels of CORT stress. Conversely, those with reactive personalities exhibit passive behaviours alongside heightened CORT reactions (Cockrem, 2013; Littin & Cockrem, 2001). No assessment of character was

included in this analysis, but there is reason to believe that incorporating such an evaluation could provide a more comprehensive understanding of the CORT response to stress in birds.

When analysing the individual CORT stress responses, there was a marked variation between individuals, ultimately contributing to a lack of uniform CORT expression changes across the different experimental groups. It is crucial to consider the individual's life history, particularly when working with adult subjects, as is the case in this experiment. Adult individuals, having undergone a spectrum of life experiences, may have developed distinctive stress-coping mechanisms compared to their younger counterparts. (de Haas *et al.*, 2013, 2014). Individual differences in stress susceptibility, life history coping mechanisms, and social dynamics within the flock could have contributed to the observed CORT patterns.

Finally, these differences may be partially attributed to variations in the experimental approach. When comparing my experimental approach to previous research, the restraint method has been employed in numerous studies to induce a stress response in chickens, demonstrating its effectiveness in elevating plasma CORT concentration levels and triggering the expression of stress-related genes in key areas such as the hippocampus, hypothalamus, and adrenal glands (Ericsson *et al.*, 2014; Fallahsharoudi *et al.*, 2015; Løtvedt *et al.*, 2017). However, it is crucial to acknowledge that the specific environmental conditions during the treatment, along with variations in the restraint procedures applied to the birds, may have introduced potential confounding factors.

For instance, in my study, chickens were restrained using a hanging bag, a technique akin to the one employed by Ericsson and colleagues (2014) in which the observer catches the bird in a net originally designed for fishing, and subsequently, the bird is suspended inside the hanging net. Other studies, however, have adopted diverse approaches to restrict the movement of chickens, such as utilizing a cone or shackle method (Ismail *et al.*, 2019), or employing a harness that immobilizes the wings and prevents the birds from standing (Aman *et al.*, 2016; Kadhim & Kuenzel, 2022). These variations in restraint techniques highlight the need for careful consideration and standardization when interpreting results across studies, as different methods may yield distinct physiological and behavioural responses in the study subjects.

In summary, my findings suggest that the stress treatment employed in this study may not have effectively induced an effective stress response. These observations underscore the importance of choosing appropriate stress induction methods when investigating the hippocampus and emphasize the need to consider various contextual factors to differentiate between FOS induction patterns attributed to spatial context and those associated with the stressfulness of the experience.

### 2.4.3. Hippocampal activation in response to restraint stress

In the present study, the avian hippocampus exhibited a region-specific response to the stress manipulation employed, as evident in the differences in FOS immunoreactivity observed between the rostral and caudal hippocampus. The rostral hippocampus displayed a higher density of FOS-positive cells in the V, DM, and DL subregions as corroborated by density maps exhibiting cell-dense areas across the three subregions.

Despite the observed neuronal activity in the rostral hippocampus, there was a lack of activation of the HPA axis. This is evidenced by non-significant changes in CORT levels and the absence of activation in stress-related genes in the pituitary when comparing stressed and unstressed animals. Additionally, no significant changes in FOS activation were observed in the PVN, BSTL or NHpC. While the expression of the immediate early gene FOS has been a longstanding marker in stress studies (Ceccatelli *et al.*, 1989), it is crucial to emphasize that the presence of FOS protein immunoreactivity or mRNA in cell nuclei specifically denotes neural excitation. This implies that the FOS-like immunoreactivity in the hippocampus could have been caused by stimuli not related to the stress induction treatment.

Given the established role of the hippocampus in detecting novel spatial features, it is reasonable to infer that the neural response observed in this study is linked to the recognition of a novel spatial context. When it comes to the environmental conditions of the animals in this study, red lights were incorporated to maintain dark conditions during the restraint stress induction, a method commonly used to reduce visual input in rodent behavioural experiments. However, unlike rodents, chickens possess a sophisticated visual system with seven distinct types of photoreceptors and the full complement of four distinct spectral types of single cones (SWS1, SWS2, RH2, LWS), each finely tuned to specific wavelengths in the visual spectrum such as violet, blue, green, and red. Notably, these single cones incorporate an organelle known as the oil droplet at the inner segment's distal end. These oil droplets finely tune the spectral sensitivities of individual cones, thereby enhancing birds' capacity for precise colour discrimination (Nikbakht & Diamond, 2021; Seifert *et al.*, 2022; Wilby & Roberts, 2017). Hence, the use of red light intended to preserve dark conditions may have inadvertently served as effective illumination for the visual input of the animals, thereby potentially offering cues about changes in their spatial context. These spatial cues could encompass changes in the lighting conditions and in shapes and patterns from one room to the other, as well as the introduction of unfamiliar objects, for example by introducing the animals in the pillowcase during the restraint treatment.

Comparable findings in rodent studies have associated the detection of environmental novelty with the septal hippocampus, as evidenced by impaired recognition of novel spatial information following neurotoxic lesions (Lee *et al.*, 2005). If hens indeed possessed the capability to distinguish objects under red lights and considering the introduction of novel spatial conditions

during stress induction, it raises the possibility that the observed neuronal activation in the rostral hippocampus may be a response to changes in the spatial context.

In chickens, however, the neuronal representation of environmental shape appears to involve the entire hippocampus with no reported differences at a subregional level (Mayer *et al.*, 2018; Morandi-Raikova & Mayer, 2020), although it is important to acknowledge that more evidence is needed, particularly as direct comparisons between the caudal and rostral hippocampus of chickens have not yet been thoroughly addressed in the existing literature. In fact, the consensus that the temporal lobe of the hippocampus does not contribute to the processing of novelty and spatial information is not universally agreed upon, with previous studies showing increased FOS expression in the temporal hippocampus of rodents when exposed to novel objects and in response to spatial memory tests (Bernstein *et al.*, 2019; Vann *et al.*, 2000). Notably, the temporal dentate gyrus has been implicated in detecting environmental novelty and transmitting this information to the septal hippocampus (Fredes *et al.*, 2020).

These findings strongly suggest the necessity for a refined method in examining hippocampal activation, particularly to account for more subtle differences in neuronal activation. Implementing a method that can discern subtle differences in activation patterns across various subregions and rostrocaudal levels would significantly enhance our understanding of the complex neural processes underlying stress responses.

## 2.5.    Conclusion

In this study, hippocampal FOS induction appears to operate independently of the acute stress induction treatment as evidenced by increased immunoreactivity in the rostral hippocampus and an overall lack of differences between stressed and unstressed animals in the analysis of additional stress indicators involved. These outcomes challenged several assumptions about the chosen experimental design employed, prompting a revaluation of how the stress response is assessed, particularly when the hippocampus is involved. By addressing the limitations of the study, I recognize the interplay between stress induction methods, region-specific dynamics, spatial context, and individual variabilities.

In providing a novel perspective, this study not only contributes to the current understanding of the mechanism underlying avian stress response but also sets the stage for an in-depth exploration into the molecular processes and brain network interactions governing the avian hippocampal response to stress.

# Chapter 3. Mapping Hippocampal Response to Isolation Stress in Young Chicks

## 3.1.   Introduction

The hippocampus is a crucial brain region that plays a vital role in regulating the activity of the Hypothalamic-Pituitary-Adrenal (HPA) axis. However, little is known about the functional specialization along the longitudinal axis of the avian hippocampal formation (HF).  In Chapter 2, I explored the immunohistochemical induction of FOS protein and HPA-axis activation in adult hens under restraint stress. The study aimed to investigate the activation of different subdivisions, namely the ventral (V), dorsomedial (DM), and dorsolateral (DL), along the longitudinal axis of the avian HF in response to acute restraint stress. However, an increase in FOS density in the rostral hippocampus and the absence of additional markers of HPA axis activation suggested a limited impact of the stress induction procedure, with substantial environmental influences affecting hippocampal neuronal activation.

In this chapter, I explore the use of conspecific isolation as a stressor and employ the analysis of vocalisations as a tool for measuring stress response in chicks. By using conspecific isolation in young chicks as the stress induction treatment, I expect to elicit a robust HPA axis activation. Conspecific isolation is a well-established stressor in animal studies and is often used to study the stress response in social animals, particularly in chicks or fowl where young individuals form strong social bonds among individuals of the same species (Bolhuis, 1991; Nakagawa & Waas, 2004; Remage-Healey *et al.*, 2003).

Previous research shows that in the presence of companions, chicks produce minimal vocalisations described as twittering or pleasure calls. However, when socially isolated, chicks produce high-pitched calls known as distress vocalisations (Eiserer, 1990; Sufka & Weed, 1994). A study by Marx *et al.* (2001) analysed the vocal expressions of chicks during social isolation. The analysis revealed that these vocalisations primarily comprised four types of calls: distress calls, short peeps, warbles, and pleasure notes. While low-energy vocalisations dominated in group sizes of three or more chicks, the number of distress calls increased as the group size decreased constituting the majority (43.72%) of the recorded vocalisations. This highlights the significance of vocalisations as a valuable tool for discerning an animal's emotional state and, consequently, assessing its response to stress.

In addition, research has shown that individuals' character traits can influence their stress response, with some individuals being more resilient than others. For instance, the bold-shy continuum, attributable to genetic changes in the stress axis, is associated with various traits such as aggressiveness, foraging behaviour, recovery time, and reaction to stress with shy individuals exhibiting higher basal and stress-induced cortisol levels (Gebauer *et al.*, 2023; Øverli *et al.*, 2007;

Susman *et al.*, 1999). In the context of animal behaviour research, boldness refers to a willingness to take risks and fearlessness in novel situations, while shyness is characterized by timidity or avoidance behaviour (Wilson *et al.*, 1994).

Although the literature on stress-coping styles in mammals is extensive, less is known about the relationship between stress-coping mechanisms and character in birds. Indeed, the analysis of the relationship between bird calls and character measures in this study adds depth to our understanding of avian stress response. Previous studies in birds suggest that those individuals exhibiting increased alarm calls under stressful situations may also demonstrate a bold, more exploratory nature in unfamiliar settings (Guillette & Sturdy, 2011). Hence, employing conspecific isolation as a stressor and the use of vocalisations as a metric for assessing the stress response in animals could provide a deeper understanding of the intricate relationship between character traits, stress response, and *FOS* gene expression in the hippocampus and HPA axis activation.

For this study, it is anticipated that conspecific isolation will trigger activation in the caudal hippocampus of young chicks, with a predilection for the DL hippocampus, a prediction informed by the research conducted by Takeuchi *et al.* (1996). The expectation is that the activation within the caudal hippocampus should be evident, reflecting behavioural and hormonal changes in response to isolation stress. Simultaneously, an increase in distress vocalisations is anticipated, serving as a behavioural manifestation of the experienced stress. Furthermore, I predict a physiological reaction characterized by elevated corticosterone (CORT) levels, which will be particularly pronounced in individuals identified as possessing a shy character.

## 3.2. Methods

### 3.2.1. Animals and housing

A total of 130 one-day-old broiler chicks, consisting of 65 males and 65 females were collected from Dalton Hatchery (Thirsk, UK) on three separate occasions: one batch of 46 and 2 batches of 42 animals on July 26th, August 2nd, and August 9th, 2022. Chicks were transported to Newcastle University in separate female and male boxes.

Upon arrival, chicks were housed in the Comparative Biology Centre Large Animal Unit (LAU) in separate pens for females and males. They were provided with *ad libitum* access to food and water and housed in two pens each one of 1.5 $m^2$, and equipped with bedding and enrichment materials, maintaining a room temperature between (RT) and heat lamps set at 27◦C as approved by the Animal Welfare and Ethical Review Body (AWERB) under the Project License PB536696A.

Individual weight and overall physical condition were evaluated on arrival and a subset of 30 chicks per batch (15 males and 15 females) were randomly selected and identified using

numbered leg rings. Birds were given two days to acclimatize to the arrival pens under a 14L:10D light cycle, with lights on at 4 a.m. and off at 6 p.m.

Chicks without leg rings were designated as companion birds and did not undergo any experimental procedures but accompanied the birds within groups B, C, and D (described below). At the end of the experiment, all birds, those involved in the experiment and their companions, were humanely euthanized using cervical dislocation, adhering to the Schedule 1 method.

### 3.2.2. Character assessment

Two days post-hatch, the animals underwent a behavioural assessment aimed at determining their individual personalities within a bold/shy spectrum. For logistical reasons, they were initially transferred from their arrival pen to an identical new pen, maintaining separate pens for males and females. On the same day, 30 chicks per batch, identified by leg rings, were individually transported to and from a designated test room in black plastic boxes to undergo the behavioural test.

The assessment took place in a soundproof chamber equipped with a plastic box (length: 0.71m, width: 0.44m, height: 0.38m) without a top, and a video camera positioned above it (approximately 20 cm above the box). The soundproof chamber was maintained at RT, with ambient background noise, and had lights turned off (except for the duration of the behavioural test).

Upon entering the test room, each bird was placed at the centre of the plastic box to undergo an open field (OF) test. The test started when the lights were switched on. Over a span of 1 minute, the bird's behaviour and vocalisations were recorded via video. After the test, the weight and physical condition of the birds were assessed. The birds were identified using non-toxic markers and returned to the home pen where they remained undisturbed for the next 4 days.

The recorded videos were analysed using BORIS version 8.19.3 for Windows. Latency to step, latency to vocalize, number of movements, and number of vocalisations were scored for each bird. Based on these scores, the birds were categorized along a continuum ranging from shy to bold. A ranking system was established using 4 parameters: the latency to step, the count of steps taken, the latency to vocalize, and the number of vocalisations. The top 15 most proactive individuals were considered bold individuals while the top 15 most reactive individuals were categorized as shy individuals similar to the methodology used in Gebauer *et al.*, 2023.

### 3.2.3. Stress induction

On day 10 post-hatching, beginning at 8:00 a.m., the birds underwent stress induction treatment in the same room as previously described. The stress induction consisted of conspecific isolation of individual chicks and their comparison to non-isolated birds. To achieve this, the animals were distributed into 5 different groups, and these groups were balanced across

experimental rounds according to the bird's character, sex, and the experiment's time of the day (Figure 3.1).
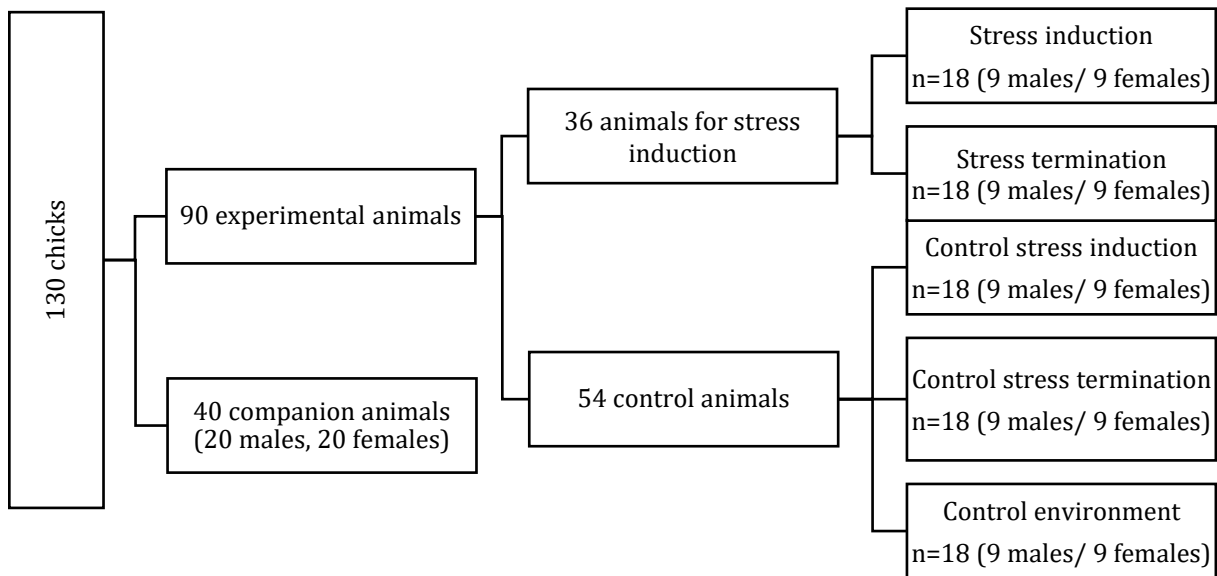


**Figure 3. 1.** Distribution of the animals into experimental, companion, and control groups.

**GROUP A** –*Stress induction group*- Birds were transported from their home pen in individual plastic boxes to the stress induction room. Once there, they experienced 20 minutes of isolation in a plastic box illuminated by a light source. Their vocalisations and movements were captured via video recordings. Following the stress induction, the chicks were immediately euthanized.

**GROUP B** –*Stress termination group*- Like Group A, birds from the home pen were placed in individual plastic boxes and taken to the stress induction room. These birds also underwent 20 minutes of conspecific isolation, with their vocalisations and movements recorded. Following the stress induction, the chicks were reunited with two companion birds for an additional 20 minutes before being euthanized. The companion birds were then returned to the pen while the isolated chick was immediately euthanized.

**GROUP C** –*Control stress induction group*- One experimental bird and two companion birds were moved from the pen to a separate area of the home pen room. These animals were placed in a box identical to the one used in the stress induction room. The group remained undisturbed within the box for 20 minutes. Subsequently, they were transported to the stress induction room where the experimental bird was euthanized immediately, and the two companion animals were returned to the home pen. By being in the same environmental conditions as the stress induction animals, they served as a control group to evaluate any effects caused by spatial context cues.

**GROUP D** –*Control stress termination group*- Like Group C, one experimental bird, and two companion birds were moved from the pen to a separate area of the home pen room. These

animals were placed in a box identical to the one used in the stress induction room. The group remained undisturbed within the box for 40 minutes. Subsequently, they were transported to the stress induction room where the experimental bird was euthanized immediately, and the other two companion animals were returned to the home pen. By being in the same environmental conditions as the stress termination animals, they served as a control group to evaluate any effects caused by spatial context cues.

GROUP E –*Control environment group*- Animals in this group did not receive any stress induction treatment, they were taken directly from the home pen into the stress induction room and immediately euthanized. By being euthanized directly after their transportation to the stress induction room, they serve as a control of any effects due to the change in spatial context during both stress induction and stress termination treatments.

The procedures of stress induction, euthanasia, brain dissection, and blood collection all occurred within the same room.

### *3.2.4. Vocalisation analysis*

The quantification of vocalisations was carried out using BORIS version 8.19.3 for Windows. For the analysis of vocalisations, distress calls (Figure 3.2, B) were differentiated from regular calls (Figure 3.2, C) and added to the software analysis as different behaviours. After adding behaviours, appropriate codes were assigned to each identified behaviour. The occurrence of the behaviours was recorded by selecting the corresponding coded key whenever they occurred during the video playback. To ensure accurate counting of behaviours, all videos were viewed at a playback speed of 0.800x.
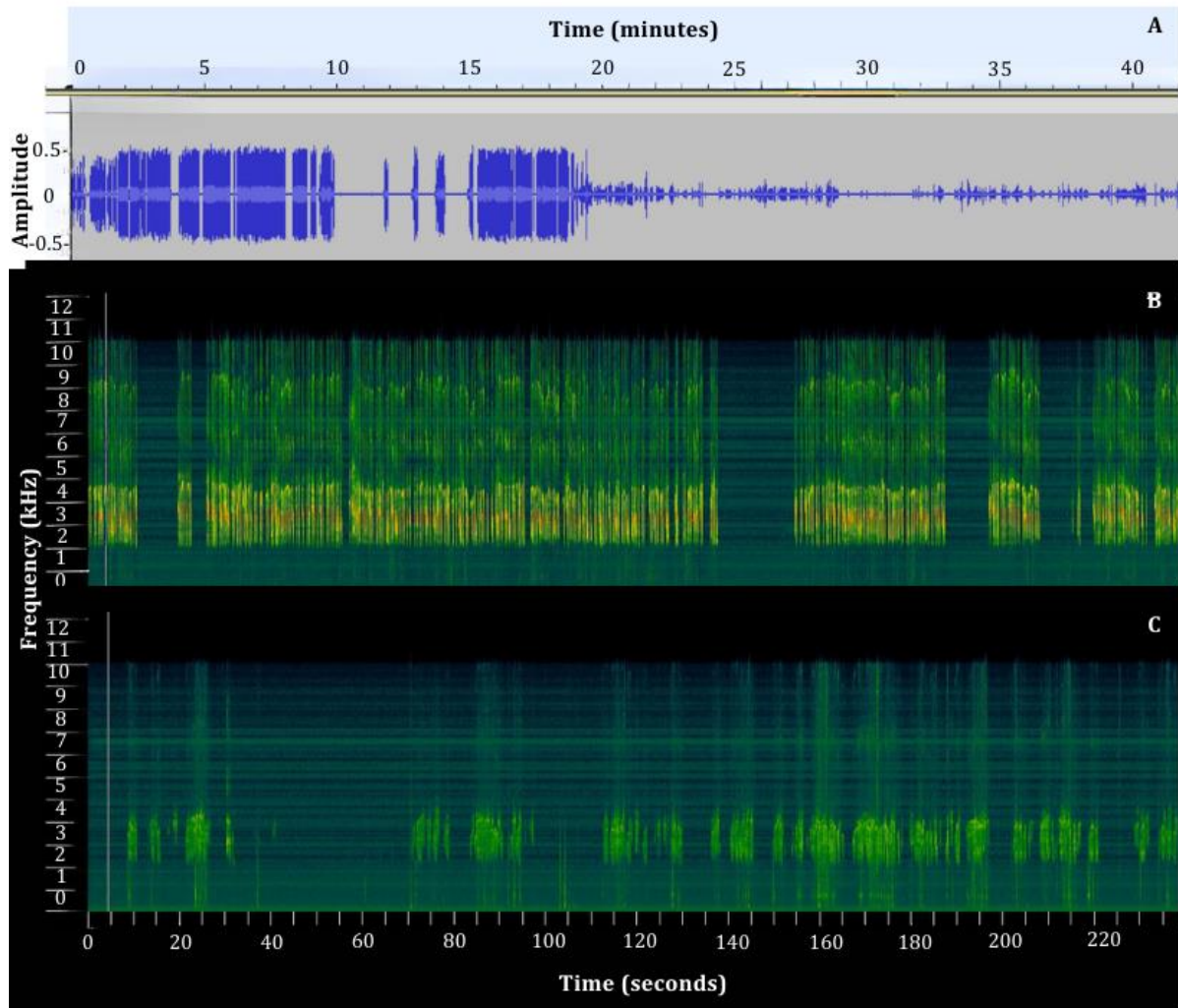
**Figure 3. 2.** The waveform diagram (A) illustrates chick vocalisations over 40 minutes, starting with a 20-minute isolation period followed by a 20-minute reunion with companions. The x-axis represents Time (seconds), and the y-axis shows Normalised Amplitude (unitless), ranging from -.5 to .5. Spectrograms of 20-second segments (B and C) detail distress calls during isolation (B) and regular calls during reunion (C). In these spectrograms, the x-axis represents Time (seconds), and the y-axis represents Frequency (Hz). Spectrograms were created using Kaleidoscope Lite (B and C) and the waveform diagram was created using Audacity (A) software.

A different approach was employed for videos with multiple chicks. Due to the rapid and frequent occurrence of calls, distress calls were quantified using the software codes while regular calls were manually counted using a clicker counter. The manual approach was preferred over the software due to the limited capacity of the software to accurately capture frequent calls, including occasional software crashes caused by rapid keyboard inputs.

The abovementioned process was consistently applied to every video encompassed within the study, guaranteeing a thorough and systematic evaluation of vocalisation occurrences. The execution of video analysis was entrusted to a placement student, Ellisa Foulkes, who remained blind to the experimental conditions of the video subjects. This approach further fortified the objectivity of the analysis.

### 3.2.5. Blood sampling and CORT levels

Blood samples were collected by allowing blood to flow directly into 1.5 ml Eppendorf tubes as drops fell from the site of decapitation. The tubes were promptly placed on fresh ice to maintain sample integrity until centrifugation.

Blood was centrifuged at 3000 rpm x 15 min to separate plasma from blood cells. Plasma was collected into a separate tube and plasma and blood cells were then placed in dry ice throughout the day and stored at -80 °C until used for the determination of CORT levels.

Plasma CORT levels were determined using the Corticosterone Enzyme-Linked Immunosorbent Assay (ELISA) kit from Enzo Life Sciences (ADI-900-097-96 well kit) as described in the methods section of Chapter 2. Furthermore, samples from various animals (n=5) were combined into pooled samples of high and low CORT responders (HR and LR, respectively), which were used across plates to standardize the data and account for any plate-specific variations.

Samples from different groups of animals (treatments) were evenly distributed across 3 plates and measured in triplicates. However, upon reviewing the results from the first two plates, some samples were identified as inconsistent between triplicates. To ensure accuracy, we decided to re-run those specific samples on a third plate. Interestingly, the third plate showed higher values for the pooled samples compared to the previous two plates which were consistent with each other. As a result, just like in the previous chapter, the values obtained from the pooled samples were averaged and a correction factor was obtained by calculating the ratio of the mean value of the pooled samples between plates. A correction factor of 0.655 was applied for the analysis of samples in the third plate containing repeated samples.

### 3.2.6. Tissue sample collection

The brain was extracted from the skull and sliced using a chilled and sterile tissue matrix (Electron Microscopy Sciences) and microtome blades (HP35 coated, ThermoScientific). Following the extraction of the brain, the pituitary gland was dissected immediately and collected in a 2ml RNAse-free Eppendorf tube, however, due to time constraints, results from the pituitary gland were not analysed and will not be reported in this thesis. Collected samples were immediately frozen using dry ice.

The brain was then placed within the matrix, ventral side facing upward, and oriented at the desired angle. The blades were positioned in the desired channels (target positions were -0.06 mm, 1.6mm, and 3.6 mm interaural) and brought down in a single fast movement. To remove the slices from the matrix, the blades were lifted at the same time. Following the removal of the blades, they were placed over an ice-cold metal platform and the slices were carefully detached from the blades and directly placed over the platform.

The regions of interest that were dissected include the caudal hippocampus (V, DM, and DL subregions), rostral hippocampus (V, DM, and DL subregions), the bed nucleus of the stria *terminalis lateralis* (BSTL), and capsular amygdala (CeC). The dissection of these regions was meticulously conducted using tissue punches (UniCore punches 1.00 mm, Qiagen) and the chick brain atlas by Puelles *et al.* (2007) as a reference (Figure 3.3). To avoid damaging the tissue and the quality of the samples, tools were kept ice-cold and cleaned using 70% ethanol and RNase Away decontamination solution (Thermo Fisher Scientific) between each animal.
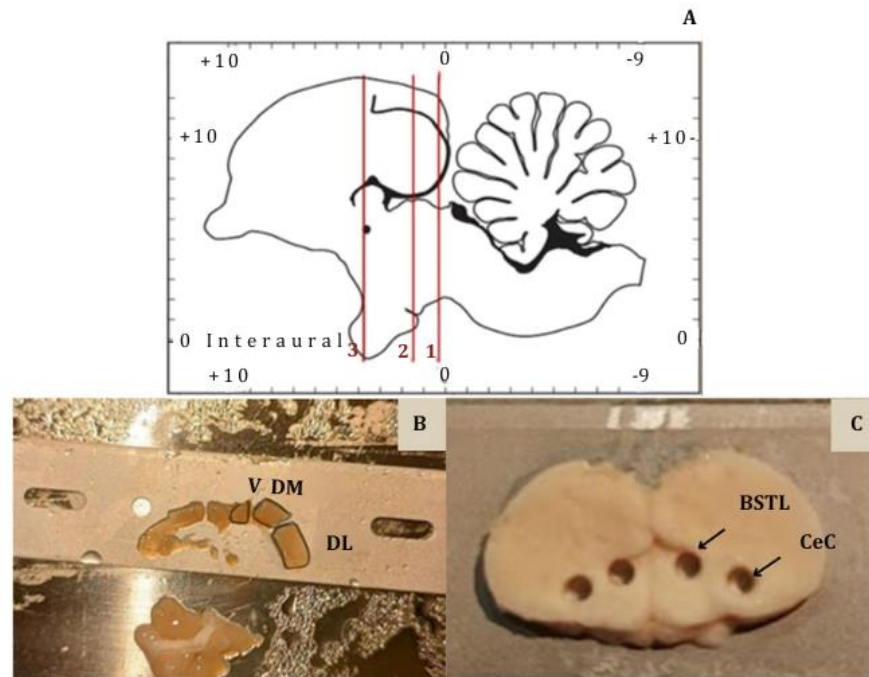


**Figure 3. 3.** Tissue collection. Tissue slices were collected using three blades along the longitudinal axis of the avian forebrain (A, marked by the red lines). Ventral (V), dorsomedial (DM), and dorsolateral (DL) hippocampal subdivisions were collected in left-right pairs of one punch for each region or by manually slicing it into three portions from both the caudal and rostral hippocampus (B), while the capsular amygdala (CeC) and the BSTL were collected using a single 1 mm tissue punch (C).

After extraction, tissue samples were placed within 2 ml Eppendorf tubes (RNase-free microcentrifuge tubes, Invitrogen) and transferred to dry ice. For long-term storage, the samples were stored at -80 °C until RNA extraction.

### 3.2.7. Quantitative real-time PCR

Due to time constraints, only a subset of the samples extracted from the hippocampal formation were processed for the qPCR analysis (n=24). For these samples, RNA extraction was performed from cryosections of both caudal and rostral regions using RNeasy® Plus Micro Kit (Qiagen) and gDNA eliminator mini spin columns according to the manufacturer's instructions.

Complete sample disruption was achieved by the addition of lysis buffer at RT for 25 minutes without any homogenization.

Reverse transcription was carried out using a 20μg RNA reaction mix and an Invitrogen® Superscript IV VILO Master Mix Kit (Invitrogen) following the manufacturer's guidelines. The generated cDNA was subsequently diluted 1.5x before use in the qPCR.

Quantification of mRNA levels was performed via qPCR, employing a *FOS* primer designed to amplify a target region of 120 base pairs (bp), the forward primer sequence was 5'-ACAGCCTCACCTACTACCCGT (positions 198-218 of accession number NM_204305.1) and reverse primer 5'-TCACGGTGGGCACGAAGTTG (positions 317-298 of accession number NM_204305.1). Glyceraldehyde 3-phosphate dehydrogenase (*GAPDH*) was used as the reference gene for normalisation. The *GAPDH* primer was designed to amplify a target region of 137 bp using the forward primer 5'-CTCCACCTTTGATGCGGGTG (positions 927-946 of accession number NM_204305.1) and the reverse primer 5'-TGGCTCACTCCTTGGATGCC (positions 1063-1044 of accession number NM_204305.1). Primers were designed by Alessandra Pross (IRB Lleida, Spain) using Primer-BLAST (NCBI, USA).

DNA standards were generated for absolute quantification using end-point PCR on brain tissue DNA for each gene. The resulting PCR products were purified from a gel using the MinElute PCR purification kit (QIAGEN) under the manufacturer's protocol. Standard concentrations were determined using a NanoDrop spectrophotometer (Thermo Fisher Scientific.) Serial dilutions of the standards were produced beginning with a 1:100 dilution followed by 5-fold dilutions.

Real-time qPCR was performed using a CFX-Connect qPCR cycler (Bio-Rad, UK) with an initial step of 95°C for 10 min, followed by 40 cycles of 95°C, 60°C and 72°C, each for 15 seconds. Reaction mixtures in 10μl volume included 4μl cDNA, 5μl SYBR mix (Meridian Bioscience SensiFAST SYBR No-ROX Kit), and 0.4μl (400 nmol) of each forward and reverse primer. In the no-template control, 4μl of cDNA was replaced by water. While the standard curve was run in singlicate, the samples were run in triplicate within an assay run. To ensure consistency and mitigate plate-to-plate variability affecting within-bird comparisons, samples were analysed in 6 different plates with samples corresponding to the same region (caudal hippocampus, 3 plates: V, DM, and DL; rostral hippocampus, 3 plates: V, DM, and DL). A melting curve analysis was performed to confirm the specificity of the reactions.

The results were evaluated as the ratio of the expression of *FOS* to that of the reference gene *GAPDH* in the same individual samples.

### 3.2.8. Statistical analysis

Prior to statistical analyses, the homogeneity of variances was assessed using Levene's test while a careful examination of the distribution of the normalised data was conducted using

graphical methods, including histograms. These steps were crucial in validating the appropriateness of the chosen statistical analyses and ensuring the reliability of the results.

Videos were analysed as follows: first, videos were analysed and the total number of calls for individuals and groups were recorded. Subsequently, to standardise the assessment, the number of calls per minute was calculated by dividing the total number of individual calls or the number of calls per group by the respective video length. Finally, for those animals that were in groups, the number of calls was also divided by three, accounting for the number of animals within each group.

A Generalized Linear Model (GLM) was used to compare groups C and D (20- and 40-min control groups), because of health complications, the sample size for group D was one fewer bird (n=35). Distress and regular calls were analysed separately, each analysis included two between-subject factors: treatment (2 levels: C and D) and character (2 levels: bold and shy). The statistical significance of the relationship was determined using P values derived from Wald's χ2 test statistics. A second GLM was used to compare vocalisations in group A against group C (isolated vs accompanied birds) using the same factors.

A Generalized Estimating Equations (GEE) model was used for the analysis of group B. For this analysis, the ID of the animal was included as a subject effect and treatment was analysed as a within-subject variable (2 levels: isolated and accompanied), while character was included as a between-subject variable (bold and shy).

For the analysis of CORT concentration values, a GLM was carried out in CORT (ng/ml) normalised data (logarithmic transformation base 10). The analysis included three between-subject factors (treatment 3 levels: isolation, companions, and home pen), plate (3 levels: plates 1 to 3), and character (2 levels: bold and shy). The statistical significance of the relationship was determined using P values derived from Wald's χ2 test statistics.

For the analysis of *FOS* gene expression, ratios obtained by dividing the expression level of each target gene by the expression level of the reference gene (*GAPDH*) were normalised using logarithmic transformation base 10. Original Ct values are provided in Annexes 2 and 3.

A GEE analysis was used to evaluate the relationship between treatments across the rostral and caudal hippocampus. The significance of the relationship was determined using P values derived from Wald's χ2 test statistics, while parameter estimates were obtained by a maximum likelihood approach. The analysis included one between-subject factor (treatment with 3 levels: control stress termination, stress termination, and stress induction), 2 within-subject factors (rostrocaudal position with 2 levels: caudal and rostral, and subregion with 3 levels: V, Dm, and Dl). In data preprocessing, values outside 3 standard deviations from the mean were identified as outliers and subsequently excluded from the analysis (n=2).

All analyses were performed using IBM SPSS Statistics version 28.0 for Windows (IBM Corp., Armonk, N.Y., USA). In all cases, statistical significance was accepted at p<0.05.

## 3.3. Results

### 3.3.1. Analysis of vocalisations

As a first step in analysing regular and distressed vocalisations, a GLM was used to examine any potential variations between the vocalisation patterns of the control groups. The 20-min control group (group C) was compared to the 40-minute control group (group D) revealing no statistically significant effect of the treatment on the number of distress calls ($X^2_{(1)} = 0.603$, p=0.437) but an effect on the number of regular calls ($X^2_{(1)} = 16.667$, p<0.001), with the 20-min group displaying a higher number of regular calls than the 40-min group (Figure 3.4). The character did not influence the number of both distress calls ($X^2_{(1)} = 3.150$, p=0.076) and regular calls ($X^2_{(1)} = 0.229$, p=0.632), nor was there a significant interaction between both factors (distress calls: $X^2_{(1)} = 1.577$, p=0.209, regular calls: $X^2_{(1)} = 2.175$, p=0.140).
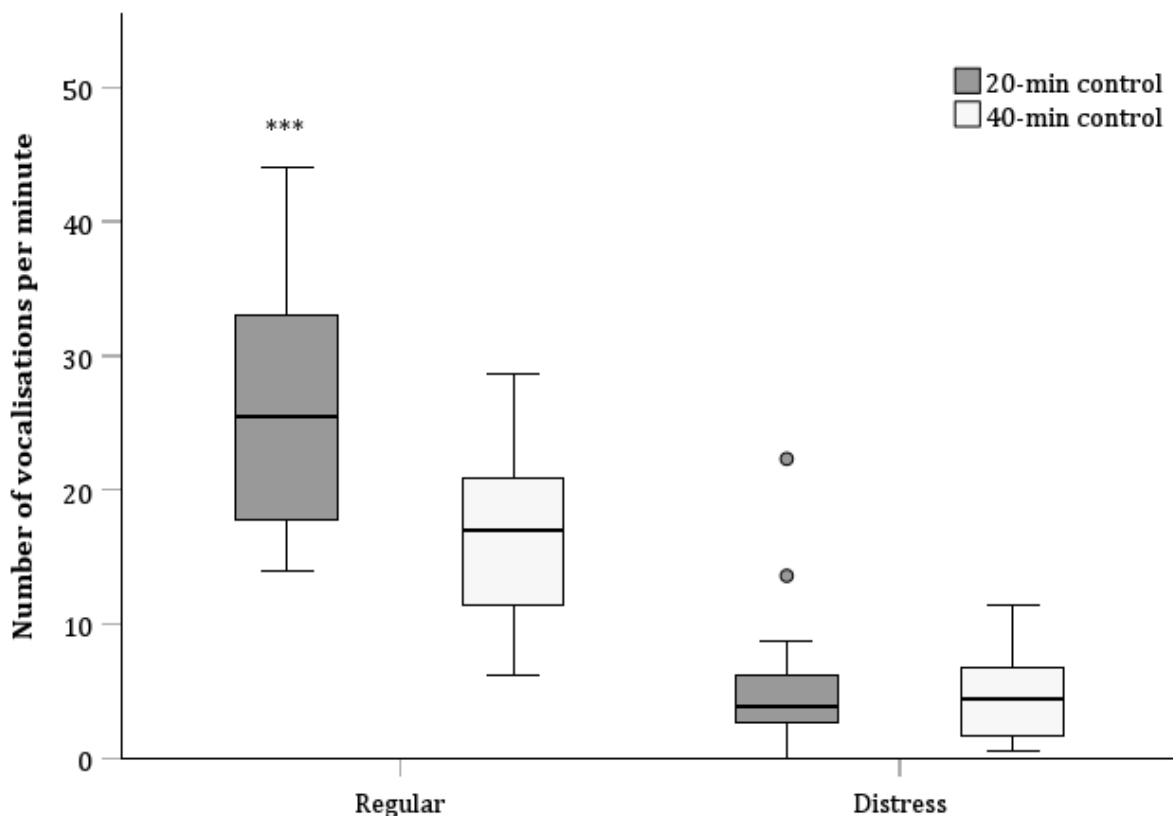


**Figure 3. 4**. Comparison of regular and distress calls in unstressed chick control groups following 20-min and 40-min call registrations.  The findings reveal that chicks produced more regular calls per minute during the 20-minute period compared to the 40-minute period. The box plot showcases the distribution of vocalisations, with the central box indicating the interquartile range (IQR) and the horizontal line inside the box representing the median value. The whiskers extend to the minimum and maximum values within 1.5 times the IQR from the first and third

quartiles, respectively. Points represent outliers (more than 1.5 times the IQR). Asterisks indicate significant differences against animals in the 40-min group (***p<0.001).

A second analysis involved the comparison of stressed isolated animals (Group A) versus their unstressed counterparts (Group C). The GLM analysis showed that stressed animals exhibited a notably higher number of distress calls compared to unstressed animals. The statistical analysis indicated a significant effect due to the treatment ($X^2_{(1)}$ = 50.290, p<0.001, with no influence of character as a factor ($X^2_{(1)}$ = 0.022, p=0.882). Similarly, the two-way interaction of treatment and character ($X^2_{(1)}$ = 0.583, p=0.445) demonstrated no effect on the number of vocalisations (Figure 3.5).

For the regular calls, there was a statistically significant effect of the treatment ($X^2_{(1)}$ = 122.186, p<0.001), where unstressed animals exhibited a higher number of regular calls than stressed animals. The effect of the character was not statistically significant ($X^2_{(1)}$ = 0.747, p=0.388), nor was the interaction between treatment and character ($X^2_{(1)}$ = 0.083, p=0.773) (Figure 3.5).
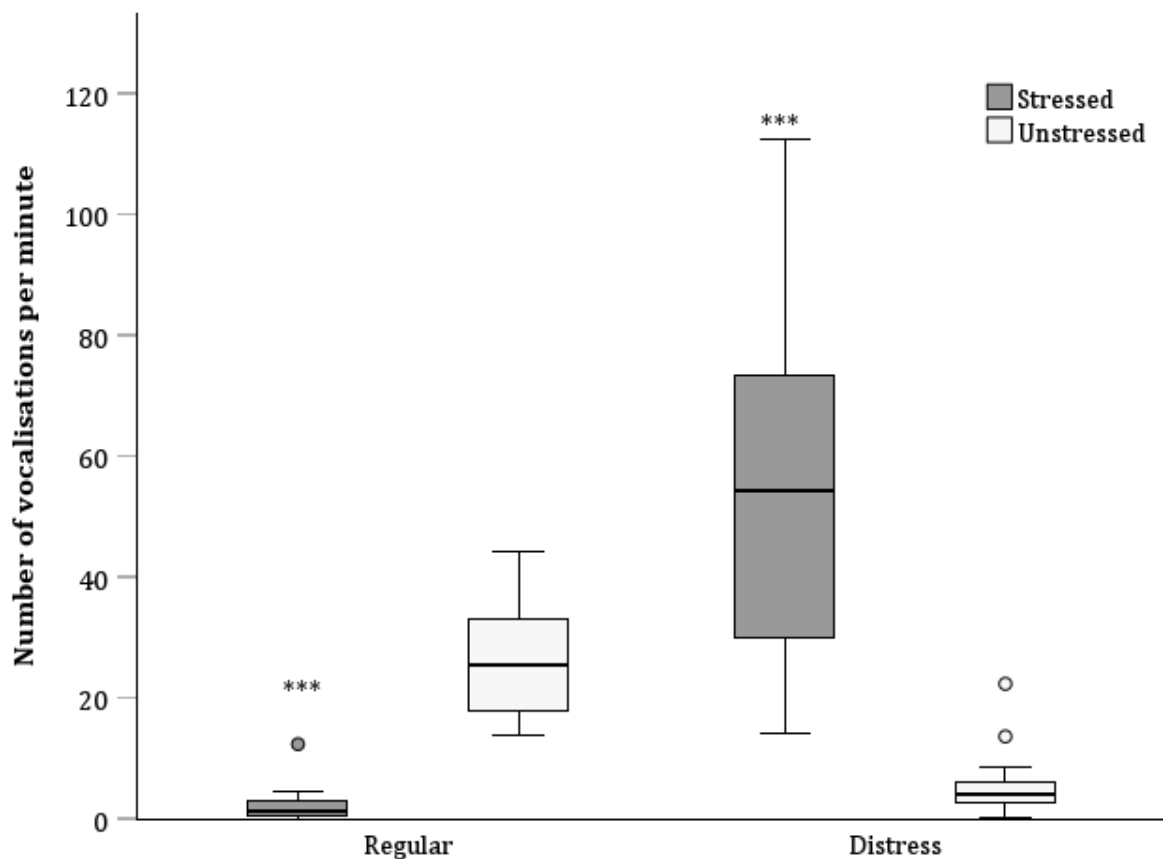


**Figure 3. 5**. Estimated number of regular and distress calls for stressed and unstressed birds. Results show a higher number of regular calls in unstressed animals and a higher number of distress calls in stressed animals. The box plot showcases the distribution of vocalisations, with the central box indicating the interquartile range (IQR) and the horizontal line inside the box representing the median value. The whiskers extend to the minimum and maximum values within 1.5 times the IQR from the first and third quartiles, respectively. Points represent outliers (more

than 1.5 times the IQR). Asterisks indicate significant differences against the control unstressed animals (***p<0.001).

The final analysis focused on group B, consisting of birds isolated for a 20-minute duration and subsequently reunited with companions. The GEE analysis revealed that the number of distress calls increased significantly when birds were alone. The substantial increase in distress vocalisations among birds in isolation was statistically significant due to the treatment ($X^2_{(1)}$ = 46.353, p<0.001) but not to the character ($X^2_{(1)}$ = 0.026, p=0.872). Additionally, the interaction between treatment and character was also not significant ($X^2_{(1)}$ = 0.009, p=0.923) (Figure 3.6).

An inverse effect was observed when analyzing the number of regular calls. When birds are reunited with companions there is an increase in the number of regular calls. While the effect of the treatment in this interaction was statistically significant ($X^2_{(1)}$ = 31.267, p<0.001), there was no effect of the character ($X^2_{(1)}$ = 0.223, p=0.636), and no interaction of the treatment and character ($X^2_{(1)}$ = 0.138, p=0.710) (Figure 3.6).
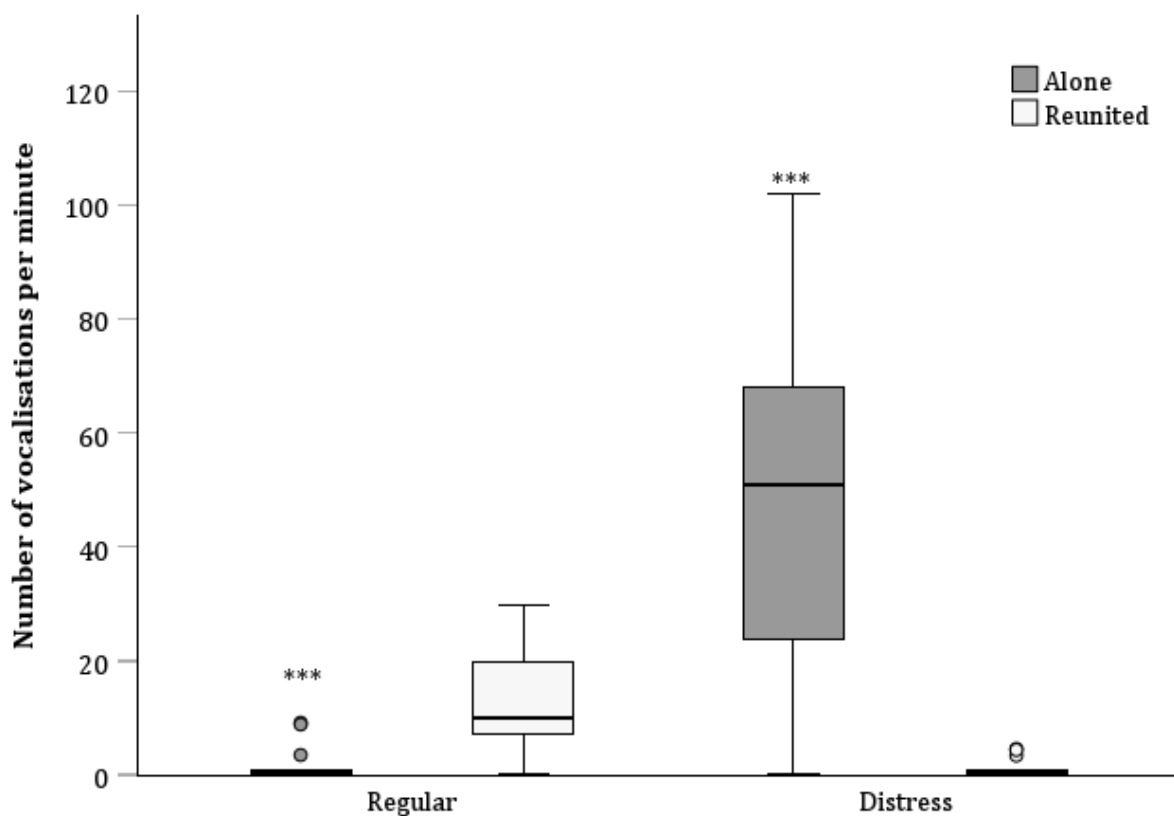


**Figure 3. 6.** Estimated counts of regular and distress calls emitted by animals during isolation and after reunion with companions. The findings reveal a higher number of regular calls among accompanied animals, contrasting with a higher occurrence of distress calls when animals are alone. The box plot showcases the distribution of vocalisations, with the central box indicating the interquartile range (IQR) and the horizontal line inside the box representing the median value. The whiskers extend to the minimum and maximum values within 1.5 times the IQR from the first and third quartiles, respectively. Points represent outliers (more than 1.5 times the IQR). Asterisks indicate significant differences against animals reunited with companions (***p<0.001).

### 3.3.2. Corticosterone analysis

As already mentioned, the study investigated CORT concentration (ng/ml) in birds subjected to different conditions: isolation (Group A), unstressed animals in the same environmental conditions (Group C), birds sampled directly from the home-pen without any interventions (Group E). The GLM analysis revealed a statistically significant main effect due to the treatment ($X^2_{(2)}$ = 7.031, p=0.030). This effect resulted primarily from elevated CORT levels in isolated animals against their unstressed control group (p=0.008). The interaction between isolated animals and those sampled directly from the home-pen did not result in a significant interaction (p=0.434) (Figure 3.7).

There was no effect due to the bird's character ($X^2_{(1)}$ = 0.030, p=0.862), but there was an effect due to the specific ELISA test plate used to analyse the samples ($X^2_{(2)}$ = 6.999, p=0.030) indicating variability between plates. Moreover, there were no statistically significant two-way interactions between character and treatment ($X^2_{(2)}$ = 0.034, p=0.983), character and plate ($X^2_{(2)}$ = 0.744, p=0.689), or plate and treatment ($X^2_{(4)}$ = 1.980, p=0.739). The three-way interaction between plate, character, and treatment ($X^2_{(3)}$ = 0.566, p=0.904) lacked statistical significance.
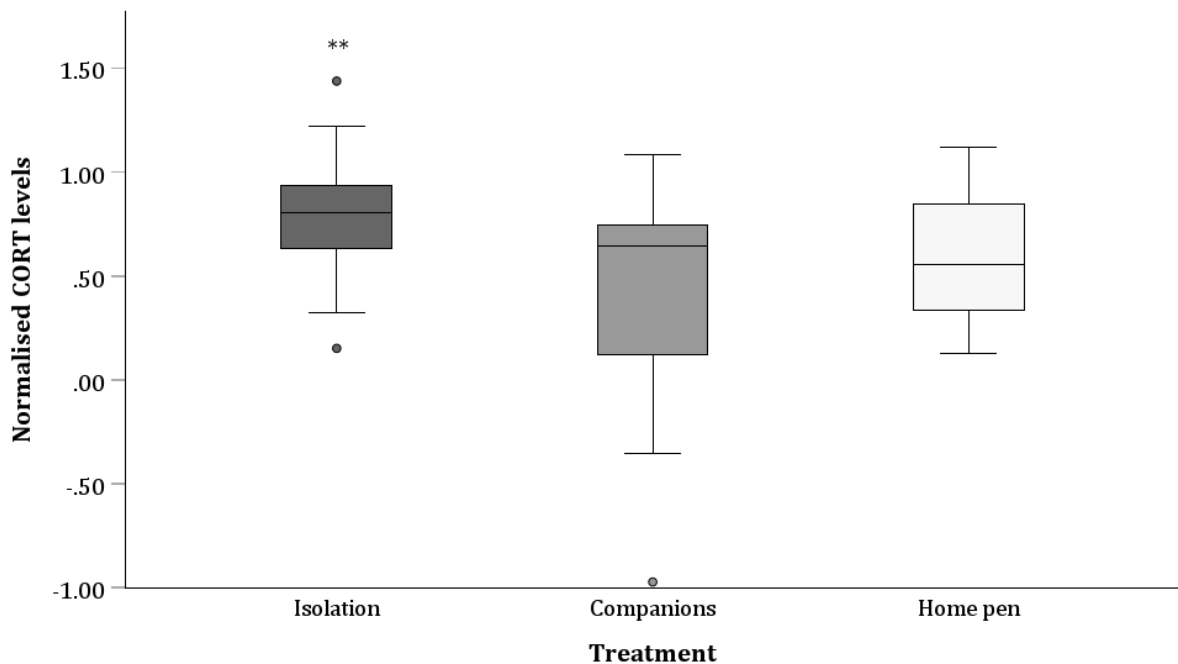


**Figure 3. 7**. Comparison of plasma corticosterone (CORT) concentration (ng/ml) between isolated chicks, chicks in the presence of companions, and unstressed chicks in their home pen. Results showed that under identical environments, isolated chicks exhibit higher levels of CORT in plasma when compared to chicks with companions. The box plot showcases the CORT levels with the central box indicating the interquartile range (IQR) and the horizontal line inside the box representing the median value. The whiskers extend to the minimum and maximum values within 1.5 times the IQR from the first and third quartiles, respectively. Points represent outliers (more than 1.5 times the IQR). Asterisks indicate significant differences against accompanied animals (**p<0.01).

### 3.3.3. Hippocampal FOS gene expression

A GEE analysis was employed to investigate the impact of the treatment, rostrocaudal level, and subregion on the expression of the *FOS* gene in the hippocampus. The analysis revealed a significant main effect due to the rostrocaudal level ($X^2_{(1)}$ = 6.683, p=0.010) and hippocampal subdivision ($X^2_{(2)}$ = 58.503, p<0.001). The caudal hippocampus exhibited the lowest *FOS* expression, with the V subdivision displaying reduced *FOS* levels compared to the DM and the DL subdivisions across both rostrocaudal levels.

Additionally, a significant main effect due to the treatment ($X^2_{(2)}$ = 10.760, p=0.005) was also observed, primarily due to an overall increased expression of *FOS* across the entire hippocampus in both the stress induction (p=0.009) and stress termination groups (p=0.002), which did not differ significantly from each other.

The analysis also revealed a significant interaction between the rostrocaudal level and the subdivision ($X^2_{(2)}$ = 30.550, p<0.001). The V subdivision exhibited lower *FOS* expression compared to the DM and DL subdivisions for both rostrocaudal levels. In the caudal hippocampus, the difference in the V subdivision is significant against the DL subdivision (p=0.001) and against the DM subdivision (p=0.029) which are not different from each other. For the rostral hippocampus, the difference in the V subdivision is significant against the DL subdivision (p<0.001) and against the DM subdivision (p<0.001) which also differ from each other (p<0.001) (Figure 3.8).

Moreover, the interaction between the rostrocaudal level and the treatment ($X^2_{(2)}$ = 9.811, p= 0.007) was also significant with the lowest *FOS* expression in both the caudal and rostral levels of the control group. In the caudal hippocampus, the stress induction group showed the highest *FOS* expression (p=0.018 *versus* control). In the rostral hippocampus, *FOS* levels decreased during stress induction (p=0.048) and they increased in response to stress termination (p<0.001) when compared to the control group, with the stress termination also statistically different from the stress induction group (p=0.030) and displaying the highest *FOS* levels.

However, when considering the combined effect of treatment and subdivision ($X^2_{(4)}$ = 9.811, p=0.739), as well as the three-way interaction among treatment, rostrocaudal level, and subdivision ($X^2_{(4)}$ =1.952, p= 0.745), no significant effects on the *FOS* expression was found.
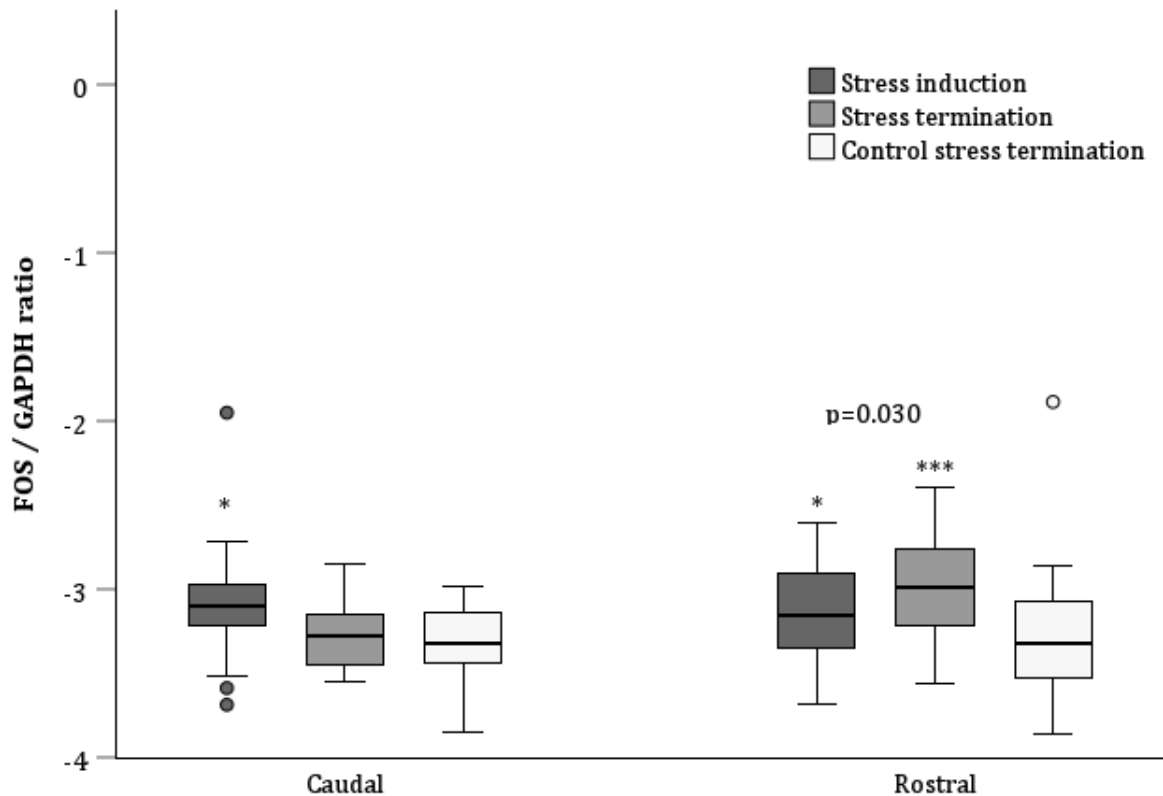
**Figure 3. 8**. Expression levels of *FOS* gene in the chicken hippocampus. Results show a higher expression of *FOS* in the caudal hippocampus during stress induction and a higher expression of *FOS* in the rostral hippocampus during stress termination. The box plot showcases the *FOS* gene expression in relation to the reference gene GAPDH with the central box indicating the interquartile range (IQR) and the horizontal line inside the box representing the median value. The whiskers extend to the minimum and maximum values within 1.5 times the interquartile range (IQR) from the first and third quartiles, respectively. Points represent outliers (more than 1.5 times the IQR). Values in the figure are not log-transformed ratios but rather represent the obtained ratios of the target gene's expression. Asterisks indicate significant differences vs the control group (*p<0.05; **p <0.01, ***p<0.001).

## 3.4.    Discussion

### 3.4.1.  Summary

In the present study, the aim was to detect the expression of the *FOS* IEG induced by social isolation and to map the hippocampal subregions involved in the stress response in the chicken brain. At the same time, efforts were made to address potential confounding factors related to spatial context, such as environmental novelty. The central hypothesis of this study was that the caudal hippocampus would exhibit higher *FOS* gene expression in response to stress termination, given its proposed role in the feedback regulation of the HPA axis. Additionally, recognizing the impact of character on stress reactivity, the analysis included an assessment of character, with the hypothesis that shy individuals would be more susceptible to isolation.

The effectiveness of the stress induction and its impact on the activation of the HPA axis was confirmed through the use of different indicators. First, there was a notable increase in distress vocalisations among the chicks subjected to the stress induction protocol. This behavioural response was consistent across both shy and bold chicks, indicating the effectiveness and overall stressfulness of the conspecific isolation treatment. Second, measurements of CORT levels in the blood revealed a significant increase in response to isolation, further corroborating the physiological response to acute stress.

In contrast to the methods employed in Chapter 2, the stress induction protocol, which entailed isolating 10-day-old chicks from conspecifics for a duration of 20 minutes, proved successful in eliciting a stress response. This stressor triggered distinct regional activation patterns within the hippocampus, as observed by significant differences between rostral and caudal levels with the activation of the caudal hippocampus during stress induction and the activation of the rostral hippocampus during stress termination. Interestingly, the rostral hippocampus also showed a reduction in *FOS* expression in response to stress induction.

### 3.4.2. *Social isolation as a stress induction method*

As a first approach, I set out to assess the efficacy of the stress response elicited by conspecific isolation. According to previous studies, young animals that exhibit social attachment experience painful feelings of separation manifested as intense and persistent distress vocalisations when isolated from their sources of social support (Panksepp *et al*., 1997). In the present study, the analysis of vocalisations between stressed and unstressed animals revealed a clear and consistent pattern: isolation led to an increase in distress calls and a reduction in regular calls, whereas social companionship resulted in the opposite effect with fewer distress calls and a noticeable increase in regular calls, however, these changes were not linked to shy or bold character types as hypothesized.

Distress calls, characterized by their loud and high-pitched nature, emerge within a week after hatching and gradually decrease with age (Takeuchi *et al*., 1996). Notably, my findings align with previous studies in birds, such as Marx *et al*. (2001), Sufka *et al*. (1994), and Takeuchi *et al*. (1996), which reported an increase in distress calls in response to isolation and a reduction or almost complete absence of any other type of vocalisation. This consistency across studies highlights the reliability of distress calls as an indicator of emotional distress and the overall emotional well-being of the chicks as proposed by Pereira *et al*. (2022).

Despite the proposition that distress vocalisations may be elicited in response to environmental unfamiliarity (Montevecchi *et al*., 1973), my findings challenge this notion. In identical novel environments, animals exhibited an increase in distress calls in response to isolation rather than the environment itself, as evidenced by the minimal number of distress vocalisations in the control group subjected to an unfamiliar environment.

This isolation-induced alteration in vocalisation patterns was further corroborated through a subsequent analysis involving birds isolated for 20 minutes and then reintegrated with their companions. Consistent with prior research, the analysis revealed a marked decrease in distress calls during the reintegration period (Kaufman & Hinda, 1961). This decrease in distress calls following reintegration suggests a potential relief from the stressful experience experienced by the previously isolated individual, a phenomenon known as social buffering. This concept refers to the ability of a conspecific's presence to alleviate an individual's stress response and has been previously demonstrated in chicks (Edgar *et al.*, 2015).

The increase in regular calls observed during social reunification also demonstrates the preference for regular vocalisations in a group setting, as expected. It is worth noting that my study did not distinguish between different types of vocalisations englobed as regular calls; however, other research has identified various call types linked to the social environment, including short peeps, pleasure notes, and warbles, with the latter being the most prevalent in group communication (Marx *et al.*, 2001). A detailed analysis of these regular calls and their characterization could provide valuable insights into the vocalisation dynamics of the animals during reunification and separation.

While regular calls were not subdivided by type, the comparison between the 20-minute and 40-minute groups provided further insights into the dynamics of the regular vocalisations in chicks. The 20-minute group exhibited a higher frequency of regular calls compared to the 40-minute group, suggesting that over time, animals' inclination towards social vocalisations decreases as they progressively acclimated to the novel environment and the alterations in the composition of their social group. It is important to note that, before the experiments, animals underwent a one-week habituation period to their home pens, during which they familiarised themselves with their companions. It has been established that the nature of the relationship between individuals plays a crucial role in determining whether social buffering of the stress response will manifest (Gust *et al.*, 1994; Loconsole & Regolin, 2022), and given that these animals were well-acquainted with each other, there was an expectation that their companionship would be able of buffering the stress response elicited by the novel environment.

Although the decrease in distress calls does not necessarily confirm a direct reduction in stress, the impact of the isolation treatment was also manifested in changes in the CORT levels. Previous research has shown that social species may display an 'isolation syndrome,' characterized by heightened stress responses in isolated individuals across various stimuli, including endocrine, behavioural, and autonomic indicators (Kikusui *et al.*, 2006). The present study's findings indicate that isolated birds exhibited significantly elevated CORT levels compared to unstressed birds with companions. These findings are consistent with existing literature showing increased CORT in response to conspecific separation in chicks (Feltenstein *et al.*, 2003).

In contrast to the stress induction method employed in Chapter 2, the conspecific isolation approach emerged as a robust and reliable means to induce stress in chicks, as evidenced by the distinct vocalisation patterns and the changes in CORT levels. Given the effective elicitation of the stress response, the subsequent step was to examine the changes in hippocampal *FOS* gene expression resulting from the induced stress response.

### 3.4.3. *Hippocampal regulation of stress in birds*

The exploration of hippocampal *FOS* IEG expression in this study revealed complex patterns influenced by treatment, rostrocaudal level, and hippocampal subdivision. The overall increased *FOS* expression in both the caudal and rostral regions highlights the crucial role of the hippocampus in regulating emotional responses in birds.

Contrary to the initial hypothesis, the current findings reveal the activation of the rostral hippocampus during stress termination, along with an inhibitory effect resulting from the stress induction treatment. Surprisingly, in the caudal hippocampus, expression of the *FOS* gene was observed in response to stress induction. These findings contradict the hypothesis that the rostral hippocampus, considered the avian equivalent of the septal hippocampus in rodents, would remain inactive as it is primarily linked to spatial navigation and episodic memory (Moser & Moser, 1998). Instead, the findings support the involvement of the rostral hippocampus in stress regulation in birds. This aligns not only with previous studies in mammals, which link the septal hippocampus to the regulation of emotional responses such as fear and anxiety (Carvalho *et al*., 2008; Maren *et al*., 1997) but also with findings in birds (Takeuchi *et al*., 1996) in which hippocampal activation in response to stress extends throughout the entirety of the rostral to caudal hippocampal formation, indicating the absence of a functional division.

Initially, considering the hippocampus's role in regulating the HPA axis via inhibitory feedback mechanisms, one might anticipate hippocampal activation only upon stress termination. However, the observed activation of the caudal hippocampus during stress induction prompts consideration of two plausible explanations: either the observed activity is in response to spatial processing and environmental novelty, or it engages in processing the stress stimulus itself, independent of its feedback function.

To discern between these possibilities, a comparison with a control group experiencing similar environmental conditions was provided in this study. If the activation of the caudal hippocampus was due to environmental novelty, similar levels of activation in both stressed and unstressed control groups would be expected, given their shared identical environmental contexts. This, however, was not supported by the analysis as the stressed animals exhibited statistically significant increases in activation compared to the control group.

As the activation pattern remained unique to stressed subjects, it strengthens the argument that the hippocampal activation observed in the current study is directly involved in the

processing of stress stimuli. This interpretation finds support in research on house sparrows, where similar activation patterns in the caudal HF correlate with approach-avoidance conflicts, indicative of anxiety or acute stress (Kimball *et al.*, 2022; Madison *et al.*, 2024). These findings also indicate a cross-species consistency in hippocampal activation under stress conditions, suggesting a more direct involvement of the hippocampus in emotional processing.

Regarding the inhibitory effect of stress induction observed in the rostral hippocampus, previous studies linking severe acute stress with stress-induced cognitive deficits might shed light on this finding. Research in mammals has shown that stress has profound cognitive effects, with acute stress extensively activating the CA1 region, which is pivotal for hippocampus-dependent memory, disrupting synaptic structure and function. Previous research in mice has demonstrated that acute severe stress can impair spatial memory (Yu *et al.*, 2018). This notion has been supported by studies indicating that acute stress impairs hippocampus-dependent memory, particularly during memory retrieval (Gagnon & Wagner, 2016). These effects tend to be more rapid and pronounced in young individuals compared to fully mature adults (Chen *et al.*, 2006). Moreover, stress's impact on cognitive functions tends to affect the septal CA1 region but not the temporal CA1 region which remains largely unaffected in response to stress (Maras *et al.*, 2014). In essence, the inhibition of the rostral hippocampus during stress induction may represent a mechanism by which the brain modulates its response to stress, prioritizing certain functions while temporarily dampening cognitive processing to cope with the immediate demands of the stressful situation.

Overall, these findings prompt a reconsideration of our understanding of the role of the hippocampus in emotional regulation. The activation of both the rostral and caudal hippocampus after an effective stress induction method challenges previous findings supporting the dominant perspective of a rostral-caudal functional dichotomy where manipulations of the mammalian temporal hippocampus (the potential equivalent of the avian caudal hippocampus) affect emotional responses (Fanselow & Dong, 2010; Henke, 1990; Kjelstrup *et al.*, 2002; Maren & Holt, 2004). Instead, it supports a functional organization as previously proposed by Strange *et al.* (2014) in which differences along the mammalian septotemporal axis (equivalent to the avian rostrocaudal axis) exhibit a gradient-like organization as supported by neuroanatomical and electrophysiological data (Amaral & Witter, 1989; Kjelstrup *et al.*, 2008), where both the caudal and rostral hippocampus could participate in emotional regulation.

Moreover, despite sharing a similar functional role, the activation of the rostral and caudal hippocampus does not overlap revealing a temporal distinction, manifested as differences in *FOS* gene expression occurring at different stages (during stress induction versus termination). These results suggest that the rostral and caudal hippocampus may have differential sensitivities and unique gene activation patterns during emotional responses, potentially influenced by variations

in anatomical connectivity along the longitudinal axis that have not yet been addressed in chickens.

### 3.5. Conclusion

This study successfully induced stress responses in chicks through conspecific isolation, revealing distinct regional *FOS* activation patterns in the hippocampus. The isolation method proved effective, as evidenced by increased distress calls, and elevated CORT levels. Contrary to expectations, the hippocampal *FOS* gene expression exhibited complex patterns, challenging the existence of a rostrocaudal functional dichotomy, with both rostral and caudal regions contributing to emotional regulation.

Findings prompt a reconsideration of the traditional understanding of the hippocampus's role in emotional regulation and challenge the existence of rostral-caudal functional dichotomy in the avian hippocampus resembling that existing in mammals. Instead, it supports a gradient-like organization along the rostrocaudal axis, emphasizing the need for a comprehensive understanding of hippocampal function integrating hippocampal neuroanatomy and functional studies to advance our understanding of the function of the avian hippocampus.

# Chapter 4. Hippocampal Connectivity Involved in Stress Regulation in the Chicken Brain

## 4.1.    Introduction

Stress regulation is a complex process that involves a network of neural circuits and pathways. By examining the connectivity of the key components involved, we can gain valuable insight into the shared mechanisms governing the stress response across species.

In previous chapters, I explored the mapping of the areas activated in response to acute stress in the chicken brain. I discussed the differences between the rostral and caudal regions of the avian hippocampal formation (HF) and the implications of c-Fos activation in each of these regions. This chapter presents the findings of the study on connectivity in the chicken brain with a particular focus on characterizing the connections between the hippocampus and the hypothalamic paraventricular nucleus (PVN) identifying any potential relay area between these two regions, if present.

As highlighted in Chapter 1, despite the apparent structural organisation differences between the HF of mammals and birds, comparative studies of the hippocampus consistently confirm its status as an evolutionarily conserved brain structure, featuring homologues across vertebrate taxa (Bingman *et al.*, 2009; Striedter, 2016). This notion stems from its shared origin in amniotes (Medina & Abellán, 2009) and a generally conserved function, particularly in its role in spatial memory processes (Muzio & Bingman, 2022; Salas *et al.*, 2003).

Moreover, the mammalian and avian HF share similar connectivity patterns including extra-hippocampal connections linking the HF to the lateral septum (SL) and medial septum (SM), hypothalamus, the lateral part of the bed nucleus of the stria *terminalis lateralis* (BSTL), the nucleus of the diagonal band (NDB), amygdala, the brainstem monoaminergic nuclei, and telencephalic sensory processing regions (Atoji & Wild, 2004, 2006; Bingman *et al.*, 2009; Bouillé *et al.*, 1977; Casini *et al.*, 1986, Herold *et al.*, 2019; Krayniak & Siegel, 1978), while intrahippocampal connections within the avian HF are reminiscent of the trisynaptic circuit found in the mammalian hippocampus (Kahn *et al.*, 2003). Nevertheless, direct comparisons between avian and mammalian hippocampal subdivisions and precise interpretations of their functional roles in stress regulation remain largely unresolved.

In the early 1980s, studies in rodents by Fischette *et al.* (1980, 1981) were among the first to focus on the temporal and septal hippocampal differences in mammals, suggesting that the temporal hippocampus played a role in glucocorticoid regulation. Their research showed that fimbria-fornix lesions, which disrupt temporal subicular efferents, altered the circadian rhythmicity of plasma corticosterone (CORT) levels. Posterior investigations found that cytotoxic lesions or pharmacological inactivation of the temporal hippocampus, but not the septal

hippocampus, had anxiolytic effects with minimal effect on spatial learning (Bannerman *et al.*, 2003; Kjelstrup *et al.*, 2002; Moser *et al.*, 1995). In contrast, septal hippocampus lesions affected spatial learning without affecting anxiety-related measures. Additional support for this functional differentiation in mammals came from the discovery that place cells, which contribute to spatial representation of the environment, are more abundant in the septal hippocampus relative to the temporal hippocampus (Jung *et al.*, 1994; Royer *et al.*, 2010).

Today, the temporal hippocampus of mammals is recognized as an important site for the control of emotional behaviours including anxiety (Adhikari *et al.*,2010; Bannerman *et al.*, 2003; Felix-Ortiz *et al.*, 2013; Jimenez *et al.*, 2018; Kheirbek *et al.*, 2013), fear (Kjelstrup *et al.*, 2002), and stress (Herman *et al.*, 1998, 2003; Herman & Cullinan, 1997; Herman & Mueller, 2006; Mueller *et al.*, 2006; Radley & Sawchenko, 2011).

Anatomical studies suggest that the temporal subiculum, in particular, is responsible for the control of hippocampal inhibition of the Hypothalamic-Pituitary-Adrenal (HPA) axis in mammals (Herman *et al.*, 1998; Mueller *et al.*, 2004, 2006). There is, however, no evidence of a direct projection from the temporal subiculum cells to the PVN (Swanson & Cowan, 1977) suggesting the existence of one or more neuronal relays between the HF and the PVN with numerous studies supporting the bed nucleus of the stria *terminalis* (BST) as an intermediary structure connecting the temporal HF to the PVN (Avery *et al.*, 2014; Cole *et al.*, 2022; Cullinan *et al.*, 1993; Gergues *et al.*, 2020; Herman & Cullinan, 1997; Larsen *et al.*, 1994; Ulrich-Lai & Herman, 2009). While evidence of the temporal subiculum's role in stress regulation in mammals is well documented, the same cannot be said about the chicken brain.

Understanding the connectivity of the avian hippocampus is crucial in comprehending its regulatory role on the HPA axis. As reviewed by Striedter (2016), data on the intrinsic and extrinsic connections of the hippocampus in birds come mainly from studies in pigeons (Erichsen *et al.*, 1991; Krebs *et al.*, 1991; Székely, 1999; Kahn *et al.*, 2003; Atoji & Wild, 2004, Herold *et al.*, 2019) which vary widely in the number of proposed hippocampal subdivisions, the rostrocaudal levels of interest, the boundaries between divisions, and in the nomenclature employed.

Although 50 years have passed since Bouillé and Baylé (1973 a,b,c) proposed an inhibitory role of the HF in regulating the HPA axis in birds, the specific hippocampal connectivity and subdivisions involved in this process remain largely unexplored. Their research on pigeons (*Columba livia*) demonstrated that hippocampal lesions disrupt the circadian rhythm of CORT secretion, leading to sustained elevated levels throughout the day. Additionally, electrical stimulation of the HF led to significant suppression of plasma CORT levels (Bouillé & Baylé, 1973b), affirming its inhibitory role in HPA axis regulation.

Anterograde tract-tracing studies have confirmed direct connections from the avian HF to various hypothalamic regions, including the lateral hypothalamus, medial and lateral septal nuclei, nucleus of the diagonal band, and BST (Atoji *et al.*, 2002, 2006; Atoji & Wild, 2004; Casini

*et al.*, 1986; Herold *et al.*, 2019; Székely & Krebs, 1996). While a recent investigation in pigeons proposes a direct link from the HF to the PVN (Herold *et al.*, 2019) the evidence in chickens is absent and details regarding the subregional origin of such a connection remain to be explored. Moreover, it is plausible that communication between the HF and the PVN may rely on indirect pathways, akin to mammalian models, potentially including pathways via the septum and the BST.

Furthermore, there is a notable gap in retrograde tracing studies between the avian PVN and the hippocampus. For this reason, this study aims to elucidate the pathways communicating the HF and the PVN using three different approaches: *in vivo* tract tracing injections, *ex vivo* organotypic slice cultures, and an exploratory investigation involving the production of avian adeno-associated viral (AAV) vectors. The *in vivo* tract-tracing approach involves fluorescent tracers being injected into the hippocampus to label axonal projections from the hippocampus to other brain regions such as the BSTL and the PVN (anterograde), as well as from those brain regions back to the hippocampus (retrograde). The *ex vivo* organotypic slice culture method involves the preparation of brain slices from chicken embryos, which were then injected with an anterograde tracer in the hippocampus and a retrograde tracer in the PVN. Lastly, the exploratory study involving the production of avian AAV vectors aims to develop a new tool for studying transsynaptic connections in the chicken brain.

Drawing parallels to mammalian counterparts, the chicken hippocampus is anticipated to send projections to the avian BST, in turn, the BST may also communicate the hippocampus with the PVN. At a rostrocaudal level, this communication should originate at the level of the caudal hippocampus and not from the rostral hippocampus supporting the existence of a functional gradient homologous to mammals (Smulders, 2017). At a subregional level, this communication should involve the dorsolateral (DL) subregion given its proposed homology to the mammalian subiculum (Abellán *et al.*, 2014; Erichsen *et al.*, 1991; Kahn *et al.*, 2003; Székely & Krebs, 1996). Overall, it is expected that the combination of tracing techniques will provide a more comprehensive understanding of the neural circuits involved in hippocampal-mediated stress responses in the chicken brain.

## 4.2. Methods

### 4.2.1. Tract-tracing experiments

A series of studies were undertaken to investigate the connections between the hippocampus and other brain regions associated with stress regulation in the chicken brain, particularly focusing on the PVN. These studies combined *in vivo* tract tracer injections conducted at Newcastle University and *ex vivo* tracing in organotypic slice cultures performed during an academic secondment in collaboration with the IRBLleida in Spain. In addition to these approaches, the study considered using AAV for neuronal tracing. Preliminary steps to establish

and optimize this tracing protocol were initiated at Newcastle University and are described in the following sections.

### 4.2.1.1. In vivo tract-tracing injections

#### 4.2.1.1.1. Animals

A total of 22 Lohmann Brown laying hens (*Gallus gallus*) of 46 weeks of age were collected from Lintz Hall Farms (Newcastle Upon Tyne, UK) on March 15th, 2021. After arrival, animals were habituated to the new environment for two weeks. The hens were housed at the Comparative Biology Centre Animal Unit at Newcastle University following the Home Office code of practice, under the project license number PB536696A. The birds were maintained on a 15.5L:8.5D lighting schedule (lights off at 10 pm), provided with *ad libitum* access to food and water, and offered various environmental enrichment materials including nest boxes, hay, perches, and hanging enrichment.

The animal unit consisted of 2 rooms, namely R1 and R2. Initially, animals were housed together in R1. The second room, R2, was designated for hens to stay overnight before undergoing surgical procedures and later as a post-surgical recovery room. To ensure proper recovery of animals in R2, 2 separate pens were available. Companion animals were housed in R2 only to accompany the hens in recovery.

#### 4.2.1.1.2. Surgical preparation

Before the surgical procedures, preliminary experiments were conducted on March 22nd (n=1, carcass) to determine the precise positioning of the hens' heads in the stereotaxic frame. Subsequently, a stereotaxic injection procedure involving the precise positioning of the hens' heads in the stereotaxic frame, followed by injections of Fluoro-Ruby (FR) into the rostral and caudal hippocampus as well as the BSTL, and injections of green Retrobeads™ into the PVN and BSTL, was performed on a total of 8 adult Lohmann Brown laying hens according to the procedures outlined in the next sections. Surgeries were performed on March 29th (n=2), May 10th (n=2), June 28th (n=2), and July 15th (n=2) of 2021, the rest of the birds were used as companion animals and rehomed at the end of the experiment.

The night before each surgery, hens (two at a time) were food-deprived and transferred to a focal pen at 10 p.m. On the day of the experiment, the hens were transported to the surgery room in carrier boxes where they were weighed before the surgery. All surgical procedures were conducted with the assistance of the Comparative Biology Centre (CBC) veterinary team and carried out in conjunction with Dr Tom Smulders, who performed the stereotaxic injections.

### 4.2.1.1.3. Anaesthesia

Anaesthesia was initiated using an induction mask containing 8% sevoflurane mixed with oxygen. Immediately after, the birds were intubated, with lidocaine applied to the glottis beforehand, and the intubation tube was secured to the beak.

Anaesthesia was maintained throughout the procedure with a continuous delivery of 2.4-4% sevoflurane at a rate of 0.5-1 L/min. Additionally, butorphanol was provided at intervals (2 hours) during surgery. In addition, an intravenous saline drip (3 mg/kg/h) with a port for drug administration was placed into the medial metatarsal vein and hens were placed on a temperature-regulated homeothermic blanket and covered with a surgical drape. Before starting, the absence of reflexes was confirmed by administering a comb pinch.

### 4.2.1.1.4. Stereotaxic procedure

The stereotaxic frame was disinfected with alcohol before use. The anteroposterior (AP) axis was zeroed using the ear bars as a reference. The bird was then positioned in the stereotaxic frame and feathers from the comb to the neck were shaved and removed via vacuum. The head was positioned relative to the stereotaxic frame using a 46° plate.

The incision site was cleaned using Hydrex spray (Ecolab), and following a second confirmation of the anaesthesia, an incision was made from behind the comb to behind the ear bars. Sterile clamps were used to keep the incision open, and cotton or blue roll twists soaked in saline were used to stem the bleeding and prevent the skin margins from drying out.

The periosteum was scraped, the skull was cleaned and the mediolateral (ML) zero point was calculated by measuring the midpoint between two points (the skull is the same height on a ML axis). Once localized, the zero point was marked using a sterile marker.

### 4.2.1.1.5. Tracer injections

Before the surgery, coordinates were estimated by meticulously examining cresyl-violet stained slides obtained from adult hens. These estimations were made by comparing the observed anatomical landmarks with the chick brain atlas by Puelles *et al.* (2007). The estimated coordinates for the regions of interest are shown in Table 4.1.

| Table 4. 1. *Estimated locations of the regions of interest in adult hen brain.* | | | | |
|---|---|---|---|---|
| | Anteroposterior | Mediolateral | Dorsoventral | Angle |
| **Rostral hippocampus** | 1.84 | 5 mm | 0.22 mm | 0° |
| **Caudal hippocampus** | 0.64 | 3.83 mm | 0.65 mm | 0° |
| **BST** | 3.28 | 5.2 mm | 8.2 mm | 0° |
| **PVN** | 3.28 | 2.29 | 11.38 mm | 11.34° |

Nevertheless, it is important to note that these coordinates were subjected to adjustments on the day of the surgery. This adaptation was necessary due to inherent variations in the size and shape of the adult hen skulls, variations were noticed while calculating the zero-point as described before.

After locating the injection coordinates using the stereotaxic touchscreen display and marking them on the skull directly above the target area, a small hole with a diameter of 1.4 mm was carefully drilled using an engraving burr attached to an electric drill. One hole was drilled at a time, with the next hole drilled only after the injection and coverage of the previous hole was completed.

For the injections, a Nanoject II™ (Drummond Scientific) automatic injector was employed. The injector was carefully preloaded with mineral oil and used in conjunction with pulled microinjection capillary tubes each measuring 3.5-inch length and designed for the Drummond Nanoject™ II. The preparation of these capillary tubes involved using the Narishige Glass Microelectrode Puller PE-2 with the coil adjusted to 6.5 to achieve a slender and elongated taper. To ensure the functionality of the Nanoject, a quality check was performed before insertion. This involved testing the Nanoject on a white piece of filter paper to confirm the absence of any clogs or impediments guaranteeing the reliability of the injection process.

For anterograde tract tracing, FR (Dextran, Tetramethylrhodamine, 10,000 MW, Invitrogen™) was injected into the hippocampus (rostral or caudal) and the BSTL of the adult hen brain. Pressure injections were performed with a 15% FR solution dissolved in sterile saline. Simultaneously, for retrograde tracing, green Retrobead™ fluorescent latex microspheres (Lumafluor Inc.) were administered into the PVN of the hypothalamus and in the BSTL. The green retrobeads were used as supplied by the manufacturer.

With the dura exposed, the injector was attached to the stereotaxic frame and moved to the zero point on the skull (AP and ML) before advancing to the specific coordinates of the regions of interest. By touching the dura, the dorsoventral (DV) was also zeroed. The injector was pulled up and the dura was pierced using a hypodermic needle before inserting the injector.

The loaded micropipette was gently lowered into the brain at a pace of 1mm every 30 seconds, followed by the activation of the Nanoject inject button. Each time the "inject" button was pressed, a predetermined volume of 0.05 µL was dispensed. To ensure thorough tracing, multiple injections were administered at each location, these were delivered with a minimum interval of 2 minutes between injections.  The maximum volume of tracer injected at any site was 0.3 µL.

### 4.2.1.1.6. Post-injection procedure

After each injection, the glass micropipette was left in place for 5 minutes before its careful removal. The surgical site was meticulously cleaned, and the cranial hole was sealed with bone wax.

Following the removal of the surgical clamps, the margins of the skin were anaesthetized with lidocaine in preparation for suturing the scalp. Next, the animal was gently released from the ear bars and extubated. Any mucus within the trachea was removed using a vacuum.

### 4.2.1.1.7. Post-operative protocol

After the surgical procedure, a mask connected to $O_2$ was placed over the bird's head while its overall state was monitored, and the bird was awake. Before transporting the bird to the recovery room (R2), the bird was visually monitored by a team of veterinarians until the bird exhibited unrestricted movement and appeared free from pain and distress.

To mitigate postoperative pain and discomfort, comprehensive peri-surgical care was administered on the day of surgery and the subsequent 6 days. The approach included the use of specific medications: Butorphanol (2 mg/kg) for post-surgery pain management, meloxicam (1 mg/kg) as a non-steroidal anti-inflammatory drug to alleviate inflammation and pain, enrofloxacin (10 mg/kg) to prevent bacterial infections, and dexamethasone (0.5 mg/kg) to prevent inflammation and reduce swelling in the brain. These interventions were implemented following the recommendations provided by the veterinary team and coupled with daily visual assessments to monitor signs of pain or distress.

Throughout the experiment, the welfare of the animals was a top priority. All hens that underwent surgical procedures exhibited smooth recoveries and the postoperative assessments, including daily visual observations and interventions, revealed no signs of acute pain or distress in the days following the surgeries. The applied analgesia and antibiotics effectively minimised postoperative discomfort, ensuring the well-being of the animals throughout the recovery period. On the seventh day post-surgery, the birds were reintegrated into their home cage alongside companions.

### 4.2.1.1.8. Perfusion

After 4 weeks, the birds were anaesthetized with a combination of Ketamine (40mg/kg) and Xylazine (8mg/kg) and underwent a perfusion procedure. For this, the absence of reflexes was confirmed, and the animal was cannulated to deliver a mix of Propofol (14 mg/kg), Fentanyl (30 µg/kg), and heparin (1mL 5000 IU). After confirming the anaesthesia a second time, the thoracic cavity was opened to allow visualisation of the beating heart.

Briefly, the abdominal wall was incised at the base of the sternum, and the sternum itself was gently reflected by cutting through the sternal ribs, and the ventral ligaments connecting to

the stomach and liver. With the heart exposed, the pericardial sac was removed, a small incision was made into the left ventricle, and the blunt perfusion needle was inserted into the ascending aorta. Once in place, it was securely clamped using a haemostat.

Perfusion was initiated using a Watson Marlow Sci Q 400 pump. Initially, a washout buffer solution (500 mL, 0.9% Saline solution in $dH_2O$) was circulated at the pump's velocity on level 3 to clear residual blood. A small incision in the liver lobes facilitated exsanguination. Upon completion of the washout buffer, the perfusion line was changed into the fixative solution (500 ml, 4% paraformaldehyde (PFA) 0.1 M phosphate buffer (PB) pH 7.4, with the pump speed adjusted to level 1. Fixation was confirmed by the appearance of fixation tremors, and the perfusion was completed once the fixative solution was fully circulated.

### 4.2.1.1.9. Brain extraction

The brain extraction process began with the opening of the top of the skull allowing for a clear view of the brain's surface and securing the head in the stereotaxic apparatus to provide stability and precision while cutting the brain using a #24 scalpel at an angle of 46 degrees at the level of the cerebellum. This was done to ensure a consistent reference point for the subsequent sectioning aligning the plane of section with the orientation of the ML and DV planes during surgery.

The brain was trimmed from bone and the dura and meninges attachments to the skull were carefully removed. The extracted brain was immersed in the fixative solution for an additional 24 hours at 4 °C. After this period, the brain was immersed in 30% Sucrose in PB 0.1 M until it sank. The fixed brain was embedded in an optimal cutting temperature (OCT) compound and stored at -80 °C until cryostat slicing.

### 4.2.1.1.10. Brain processing

Cryoprotected brains were sliced into 3 series of slices at a thickness of 40 μm using a cryostat (Leica CM1860) at -20°C. Slices were treated as free-floating and counterstained using 300 nM DAPI (4', 6-diamidino-2-phenylindole, ThermoFisher) before mounting using Vectashield antifade mounting medium without DAPI (Vector Laboratories), except for the brains extracted from the first two surgeries which were mounted using Vectashield Antifade Mounting Medium with DAPI (Vector Laboratories) and without the additional counterstaining step.

Mounted brains were coverslipped and visualized using a fluorescent Leica DM-LB microscope and employing objective magnifications of 40× and 100x, and eyepiece magnification of 10x. A digital camera (Optronics, MicroFire™) was used for image capture.

### *4.2.1.2. Production of Avian Adeno-Associated Viral Vectors*

Plasmids for A3V vector generation (plasmids expressing the genes of interest: pA3V-RSV-EGFP, pA3V-RSV-mCherry, plasmid Rep-Cap: pA3V-RC, and plasmid Helper: pAd12) were obtained from the Department of Biological Sciences at Kyoto University (Japan) in collaboration with Dr Dai Watanabe. Detailed information about these plasmid constructs is available in Matsui *et al.*, 2012. The transformation, transfection, and purification processes were carried out under the supervision of Dr Lei Huang at Newcastle University (UK), while tracer injections were conducted under the supervision of Dr Tom Smulders.

#### *4.2.1.2.1. Cell culture*

All cell culture procedures were conducted using human embryonic kidney 293T cells (ATCC, UK) within a microbiological safety cabinet while employing aseptic techniques to maintain sterility. These procedures were approved by the Biosafety Sub-Committee of Newcastle University. Cell culture incubations were performed in a humidified environment at 36.7°C with 5% $CO_2$ unless specified otherwise.

The day before transfection, cells were split 1:3 using T25 cell culture flasks (Sarstedt). They were cultured in complete Dulbecco's Modified Eagle's Medium (DMEM complete, Merck) supplemented with 10% v/v Fetal Bovine Serum (FBS, Sigma Aldrich), 4 mM L-alanylDMEM -L-glutamine (Sigma Aldrich), and 1% penicillin-streptomycin (Sigma Aldrich).

After confirming 80% confluency under the microscope, the medium was discarded, and cells were rinsed once with 0.05% Trypsin-PBS solution. After gently rocking the flask a few times to ensure even coverage, the solution was quickly discarded to prevent cell detachment.

Cells were trypsinized again by adding 0.05% Trypsin-PBS solution and incubated for 5 min. After confirming cell detachment under the microscope, complete culture media was added to neutralize trypsin. After pipetting back and forth to obtain a single-cell suspension without clumps of cells, the resulting suspension was transferred to a 50 ml Falcon tube for centrifugation.

Finally, cells were centrifuged at 1200 rpm for 5 min and the resulting pellet was resuspended in complete culture media for a 1:5 ratio split. Cells were seeded into new T25 flasks and incubated for 24 h.

#### *4.2.1.2.2. Cell transfection*

Transfection was carried out in batches of ten T-75 flasks (Sarstedt). A transfection complex was prepared, consisting of viral plasmid DNA and Polyethyleneimine (PEI, 150 mM, pH 7) solutions, prepared in separate tubes using a 1:1:2 molar ratio (Helper plasmid pAd12, RC plasmid pA3V-RC, A3V plasmid coding the gene of interest mCherry or EGFP) and diluted in 0.95% saline solution. The diluted PEI was added to the diluted DNA and vortexed briefly. The transfection complex was left to incubate at room temperature (RT) for 15 min before use.

After confirming 80% cell confluence under the microscope, plated cells were trypsinized and resuspended as described previously, with the exception that approximately 2 ml of the previous medium was retained in each flask. The cell suspension was seeded into new T25 cell culture flasks containing pre-warmed (at 37°C) serum-free DMEM.

The transfection complex was added dropwise to the flasks and the flask was gently rocked to disperse the medium evenly. Cells were then incubated for 72 h, and 24 h post-transfection, the medium was replaced with DMEM complete medium.

### 4.2.1.2.3. *Iodixanol gradient purification*

To initiate purification, cells were scraped from the cell culture flasks along with the supernatant. The resulting solution was transferred to a 50 ml centrifuge tube. Cells were centrifuged at 1580 x rcf (rfc, relative centrifugal force) for 10 min at 4°C., and the supernatant was discarded. The cell pellet was resuspended in PBS (Gibco™ PBS Tablets, 1X), transferred to a new 50 ml centrifuge tube, and centrifuged at 1580 x rcf for 10 min at 4°C. After discarding the supernatant, the pellet was frozen at -80 °C until further processing.

Continuing the protocol, the pellet was lysed in 4 cycles of thawing and refreezing using a bead bath at 37.6 °C and an ice pellet bath, respectively. After the last thaw, the pellet was sonicated using 4 x 1-second pulses for a total of 9 seconds at a 20% duty. The lysate was kept on ice to prevent overheating.

Next, the lysate was incubated with benzoase 0.05 U/µl final concentration (Merck) for 45 min and then centrifuged at 2800 x rcf for 5 min at 4°C. The supernatant was collected and transferred to a 1.5 ml Eppendorf tube for an additional centrifugation step, lasting 30 min at 3500 x rcf at 4°C. The resulting supernatant was collected and stored at -80°C until iodixanol processing.

The collected supernatant was purified through an Iodixanol (OptiPrep) gradient ultracentrifugation. For this, 4 conical open-top centrifuge tubes of 15 ml (Corning™ Falcon™) were prepared with 60% Iodixanol in 1M NaCl/PBS-MK buffer for the 15% concentration tube and with 60% Iodixanol and 1X BS-MK buffer for the 25% and 40% concentration tubes. The 60% concentration tube was prepared using 60% Iodixanol and 0.45% phenol red.

The gradient was loaded by overlaying each solution from the highest to the lowest concentration. The viral supernatant was added as the final layer on top of the gradient.

Before ultracentrifugation, the tubes were carefully balanced using 1x PBS to top off the tube and adjust the weight. Tubes were centrifuged using a Beckman Coulter Optima L-80 XP Ultracentrifuge at 40,000 g for 3 hours in a SW 41 Ti rotor at 4 °C.

After centrifugation, the tubes were punctured slightly below the 60-40% interface with an 18 g needle attached to a 10 mL syringe with the bevel of the needle facing the 40% gradient. Approximately 1.5 mL were collected per tube, taking care to avoid collecting the proteinaceous

material at the 40-25% interface. The collected fractions were pooled together and stored overnight at 4°C.

The following day, the solution was concentrated using Vivaspin 20 (Sartorius) and 1X PBS containing 0.001% Pluronic F-68 (Sigma-Aldrich). The viral solution was clarified by centrifugation at 18 x g for 5 min and stored at -80 °C until used.

### 4.2.1.2.4. AAV administration to adult hens

Two brown laying hens of 20 weeks of age were collected from Lintz Hall Farms (Newcastle Upon Tyne, UK) and used in a pilot study assessing the efficacy of virus transduction in chicken brain cells. Only AAV-mediated GFP expression was assessed.

Animals were housed at the CBC Animal Unit at Newcastle University following the Home Office code of practice. Birds were kept on a 14L:10D lighting schedule, and provided with unrestricted access to food and water, and environmental enrichment materials such as nest boxes. Animals were given a two-week habituation period to the new environment before undergoing the stereotaxic procedures.

The surgical preparation, anaesthesia administration, and stereotaxic surgical procedures were identical to those outlined in the *in vivo* tracer injection protocol. However, there were differences in the tracer injections for this study. Specifically, a Hamilton syringe was used to inject the viral vector suspension and a single injection of the tracer was administered into the hippocampus in the coordinates in Table 4.2. The same post-injection and post-operative procedures were applied as previously described.

| Table 4. 2. *Coordinates for the injection of viral vector suspension in the rostral and caudal hippocampus of adult hens.* | | | |
|---|---|---|---|
| | Anteroposterior | Mediolateral | Dorsoventral |
| **Rostral hippocampus** | 1.8 | 4.4 mm | 0.22 mm |
| **Caudal hippocampus** | 0.5 | 3.87 mm | 0.65 mm |

Following an 8-week survival period, chickens were deeply anaesthetized and underwent transcardial perfusion for the extraction of the brain.

### 4.2.1.2.5. Tracer analysis

Dissected brains were sliced into 100 μm-thick sections using a cryostat. These sections were collected as free-floating slices and washed 3 times in PBS before being mounted. Slides were coverslipped using Vectashield antifade mounting medium without DAPI (Vector Laboratories). Fluorescent images were captured using a ZEISS Axioscan 7 microscope with a 10x magnification and processed using Zen Blue software (Zeiss Group).

### 4.2.1.3.    Ex vivo organotypic slice cultures

#### 4.2.1.3.1.  Animals

The eggs used in the study were incubated at the Institute of Biomedical Research in Lleida, Spain (IRBLleida), overseen by Alessandra Pross and following the methodologies outlined in Pross *et al.* (2022). The protocols used were approved by the Committees of Ethics for Animal Experimentation and Biosecurity of the University of Lleida (reference no. CEEA 08-02/19), as well as that of the Catalonian Government (reference no. CEA/9960 MR1/P3/1 for embryos, and CEA/9960 MR1/P4/1 for post-hatchlings).

Briefly, fertilized domestic chick eggs (*Gallus gallus;* Leghorn strain) were obtained from a commercial hatchery (Granja Santa Isabel, Cordoba, Spain). Incubation conditions were maintained at a temperature of 37.5°C and a relative humidity of 55%–60%, with periodic rocking. The initiation of incubation marked the first embryonic day (E0).

#### 4.2.1.3.2.  Tracer application and slice culture

Embryos between embryonic day 16 (E16) and 18 (E18) were selected for the study (N = 42). On the day of the experiment, eggs were carefully removed from the incubator and prepared for the procedure. Anaesthesia induction was achieved by creating a small hole in the eggshell, followed by an incision in the membrane at the level of the air sac. The eggs were then placed in an anaesthetic chamber infused with Halothane (2-Bromo-Chloro-1,1,1-trifluoro-ethane, Sigma-Aldrich, 1 ml Halothane/1,000 ml of chamber volume) for a duration of 10 to 15 min. Successful anaesthesia induction was confirmed by the absence of motor responses in the embryo.

Anaesthetized embryos were decapitated, and their brains were quickly extracted from the skulls. Extracted brains were immersed in ice-cold sucrose-substituted Krebs solution (240 mM sucrose, 3 mM KCl, 3 mM $MgCl_2$, 23 mM, $NaHCO_3$, 1.2 mM $NaH_2PO_4$, 11 mM D-glucose) oxygenated with carbogen (95% O2, 5% $CO_2$). After 10 min, the brains were sliced coronally at the level of the anterior commissure using a chilled, sterile tissue matrix (Electron Microscopy Sciences) and microtome blades (HP35 coated, ThermoScientific). Slices were promptly transferred onto the stage of a dissecting microscope. To maintain their viability, slices were supported by a porous membrane (Millipore 0.45 μm pore size) and located inside a chamber containing artificial cerebrospinal fluid (ACSF; 119 mM NaCl, 2.5 mM KCl, 1.3 mM $Mg_2SO_4$, 1.0 mM $NaH_2PO_4$, 26.2 mM $NaHCO_3$, 11 mM D-glucose, 2.5 mM $CaCl_2$) while on under the dissecting microscope.

Target sites for injections were identified using anatomical landmarks and chick brain atlas by Puelles *et al.* (2007) as a reference. Retrograde tracing was conducted by placing biocytin crystals directly in the PVN, while anterograde tracing was achieved via microinjections of diluted Texas Red (TR, dextran, 3000 MW, Invitrogen) in two different subregions of the hippocampus:

ventral (V, n=10) and the DM-DL boundary (n=10). The selection of these specific regions of interest was based on findings derived from the density maps outlined in Chapter 2, alongside similar observations from prior studies (Takeuchi *et al.*, 1996). Before injecting, TR pure lyophilized powder was diluted in heated (40-50 °C) phosphate-buffer saline (PBS) at a maximum solubility of 100 mg/mL and introduced to the tissue using glass capillary tubes pulled into fine needles. For both crystals and the microinjections, only one application of the tracer was done per site.

After the injections, the slices were maintained for approximately 6 hours in a chamber containing ACSF at RT and oxygenated with carbogen, the ACSF was replaced every 30 min. Brains were then transferred to a room at -20°C. In this room, slices were fixed for four hours by immersion in 4% PFA in 0.1 M PB (pH 7.2) followed by immersion into a cryoprotective 30% sucrose solution until they sank.

### 4.2.1.3.3. Chromogenic staining

Cryoprotected slices were sectioned into 3 consecutive series of 100 μm-thick sections with a freezing sliding microtome (HM 450, Thermo Scientific) and processed as free-floating sections.

Slices containing biocytin were incubated in an avidin-biotin-peroxidase complex solution (Vectastain Elite ABC Kit, Vector Laboratories). First, slices were washed 3 times for 10 min in PBS 0.3%, and endogenous peroxidase activity was inhibited in 5% $H_2O_2$ and 10% methanol in PBS for 30 min. Then, the tissue was washed with PBS 3 times for 10 min, followed by incubation in ABC solution for 1 hour at RT. The Vectastain solution was prepared 30 min before use following the manufacturer's instructions.

After the incubation period, the sections underwent 2 rinses in PBS 0.3% each for 10 min, followed by an additional wash in Tris 0.05 M pH 7.6 for 10 min. Finally, slices were immersed for 10 min in DAB (3, 3'-diaminobenzidine, Sigmafast, Sigma-Aldrich) diluted in Milli-Q water, following the manufacturer's instructions. Slices were then rinsed 3 times in Tris 0.05M pH 7.6 for 10 min.

Processed slices were mounted on gelatin-coated slides, dehydrated and cleared via alcohol and xylene, and finally, coverslipped using Permount (Fisher Scientific). One of the series was counterstained with toluidine blue 1% at a pH of 4.6.

### 4.2.1.3.4. Fluorescent staining

Texas Red (TR) is inherently fluorescent without requiring additional staining. Biocytin, on the other hand, needs to be stained to be visualized. This staining can be achieved through chromogenic methods, as described in the previous section, or through fluorescent staining, as discussed in this section.

The cryoprotected brain slices were sectioned into 3 consecutive series of 100 μm-thick sections using a cryostat (Leica CM1860) at -20°C and processed as free-floating sections. Slices containing both TR and biocytin were washed 3 times for 10 min each in PBS 0.3% and incubated in a solution of iFluor 488 streptavidin conjugate (Stratech) at a 1:500 dilution. This solution had been previously prepared by diluting iFluor 488 in a mixture of 1% Bovine Serum Albumin (BSA) and glycerol at a 1:2 ratio.

After a 2-hour incubation period, the slices were washed 3 times in PBS 0.3% for 10 min each before mounting using Vectashield antifade mounting medium without DAPI (Vector Laboratories). Selected sections were counterstained with 300 nM DAPI (ThermoFisher) before coverslipping to facilitate the visualisation of nuclear DNA and aid in the anatomical description of the tract-tracing procedure.

### 4.2.1.3.5. Image analysis

Digital microphotographs from chromogenic experiments were captured using a ZEISS Axioscan 7 microscope with a 10x magnification. For images derived from fluorescent material, a fluorescent microscope (Zeiss AxioImager with apotome) was used with objectives of ×100 and ×40.

To ensure optimal image quality, adjustments were made to the brightness and contrast, and images were processed using Zen Blue software (Zeiss Group). The analysis of images and the anatomical descriptions were conducted through visual examination and using the chick brain atlas by Puelles *et al.* (2007) as a reference.

## 4.3. Results

### 4.3.1. In vivo tract-tracing injections

Despite careful adherence to the established protocol, the stereotaxic injections in the adult Lohmann Brown laying hens did not yield the intended results. Microscopic examination of the processed brain slices showed the successful detection of the retrograde green Retrobeads™ and the anterograde FR tracer signals following visualisation under the fluorescent Leica DM-LB microscope. However, the tracers failed to diffuse adequately from the injection sites within the targeted brain regions preventing the visualisation of the neural fibres and pathways of interest and hindering any meaningful analysis of the connectivity.

Several challenges were encountered throughout the surgical procedure. The variability in the size and shape of the adult hen skulls posed difficulties in precisely locating the injection coordinates and the adaptation of coordinates on the day of surgery did not compensate for these inherent anatomical variations, leading to inaccurate placements of the tracers and making it

impossible to replicate the coordinates of target sites between surgeries. Additionally, at least one brain revealed spillage of the tracer as the pipette was retracted from the injection site (Figure 4.1, B) and one more completely lacked any signs of tracer which could be attributed to a possible occlusion of the injection pipette during the surgical procedure.

After the surgery, limitations in the microscopic analysis significantly impacted the interpretation of the results and added a layer of complexity to the experimental findings. First, the microscope utilized for this study, despite its capabilities, proved inadequate for the detailed visualisation of the tracer diffusion and neural fibres. The lack of clarity and resolution in the images obtained hindered a comprehensive analysis of the tracer spread within the brain tissue. Second, the lack of discernible fibres in the examined brain sections posed a question on the effectiveness of the chosen tracers for this experimental setup, particularly for the selection of the anterograde tracer.

The injection sites of the anterograde tracer (FR) revealed signs of tissue damage (e.g., holes, spill, and breakage), indicating possible oedema (Figure 4.1, C). The presence of oedema suggested an inflammatory response at the injection sites, which could have influenced the diffusion patterns of the tracers. This observation raises concerns about the potential impact of tissue damage on the accurate assessment of neural connectivity and emphasizes the need for meticulous selection not only of the type and amount of tracer injected but also of the injector used for this procedure.

The unsuccessful outcomes and challenges faced highlighted the need for a change in the tracing strategy and the incorporation of innovative techniques to account for anatomical variability and tracer diffusion issues to ensure the precise mapping and analysis of neural pathways in the targeted brain regions. The refinement in tract-tracing procedures and microscopic examination involved the contemplation of viral tracing methods to circumvent the problems of diffusivity and multiple injections, as well as the adoption of *ex vivo* tract-tracing methods coupled with the addition of a higher-resolution microscope and appropriate imaging equipment.
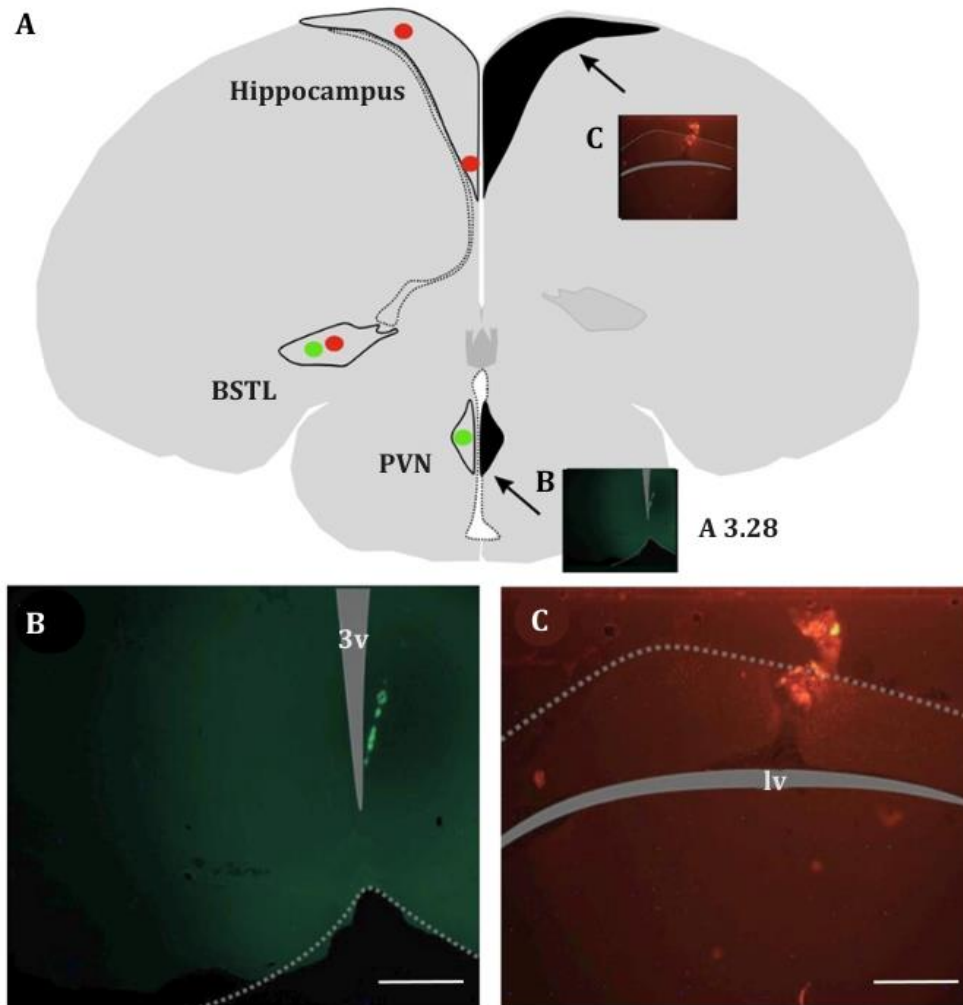
**Figure 4. 1**. Overview of the targeted injection sites. Retrograde Retrobeads™ (green) and anterograde Fluoro-Ruby (FR) (red) tracing within the chicken hippocampus (anterograde tracer), the bed nucleus stria *terminalis lateralis* (BSTL, both anterograde and retrograde tracers), and the paraventricular nucleus of the hypothalamus (PVN, retrograde tracer) (A). In some cases, spillage of the tracer occurred during the injection process as indicated by the presence of the tracer along the route of the micropipette injection (B). Tissue holes were found in some of the brains and could indicate localized tissue oedema (C). The scale bar represents 100 μm. A indicates the approximate anteroposterior (AP) position described in the chick brain atlas by Puelles *et al.* (2007).

### 4.3.2. Production of Adeno-Associated Viral (AAV) Vectors

Upon analysis, the brain sections from the AAV-administered hens revealed distinct and robust green fluorescent protein (GFP) expression within the injection site confirming the success of the gene delivery and expression process and establishing a reliable experimental approach for viral-tracing studies on the avian brain. Labelled cell bodies and fine dendritic processes were mainly found in the hippocampus near the injection site (DL region) and in the V subregion. Scattered GFP-positive neurons were found in lower quantities bilaterally across the SL. No labelled cells were found near or in the PVN.

The specificity and intensity of GFP expression demonstrated the efficient transduction of hen brain cells by the AAV vector 8 weeks after the injection of A3V-RSV-EGFP (Figure 4.2)
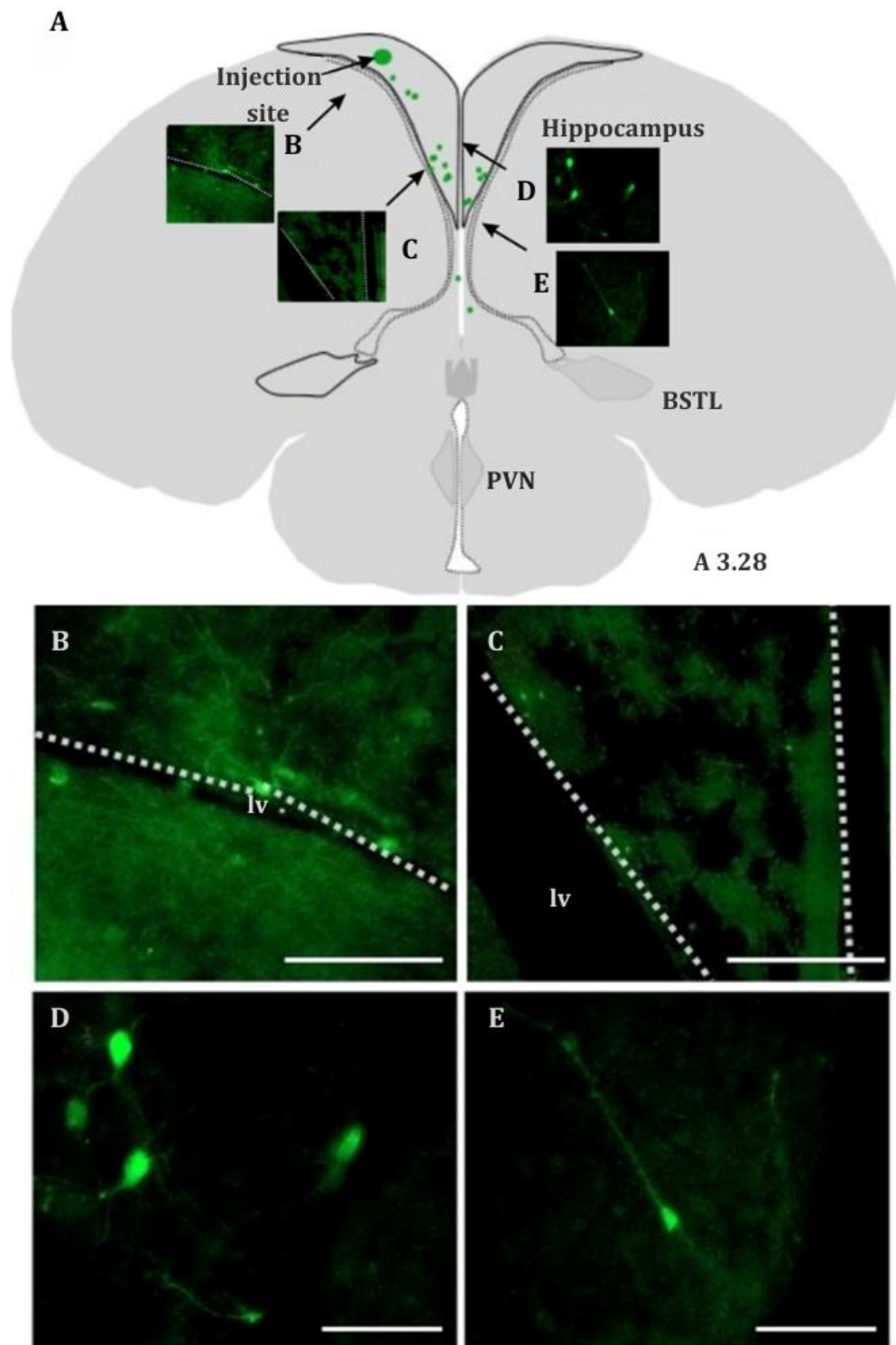


**Figure 4. 2.** The diagram shows the approximate location of stereotaxic injections. Injections of A3V-RSV-EGFP were applied into the dorsolateral (DL) subregion of the hippocampus of adult hen (A). Injections resulted in the labelling of hippocampal neurons near the site of the injection (B) and into the ventral (V) subregion of the hippocampus reaching the septum (C). Higher magnification images (D-E) show labelled cell bodies of neurons. Scale bars: B-C 100 μm and D-E 25 μm. A indicates the approximate anteroposterior (AP) position described in the chick brain atlas by Puelles *et al.* (2007).

### 4.3.3. Ex vivo organotypic slice cultures

#### 4.3.3.1. Anterograde tracing

Anterograde microinjections of diluted TR dextran amine tracer were applied to 20 brains, successful application was achieved in 12 out of the 20 brains targeting the V subdivision (n=5) and the DM-DL intersection of the hippocampus (n=7) (Figure 4.3). It is worth noting that the ventral injection, due to its proximity to the lateral ventricle and the small injection site, posed a greater challenge compared to the injection in the DM-DL intersection.

**B**

Hippocampus

Texas red

PVN

Biocytin
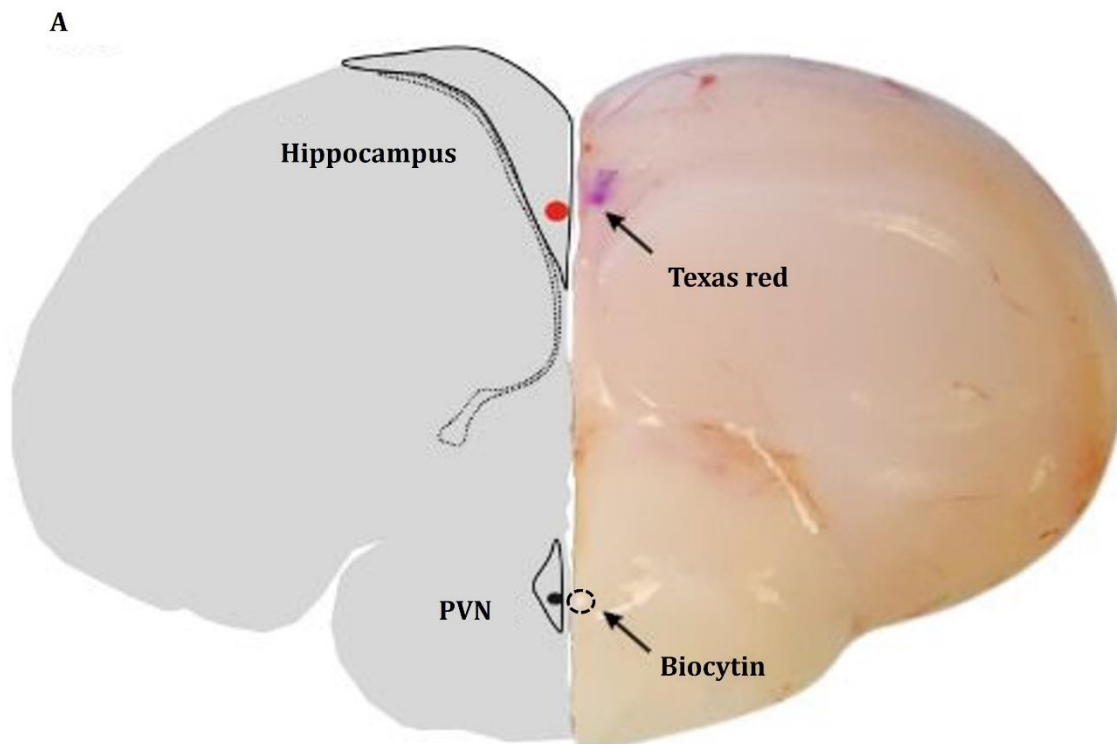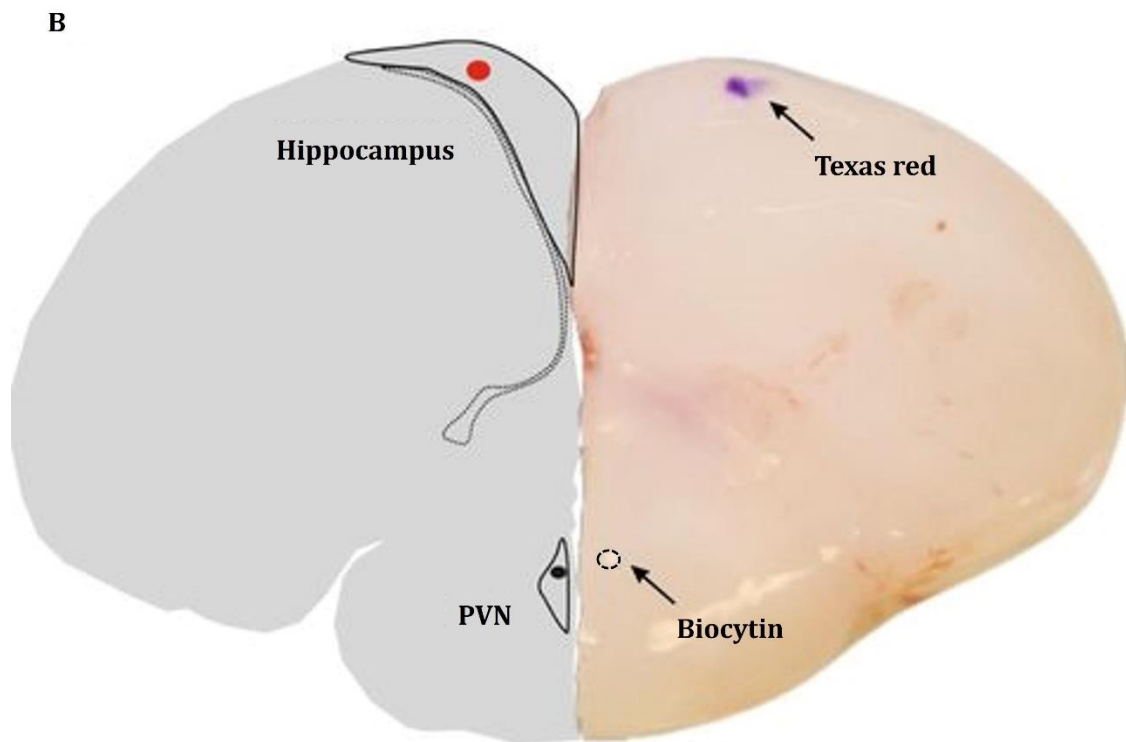
**Figure 4. 3.** Distribution of organotypic slice tracing injections in the brain slice culture of chick embryos (E16-E18). The left side shows a schematic drawing of the brain, indicating the regions where tracers were injected. The right side presents a photograph of the brain's right hemisphere with the corresponding injection sites. The schematic and photograph are aligned for direct comparison. Annotations and arrows on the photograph highlight the specific tracer injection sites corresponding to the schematic. Tracer types are as follows: anterograde Texas Red (TR) injections are marked by a purple dot on the right side and a red dot on the left side, while retrograde biocytin injections are indicated by an inner dashed circle on the right side and a black dot on the left side. In total, 10 anterograde injections were placed in the ventral (V) subregion (A) and 10 in the dorsolateral (DL) subregion (B) of the hippocampus. Arrows point to the tracer positions for clarity.

Across all analysed brains, consistent patterns of projections were observed. These projections were exclusively ipsilateral, originating from the injection sites within the hippocampus, and remained confined within the boundaries of the hippocampus (Figure 4.4). When the course of the descending fibres was followed, these appeared as dispersed fibres in the immediate vicinity of the injection site and as fibre bundles approaching the midline along the interhemispheric foramen. No extensions of the traced fibres were observed outside the confines of the hippocampus in any of the analysed tissue sections.
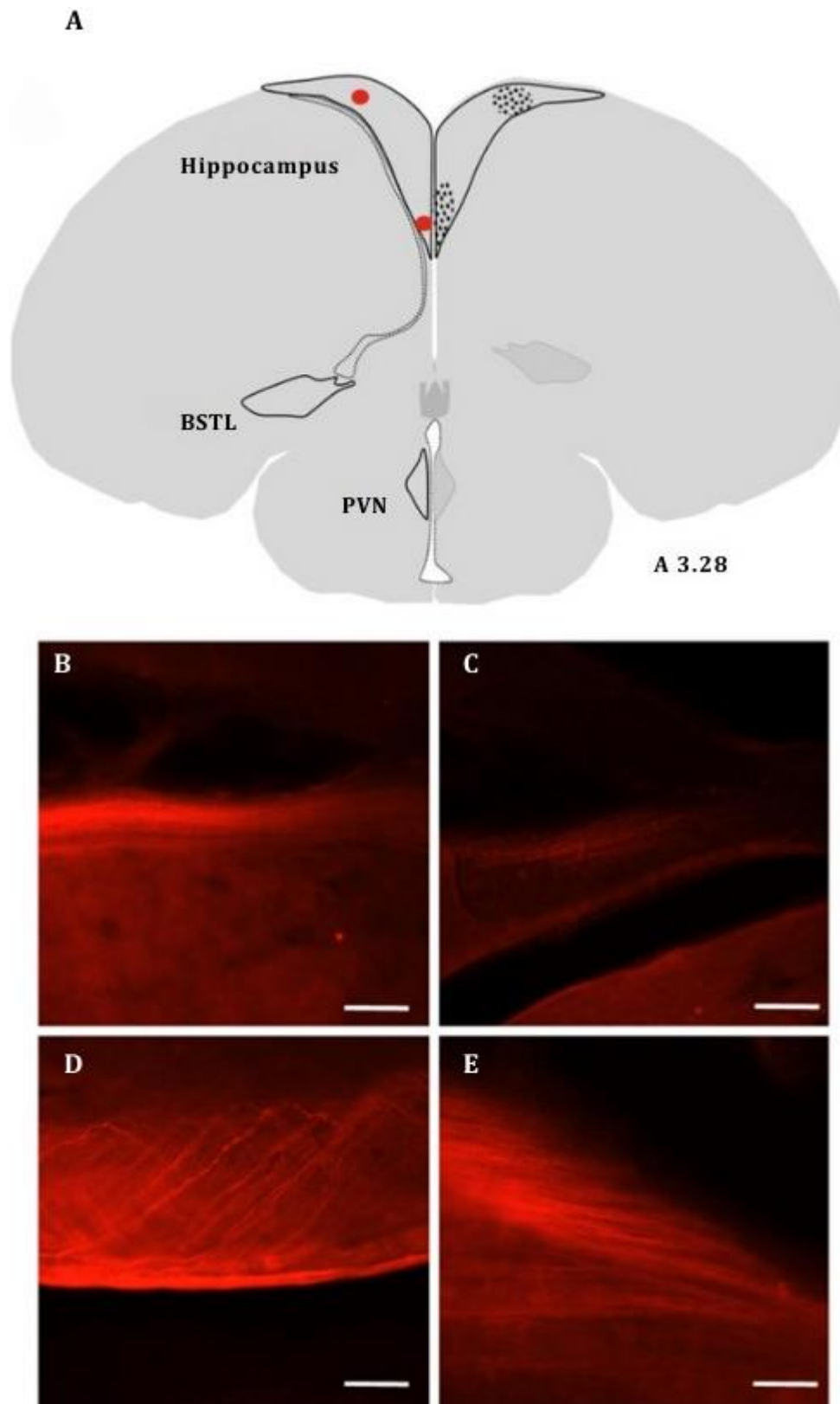
**Figure 4. 4.** Anterograde tract-tracing in coronal sections from chicken embryo hippocampus. In panel (A), Texas Red-containing fibres are represented as small dots, illustrating the distribution of several fibres alongside the location of the tracer injection sites represented as red dots. The fluorescent images reveal the appearance and limited extension of fibres from the injection site and within the injection area (B-E). Scale bars represent 100 μm. A indicates the approximate anteroposterior (AP) position described in the chick brain atlas by Puelles *et al.* (2007).

### 4.3.3.2.  Retrograde tracing

In the retrograde tracing study, biocytin crystals were placed in the PVN resulting in a consistent labelling pattern with slight variations due to the positioning of the biocytin crystal and the size of the crystal resulting in differences in the extension of the tracer's site. Case 20C1 was chosen as the most representative case due to the small and accurate injection site, along with the high quality of the retrograde labelling observed.  The labelling pattern identified in this specific case will be outlined in this section. The nomenclature for the areas described, as well as the locations referred to in the present section, were based on the chick brain atlas by Puelles *et al*. (2007).

The injection site was located at A. 2.08 and spread laterally into the hypothalamic area. However, the centre of the injection site was restricted to the magnocellular (PaMC) and parvicellular (PaPC) areas of the PVN. Within this injection site, a substantial number of neurons in the PVN exhibited clear labelling, and the demarcations of the injection site were well-defined, demonstrating minimal diffusion into surrounding regions. Labelling was observed laterally in the prethalamus, specifically in the reticular nucleus (Rt) (Figure 4.5 B).
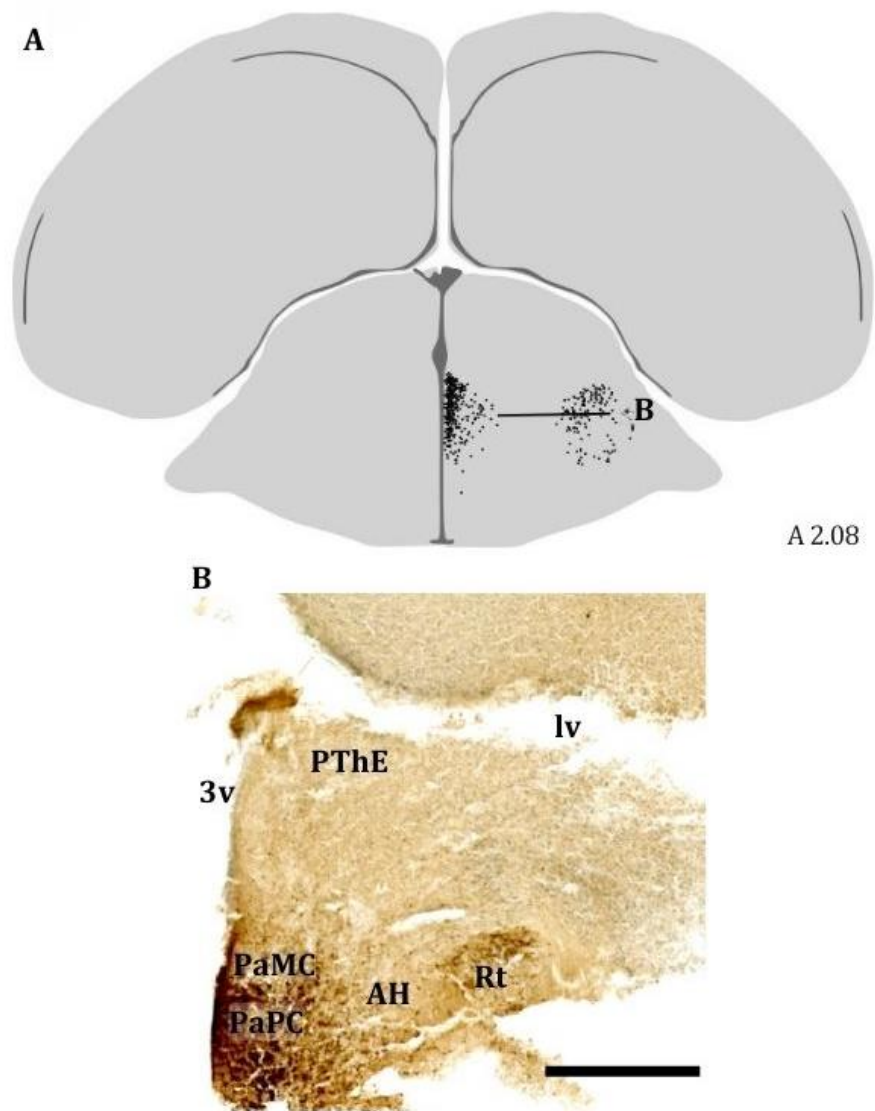
**Figure 4. 5.** The schematic drawing of a chick brain slice containing the injection site of biocytin in the PVN. Dots represent neurons retrogradely labelled with biocytin. The microphotograph shows the injection site in the stained brain slice (B). The scale bar represents 500 μm. A indicates the approximate anteroposterior (AP) position described in the chick brain atlas by Puelles *et al.* (2007). 3v, third ventricle; AH, anterior hypothalamic area; lv, lateral ventricle; PThE, prethalamic eminence; Rt, reticular nucleus.

Moving rostrally, the injection site became even more sharply delineated as the spread of the tracer reduced in size. Contralaterally, a sparse population of neurons was labelled in the PVN of the left hemisphere (Figure 4.6 E). Additionally, at the level of the reticular nucleus (Rt), the site was prominently stained in the right hemisphere (Figure 4.6 D), and a discernible presence was also observed in the left hemisphere with a comparatively lighter colouration (not shown).

Further analysis revealed consistent bilateral staining patterns in telencephalic pallial and subpallial regions. In addition to the retrograde labelling in the PVN, numerous labelled neurons were observed bilaterally in the auditory area (Au) of the caudomedial nidopallium (NC) and throughout the periventricular region of the mesopallium (MVPe) (Figure 4.6 C). Labelled cells extended from the septofimbrial nucleus (SFi) and into the fimbria of the hippocampus (fi)

continuing into the hippocampal region (Hi). In the HF, labelled cells were restricted to the V hippocampus which was slightly more prominent in the contralateral hemisphere (Figure 4.6 C). Sparsely labelled cells were observed extending from the PVN into the subparaventricular nucleus (SPa). Other areas with sparsely labelled cells included the nucleus of the stria *medullaris* (sm), the periventricular stratum (Pe), and the posterior portion of the nucleus of the hippocampal commissure (NHpC) (Figure 4.6 B).
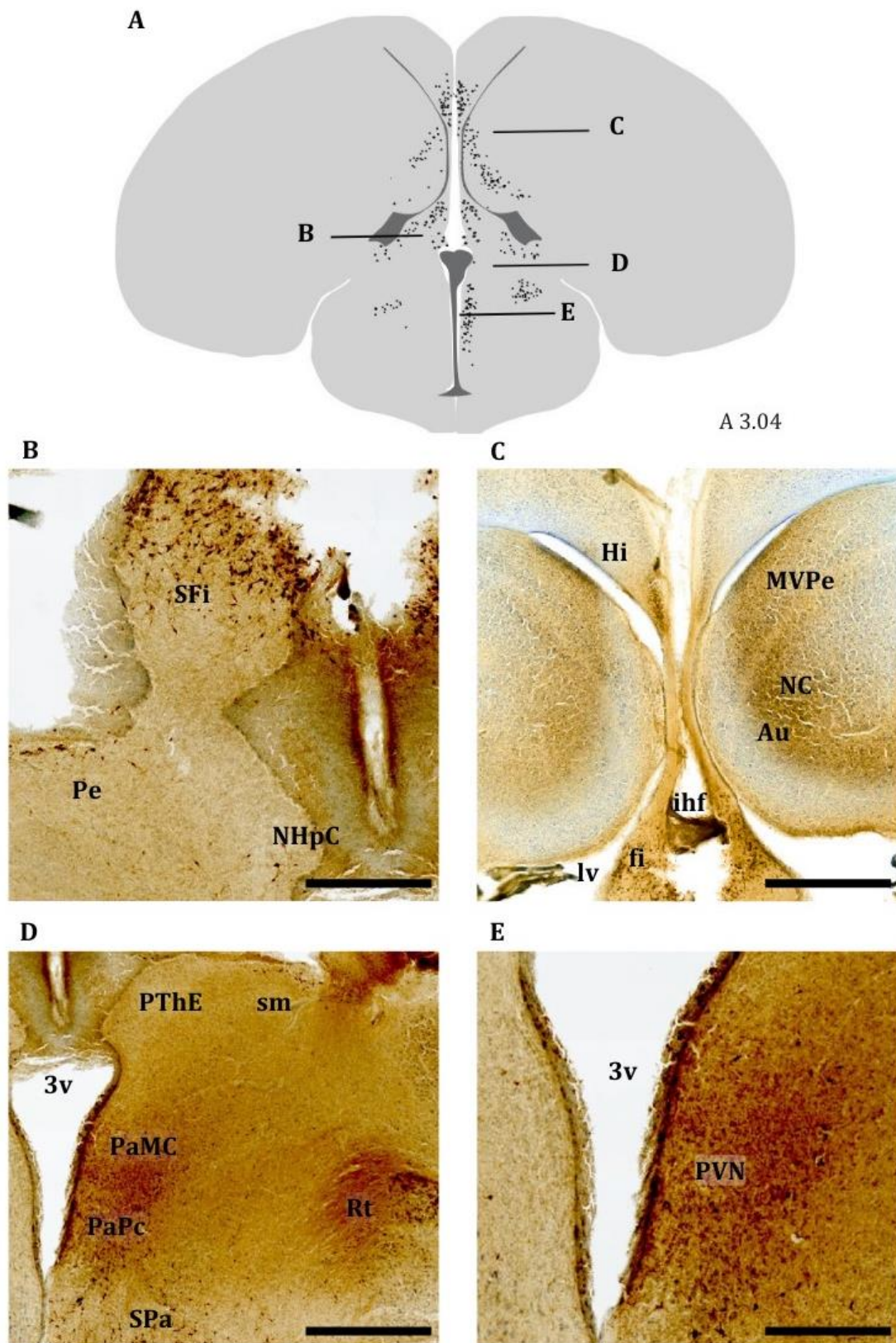
**Figure 4. 6.** The schematic drawing illustrates coronal section A 3.04 of retrogradely labelled chick brain slices. Dots in panel A represent neurons retrogradely labelled with biocytin. The accompanying microphotographs provide a detailed visualisation within specific regions of interest in tissue sections counterstained with toluidine blue 1%. Scale bars: C:1000 µm, D: 500 µm, and B & E: 200 µm. A indicates the approximate anteroposterior (AP) position described in the chick brain atlas by Puelles *et al*. (2007). For abbreviations see text.

While the overall staining pattern remained relatively consistent between A 3.04 and A 3.28, subtle differences became apparent. For instance, in the caudomedial nidopallium and throughout the periventricular region of the mesopallium, the staining in A 3.28 tended to concentrate more towards the midline, extending to the boundary with the lateral ventricle (Figure 4.8 B). Similarly, labelled cells within the hippocampal region became increasingly more conspicuous across the entire V subdivision as marked by the presence of intensely dark stained cells (Figure 4.8 B).

Labelled cells extended from the fimbria of the hippocampus into the septum (Se) and septal neuroendocrine systems. Numerous cell bodies were found in the septofimbrial nucleus (Sfi), the septohippocampal nucleus (Shi), and the SM (Figure 4.8 C, 4.9 D). Stained nuclei were absent in the SL and sparse nuclei were found in the NHpC and the hippocampal commissure (hic, Figure 4.7).
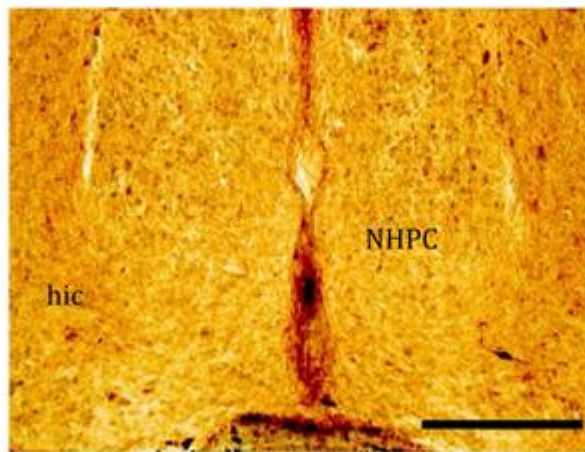


**Figure 4. 7**. Retrogradely labelled cells in the nucleus of the hippocampal commissure (NHpC) and the hippocampal commissure (hic). The scale bar represents 200 µm.

Moreover, retrogradely labelled cells were found bilaterally in the central extended amygdala (CEA) and the medial extended amygdala (MEA, Figure 4.8 D-E), particularly in the lateral and medial parts of the bed nucleus of the stria *terminalis* (BSTL and BSTM, respectively) and in the horizontal limb of the diagonal band (HDB). Within the dorsal somatomotor basal ganglia, abundant labelled cells were found in the medial striatum (MSt) and in the ectopic intrastriatal part of the globus pallidus (PalE) with weakly stained cells in the striopallidal area (StPal). Only weakly labelled cells were found in the lateral striatum (LSt) (Figure 4.8 D).
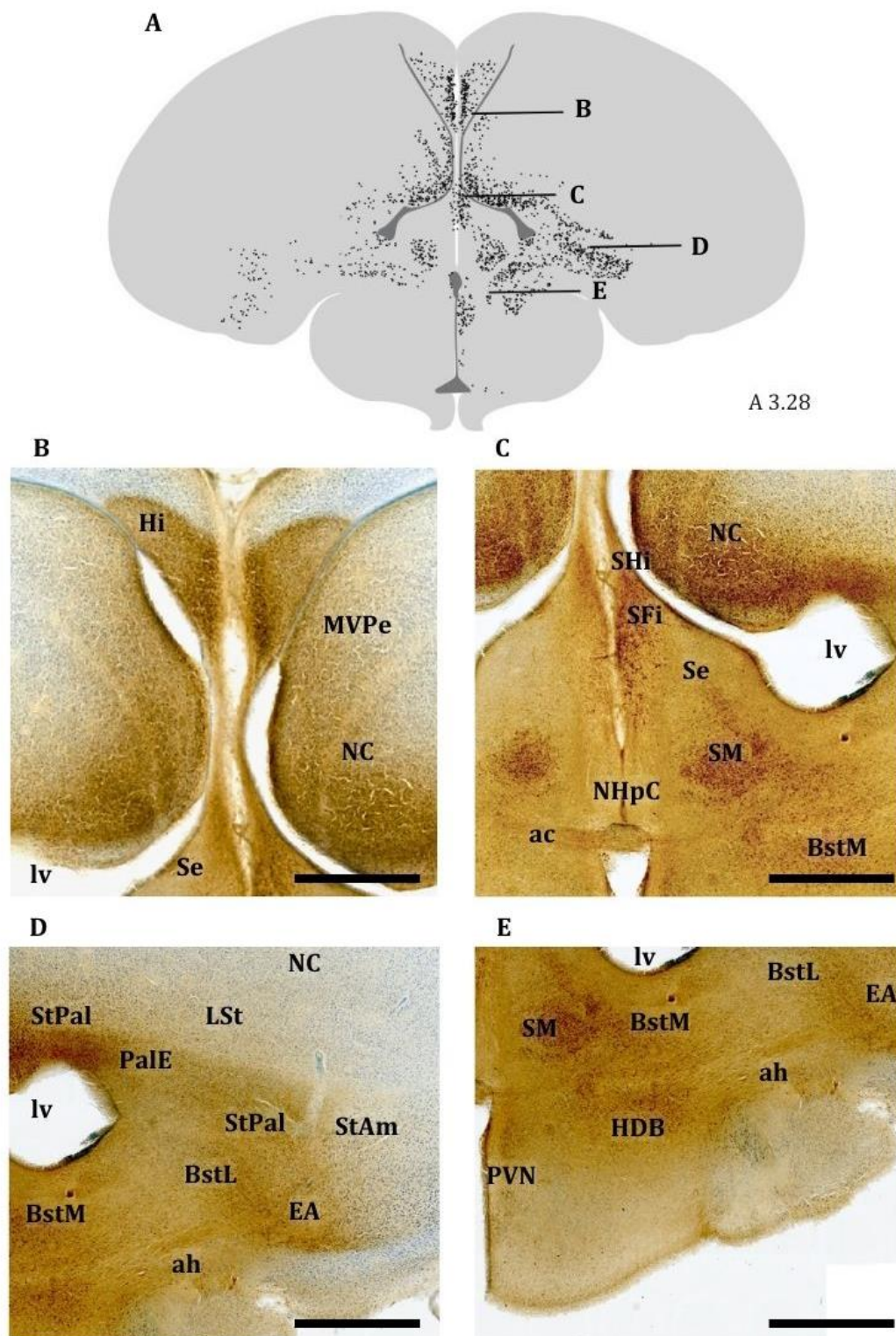
**Figure 4. 8.** The schematic drawing illustrates coronal section A 3.28 of retrogradely labelled chick brain slices. Dots in panel A represent neurons retrogradely labelled with biocytin. The accompanying microphotographs provide a detailed visualisation within specific regions of interest in tissue sections counterstained with toluidine blue 1%. The scale bar represents 1000 µm. A indicates the approximate anteroposterior (AP) position described in the chick brain atlas by Puelles *et al.* (2007). ac, anterior commissure; ah, amigdalohypothalamic tract; EA, extended amygdala; StAm, strioamygdaloid transition area. For other abbreviations see text.

At the level of A 3.76, the distinct boundary formed by the labelling of hippocampal neurons was still easily discernible but underwent a slight fading while expanding in size towards

the DM hippocampus. The most intense staining, however, persisted prominently within the boundaries of the V subdivision (Figure 4.9 B). Simultaneously, the labelled neurons in the caudomedial nidopallium and the mesopallium experienced a significant attenuation, appearing notably fainter (Figure 4.9 B) and ultimately disappearing in a 4.74 (Figure 4.10 B).

At this level, retrogradely labelled cells in the CEA and the MEA exhibited increased abundance and more intense staining. This heightened labelling delineated clear boundaries between the medial and lateral striatum, as well as the globus pallidus (Figure 4.9 C & E). This same pattern was also observed more rostrally in a 3.76 (4.10 C).

As the hippocampus decreased in size, the extension of the labelling becames more confined, retracting within the V subdivision of the hippocampus (Figure 4.10 B, 4.11 B). Furthermore, labelled structures in the septum were replaced by the emergence of the lamina terminalis (LTer) and the medial preoptic area (MPA) which appeared retrogradely stained (Figure 4.10 B, D).

Additional labelled structures were found in the periventricular stratum (Pe), the basal nucleus (B), NDB, the nucleus of the ventral limb of the diagonal band (VDB), and a few labelled neurons in the nucleus of the HDB (Figure 4.11 D).
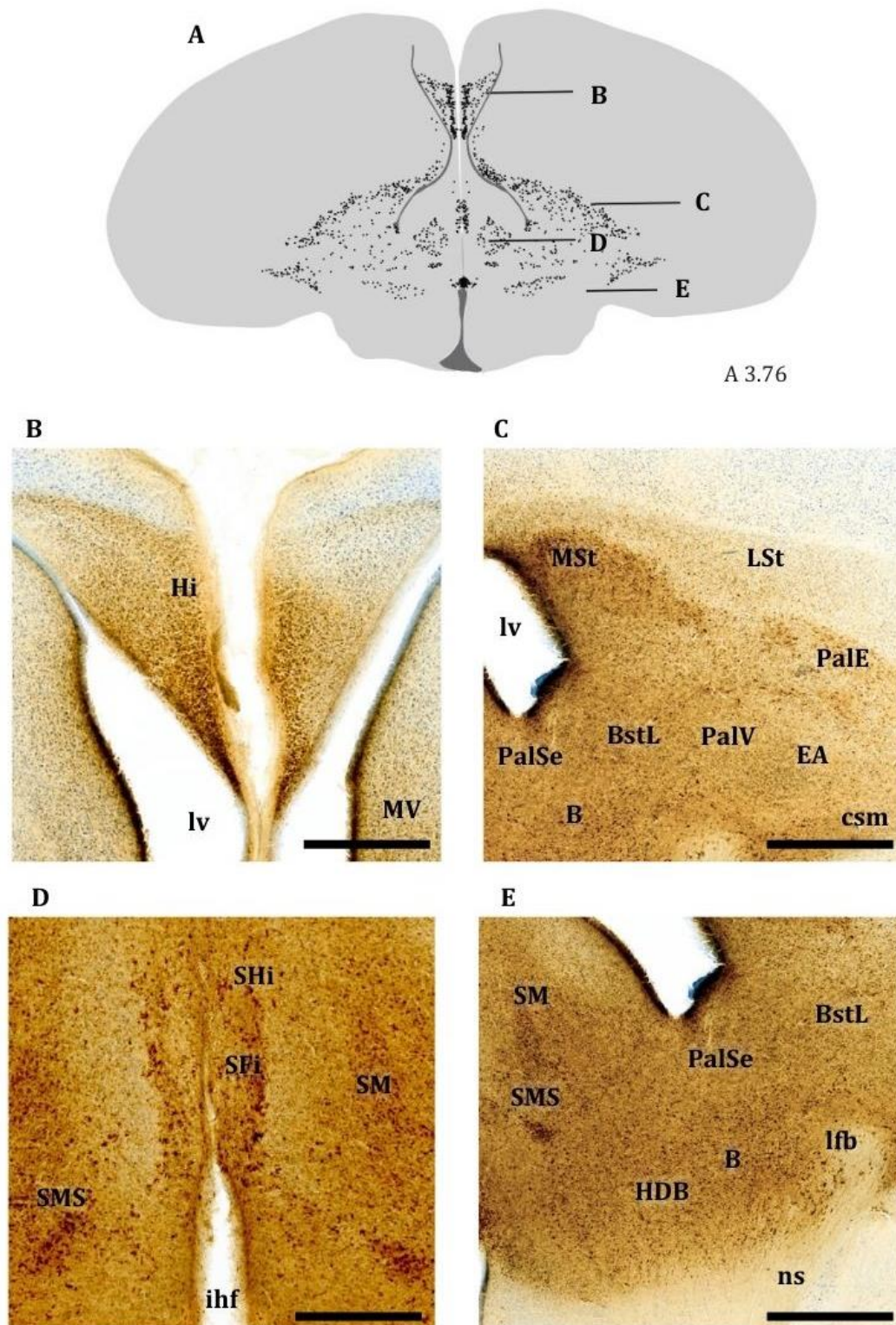
**Figure 4. 9.** The schematic drawing illustrates coronal section A 3.76 of retrogradely labelled chick brain slices. Dots in panel A represent neurons retrogradely labelled with biocytin. The accompanying microphotographs provide a detailed visualisation within specific regions of interest in tissue sections counterstained with toluidine blue 1%. The scale bar in B, C and E represent 1000 μm, and the scale bar in D represents 500 μm. A indicates the approximate anteroposterior (AP) position described in the chick brain atlas by Puelles *et al.* (2007). lfb, lateral forebrain bundle; ns, nigrostriatal tract; SMS, submedial septal nucleus. For other abbreviations see text.
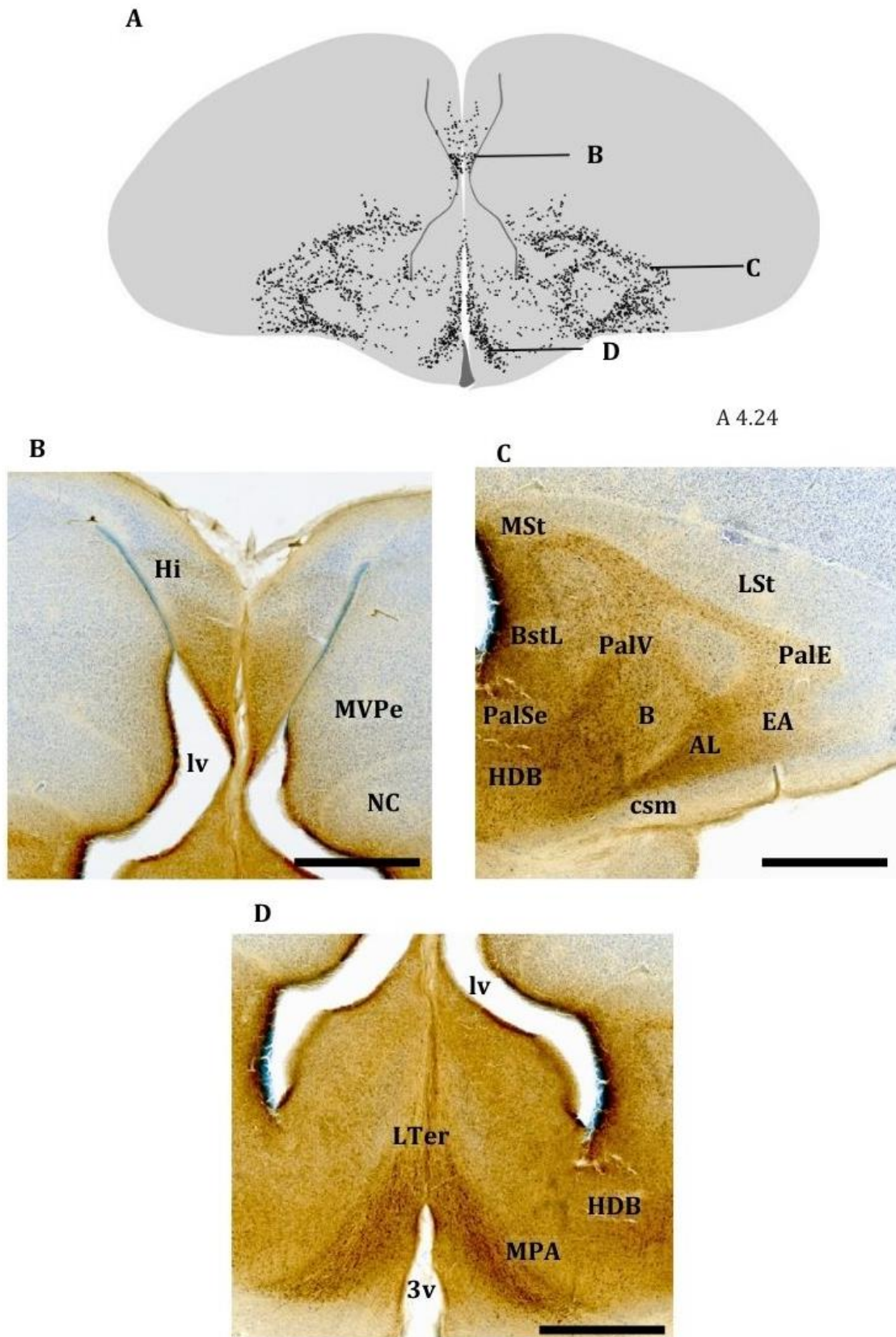
**Figure 4. 10**. The schematic drawing illustrates coronal section A 4.24 of retrogradely labelled chick brain slices. Dots in panel A represent neurons retrogradely labelled with biocytin. The accompanying microphotographs provide a detailed visualisation within specific regions of interest in tissue sections counterstained with toluidine blue 1%. The scale bar represents 1000 μm. A indicates the approximate anteroposterior (AP) position described in the chick brain atlas by Puelles *et al*. (2007). For abbreviations see text.
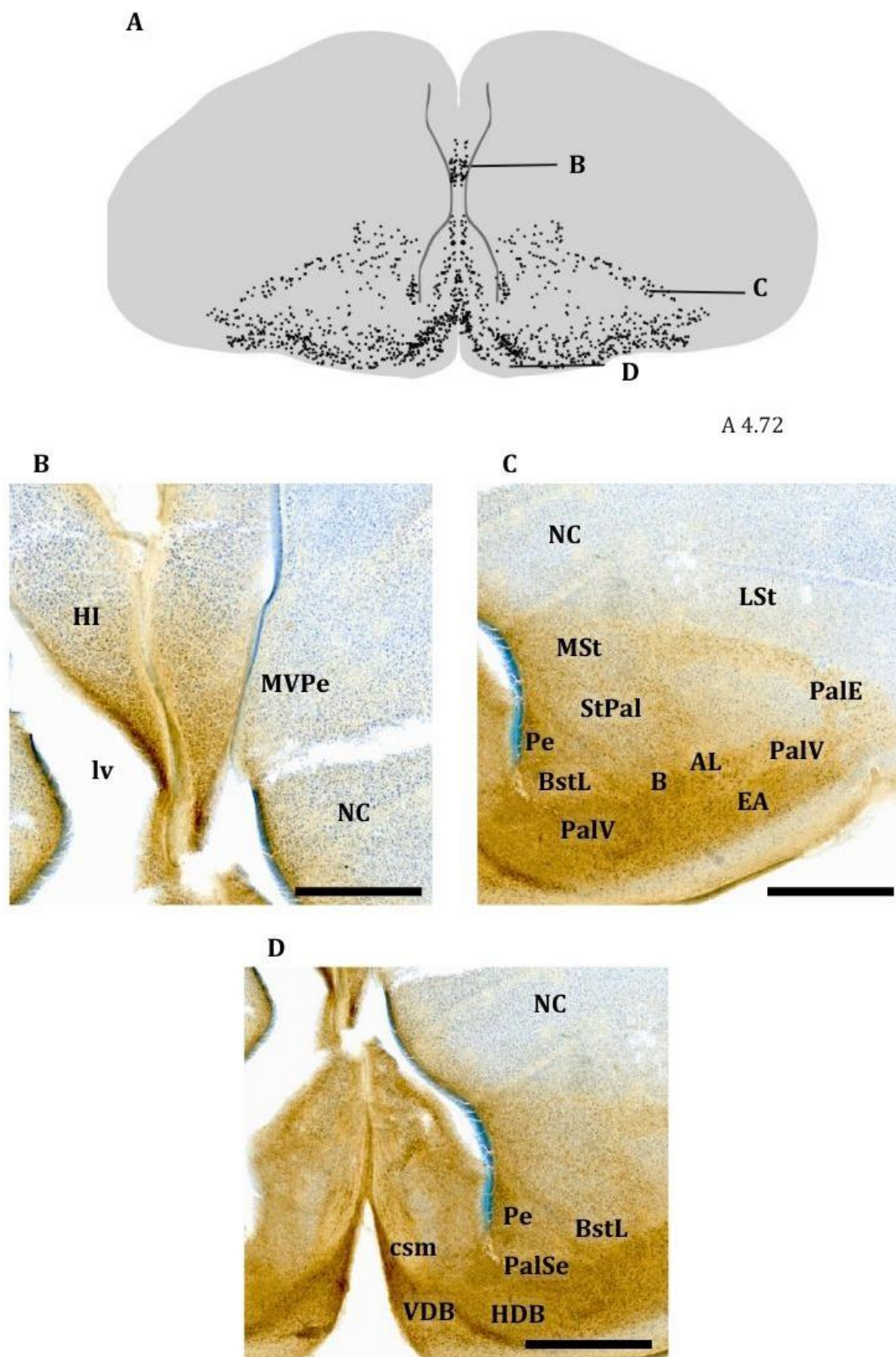
**Figure 4. 11.** The schematic drawing illustrates coronal section A 4.72 of retrogradely labelled chick brain slices. Dots in panel A represent neurons retrogradely labelled with biocytin. The accompanying microphotographs provide a detailed visualisation within specific regions of interest in tissue sections counterstained with toluidine blue 1%. The scale bar represents 1000 µm. A indicates the approximate anteroposterior (AP) position described in the chick brain atlas by Puelles *et al.* (2007). For abbreviations see text.

## 4.4. Discussion

### 4.4.1. Summary

The tract-tracing studies conducted in this research provided valuable insights into the chicken brain connectivity involved in regulating stress. Despite the limitations of both *in vivo* and *ex vivo* approaches, these findings contribute to our understanding of the connectivity between the hippocampus and PVN in the chicken brain. An outstanding revelation is the potential existence of a direct pathway linking the ventral rostral hippocampus with the PVN, a connection not previously documented. Additionally, the observations from this study corroborate previous observations of similar PVN pathways in mammals. These novel connectivity patterns in the avian PVN emphasize the need for further exploration to fully understand the functional implications of these connections in stress regulation.

### 4.4.2. Tract-tracing methodological considerations

The experimental approach encompassed both *in vivo* and *ex vivo* tract-tracing techniques. Unfortunately, the *in vivo* method posed great challenges due to substantial variations in the size and shape of hen skulls and the overall complexity of tracer injections. The use of conventional non-transsynaptic tracers required multiple injection sites, demanding precise and consistent coordinates to identify target sites, ultimately making replication between surgeries nearly unattainable due to the variations between subjects. Conversely, the *ex vivo* experimental approach provided a more direct and precise means of targeting the areas of interest, facilitating the visualisation of the target areas and thereby improving the accuracy of tracing experiments. This approach has been effectively employed in previous chick studies as demonstrated by Ahumada-Galleguillos *et al.* (2015).

Organotypic cultures of thick brain slices offered a solution to the challenge of localizing specific target areas while minimizing damage to surrounding brain regions, particularly those positioned above the PVN. Intending to characterize the complex communication dynamics between the hippocampus and the PVN, I employed biocytin and dextran amines as retrograde and anterograde tracers, respectively. Tracers were applied in the PVN (retrograde labelling) and hippocampus (anterograde labelling) of slices obtained at the level of the anterior commissure, a level chosen for its unique advantage in enabling the visualisation not only of the hippocampus and PVN but also of other regions linked with emotional responses, such as the extended amygdala.

Despite its advantages, the organotypic slice culture method also presents a significant limitation in fully examining the entire HF. For instance, the brain slices used in this study

predominantly covered the rostral portion of the hippocampus, with minimal coverage of the caudal hippocampus, particularly the caudal-most region which was completely absent. The range of slices extended from interaural 2.08 to interaural 4.72, equivalent to A5.50 to A9.25 in Karten & Hodos (1967), and categorized as medial and rostral sections, respectively, according to Atoji *et al*. (2002). Moreover, fibre disconnection during slice preparation is also a possibility. For instance, if the fibre pathways from the dorsal lateral (DL) region of the brain run in a caudal and lateral direction before reaching the hypothalamus, slicing the brain could sever these connections influencing the observed outcomes.

The absence of anterograde tracer diffusion observed in the slice culture experiment highlights another significant limitation inherent to this technique: the restricted time frame available for tracer diffusion. Unlike *in vivo* experiments, where tracer diffusion can persist over days, weeks, or even months depending on the experimental design, tissue slice culture experiments offer a relatively short time frame for diffusion, typically spanning hours to days based on the experimental setup. Moreover, the reduced metabolic activity in tissue slice culture compared to *in vivo* conditions can further impact the rate of tracer diffusion. Consequently, the 6-hour duration allotted in the experiment may have been insufficient for complete anterograde tracer dissemination.

In this study, I also put forward a novel approach to investigate the connectivity of the hippocampus in the chicken brain. I suggest the use of avian adeno-associated viral vectors as an additional option, which can yield promising results. Although I had limited time to work on this process, the initial steps yielded promising results. I successfully produced the GFP viral vector from plasmids and purified it to a level where it could be effectively expressed upon injection into the chick hippocampus. This outcome is highly encouraging, and I believe that this method has great potential to further our understanding of chicken brain connectivity.

### 4.4.3. *Stress Regulation Circuitry in Chickens*

In this section, we explore the results of our study on connectivity in the chicken brain. Specifically, the identification of retrogradely labelled cells in brain regions involved in emotional processes, including stress, such as the hippocampus, septum, and key components of the central and lateral extended amygdala. It is important to mention that our study revealed additional retrogradely labelled cells in other areas of the brain, such as the reticular nucleus, mesopallium, nidopallium, and the dorsal somatomotor basal ganglia, including the MSt, and globus pallidus. While these areas are known to play a crucial role in various cognitive processes, they are outside the scope of this thesis and therefore will not be part of this discussion.

### *4.4.3.1.* *Hippocampus*

Early functional studies conducted by Bouillé and Baylé (1973b) demonstrated that lesions within the posteromedial hypothalamic nucleus (PMH) induced a notable decrease in plasma CORT levels, while stimulation of the same area led to a significant increase in plasma CORT levels (1973a). Building upon these findings, subsequent research by Bons *et al.* (1976) identified degenerating nervous fibres and synaptic boutons within the PMH following hippocampal lesions, suggesting an anatomical connection between these brain regions. These discoveries highlighted the communication between the hypothalamus and hippocampus paving the way for the exploration into the neural circuitry underlying stress regulation in birds.

At the time, the corticotropic region was identified as the nuclei PMH, as it would take years before the PVN was identified (Bons *et al.*, 1985, 1988) so it was not included in the atlas by Karten and Hodos (1967) which served as the reference atlas during that period (Smulders, 2021). We now know that it is the PVN, rather than the PMH, that houses neurons responsible for the release of corticotropin-releasing hormone (CRH) and arginine vasotocin (AVT) in birds. These neurons serve as the ultimate destination for central projections from brain regions that are sensitive to stress, where they converge to regulate the activity of the HPA axis. The observations made by Bouillé and Baylé (1973a,b) are now attributed to the existence of fibres of passage as CRH-containing neurons from the PVN run together and traverse the PMH on the way to the median eminence (Smulders, 2021).

One of the pioneering investigations into characterizing the neural connections between hypothalamic and extrahypothalamic structures involved in regulating corticotropic cells in birds was conducted by Bouillé *et al.* (1977). In this study, they aimed to explore the presence of direct neural connections between hippocampo-septal structures and the corticotropic region of the hypothalamus. The investigation employed stereotaxic injections of horseradish peroxidase (HRP) into the PMH and resulted in the visualisation of retrograde transport of peroxidase in both the hippocampus and the SM with labelling observed bilaterally. These results further supported the role of the hippocampus in stress regulation in birds and suggested a potential direct connection between the hippocampus and the hypothalamus.

Consistent with the observations made by Bouillé *et al.* in 1977, the present study employing organotypic slice cultures revealed that the placement of biocytin crystals in the PVN resulted in bilateral labelling of the hippocampus. Furthermore, akin to Bouillé *et al.* (1977), we observed that the labelled fibres were predominantly situated in the V subdivision suggesting its participation in the neural circuitry underlying the regulation of the stress response.

These results, however, contrast with studies in mammals where evidence at a subregional level suggests that communication between the hippocampus and the PVN is facilitated through a relay area, the BSTL, with the involvement of the temporal subiculum. This insight was initially presented by Fischette *et al.* (1980, 1981) and further supported by

subsequent research by Cullinan *et al.* (1993). If indeed the DL subregion of the avian hippocampus corresponds to the mammalian subiculum (Abellán *et al.*, 2014; Erichsen *et al.*, 1991; Kahn *et al.*, 2003; Székely & Krebs, 1996), one might anticipate it to play a role in mediating communication to the PVN in birds.

At least in pigeons, substantial evidence indicates that efferent projections from the hippocampus originate mainly from its DM and DL divisions (Striedter, 2016). Early studies in pigeons by Benowitz and Karten (1976) documented the potential involvement of the DL subregion. In their investigation, labelling of the hypothalamus, including the parvocellular portion of the PVN (then referred to as the *stratum cellulare internum*, SCI) occurred following HRP injections into the lateral portion of the area parahippocampalis (APH) which would be equivalent to the DL subregion. Like mammals, this connection was exclusively observed in the caudal hippocampus.

However, in line with the findings in this study, a subsequent study by Casini *et al.* (1986) observed that injections into both the hippocampus (corresponding to the V subdivision) and the APH (corresponding to the DM, and DL subregions) of pigeon brains led to a similar labelling of the SCI. Atoji *et al.* (2002) would later corroborate Casini's findings. Employing the cholera toxin B subunit (CTB) to retrogradely label the pigeon hippocampus, Atoji and colleagues (2002) targeted the V subdivision of the hippocampus, resulting in labelled cells in the SCI. Interestingly, unlike the observations of Benowitz and Karten, as well as those of the current study, both Casini *et al.* (1986) and Atoji *et al.* (2002) found this connection when the injection in the hippocampus was situated at an intermediate rostrocaudal level (A6.5 based in the atlas by Karten & Hodos, 1967). Notably, in the latter study, the projection into the SCI was not observed either moving rostrally or caudally from this level.

Admittedly, the labelling of the V subdivision is somewhat surprising and was not contemplated in the hypothesis of the study. While this subregion does indeed possess telencephalic projections, they do not seem to consist of long descending pathways. Instead, such projections are more characteristic of the DL subdivision, which notably gives rise to extensive anterograde projections reaching into areas such as the SL, the *stratum cellulare externum* (SCE), and the medial periventricular hypothalamus. This pattern has been documented in the zebra finch (Székely & Krebs, 1996) and pigeons (Krayniak & Siegel, 1978; Casini *et al.*, 1986) emphasizing the need for studies across different species.

More recently, Herold *et al.* (2019) also identified a direct connection between the hippocampus and the hypothalamus, more specifically in the nucleus *periventricularis magnocellularis* (PVM), the presumed homologue of a portion of the mammalian PVN as proposed by Berk in 1987. Their research, however, reveals that this connection is limited to a specific area within the dorsomedial (DM) subdivision of the hippocampus and is exclusively observed in the

caudal region of the hippocampus in adult homing pigeon brains contrasting with the observations in this study.

However, similarly to the results observed in my study, unilateral AAV-GFP injections into the PVN led to the bilateral expression of GFP-positive fibres in the CA2 region of the septal pole of the mouse hippocampus (Cui *et al.*, 2013). Based on this, it is noteworthy to consider previous research suggesting homology between the ventral subregion of the avian HF and the mammalian Ammon's horn (Benowitz & Karten, 1976; Casini *et al.*, 1986; Erichsen *et al.*, 1991; Montagnese *et al.*, 1996; Székely, & Krebs, 1996).

Furthermore, studies have traced vasopressin and oxytocin pathways from the PVN to the septal subiculum in rats. These fibres then extend from the septal hippocampus into the temporal hippocampus (Buijs,1978). Subsequently, Silverman *et al.* (1981) employed iontophoresis of HRP into the PVN, resulting in HRP-filled cells restricted to the subiculum in both the temporal and septal hippocampal regions in the rat brain, albeit with fewer cells observed in the septal pole.

The discrepancies in connectivity findings across studies could be attributed to potential species-specific and age-related variations, as elucidated by existing literature such as Tömböl *et al.* (2000), which outlined species-specific connectivity differences such as profuse arborisation of projection neuron axon collaterals and a higher density of GABA immunopositive local circuit neurons in the homing pigeon hippocampus when compared to the chicken hippocampus. Moreover, it is plausible that variations in methodology may yield different results. Specifically, the majority of the observations reported here were derived from anterograde tracing using tracers different from the ones employed in our study, which may yield differing results and could explain why my findings closely resemble those of the only other retrograde avian tracing study available for comparison (Bouillé *et al.*, 1977). Considering that PVN tracing studies into the mammalian hippocampus have yielded variable results, as shown in this discussion, and evidence of retrograde tracing from the PVN into the avian hippocampus is almost nonexistent further studies are warranted to confirm the observations proposed in this study.

To corroborate retrograde findings, dextran amine was applied in the hippocampus as an anterograde tracer. Unfortunately, as mentioned in the previous section, these injections, as well as the anterograde *in vivo* injections, were unsuccessful and diffusion of the tracer was inadequate to characterize any connections between the hippocampus and the PVN. Consequently, we cannot dismiss the possibility that the retrograde labelling observed in the hippocampus might stem from fibres of passage carrying the tracer. Nevertheless, the pattern of retrograde labelling provided us with interesting insights into the circuitry involved in the hippocampus-PVN communication, particularly regarding the potential reliance on multiple synaptic connections within this circuit.

#### *4.4.3.2.* *Septum*

The organization of the avian septum is comparable to that of the mammalian structure and contains distinct anatomical subdivisions: SL, SM, septohippocampal septum, and caudocentral septum (Goodson *et al.*, 2004; Kuenzel & Jurkevich, 2022). In general, the literature exhibits a notable emphasis on the SL in comparison to the SM, with studies identifying input to the PVN originating from the LS in both mammals (Silverman *et al.*, 1981; Singewald *et al.*, 2011) and birds including the domestic mallard (Korf, 1984). However, in this study, cells were exclusively observed in the SM following retrograde tracing in the chicken PVN.

Retrograde labelling was observed across the SM with additional labelling of the SFi, Shi, and SMS. This finding is in line with the research conducted on pigeons by Bouillé *et al.* (1977), which demonstrated similar hypothalamic retrograde labelling patterns from the PMH. Conversely, projections from the SM to the PVN have been previously identified using small iontophoretic injections of the anterograde tracer *Phaseolus vulgaris* leucoagglutinin (PHAL) in domestic chick brains (Montagnese *et al.*, 2004).

In mammals, PVN connectivity has been extensively studied in the context of vasopressin and oxytocin pathways. In a study by Buijs (1978), PVN vasopressin and oxytocin-containing fibres were found to reach the medial and lateral septum of the rat brain. Moreover, HRP iontophoresis into the PVN also results in labelled neurons in the rat SM and the septofimbrial nucleus (Silverman *et al.*, 1981) further supporting the findings of this study.

It is worth noting that, further research is needed to fully elucidate the functional implications of this observation and to gain a more comprehensive understanding of whether the SM relays information to the hippocampus from the PVN, particularly in its role regulating the HPA axis. Functionally, the SM participates in a wide range of functions such as sensorimotor integration, affect-motivation, and cognition (Ang *et al.*, 2017: Calandreau *et al.*, 2007), as such, it has not received much attention for its involvement in stress regulation.

In birds, namely pigeons (Atoji & Wild, 2004), zebra finch (Székely & Krebs, 1996), and chick (Montagnese *et al.*, 2004), hippocampal efferents have been observed in the septum. For instance, PHAL injections into the V subregion give rise to labelled fibres coursing through the septohippocampal junction, arborising within the SM, and invading the contralateral septum in the zebra finch (Székely & Krebs, 1996). In general, there appears to be a general agreement in the literature that axons arising from the avian V subdivision extend into the SM, whereas fibres from the DM and DL innervate the SL (Atoji &Wild,  2004; Casini *et al.*, 1986; Krayniak & Siegel, 1978; Székely & Krebs, 1996). Conversely, the SM sends projections to the HF, the nucleus of the diagonal band, the commissural septal nucleus, and the BSTL (Atoji & Wild, 2004; Montagnese *et al.*, 2008).

#### *4.4.3.3.    The Lateral Bed Nucleus of the Stria Terminalis*

In both avian and mammalian species, the BST is divided into two major divisions: the lateral (BSTL) and the medial (BSTM) divisions. The BSTL forms part of the CEA and is known to play a key role in the regulation of the stress response in both mammals (Phelps & LeDoux, 2005; Davis *et al.*, 2010) and birds (Pross *et al.*, 2022). The BSTM forms part of the MEA and participates in social and reproductive behaviours (Goodson, 2008; Martínez-García *et al.*, 2008; Medina *et al.*, 2017, Ulrich-Lai & Herman, 2009).

In this study, numerous retrogradely labelled cells were identified in both BSTL and BSTM. These findings are consistent with studies in mammals where discrete iontophoretic injections of the retrograde tracer Fluoro-gold in the PVN of rat brains result in Fluoro-gold-labelled neurons distributed across the anterior medial, ventral medial, ventral lateral, and posterior intermediate subdivisions of the BST (Cullinan *et al.*, 1993). Similarly, following HRP iontophoresis into the PVN, labelled neurons are found in the BST at the level of the medial preoptic area in the rat brain (Silverman *et al.*, 1981).

As in mammals (Conrad & Pfaff, 1976), studies in birds, particularly in pigeons (Atoji *et al.*, 2006) and chicks (Bálint *et al.*, 2011) have documented projections from the BSTL to both the magnocellular and parvocellular divisions of the PVN further supporting the findings of this study.

Functionally, the BSTL plays a crucial role in the regulation of stress responses (Martínez-García *et al.*, 2008; Medina *et al.*, 2017; Pross *et al.*, 2022). Previous findings in chickens (Nagarajan *et al.*, 2014) align with observations in mammals (Cecchi, 2002), indicating that the BSTL is activated in response to acute stress. Additionally, CRH-containing neurons have been identified within this structure (Richard *et al.*, 2004), further implicating its involvement in stress regulation. As in mammals, the avian  BSTL contains mainly GABA-ergic projection neurons (Bruce *et al.*, 2016), however, as we did not study the neurochemical properties of the labelled cells, only future research can provide more information about the functional relationship of the reported connections.

In mammals, excitatory projections from the hippocampus relay in the BST activating an inhibitory GABAergic relay causing disinhibition of the PVN CRH neurons (Herman *et al.*, 2016). Conversely, anterograde tract-tracing of the rat hippocampus results in projections originating in the temporal subiculum coursing to the BST via either the fimbria-fornix or a pathway involving the *stria terminalis* via the amygdala (Cullinan *et al.*, 1993). While these investigations emphasize the involvement of the mammalian temporal hippocampus, avian studies suggest that projections to the BSTL involve both the rostral and caudal regions of the hippocampus. Communication from the hippocampus to the BSTL has been reported to originate throughout the rostrocaudal extent of the HF, with small but consistent projections from the ventral HF and stronger connections from the DM subdivision (Atoji *et al.*, 2002, 2006). It is worth noting, however, that this pattern is

not consistently reported in every study, with some studies indicating a lack of direct connections from the DM subdivision to the BSTL (Herold *et al.*, 2019).

### 4.4.3.4.  *NHpC*

Our findings revealed sparse retrogradely stained cells in the NHpC (previously known as the bed nucleus of the pallial commissure). These findings are in line with previous connectivity studies in pigeons where iontophoretic injections in the PVM resulted in labelled cells in this region (Berk & Finkelstein, 1983).

Although no mammalian counterpart of this structure has been identified in mammals, the mammalian medial and the triangular septal nuclei have been suggested as plausible candidates (Kadhim *et al.*, 2019, 2020 in Smulders, 2021). Notably, labelled cells have been found in both the medial and triangular septal nuclei of rats following HRP iontophoresis in the PVN (Silverman *et al.*, 1981).

Functionally, recent studies show a significant number of CRH neurons in the NHpC of birds which activate in response to acute restraint stress suggesting a role in the initial activation of the HPA axis (Nagarajan *et al.*, 2014, 2017a,b; Kadhim *et al.*, 2019). The specific interaction between this structure and the avian hippocampus, if existent, remains an area yet to be thoroughly examined.

## 4.5.   Conclusion

This study sheds light on the connectivity of the chicken hippocampus involved in stress regulation. Findings provide evidence of the existence of direct connections between the hippocampus and the PVN in chickens and support the possibility of indirect communication via the septum and the BSTL. Contrasting with the hypothesis of a preferential innervation of the caudal hippocampus, the communication pattern in this study was observed at the level of the rostral hippocampus, involving the V subdivision. Moreover, our findings highlight the communication between the PVN and the SM, BSTL, and the NHpC, suggesting a potential involvement of these structures in the relay of information associated with the feedback regulation of the HPA axis. Further studies are necessary to fully understand the intricate functions of these brain regions in birds, and we propose the use of avian AAV vectors as a promising tool. Altogether, our study provides a more detailed view of the connectivity of key structures involved in stress regulation in chickens and provides the groundwork for future research investigating the functional relationship of these regions.

# Chapter 5. The Role of the Hippocampus in Stress Regulation: Understanding the Complexity

## 5.1. Summary of findings

Starting with the question of what the role of the hippocampus in stress regulation in the chicken brain is, this research project focused on two key objectives: firstly, to identify the specific subdivisions and regions of the chicken hippocampal formation (HF) that activate in response to acute stress, and secondly, to elucidate the neural pathways that connect the hippocampus to the paraventricular nucleus (PVN) of the hypothalamus. The PVN is a key component of the Hypothalamic-Pituitary-Adrenal (HPA) axis, one of the main systems involved in the regulation of the stress response. By addressing these objectives, the study aimed to further our understanding of stress regulation in birds. This, in turn, could have important implications for advancing our knowledge of the principles that govern brain evolution and the unique adaptive stress responses that are characteristic of the avian brain.

As a first approach to the research question, Chapter 2 investigated FOS induction and HPA-axis activation in adult hens under restraint stress. The initial hypothesis was that the caudal portion of the hippocampus in hens would exhibit FOS activation in response to acute stress, as opposed to the rostral portion. This hypothesis was based on the proposed functional equivalence between the caudal hippocampus in birds and the temporal hippocampus of mammals, specifically in their roles concerning the feedback regulation of the HPA axis (Smulders, 2017). Methodologically, the study employed a combination of immunohistochemical, corticosterone level measurements, and gene expression analyses to assess the impact of stress-inducing treatments on overall HPA axis activation. The study findings were unexpected, as the rostral region of the hippocampus showed significant activation following acute stress treatment, while the caudal portion did not. Interestingly, no increase of FOS activity in other brain areas, elevated corticosterone levels, or the expression of stress-related genes of interest was observed. After carefully considering various potential contributing factors, such as specific spatial context conditions and the employed techniques, it was concluded that the stress-inducing treatment failed to elicit a robust activation of the HPA axis. The unexpected findings prompted the refinement of the experimental methods for a second examination of the same hypothesis.

Continuing the quest to identify hippocampal subregions involved in the stress response, Chapter 3 of the research project investigated the expression of the *FOS* immediate-early gene (IEG) induced by social isolation in chick brains. Building upon the hypothesis established in Chapter 2, it was anticipated that the caudal hippocampus would demonstrate elevated *FOS* gene expression following stress termination, mirroring the function of the mammalian temporal hippocampus. Unexpectedly, the rostral hippocampus exhibited activation during stress termination, with an inhibitory effect resulting from the stress induction. On the other hand, the caudal hippocampus did not show activation following stress termination, but notable *FOS* activity was observed during the stress induction phase. These activation patterns were accompanied by observable behavioural manifestations and hormonal changes

indicative of distress in the animals, providing compelling evidence that the observed hippocampal activation resulted from stress. Overall, the study provided significant insights into the relationship between hippocampal function and stress response in birds.

Finally, Chapter 4 aimed to elucidate the communication pathways between the hippocampus and the PVN, with a hypothesis that an intermediary relay region, specifically the bed nucleus of the stria terminalis lateralis (BSTL), is involved. The study revealed retrogradely labelled cells within the ventral subdivision of the hippocampus present in the rostral portion and confirmed pathways extending towards the central and medial extended amygdala, including the BSTL, in addition to retrograde labelling of regions of interest such as the septum and the nucleus of the hippocampal commissure (NHpC).

Taken together, the results from this study underscore the role of the avian HF in stress regulation. Notably, we found that the rostral hippocampus in chickens functions similarly to the mammalian temporal hippocampus, playing a key role in the negative feedback regulation of the HPA axis. On the other hand, the caudal portion of the avian HF is sensitive to acute stressors but appears to be primarily involved in the cognitive processing of this experience, akin to the functions of the mammalian septal pole. These findings raise intriguing questions about the potential functional segregation within the longitudinal axis of the avian hippocampus and its similarities and differences with the mammalian hippocampus.

## 1.5. Functional segregation in the mammalian hippocampus

The hippocampus is a complex and highly organized brain structure that is crucial for both cognitive and emotional processes, including learning, memory, spatial navigation, and stress regulation. One of the most fundamental questions in the study of the hippocampus is whether it is functionally segregated or not. Functional segregation refers to the notion that different subregions of the hippocampus have distinct roles in processing and integrating information. The identification of functional segregation in the hippocampus has important implications for understanding the complex dynamics behind these processes.

One of the earliest reviews suggesting the functional differentiation of the hippocampus was by Moser and Moser (1998). They argued that the input and output connections of the septal and temporal hippocampus are distinct (Swanson & Cowan, 1977), while spatial memory appears to depend on the septal pole rather than the temporal (Moser *et al*., 1995) and lesions in the temporal hippocampus, but not the septal, affect stress responses and emotional behaviour in mammals (Henke, 1990). Over the years, evidence has accumulated supporting the claim of functional segregation in the mammalian hippocampus (Ferbinteanu & McDonald, 2001; Henke, 1990; Hunsaker & Kesner, 2008; Jung *et al*., 1994; Kjelstrup *et al*., 2002; Klur *et al*., 2009; Kumaran *et al*., 2009; Pothuizen *et al*., 2004; Rogers & Kesner, 2006; Strange *et al*., 2014).

While there is considerable evidence supporting functional segregation within the hippocampus, it is important to acknowledge the limitations of many of these studies, in particular the functional

studies which often rely on hippocampal lesions. Lesion studies, though informative, often lack the precision required to selectively target specific subdivisions of the hippocampus. The variability in lesion placement, potential damage to associated areas, lesion overlap, and lesion extent across studies pose challenges in evaluating the precise relationship between lesioned regions and corresponding functional deficits.

Consequently, discrepancies have emerged between the findings of studies employing electrolytic and neurotoxic procedures, as highlighted in research conducted by Moser *et al.* in 1993 and 1995. Moreover, there have been variations due to the extent of the lesions, with some studies reporting deficits with hippocampus lesions of 25-45% for septal and 45-50% for temporal hippocampus lesion size (Bannerman *et al.*, 1999, 2002), while contrasting outcomes have been observed in studies utilizing identical lesions and methodologies and reporting no impairment from either septal or temporal hippocampal lesions of an average of 55% of total septal volume and an average of 45-50% of total temporal hippocampus volume (Richmond *et al.*, 1999).

Complicating matters further, unlike the septal pole, lesions involving the temporal hippocampus pose additional challenges due to its orientation. Most rodent studies focus on the septal hippocampus because its positioning facilitates stereotactic placement studies, as it is located toward the top of the skull; in contrast, much of the temporal hippocampus lies below the thalamus and extends posteriorly (Paxinos and Watson, 1998). This positioning makes it considerably arduous to perform lesion placements that avoid causing damage beyond the hippocampus itself (Rogers & Kesner, 2006).

Hence, to fully understand the functional organization of the hippocampus, it's important to consider a variety of evidence beyond just lesion studies. Luckily, other types of evidence can provide valuable insights into this topic. Among these, perhaps the most compelling evidence comes from studies on hippocampal connectivity. Specifically, these studies have demonstrated that the output of the hippocampus varies depending on its location along the septotemporal axis, which suggests that different downstream structures may be activated depending on where the output originates (Swanson & Cowan, 1977). For instance, denser connectivity of the temporal pole with the amygdala and hypothalamic endocrine and autonomic nuclei support its role in the endocrine stress response (Canteras & Swanson, 1992; Kishi *et al.*, 2006; Maren & Fanselow, 1995; Pitkänen *et al.*, 2000; Risold & Swanson, 1996).

However, the notion that the temporal hippocampus is solely responsible for emotional processing and the septal hippocampus exclusively manages cognitive functions is not widely agreed upon and anatomical studies in rodents and primates show that hippocampal extrinsic connectivity and gene expression data are organized as both sharply demarcated domains and smooth topographical gradients rather than an absolute temporal-septal dichotomy (Amaral & Witter, 1989; Kjelstrup *et al.*, 2008; Strange *et al.*, 2014; Thompson *et al.*, 2008; Vogel *et al.*, 2020). If differences along the septotemporal axis are gradual rather than absolute, then functional differences along the longitudinal axis may also exhibit a gradient-like organization meaning that the temporal hippocampus may also participate in spatial processing and the septal hippocampus in emotional processing.

Indeed, data reveals a lower proportion of cells that express place fields in the temporal hippocampus compared to the septal pole, alongside lower spatial selectivity in cells within the temporal pole (Jung *et al*., 1994), suggesting that a role for the temporal hippocampus in the processing of large-scale spatial information may exist (Kjelstrup *et al*., 2008). Regarding the emotion-related functions of hippocampal regions, much attention has been directed towards their communication with the amygdala for emotional processing. In this regard, it has been noted that except for the septal-most portion of the hippocampus, all other parts innervate the amygdala (Kishi *et al*., 2006) which may offer insight into the inconsistent outcomes seen in rodent fear-conditioning studies involving lesions or inactivation of either the septal or temporal hippocampus (Carvalho *et al*., 2008; Maren *et al*., 1997). However, it remains unclear what the functional implications are in the context of stress.

Furthermore, there is evidence to suggest that differences along the longitudinal axis of the hippocampus extend to adult neurogenesis as well, which could reflect differences in information processing and information relayed to downstream connected brain structures (Anacker & Hen, 2017). Research in rodents indicates that the septal hippocampus displays elevated levels of adult neurogenesis, quantified by the number of adult-born cells expressing doublecortin, whereas the temporal hippocampus demonstrates reduced levels of adult neurogenesis (Jinno, 2011; Snyder *et al*., 2009). Complex spatial and contextual stimulation is linked with septal neurogenesis, whereas chronic stress is associated with a decrease in neurogenesis specifically in the temporal dentate gyrus (Kempermann *et al*., 1997; Lehmann *et al*., 2013; Tanti *et al*., 2012, 2013). Conversely, chronic treatment with antidepressants has been shown to increase neurogenesis in the same temporal area (Boldrini *et al*., 2009; Wu & Hen, 2014).

Overall, the available evidence suggests the presence of functional segregation within the hippocampus. However, the interpretation of this evidence seems to point towards highly intertwined functions in the hippocampus rather than a distinct independent separation along the mammalian septotemporal axis. The complete nature and impact on cognitive and emotional processing is still not entirely comprehended.

## 1.6.    Is there functional segregation in birds?

The proposed conservation of the hippocampus across different vertebrates raises the question of whether its functional segregation is also present in other animals, for example, birds.

Despite a vast literature on the mammalian hippocampus, the functional attributes of the avian hippocampus, particularly its potential for functional segregation along its longitudinal axis, have received relatively limited attention. In general, when it comes to the avian hippocampus there is a lack of availability of comparative anatomy data. The relative lack of research on the functional segregation of the avian hippocampus may be attributed to two main factors. Firstly, varying anatomical configurations of the hippocampus across vertebrates (Muzio & Bingman, 2022; Striedter, 2016) may have likely limited comparative analysis and interpretations of functional studies. Secondly, there has

been a greater emphasis on the study of the cognitive properties of the hippocampus overlooking its crucial contribution to emotional regulation.

While the avian hippocampus is structurally different from the mammalian hippocampus, it is clear from the available evidence that it is crucial for both processing spatial information and regulating the HPA axis, similar to the mammalian hippocampus, indicating functional conservation. This conclusion is supported by recent comprehensive reviews by Smulders (2017, 2021) and Madison *et al*. (2024), which highlight the importance of the avian hippocampus in these functions.

If we want to understand whether the functional segregation of the mammalian hippocampus is conserved or divergent in birds, comparative studies are necessary. Examining the connectivity patterns, and functional roles of hippocampal regions in both mammals and birds should reveal either similarities or differences between the two groups. However, while it is reasonable to expect that the avian hippocampus will exhibit some degree of functional segregation, it is unlikely to manifest as a clear rostral versus caudal difference, just like in mammals this functional segregation appears to be more nuanced than a simple septal-temporal divide. Instead, the avian hippocampus may exhibit a more complex organization with gradient-like functional subregions.

Admittedly, the approach to this question in this research project was under the assumption that functional segregation would present as a clear rostrocaudal divide as evidenced by the hypotheses proposed in Chapters 2 and 3, as well as in the rather limited sampling of the hippocampus across different rostrocaudal levels. It was expected the rostral end would be involved in cognitive abilities, akin to the mammalian septal pole, while the caudal end would participate in stress regulation, akin to the temporal mammalian hippocampus. Under this framework, the finding of *FOS* activation in the rostral hippocampus in response to stress termination (Chapter 3), along with its connectivity to the PVN indicative of a potential role in the negative feedback of the HPA axis (Chapter 4), would imply that the structural properties of the hippocampus, such as the intrinsic and extrinsic circuitry, may have undergone evolutionary modifications while retaining core functions.

However, it is crucial to consider two alternative perspectives. First, while our study focused on a limited sampling of the hippocampus across rostrocaudal levels, a more exhaustive sampling across different rostrocaudal levels may have revealed a gradient-like activation pattern of the hippocampus in response to stress, reflecting varying degrees of involvement across different regions along the rostrocaudal axis. Second, the exploration of the connectivity patterns of the caudal hippocampus could have offered further insights. It cannot be ruled out that similar connections to those observed in Chapter 4, supporting communication between the rostral hippocampus to the PVN, may also exist across the caudal hippocampus. If confirmed, these alternative possibilities would suggest the evolutionary conservation of functional segregation in the avian hippocampus.

Indeed, retrograde tracing studies conducted in songbirds have revealed a distinct pattern: the rostral hippocampus receives a greater number of inputs from the thalamus, while the caudal hippocampus receives more inputs from amygdalar regions (Applegate *et al*., 2023). Similarly, research in pigeons has identified a direct connection from the caudal hippocampus to the nucleus

*periventricularis magnocellularis* (PVM), the presumed homologue of a portion of the mammalian PVN (Herold *et al*., 2019). Like mammals, the connectivity of the hippocampus appears to be organized in a topographical manner along the longitudinal axis (Atoji *et al*., 2002, 2006; Herold *et al*., 2019; Krayniak & Siegel, 1978).

Once again, just like in mammals, most of the evidence regarding hippocampal function in birds comes from lesion studies which can pose challenges in interpretation. Functional studies have reported that activation of the HF in response to isolation extends throughout the entirety of the rostral to caudal hippocampal formation in quail chicks (Takeuchi *et al*., 1996) and that the effect of lesions in both the caudal and rostral hippocampus has a stronger effect on CORT titres in pigeons than when the lesion is restricted to only the caudal hippocampus (Bouillé & Baylé, 1973). The lack of consensus in defining the boundaries between the rostral and caudal hippocampus adds further complexity to these interpretations. Some descriptions delineate the boundary at A7.00 (Atoji *et al*., 2002), while others extend it as far rostrally as A11.00–A11.50 (Erichsen *et al*., 1991; Krebs *et al*., 1991), based on the atlas of Karten and Hodos (1967).

Additional evidence regarding the stress sensitivity of the avian hippocampus comes from studies focused on how the avian hippocampus responds to chronic stress and neurogenesis. Like mammals, anteroposterior differences in adult neurogenesis have been reported in chickens showing stress-induced decreases in adult neurogenesis in the caudal hippocampus (Armstrong *et al*., 2020; Gualtieri *et al*., 2019) but also across both the caudal and rostral hippocampus (Armstrong *et al*., 2022; Robertson *et al*., 2017).

To sum up, while the current study supports the existence of functional segregation in the avian HF, it also proposes some modifications in connectivity patterns may have occurred through evolution resulting in functional differences. It is essential to acknowledge methodological constraints that may contribute to variations in reported data when investigating avian hippocampal functions. The complexity of the hippocampal circuitry, combined with species-specific differences, adds another layer of complexity to the interpretation of experimental findings. Therefore, further research is necessary to fully understand this phenomenon and its potential impact on our understanding of the neural basis of avian cognition and behaviour.

## 1.7.    Reflection on methodological challenges

While the present study has provided valuable insights into the role of the avian hippocampus in the regulation of stress, it is important to acknowledge several limitations encountered during the project and to offer cautionary tales to guide future similar endeavours.

One of the key lessons learned from the study in Chapter 2 is the considerable challenge of disentangling the hippocampus's role in stress from its involvement in spatial memory and navigation. Our initial study design aimed to elucidate the specific contribution of the hippocampus to stress response mechanisms. However, I encountered difficulties in inducing a robust stress response while controlling for spatial cues. Surprisingly, the spatial context overshadowed the effects of the stressor,

indicating the need for a more refined stress induction procedure. It became evident that moving forward a more robust and effective stress induction procedure was required, as well as more exhaustive measures to minimize any novel spatial influences. Future studies in this domain should carefully consider the experimental design to ensure the isolation of stress-related effects from spatial context. This may involve modifying the stress induction protocol, additional control groups accounting for environmental novelty, as well as controlling environmental variables more tightly, or employing innovative experimental paradigms that mitigate spatial confounds.

In addition to methodological considerations, logistical challenges also arose. As we embarked on designing a new experiment, it became apparent that a meticulous selection of stress induction methods that would evoke a physiological stress response without significantly altering the animals' surroundings would only be possible by changing the experimental subjects from adult hens to chicks. Securing appropriate space for administering the stress induction treatment without alerting other animals in the group was essential to prevent the stressor from becoming a constant feature in the lives of the animals, which could potentially attenuate their response to the stimuli by the time of experimentation. For instance, standard stressors such as transportation, noise, restriction, or handling, which are commonly employed in laboratory settings, were unsuitable due to their potential to introduce confounding environmental variables by requiring moving the animals to a separate room to avoid disrupting the natural behaviours of the experimental subjects in the home pen.

The size of the chicks allowed for more effective control of the environment and the spaces available to perform the stress induction treatment without alerting the other animals while using conspecific isolation as a stressor, a method that has proven its effectiveness in previous research (Bolhuis, 1991; Nakagawa & Waas, 2004; Remage-Healey *et al*., 2003). This time around, the stress induction method employed proved to be effective.

Another potential pitfall is the overreliance on a single methodology. As discussed in Chapter 4, the *in vivo* tract-tracing experiments encountered numerous challenges, leading to an overall inefficacy in retrograde and anterograde labelling of the circuitry, with low replication across individuals. In addition to the aforementioned challenges, a critical consideration is the precise localization of the tracer injection sites. Notably, incorporating retrograde tracers presents significantly greater difficulty compared to anterograde tracers, primarily due to the distance, positioning, and small size of the regions of interest. Structures such as the PVN have posed particular challenges owing to their size and location, as acknowledged in previous studies (Cullinan *et al*., 1993; Kahn *et al*., 2003). How most of these studies resolve such problems is by additive and subtractive inferences, which depend on identifying overlap or lack of overlap in injection sites across multiple cases. However, if there is low replicability across subjects it becomes impossible to solve such problems.

The incorporation of organotypic slice cultures instead of relying only on the *in vivo* tract tracing provided a valuable alternative approach for obtaining the necessary data to support the study's objectives. This approach allowed for greater control over the injection sites and provided a more accurate representation of the target circuitry. The results obtained through this approach were consistent

with the study's hypotheses and provided new insights into the hippocampal communication with the PVN.

In addition, to complement the study, we planned for the use of intracranial injections of the green fluorescent protein (GFP) viral vector, which was successfully generated from plasmids and purified to a level where it was effectively expressed upon injection into the chick hippocampus. By using intracranial injections of the GFP viral vector, we expected to overcome some of the challenges faced during the *in vivo* experiments. This approach would reduce the number of injection sites, facilitate transsynaptic expression, and accessibility to visualize the expression of the vector with minimal processing of the tissue, thus offering additional advantages.

I find this approach particularly exciting because viral vector-mediated labelling techniques have the potential to greatly enhance our understanding of avian brain connectivity and function. For instance, the use of viral vectors opens the possibility for future research to explore the functional implications of the hippocampal connectivity patterns proposed here. In recent years, chemogenetic approaches using designer receptors exclusively activated by Designer Receptors Exclusively Activated Designer Drugs (DREADDs) have advanced our understanding of the relationship between brain function and behaviour, including the role of the mammalian hippocampus in emotional regulation (Parfitt *et al*., 2017). This methodology enables selective mapping of neuronal circuitry and manipulation of the behavioural output. Moreover, it facilitates the reversible remote control of cell populations and neural circuits via systemic injection or microinfusion of an activating ligand (Alexander *et al*., 2009; Armbruster *et al*., 2007). Typically, DREADD expression in behavioural neuroscience experiments is mediated by viral vector-induced neuronal transfection. Among the most common methods used for neuronal transfection are the intracranial injections of recombinant adeno-associated viral vectors (AAVs) encoding DREADDs (Campbell & Marchant, 2018). Therefore, validating viral vectors effective for neuronal transduction in chickens represents a significant advancement in this technique's development and could lead to new insights regarding hippocampal control of avian behaviour.

In hindsight, however, I recognize that access to up-to-date imaging instruments and ongoing refinement of our experimental approach could have significantly improved connectivity detection during the *in vivo* tract-tracing experiments. However, logistical constraints inherent in the research process, such as the need to source and transport animals to university facilities, along with daily housing and veterinary costs, as well as time limitations, posed significant challenges. These constraints hindered our ability to perhaps take a pause after each surgery, evaluate our options, and implement this approach more effectively. Had we been able to continually update our methodology, we might have been better equipped to overcome the challenges we encountered and achieve more robust results. Nonetheless, these reflections are speculative, and it is up to future research to determine their validity.

As always, the greatest obstacle of this whole endeavour was time. Due to the time constraints of the study, conducting additional tests was just not feasible. Additional experiments employing state-of-the-art tracing and functional analyses will be necessary to validate the functional properties of the

avian hippocampus, including those proposed in this study. However, I firmly believe that this research significantly contributes to our comprehension of hippocampal connectivity in the chicken brain, offering valuable insights into the evolutionary and functional aspects of this critical brain region.

Overall, the methodology used in this research project was effective in answering the project's aims and understanding the phenomenon under investigation. However, it is important not to lose sight of the fact that the stress response involves a complex interplay of interconnected neuroendocrine, cellular, and molecular mechanisms. Just at the level of the brain, there is still much to be uncovered regarding the interactions of the hippocampus with the avian amygdala and other relevant components. As ongoing refinements and validations of these techniques progress, it becomes increasingly evident that they hold the potential to advance previously unexplored aspects of avian neurobiology. I believe that through collaborative interdisciplinary efforts, future research will enhance the opportunity to critically assess the morphology of the avian brain, ultimately contributing to a more nuanced understanding of the hippocampal function.

## 1.8.  Take-home message

Understanding the neurobiological mechanisms underlying stress regulation in birds is crucial for advancing our knowledge of both the fundamental principles governing brain evolution and the unique adaptive stress responses that characterize the avian brain. One of the primary motivations behind this research project was to uncover insights into the evolutionary trajectory of the avian hippocampus and the conservation of hippocampal function across vertebrates by exploring the role of the hippocampus in stress regulation in chickens.

Throughout this work, I have consistently highlighted numerous similarities between the mammalian and avian hippocampus, serving to either support or contrast the findings presented in this thesis. However, it remains crucial to acknowledge that while identifying homologies can offer a valuable framework for analysing brain morphology across vertebrates, the pursuit of these relationships should not be the first and only goal when trying to understand the structural organization and function of the avian HF. By solely focusing on similarities, there is a risk of overlooking fresh insights into the distinct adaptations of birds to stress, among other aspects of their unique evolutionary trajectory.

As noted by Striedter (2005), "explaining species differences is considerably harder than explaining species similarities, which are easily attributed to common ancestry or convergence". Yet, it is within these differences that the key to unveiling novel research avenues lies. For instance, delving deeper into the discoveries outlined in this thesis, along with a thorough examination of the neuroanatomy and connectivity of structures specific to the avian stress response, such as the NHpC, holds the potential to uncover valuable information regarding the mechanisms by which birds cope with stressors.

To the best of my knowledge, the work on this dissertation represents the first documentation of hippocampal activity in response to acute stress induction. Furthermore, the observation of retrograde labelling from the PVN into the hippocampus, spanning across the rostral HF (as discussed in Chapter

4), provides additional support for the involvement of the rostral region in stress regulation. Consequently, I find no compelling reason to exclude the rostral hippocampus from consideration in the context of stress regulation. When considering the question of which subdivision and rostrocaudal region of the chicken hippocampus is involved in stress regulation, the main takeaway is there is not enough evidence to say that one specific region is solely responsible, while others are not involved. This lack of evidence, however, does not imply that all regions perform identical functions.

Overall, the complexity of the avian HF and its functional organization, underscore the need for further research on the anatomy and underlying mechanisms of the avian HF, particularly as stress regulation is a crucial aspect of avian adaptation and survival. The existing data, including the findings from this study, strongly suggest that dividing the avian hippocampus into distinct portions with clear-cut separate functions would be an oversimplification of the properties of this structure.

While these results shed light on the complexity of hippocampal function, further investigations are necessary to fully grasp the functional implications of these findings. Further research in this field could contribute to a deeper understanding of the mechanisms underlying avian cognition and behaviour, leading to the development of new strategies and interventions aimed at improving the health and welfare of avian species, both in the wild and in captivity.


## 1.9.    Conclusion

In conclusion, the findings from this study highlight the importance of the hippocampus in stress regulation in the chicken brain and provide valuable insights into the subdivisions of the avian hippocampus and the connectivity involved in regulating stress. These findings have important implications for our interpretation of the functional properties of the hippocampus and the overall conservation of this structure across vertebrates. The finding of rostral hippocampal activation in response to acute stress and the retrograde labelling of the ventral subdivision, also in the rostral HF, may ultimately contribute to a reinterpretation of the functional segregation of this structure in birds.

**Annexes**

**Annex1. Original Ct values for PCR analysis of genes in the chicken pituitary.**

| # | Group | Ct | Ct | ΔCt | Ct | ΔCt | Ct | ΔCt | Ct | ΔCt | Ct | ΔCt |
|---|-------|-----|------|----------|-------|-----------|-------|-----------|-------|----------|-------|----------|
|   |       | LBR | POMC | POMC/LBR | CRHR1 | CRHR1/LBR | CRHR2 | CRHR2/LBR | VT2R | VT2R/LBR | VT4R | VT4R/LBR |
| 1 | Control | 4.29E-18 | 1.48E-18 | 3.46E-01 | 1.27E-19 | 2.95E-02 | 7.34E-20 | 1.71E-02 | 2.36E-18 | 5.51E-01 | 1.85E-18 | 4.31E-01 |
| 2 | Stress | 2.21E-18 | 9.78E-19 | 4.42E-01 | 1.36E-19 | 6.14E-02 | 6.66E-20 | 3.01E-02 | 2.78E-18 | 1.26E+00 | 1.54E-18 | 6.98E-01 |
| 3 | Control | 8.33E-19 | 8.80E-19 | 1.06E+00 | 4.06E-20 | 4.87E-02 | 5.47E-20 | 6.57E-02 | 3.52E-19 | 4.23E-01 | 7.20E-19 | 8.65E-01 |
| 4 | Stress | 1.58E-18 | 1.77E-18 | 1.12E+00 | 9.59E-20 | 6.07E-02 | 7.78E-20 | 4.93E-02 | 8.41E-19 | 5.32E-01 | 1.73E-18 | 1.09E+00 |
| 5 | Control | 1.86E-18 | 1.91E-18 | 1.03E+00 | 1.29E-19 | 6.95E-02 | 4.40E-20 | 2.37E-02 | 1.46E-18 | 7.88E-01 | 1.09E-18 | 5.85E-01 |
| 6 | Stress | 3.34E-19 | 1.07E-19 | 3.21E-01 | 4.38E-21 | 1.31E-02 | 5.38E-20 | 1.61E-01 | 2.93E-20 | 8.77E-02 | 3.24E-19 | 9.71E-01 |
| 7 | Control | 2.83E-19 | 6.05E-20 | 2.14E-01 | 4.60E-21 | 1.63E-02 | 2.54E-20 | 8.99E-02 | 9.89E-21 | 3.50E-02 | 1.02E-19 | 3.61E-01 |
| 8 | Stress | 1.49E-18 | 1.57E-18 | 1.05E+00 | 8.53E-20 | 5.71E-02 | 7.31E-20 | 4.89E-02 | 1.32E-18 | 8.82E-01 | 1.04E-18 | 6.95E-01 |
| 9 | Control | 2.79E-19 | 6.34E-21 | 2.27E-02 | 1.43E-21 | 5.12E-03 | 1.25E-20 | 4.49E-02 | 1.47E-21 | 5.27E-03 | 1.69E-20 | 6.04E-02 |
| 10 | Stress | 1.81E-19 | 1.32E-21 | 7.26E-03 | 6.68E-22 | 3.68E-03 | 3.05E-21 | 1.68E-02 | 3.97E-22 | 2.19E-03 | 4.29E-21 | 2.36E-02 |
| 11 | Control | 2.52E-19 | 8.84E-21 | 3.51E-02 | 1.77E-21 | 7.02E-03 | 1.44E-20 | 5.71E-02 | 4.29E-21 | 1.70E-02 | 9.01E-20 | 3.57E-01 |
| 12 | Stress | 8.65E-20 | 1.01E-21 | 1.17E-02 | 3.27E-22 | 3.78E-03 | 3.56E-22 | 4.12E-03 | 1.04E-22 | 1.20E-03 | 7.05E-22 | 8.14E-03 |
| 13 | Control | 9.02E-20 | 5.45E-22 | 6.04E-03 | 1.72E-22 | 1.91E-03 | 7.07E-22 | 7.84E-03 | 1.58E-22 | 1.76E-03 | 5.96E-22 | 6.61E-03 |
| 14 | Stress | 1.46E-18 | 1.70E-18 | 1.16E+00 | 7.33E-20 | 5.02E-02 | 6.89E-20 | 4.72E-02 | 7.22E-19 | 4.94E-01 | 6.74E-19 | 4.62E-01 |
| 15 | Control | 8.28E-20 | 1.39E-21 | 1.68E-02 | 5.20E-22 | 6.28E-03 | 1.40E-22 | 1.69E-03 | 1.68E-22 | 2.03E-03 | 5.85E-22 | 7.07E-03 |
| 16 | Stress | 1.37E-18 | 1.36E-18 | 9.95E-01 | 7.01E-20 | 5.12E-02 | 5.13E-20 | 3.75E-02 | 1.57E-18 | 1.15E+00 | 8.73E-19 | 6.38E-01 |

**Annex 2. Original Ct values for PCR analysis of FOS in the caudal hippocampus of chicks under isolation stress (A), stressed chicks reunited with companions (B), and control chicks in home pen (D).**

| # | Group | Ventral Ct FOS | Ventral Ct GAPDH | Ventral ΔCt FOS/GAPDH | Dorsomedial Ct FOS | Dorsomedial Ct GAPDH | Dorsomedial ΔCt FOS/GAPDH | Dorsolateral Ct FOS | Dorsolateral Ct GAPDH | Dorsolateral ΔCt FOS/GAPDH |
|---|---|---|---|---|---|---|---|---|---|---|
| 1 | A | 1.11E-20 | 1.30E-17 | 8.57E-04 | 8.38E-21 | 1.15E-17 | 7.28E-04 | 9.63E-21 | 8.42E-18 | 1.14E-03 |
| 2 | A | 2.58E-20 | 2.25E-17 | 1.14E-03 | 6.39E-21 | 7.40E-18 | 8.63E-04 | 5.72E-21 | 6.84E-18 | 8.37E-04 |
| 3 | A | 4.84E-21 | 1.21E-17 | 3.99E-04 | 9.36E-21 | 1.16E-17 | 8.04E-04 | 3.36E-21 | 6.66E-18 | 5.05E-04 |
| 4 | A | 1.88E-19 | 1.66E-17 | 1.13E-02 | 3.35E-21 | 9.89E-18 | 3.38E-04 | 4.45E-21 | 6.32E-18 | 7.04E-04 |
| 5 | A | 3.13E-21 | 1.04E-17 | 3.01E-04 | 4.42E-21 | 3.03E-18 | 1.46E-03 | 5.50E-21 | 6.36E-18 | 8.64E-04 |
| 6 | A | 6.48E-21 | 2.51E-17 | 2.59E-04 | 5.60E-21 | 9.38E-18 | 5.96E-04 | 3.66E-21 | 7.90E-18 | 4.63E-04 |
| 7 | A | 2.76E-19 | 1.22E-17 | 2.27E-02 | 4.59E-21 | 7.18E-18 | 6.38E-04 | 2.96E-21 | 3.73E-18 | 7.92E-04 |
| 8 | A | 4.39E-21 | 2.13E-17 | 2.06E-04 | 2.98E-21 | 6.46E-18 | 4.60E-04 | 3.14E-21 | 3.20E-18 | 9.83E-04 |
| 9 | B | 4.27E-21 | 1.26E-17 | 3.40E-04 | 1.26E-20 | 2.11E-17 | 5.99E-04 | 1.22E-20 | 2.22E-17 | 5.48E-04 |
| 10 | B | 3.80E-21 | 7.44E-18 | 5.11E-04 | 8.56E-21 | 1.48E-17 | 5.77E-04 | 5.58E-21 | 1.16E-17 | 4.79E-04 |
| 11 | B | 8.13E-21 | 2.27E-17 | 3.58E-04 | 3.65E-21 | 8.05E-18 | 4.53E-04 | 6.54E-21 | 7.83E-18 | 8.35E-04 |
| 12 | B | 2.64E-21 | 7.97E-18 | 3.31E-04 | 5.76E-21 | 5.60E-18 | 1.03E-03 | 1.03E-20 | 8.53E-18 | 1.21E-03 |
| 13 | B | 6.34E-21 | 2.27E-17 | 2.79E-04 | 3.55E-21 | 4.07E-18 | 8.74E-04 | 1.22E-20 | 1.74E-17 | 7.00E-04 |
| 14 | B | 2.25E-20 | 1.59E-17 | 1.42E-03 | 3.63E-21 | 8.76E-18 | 4.15E-04 | 4.83E-21 | 1.06E-17 | 4.58E-04 |
| 15 | B | 3.83E-21 | 1.11E-17 | 3.46E-04 | 7.36E-21 | 7.00E-18 | 1.05E-03 | 4.51E-21 | 9.30E-18 | 4.85E-04 |
| 16 | B | 6.57E-21 | 1.93E-17 | 3.40E-04 | 9.67E-21 | 1.43E-17 | 6.75E-04 | 6.90E-21 | 6.02E-18 | 1.15E-03 |
| 17 | D | 4.56E-21 | 1.16E-17 | 3.93E-04 | 5.32E-21 | 6.91E-18 | 7.69E-04 | 1.12E-20 | 1.54E-17 | 7.28E-04 |
| 18 | D | 7.23E-21 | 2.98E-17 | 2.42E-04 | 3.44E-21 | 7.59E-18 | 4.54E-04 | 1.11E-20 | 1.13E-17 | 9.80E-04 |
| 19 | D | 3.75E-21 | 1.36E-17 | 2.77E-04 | 4.25E-21 | 7.04E-18 | 6.03E-04 | 4.14E-21 | 1.43E-17 | 2.89E-04 |
| 20 | D | 2.88E-21 | 2.04E-17 | 1.41E-04 | 4.12E-21 | 5.77E-18 | 7.15E-04 | 1.14E-20 | 1.07E-17 | 1.06E-03 |
| 21 | D | 3.71E-21 | 7.29E-18 | 5.09E-04 | 3.63E-21 | 9.81E-18 | 3.70E-04 | 1.74E-20 | 9.09E-18 | 1.91E-03 |
| 22 | D | 5.08E-21 | 1.58E-17 | 3.21E-04 | 5.08E-21 | 1.03E-17 | 4.94E-04 | 4.44E-21 | 6.51E-18 | 6.82E-04 |
| 23 | D | 3.57E-21 | 6.18E-18 | 5.78E-04 | 3.69E-21 | 7.10E-18 | 5.20E-04 | 3.40E-21 | 7.27E-18 | 4.68E-04 |
| 24 | D | 3.62E-21 | 1.99E-17 | 1.82E-04 | 5.57E-21 | 8.86E-18 | 6.29E-04 | 5.40E-21 | 3.94E-18 | 1.37E-03 |

**Annex 3. Original Ct values for PCR analysis of FOS in the rostral hippocampus of chicks under isolation stress (A), stressed chicks reunited with companions (B), and control chicks in home pen (D).**

| # | Group | Ventral Ct FOS | Ventral Ct GAPDH | Ventral ΔCt FOS/GAPDH | Dorsomedial Ct FOS | Dorsomedial Ct GAPDH | Dorsomedial ΔCt FOS/GAPDH | Dorsolateral Ct FOS | Dorsolateral Ct GAPDH | Dorsolateral ΔCt FOS/GAPDH |
|---|---|---|---|---|---|---|---|---|---|---|
| 1 | A | 8.58E-21 | 8.84E-18 | 9.71E-04 | 2.20E-20 | 9.27E-18 | 2.38E-03 | 1.96E-20 | 1.56E-17 | 1.25E-03 |
| 2 | A | 2.84E-21 | 2.00E-17 | 1.42E-04 | 3.33E-21 | 2.70E-18 | 1.24E-03 | 9.18E-21 | 1.16E-17 | 7.94E-04 |
| 3 | A | 2.38E-21 | 7.93E-18 | 3.00E-04 | 5.44E-21 | 6.85E-18 | 7.94E-04 | 2.51E-21 | 4.51E-18 | 5.55E-04 |
| 4 | A | 4.69E-21 | 1.90E-17 | 2.46E-04 | 8.38E-21 | 4.24E-18 | 1.98E-03 | 1.31E-20 | 1.16E-17 | 1.13E-03 |
| 5 | A | 5.75E-21 | 1.39E-17 | 4.12E-04 | 1.22E-20 | 6.41E-18 | 1.91E-03 | 1.29E-20 | 1.25E-17 | 1.03E-03 |
| 6 | A | 2.59E-21 | 1.24E-17 | 2.09E-04 | 2.61E-21 | 5.95E-18 | 4.38E-04 | 4.31E-21 | 3.42E-18 | 1.26E-03 |
| 7 | A | 3.57E-21 | 5.41E-18 | 6.59E-04 | 7.44E-21 | 9.11E-18 | 8.16E-04 | 1.46E-20 | 1.73E-17 | 8.46E-04 |
| 8 | A | 2.63E-21 | 1.41E-17 | 1.86E-04 | 1.36E-20 | 1.43E-17 | 9.54E-04 | 1.06E-20 | 8.99E-18 | 1.18E-03 |
| 9 | B | 5.48E-21 | 9.54E-18 | 5.74E-04 | 1.07E-20 | 8.70E-18 | 1.23E-03 | 2.41E-20 | 5.79E-18 | 4.17E-03 |
| 10 | B | 3.40E-21 | 8.67E-18 | 3.93E-04 | 1.63E-20 | 1.03E-17 | 1.58E-03 | 1.05E-20 | 2.29E-17 | 4.56E-04 |
| 11 | B | 3.46E-21 | 1.21E-17 | 2.85E-04 | 1.19E-20 | 6.14E-18 | 1.94E-03 | 1.18E-20 | 1.72E-17 | 6.91E-04 |
| 12 | B | 7.64E-21 | 1.66E-17 | 4.61E-04 | 1.77E-20 | 7.11E-18 | 2.50E-03 | 3.00E-21 | 1.05E-17 | 2.86E-04 |
| 13 | B | 2.51E-21 | 4.96E-18 | 5.07E-04 | 1.83E-20 | 4.56E-18 | 4.02E-03 | 1.39E-20 | 1.35E-17 | 1.03E-03 |
| 14 | B | 1.07E-20 | 1.90E-17 | 5.60E-04 | 8.28E-21 | 6.37E-19 | 1.30E-02 | 1.54E-20 | 3.01E-17 | 5.10E-04 |
| 15 | B | 4.89E-21 | 1.58E-17 | 3.10E-04 | 3.35E-21 | 8.49E-18 | 3.94E-04 | 3.09E-21 | 4.66E-18 | 6.64E-04 |
| 16 | B | 2.78E-21 | 2.02E-17 | 1.38E-04 | 1.35E-20 | 1.25E-17 | 1.08E-03 | 2.02E-20 | 4.92E-17 | 4.10E-04 |
| 17 | D | 3.85E-21 | 1.05E-17 | 3.67E-04 | 6.76E-21 | 5.44E-18 | 1.24E-03 | 7.40E-21 | 7.85E-18 | 9.42E-04 |
| 18 | D | 4.45E-21 | 1.43E-17 | 3.12E-04 | 6.80E-21 | 7.55E-18 | 9.00E-04 | 5.37E-21 | 1.22E-17 | 4.40E-04 |
| 19 | D | 8.47E-21 | 4.06E-17 | 2.09E-04 | 8.36E-21 | 7.68E-18 | 1.09E-03 | 1.45E-20 | 2.57E-17 | 5.66E-04 |
| 20 | D | 4.64E-21 | 1.54E-17 | 3.01E-04 | 9.31E-21 | 6.68E-18 | 1.39E-03 | 7.87E-21 | 1.32E-17 | 5.98E-04 |
| 21 | D | 7.93E-21 | 1.23E-17 | 6.42E-04 | 1.22E-20 | 3.39E-18 | 3.61E-03 | 7.16E-21 | 6.88E-18 | 1.04E-03 |
| 22 | D | 3.12E-21 | 1.15E-17 | 2.72E-04 | 2.54E-23 | 4.88E-18 | 5.20E-06 | 1.45E-20 | 9.86E-18 | 1.47E-03 |
| 23 | D | 3.08E-21 | 7.43E-18 | 4.15E-04 | 4.73E-21 | 2.46E-18 | 1.92E-03 | 4.61E-21 | 6.53E-18 | 7.06E-04 |
| 24 | D | 5.61E-21 | 1.27E-17 | 4.43E-04 | 1.44E-20 | 7.59E-18 | 1.90E-03 | 7.18E-21 | 5.41E-18 | 1.33E-03 |

# References

1.  Abellán, A., Desfilis, E., & Medina, L. (2014). Combinatorial expression of Lef1, Lhx2, Lhx5, Lhx9, Lmo3, Lmo4, and Prox1 helps to identify comparable subdivisions in the developing hippocampal formation of mouse and chicken. *Frontiers in neuroanatomy*, 8, 59.

2.  Able, K. (2003). The concepts and terminology of bird navigation. *Journal of Avian Biology*. 32. 174 - 183. 10.1034/j.1600-048X.2001.320211.x.

3.  Aboitiz, F. (2011). Genetic and developmental homology in amniote brains. Toward conciliating radical views of brain evolution. *Brain Research Bulletin*, *84*(2), 125–136. https://doi.org/10.1016/j.brainresbull.2010.12.003

4.  Acher, R., Chauvet, J., & Chauvet, M.T. (1970). Phylogeny of the Neurohypophysial Hormones. The Avian Active Peptides. *European Journal of Biochemistry*, 17(3), 509–513.

5.  Adhikari, A., Topiwala, M. A., & Gordon, J. A. (2010). Synchronized activity between the ventral hippocampus and the medial prefrontal cortex during anxiety. *Neuron*, *65*(2), 257-269.

6.  Ahumada-Galleguillos, P., Fernández, M., Marin, G. J., Letelier, J. C., & Mpodozis, J. (2015). Anatomical organization of the visual dorsal ventricular ridge in the chick (*Gallus gallus*): Layers and columns in the avian pallium. *The Journal of comparative neurology*, *523*(17), 2618–2636. https://doi.org/10.1002/cne.23808

7.  Alexander, G. M., Rogan, S. C., Abbas, A. I., Armbruster, B. N., Pei, Y., Allen, J. A., Nonneman, R. J., Hartmann, J., Moy, S. S., Nicolelis, M. A., McNamara, J. O., & Roth, B. L. (2009). Remote control of neuronal activity in transgenic mice expressing evolved G protein-coupled receptors. *Neuron*, 63(1), 27–39. https://doi.org/10.1016/j.neuron.2009.06.014

8.  Aman, N. A., Nagarajan, G., Kang, S. W., Hancock, M., & Kuenzel, W. J. (2016). Differential responses of the vasotocin 1a receptor (V1aR) and osmoreceptors to immobilization and osmotic stress in sensory circumventricular organs of the chicken (*Gallus gallus*) brain. *Brain Research*, 1649, 67-78.

9.  Amaral, D. G. (1995). The rat nervous system. *Hippocampal Formation*, 443-493.

10. Amaral, D. G., & Witter, M. P. (1989). The three-dimensional organization of the hippocampal formation: a review of anatomical data. *Neuroscience*, *31*(3), 571-591. https://doi.org/10.1016/0306-4522(89)90424-7

11. Amundson, R. (2001). Homology and Homoplasy: A Philosophical Perspective. *eLS*. doi:10.1038/npg.els.0003445

12. Anacker, C., & Hen, R. (2017). Adult hippocampal neurogenesis and cognitive flexibility - linking memory and mood. *Nature reviews. Neuroscience*, 18(6), 335–346. https://doi.org/10.1038/nrn.2017.45

13. Ang, S. T., Ariffin, M. Z., & Khanna, S. (2017). The forebrain medial septal region and nociception. *Neurobiology of Learning and Memory*, *138*, 238-251.

14. Applegate, M. C., Gutnichenko, K. S., & Aronov, D. (2023). Topography of inputs into the hippocampal formation of a food-caching bird. *Journal of Comparative Neurology*, 531(16), 1669-1688.

15. Armbruster, B. N., Li, X., Pausch, M. H., Herlitze, S., & Roth, B. L. (2007). Evolving the lock to fit the key to create a family of G protein-coupled receptors potently activated by an inert ligand. *Proceedings of the National Academy of Sciences*, 104(12), 5163-5168.

16. Armstrong, E. A., Richards-Rios, P., Addison, L., Sandilands, V., Guy, J. H., Wigley, P., ... & Smulders, T. V. (2022). Poor body condition is associated with lower hippocampal plasticity and higher gut methanogen abundance in adult laying hens from two housing systems. *Scientific Reports*, *12*(1), 15505.

17. Armstrong, E. A., Rufener, C., Toscano, M. J., Eastham, J. E., Guy, J. H., Sandilands, V., Boswell, T., & Smulders, T. V. (2020). Keel bone fractures induce a depressive-like state in laying hens. *Scientific reports*, 10(1), 3007.

18. Atoji, Y., & Wild, J. M. (2004). Fiber connections of the hippocampal formation and septum and subdivisions of the hippocampal formation in the pigeon as revealed by tract tracing and kainic acid lesions. *The Journal of comparative neurology*, *475*(3), 426–461. https://doi.org/10.1002/cne.20186

19. Atoji, Y., & Wild, J. M. (2005). Afferent and efferent connections of the dorsolateral corticoid area and a comparison with connections of the temporo-parieto-occipital area in the pigeon (Columba livia). *The Journal of Comparative Neurology*, 485(2), 165–182.

20. Atoji, Y., & Wild, J. M. (2006). Anatomy of the avian hippocampal formation. *Reviews in the neurosciences*, 17(1-2), 3–15.

21. Atoji, Y., Saito, S., & Wild, J. M. (2006). Fiber connections of the compact division of the posterior pallial amygdala and lateral part of the bed nucleus of the stria terminalis in the pigeon (Columba livia). *Journal of Comparative Neurology*, *499*(2), 161-182.

22. Atoji, Y., Sarkar, S. and Wild, J.M. (2016), Proposed homology of the dorsomedial subdivision and V-shaped layer of the avian hippocampus to Ammon's horn and dentate gyrus, respectively. *Hippocampus*, 26: 1608-1617. https://doi.org/10.1002/hipo.22660

23. Atoji, Y., Wild, J. M., Yamamoto, Y., & Suzuki, Y. (2002). Intratelencephalic connections of the hippocampus in pigeons (Columba livia). *Journal of Comparative Neurology*, *447*(2), 177-199.

24. Audhya, T., Hollander, C. S., Schlesinger, D. H., & Hutchinson, B. (1989). Structural characterization and localization of corticotropin-releasing factor in testis. *Biochimica et Biophysica Acta (BBA)/Protein Structure and Molecular*, 995(1), 10–16.

25. Avery, S. N., Clauss, J. A., Winder, D. G., Woodward, N., Heckers, S., & Blackford, J. U. (2014). BNST neurocircuitry in humans. *NeuroImage*, 91, 311–323. https://doi.org/10.1016/j.neuroimage.2014.01.017

26. Baeyens, D. A., & Cornett, L. E. (2006). The cloned avian neurohypophysial hormone receptors. *Comparative biochemistry and physiology. Part B, Biochemistry & molecular biology*, 143(1), 12–19. https://doi.org/10.1016/j.cbpb.2005.09.012

27. Bálint, E., Mezey, S., & Csillag, A. (2011). Efferent connections of nucleus accumbens subdivisions of the domestic chicken (Gallus domesticus): an anterograde pathway tracing study. *Journal of Comparative Neurology,* 519(15), 2922-2953.

28. Ball, M. J., Fisman, M., Hachinski, V., Blume, W., Fox, A., Kral, V. A., Kirshen, A. J., Fox, H., & Merskey, H. (1985). A new definition of Alzheimer's disease: a hippocampal dementia. *Lancet* (London, England), 1(8419), 14–16. https://doi.org/10.1016/s0140-6736(85)90965-1

29. Banasr, M., Soumier, A., Hery, M., Mocaër, E., & Daszuta, A. (2006). Agomelatine, a New Antidepressant, Induces Regional Changes in Hippocampal Neurogenesis. *Biological Psychiatry*, 59(11), 1087–1096.

30. Bannerman, D. M., Grubb, M., Deacon, R. M. J., Yee, B. K., Feldon, J., & Rawlins, J. N. P. (2003). Ventral hippocampal lesions affect anxiety but not spatial learning. *Behavioural brain research*, *139*(1-2), 197-213.

31. Bannerman, D. M., Yee, B. K., Good, M. A., Heupel, M. J., Iversen, S. D., & Rawlins, J. N. P. (1999). Double dissociation of function within the hippocampus: a comparison of dorsal, ventral, and complete hippocampal cytotoxic lesions. *Behavioral neuroscience*, 113(6), 1170.

32. Bannerman, D., Rawlins, J. N., McHugh, S., Deacon, R. M., Yee, B., Bast, T., Feldon, J. (2004). Regional dissociations within the hippocampus—memory and anxiety. *Neuroscience & Biobehavioral Reviews*, 28(3), 273–283.

33. Barnea, A., & Pravosudov, V. (2011). Birds as a model to study adult neurogenesis: bridging evolutionary, comparative and neuroethological approaches. *European Journal of Neuroscience*, 34(6), 884–907.

34. Barnea, A., Mishal, A., & Nottebohm, F. (2006). Social and spatial changes induce multiple survival regimes for new neurons in two regions of the adult brain: An anatomical representation of time? *Behavioural Brain Research*, 167(1), 63–74.

35. Basil, J. A., Kamil, A. C., Balda, R. P., & Fite, K. V. (1996). Differences in hippocampal volume among food-storing corvids. *Brain, behavior and evolution*, 47(3), 156–164. https://doi.org/10.1159/000113235

36. Bell, C. C. (2002). Evolution of cerebellum-like structures. *Brain, behavior and evolution*, 59(5-6), 312–326. https://doi.org/10.1159/000063567

37. Belleau, E. L., Treadway, M. T., & Pizzagalli, D. A. (2019). The Impact of Stress and Major Depressive Disorder on Hippocampal and Medial Prefrontal Cortex Morphology. *Biological psychiatry*, 85(6), 443–453. https://doi.org/10.1016/j.biopsych.2018.09.031

38. Benowitz, L. I., & Karten, H. J. (1976). The tractus infundibuli and other afferents to the parahippocampal region of the pigeon. *Brain research*, 102(1), 174–180. https://doi.org/10.1016/0006-8993(76)90584-9

39. Berk, M. L. (1987). Projections of the lateral hypothalamus and bed nucleus of the stria terminalis to the dorsal vagal complex in the pigeon. *Journal of Comparative Neurology*, 260(1), 140-156.

40. Berk, M. L., & Finkelstein, J. A. (1983). Long descending projections of the hypothalamus in the pigeon, Columba livia. *The Journal of comparative neurology*, 220(2), 127–136. https://doi.org/10.1002/cne.902200202

41. Berk, M. L., & Hawkin, R. K. (1985). Ascending projections of the mammillary region in the pigeon: Emphasis on telencephalic connections. *The Journal of Comparative Neurology*, 239(3), 330–340.

42. Bernstein, H. L., Lu, Y. L., Botterill, J. J., & Scharfman, H. E. (2019). Novelty and Novel Objects Increase c-Fos Immunoreactivity in Mossy Cells in the Mouse Dentate Gyrus. *Neural plasticity*, 2019, 1815371. https://doi.org/10.1155/2019/1815371

43. Beuving, G., & Vonder, G. M. (1977). Daily rhythm of corticosterone in laying hens and the influence of egg laying. *Journal of reproduction and fertility*, 51(1), 169–173. https://doi.org/10.1530/jrf.0.0510169

44. Bingman V. P., Salas C., Rodriguez F. (2009) Evolution of the Hippocampus. In: Binder M.D., Hirokawa N., Windhorst U. (eds) *Encyclopedia of Neuroscience*. Springer, Berlin, Heidelberg

45. Bingman, V. P., Bagnoli, P., Ioalè, P., & Casini, G. (1984). Homing behavior of pigeons after telencephalic ablations. *Brain, behavior and evolution*, 24(2-3), 94–108. https://doi.org/10.1159/000121308

46. Bingman, V. P., Ioalè, P., Casini, G., & Bagnoli, P. (1985). Dorsomedial forebrain ablations and home loft association behavior in homing pigeons. *Brain, behavior and evolution*, 26(1), 1–9. https://doi.org/10.1159/000118763

47. Bingman, V.P., Salas, C., Rodriguez, F. (2009). Evolution of the Hippocampus. In: Binder, M.D., Hirokawa, N., Windhorst, U. (eds) *Encyclopedia of Neuroscience. Springer*, Berlin, Heidelberg. https://doi.org/10.1007/978-3-540-29678-2_3158

48. Bird, C. M., & Burgess, N. (2008). The hippocampus and memory: insights from spatial processing. Nature reviews. Neuroscience, 9(3), 182–194. https://doi.org/10.1038/nrn2335

49. Boldrini, M., Underwood, M. D., Hen, R., Rosoklija, G. B., Dwork, A. J., John Mann, J., & Arango, V. (2009). Antidepressants increase neural progenitor cells in the human hippocampus. *Neuropsychopharmacology*, 34(11), 2376-2389.

50. Bolhuis, J. J. (1991). Mechanisms of avian imprinting: a review. *Biological Reviews*, 66(4), 303-345.

51. Bonne, O., Vythilingam, M., Inagaki, M., Wood, S., Neumeister, A., Nugent, A. C., ... & Charney, D. S. (2008). Reduced posterior hippocampal volume in posttraumatic stress disorder. *Journal of Clinical Psychiatry*, 69(7), 1087-1091.

52. Bons, N., Bouillé, C., Bayle, J., & Assenmacher, I. (1976). Light and electron microscopic evidence of hypothalamic afferences originating from the hippocampus in the pigeon. *Experientia, 32*, 1443-1445. https://doi.org/10.1007/BF01937423

53. Bons, N., Bouille, C., Tonon, M. C., & Guillaume, V. (1988). Topographical distribution of CRF immunoreactivity in the pigeon brain. *Peptides*, 9(4), 697-707.

54. Bons, N., Bouillé, C., Vaudry, H., & Guillaume, V. (1985). Localization Of Corticotropin-Releasing Factor Producing Neurons In The Pigeon Brain-An Immunofluorescence Study. *Comptes Rendus De L Academie Des Sciences Serie Iii-Sciences De La Vie-Life Sciences*, 300(2), 49-52.

55. Bouillé, C., & Baylé, J. D. (1973a). Effects of hypothalamic stimulation on pituitary-adrenocortical activity in conscious unrestrained pigeons. *Neuroendocrinology*, 12(4-5), 284-294.

56. Bouillé, C., & Baylé, J. D. (1973b). Effects of Limbic Stimulations or Lesions on Basal and Stress-Induced Hypothalamic-Pituitary-Adrenocortical Activity in the Pigeon. *Neuroendocrinology*, 13(4-5), 264–277.

57. Bouillé, C., & Baylé, J. D. (1973c). Experimental studies on the adrenocorticotropic area in the pigeon hypothalamus. *Neuroendocrinology*, *11*(2), 73-91.

58. Bouillé, C., & Baylé, J. D. (1976). Comparison between hypothalamic, hippocampal and septal multiple unit activity and basal corticotropic function in unrestrained, unanesthetized resting pigeons. *Neuroendocrinology*, 22(2), 164–174. https://doi.org/10.1159/000122623

59. Bouillé, C., Raymond, J., & Baylé, J. D. (1977). Retrograde transport of horseradish peroxidase from the nucleus posterior medialis hypothalami to the hippocampus and the medial septum in the pigeon. *Neuroscience*, 2(3), 435–439. doi:10.1016/0306-4522(77)90008-2

60. Bruce, L. L., Erichsen, J. T., & Reiner, A. (2016). Neurochemical compartmentalization within the pigeon basal ganglia. *Journal of chemical neuroanatomy*, *78*, 65-86.

61. Bruhn, T. O., Engeland, W. C., Anthony, E. L. P., Gann, D. S., & Jackson, I. M. D. (1987). Corticotropin-releasing Factor in the Adrenal Medulla. *Annals of the New York Academy of Sciences, 512(1)*, 115–128.

62. Buijs, R. M. (1978). Intra-and extrahypothalamic vasopressin and oxytocin pathways in the rat: pathways to the limbic system, medulla oblongata and spinal cord. *Cell and tissue research*, 192(3), 423-435.

63. Bullock, T.H., Behrend, K., & Heiligenberg, W. (1975). Comparison of the jamming avoidance responses in Gymnotoid and Gymnarchid electric fish: A case of convergent evolution of behavior and its sensory basis. *Journal of comparative physiology*, 103, 97-121.

64. Calandreau, L., Jaffard, R., & Desmedt, A. (2007). Dissociated roles for the lateral and medial septum in elemental and contextual fear conditioning. *Learning & Memory*, *14*(6), 422-429.

65. Campbell, E. J., & Marchant, N. J. (2018). The use of chemogenetics in behavioural neuroscience: receptor variants, targeting approaches and caveats. *British journal of pharmacology*, 175(7), 994–1003. https://doi.org/10.1111/bph.14146

66. *Cannon, W. B. (1915).* Bodily changes in pain, hunger, fear and rage: An account of recent research into the function of emotional excitement. *D Appleton & Company. https://doi.org/10.1037/10013-000*

67. Cannon, W.B. (1939). The wisdom of the body (2nd ed.). Norton & Co.

68. Canteras, N. S., & Swanson, L. W. (1992). Projections of the ventral subiculum to the amygdala, septum, and hypothalamus: a PHAL anterograde tract-tracing study in the rat. *Journal of Comparative Neurology*, 324(2), 180-194.

69. Carroll, S. B. (2008). Evo-devo and an expanding evolutionary synthesis: a genetic theory of morphological evolution. *Cell*, 134(1), 25–36. https://doi.org/10.1016/j.cell.2008.06.030

70. Carvalho, M. C., Masson, S., Brandão, M. L., & de Souza Silva, M. A. (2008). Anxiolytic-like effects of substance P administration into the dorsal, but not ventral, hippocampus and its influence on serotonin. *Peptides*, 29(7), 1191–1200. https://doi.org/10.1016/j.peptides.2008.02.014

71. Casini, G., Bingman, V.P. and Bagnoli, P. (1986), Connections of the pigeon dorsomedial forebrain studied with WGA-HRP and ^{3}H-proline. *Journal of Comparative Neurology*., 245: 454-470. https://doi.org/10.1002/cne.902450403

72. Ceccatelli, S., Villar, M. J., Goldstein, M., & Hökfelt, T. (1989). Expression of c-Fos immunoreactivity in transmitter-characterized neurons after stress. *Proceedings of the National Academy of Sciences of the United States of America,* 86(23), 9569–9573. https://doi.org/10.1073/pnas.86.23.9569

73. Cecchi, M., Khoshbouei, H., Javors, M., & Morilak, D. A. (2002). Modulatory effects of norepinephrine in the lateral bed nucleus of the stria terminalis on behavioral and neuroendocrine responses to acute stress. *Neuroscience*, *112*(1), 13–21. https://doi.org/10.1016/s0306-4522(02)00062-3

74. Charmandari, E., Tsigos, C., & Chrousos, G. (2005). Endocrinology of the stress response. Annual review of physiology, 67, 259–284. https://doi.org/10.1146/annurev.physiol.67.040403.120816

75. Chattarji, S., Tomar, A., Suvrathan, A., Ghosh, S., & Rahman, M. M. (2015). Neighborhood matters: divergent patterns of stress-induced plasticity across the brain. Nature neuroscience, 18(10), 1364–1375. https://doi.org/10.1038/nn.4115

76. Chen, Y., Fenoglio, K. A., Dubé, C. M., Grigoriadis, D. E., & Baram, T. Z. (2006). Cellular and molecular mechanisms of hippocampal activation by acute stress are age-dependent. *Molecular psychiatry,* 11(11), 992-1002.

77. Chowdhury, G. M., Fujioka, T., & Nakamura, S. (2000). Induction and adaptation of Fos expression in the rat brain by two types of acute restraint stress. *Brain research bulletin,* 52(3), 171–182. https://doi.org/10.1016/s0361-9230(00)00231-8

78. Chrousos, G.P. (2000), The Stress Response and Immune Function: Clinical Implications: The 1999 Novera H. Spector Lecture. Annals of the New York Academy of Sciences, 917: 38-67. https://doi.org/10.1111/j.1749-6632.2000.tb05371.x

79. Chrousos, G. P., & Gold, P. W. (1992). The Concepts of Stress and Stress System Disorders. *JAMA*, 267(9), 1244-1252.

80. Cockrem J. F. (2013). Corticosterone responses and character in birds: Individual variation and the ability to cope with environmental changes due to climate change. *General and comparative endocrinology,* 190, 156–163. https://doi.org/10.1016/j.ygcen.2013.02.021

81. Cole, A. B., Montgomery, K., Bale, T. L., & Thompson, S. M. (2022). What the hippocampus tells the HPA axis: Hippocampal output attenuates acute stress responses via disynaptic inhibition of CRF+ PVN neurons. *Neurobiology of stress*, *20*, 100473.

82. Colombo, M., & Broadbent, N. (2000). Is the avian hippocampus a functional homologue of the mammalian hippocampus? *Neuroscience & Biobehavioral Reviews*, 24(4), 465–484.

83. Conrad, C. D., Magariños, A. M., LeDoux, J. E., & McEwen, B. S. (1999). Repeated restraint stress facilitates fear conditioning independently of causing hippocampal CA3 dendritic atrophy. *Behavioral neuroscience*, 113(5), 902.

84. Conrad, C. D., Galea, L. A., Kuroda, Y., & McEwen, B. S. (1996). Chronic stress impairs rat spatial memory on the Y maze, and this effect is blocked by tianeptine treatment. Behavioral neuroscience, 110(6), 1321.

85. Conrad, L. C., & Pfaff, D. W. (1976). Autoradiographic tracing of nucleus accumbens efferents in the rat. *Brain research*, 113(3), 589–596. https://doi.org/10.1016/0006-8993(76)90060-3

86. Cornett, L. E., Kang, S. W., & Kuenzel, W. J. (2013). A possible mechanism contributing to the synergistic action of vasotocin (VT) and corticotropin-releasing hormone (CRH) receptors on corticosterone release in birds. *General and Comparative Endocrinology*, 188, 46–53.

87. Cornett, L. E., Kirby, J. D., Vizcarra, J. A., Ellison, J. C., Thrash, J., Mayeux, P. R., Crew, M. D., Jones, S. M., Ali, N., & Baeyens, D. A. (2003). Molecular cloning and functional characterization of a vasotocin receptor subtype expressed in the pituitary gland of the domestic chicken (Gallus domesticus): avian homolog of the mammalian V1b-vasopressin receptor. *Regulatory peptides*, 110(3), 231–239. https://doi.org/10.1016/s0167-0115(02)00216-1

88. Coveñas, R., de León, M., Cintra, A., Bjelke, B., Gustafsson, J. A., & Fuxe, K. (1993). Coexistence of c-Fos and glucocorticoid receptor immunoreactivities in the CRF immunoreactive neurons of the paraventricular hypothalamic nucleus of the rat after acute immobilization

stress. *Neuroscience letters*, *149*(2), 149–152. https://doi.org/10.1016/0304-3940(93)90758-d

89. Cui, Z., Gerfen, C. R., & Young, W. S., 3rd (2013). Hypothalamic and other connections with dorsal CA2 area of the mouse hippocampus. *Journal of Comparative Neurology*, 521(8), 1844–1866. https://doi.org/10.1002/cne.23263

90. Cullinan, W. E., Herman, J. P., & Watson, S. J. (1993). Ventral subicular interaction with the hypothalamic paraventricular nucleus: evidence for a relay in the bed nucleus of the stria terminalis. *Journal of Comparative Neurology*, *332*(1), 1-20.

91. Cullinan, W. E., Herman, J. P., Battaglia, D. F., Akil, H., & Watson, S. J. (1995). Pattern and time course of immediate early gene expression in rat brain following acute stress. *Neuroscience*, 64(2), 477–505.

92. Dallman, M. F. (2005). Fast glucocorticoid actions on brain: back to the future. *Frontiers in neuroendocrinology*, 26(3-4), 103-108.

93. Dallman, M. F., Akana, S. F., Cascio, C. S., Darlington, D. N., Jacobson, L., & Levin, N. (1987). Regulation of ACTH Secretion: Variations on a Theme of B. *Proceedings of the 1986 Laurentian Hormone Conference*, 113–173.

94. Dallman, M. F., Levin, N., Cascio, C. S., Akana, S. F., Jacobson, L., & KUHN, R. W. (1989). Pharmacological evidence that the inhibition of diurnal adrenocorticotropin secretion by corticosteroids is mediated via type I corticosterone-preferring receptors. *Endocrinology*, *124*(6), 2844-2850.

95. Darlington, D. N., Chew, G., Ha, T., Keil, L. C., & Dallman, M. F. (1990). Corticosterone, but not glucose, treatment enables fasted adrenalectomized rats to survive moderate hemorrhage. *Endocrinology*, 127(2), 766-772.

96. Davis, M., Walker, D. L., Miles, L., & Grillon, C. (2010). Phasic vs sustained fear in rats and humans: role of the extended amygdala in fear vs anxiety. *Neuropsychopharmacology*, 35(1), 105-135.

97. Day, T. A. (2005). Defining stress as a prelude to mapping its neurocircuitry: no help from allostasis. *Progress in Neuro-Psychopharmacology and Biological Psychiatry*, 29(8), 1195-1200.

98. de Haas, E. N., Bolhuis, J. E., Kemp, B., Groothuis, T. G., & Rodenburg, T. B. (2014). Parents and early life environment affect behavioral development of laying hen chickens. *PloS one*, 9(6), e90577. https://doi.org/10.1371/journal.pone.0090577

99. de Haas, E. N., Kemp, B., Bolhuis, J. E., Groothuis, T., & Rodenburg, T. B. (2013). Fear, stress, and feather pecking in commercial white and brown laying hen parent-stock flocks and their relationships with production parameters. *Poultry Science*, 92(9), 2259-2269.

100. De Kloet, E. R., Joëls, M., & Holsboer, F. (2005). Stress and the brain: from adaptation to disease. *Nature Reviews Neuroscience*, 6(6), 463–475.

101. De Kloet, E. R., Vreugdenhil, E., Oitzl, M. S., & Joëls, M. (1998). Brain Corticosteroid Receptor Balance in Health and Disease. *Endocrine Reviews*, 19(3), 269–301.

102. De Morais Magalhães, N. G., Guerreiro Diniz, C., Guerreiro Diniz, D., Pereira Henrique, E., Corrêa Pereira, P. D., Matos Moraes, I. A., … Wanderley Picanço Diniz, C. (2017). Hippocampal neurogenesis and volume in migrating and wintering semipalmated sandpipers (Calidris pusilla). *PLOS ONE*, 12(6), e0179134.

103. Denver, R. J. (2009). Structural and Functional Evolution of Vertebrate Neuroendocrine Stress Systems. *Annals of the New York Academy of Sciences*, 1163(1), 1–16.

104. Dranovsky, A., & Hen, R. (2006). Hippocampal Neurogenesis: Regulation by Stress and Antidepressants. *Biological Psychiatry*, 59(12), 1136–1143.

105. Dunn, I. C., Wilson, P. W., Smulders, T. V., Sandilands, V., D'Eath, R. B., & Boswell, T. (2013). Hypothalamic agouti-related protein expression is affected by both acute and chronic experience of food restriction and re-feeding in chickens. *Journal of Neuroendocrinology*, 25(10), 920–928. https://doi.org/10.1111/jne.12088

106. Edgar, J., Held, S., Paul, E., Pettersson, I., I'Anson Price, R., & Nicol, C. (2015). Social buffering in a bird. *Animal Behaviour, 105,* 11–19.

107. Eichenbaum, H., Dudchenko, P., Wood, E., Shapiro, M., & Tanila, H. (1999). The hippocampus, memory, and place cells: is it spatial memory or a memory space? *Neuron*, 23(2), 209-226.

108. Eiserer, L.A. (1990). Effects of environmental novelty on distress vocalisations of ducklings following withdrawal of an imprinting object. *Bulletin of the psychonomic society*, 28, 225-227.

109. El Falougy, H., & Benuska, J. (2006). History, anatomical nomenclature, comparative anatomy and functions of the hippocampal formation. *Bratislavske lekarske listy*, *107*(4), 103.

110. Emery, N. J., & Clayton, N. S. (2004). The mentality of crows: convergent evolution of intelligence in corvids and apes. *Science* (New York, N.Y.), 306(5703), 1903–1907. https://doi.org/10.1126/science.1098410

111. Erichsen, J. T., Bingman, V. P., & Krebs, J. R. (1991). The distribution of neuropeptides in the dorsomedial telencephalon of the pigeon (Columba livia): a basis for regional subdivisions. The Journal of Comparative Neurology, 314(3), 478–492.

112. Ericsson, M., Fallahsharoudi, A., Bergquist, J., Kushnir, M. M., & Jensen, P. (2014). Domestication effects on behavioural and hormonal responses to acute stress in chickens. *Physiology and Behavior*, 133(133), 161–169

113. Fallahsharoudi, A., De Kock, N., Johnsson, M., Ubhayasekera, S. J. K. A., Bergquist, J., Wright, D., & Jensen, P. (2015). Domestication effects on stress-induced steroid secretion and adrenal gene expression in chickens. *Scientific Reports*, 5(Sept), 1–10.

114.    Fanselow, M. S., & Dong, H. W. (2010). Are the dorsal and ventral hippocampus functionally distinct structures? *Neuron*, 65(1), 7–19.

115.    Felix-Ortiz, A. C., Beyeler, A., Seo, C., Leppla, C. A., Wildes, C. P., & Tye, K. M. (2013). BLA to vHPC inputs modulate anxiety-related behaviors. *Neuron*, *79*(4), 658–664.

116.    Feltenstein, M. W., Lambdin, L. C., Webb, H. E., Warnick, J. E., Khan, S. I., Khan, I. A., Acevedo, E. O., & Sufka, K. J. (2003). Corticosterone response in the chick separation-stress paradigm. *Physiology & behavior*, *78*(3), 489–493. https://doi.org/10.1016/s0031-9384(03)00030-1

117.    Ferbinteanu, J., & McDonald, R. J. (2001). Dorsal/ventral hippocampus, fornix, and conditioned place preference. *Hippocampus*, 11(2), 187-200.

118.    Fink, G. (2016). Stress: Concepts, definition and history. *The Curated Reference Collection in Neuroscience and Biobehavioral Psychology* (pp. 549-555). doi:10.1016/B978-0-12-809324-5.02208-2

119.    Fischette, C. T., Edinger, H. M., & Siegel, A. (1981). Temporary desynchronization among circadian rhythms with lateral fornix ablation. *Brain research*, *229*(1), 85–101. https://doi.org/10.1016/0006-8993(81)90748-4

120.    Fischette, C. T., Komisaruk, B. R., Edinger, H. M., Feder, H. H., & Siegel, A. (1980). Differential fornix ablations and the circadian rhythmicity of adrenal corticosteroid secretion. *Brain research*, *195*(2), 373–387. https://doi.org/10.1016/0006-8993(80)90073-6

121.    Fredes, F., Silva, M.A., Koppensteiner, P., Kobayashi, K., Joesch, M., & Shigemoto, R. (2020). Ventro-dorsal Hippocampal Pathway Gates Novelty-Induced Contextual Memory Formation. *Current Biology*, 31, 25 - 38.e5.

122.    Frey, B. N., Andreazza, A. C., Nery, F. G., Martins, M. R., Quevedo, J., Soares, J. C., & Kapczinski, F. (2007). The role of hippocampus in the pathophysiology of bipolar disorder. *Behavioural pharmacology*, 18(5-6), 419-430.

123.    Fujita, T., Aoki, N., Mori, C., Fujita, E., Matsushima, T., Homma, K. J., & Yamaguchi, S. (2022). Chick Hippocampal Formation Displays Subdivision- and Layer-Selective Expression Patterns of Serotonin Receptor Subfamily Genes. *Frontiers in physiology*, 13, 882633. https://doi.org/10.3389/fphys.2022.882633

124.    Gagnon, S. A., & Wagner, A. D. (2016). Acute stress and episodic memory retrieval: neurobiological mechanisms and behavioral consequences. *Annals of the New York Academy of Sciences*, 1369(1), 55-75.

125.    Gebauer, T., Gebauer, R., Císař, P., Černý, J., Roy, D. R., Zare, M., Verleih, M., Stejskal, V., & Rebl, A. (2023). Are bold-shy personalities of European perch (Perca fluviatilis) linked to stress tolerance and immunity? A scope of harnessing fish behavior in aquaculture. *Fish & shellfish immunology*, *143*, 109190. https://doi.org/10.1016/j.fsi.2023.109190

126. Gergues, M. M., Han, K. J., Choi, H. S., Brown, B., Clausing, K. J., Turner, V. S., Vainchtein, I. D., Molofsky, A. V., & Kheirbek, M. A. (2020). Circuit and molecular architecture of a ventral hippocampal network. *Nature Neuroscience*, 23(11), 1444–1452.

127. Girotti, M., Weinberg, M. S., & Spencer, R. L. (2007). Differential responses of hypothalamus-pituitary-adrenal axis immediate early genes to corticosterone and circadian drive. *Endocrinology*, 148(5), 2542–2552. https://doi.org/10.1210/en.2006-1304

128. Godoy, L. D., Rossignoli, M. T., Delfino-Pereira, P., Garcia-Cairasco, N., & de Lima Umeoka, E. H. (2018). A Comprehensive Overview on Stress Neurobiology: Basic Concepts and Clinical Implications. *Frontiers in behavioral neuroscience*, *12*, 127. https://doi.org/10.3389/fnbeh.2018.00127

129. Goerlich, V. C., Nätt, D., Elf wing, M., Macdonald, B., & Jensen, P. (2012). Transgenerational effects of early experience on behavioral, hormonal and gene expression responses to acute stress in the precocial chicken. *Hormones and behavior*, 61(5), 711–718. https://doi.org/10.1016/j.yhbeh.2012.03.006

130. Goldstein, D. S., & McEwen, B. (2002). Allostasis, homeostats, and the nature of stress. Stress (Amsterdam, Netherlands), 5(1), 55–58. https://doi.org/10.1080/102538902900012345

131. Goodson, J. L. (2008). Nonapeptides and the evolutionary patterning of sociality. *Progress in brain research*, 170, 3-15.

132. Goodson, J. L., Evans, A. K., & Lindberg, L. (2004). Chemoarchitectonic subdivisions of the songbird septum and a comparative overview of septum chemical anatomy in jawed vertebrates. *The Journal of comparative neurology*, *473*(3), 293–314. https://doi.org/10.1002/cne.20061

133. Gould, S. J. (2002). The structure of evolutionary theory. Cambridge, MA: Harvard University Press.

134. Gualtieri, F., Armstrong, E. A., Longmoor, G. K., D'Eath, R. B., Sandilands, V., Boswell, T., & Smulders, T. V. (2019). Unpredictable Chronic Mild Stress Suppresses the Incorporation of New Neurons at the Caudal Pole of the Chicken Hippocampal Formation. *Scientific Reports*, 9(1), 1–13.

135. Guillette, L. M., & Sturdy, C. B. (2011). Individual differences and repeatability in vocal production: stress-induced calling exposes a songbird's personality. *Die Naturwissenschaften*, *98*(11), 977–981. https://doi.org/10.1007/s00114-011-0842-8

136. Gupta, S., Maurya, R., Saxena, M., & Sen, J. (2012). Defining structural homology between the mammalian and avian hippocampus through conserved gene expression patterns observed in the chick embryo. *Developmental biology*, 366(2), 125-141.

137.    Gust, D. A., Gordon, T. P., Brodie, A. R., & McClure, H. M. (1994). Effect of a preferred companion in modulating stress in adult female rhesus monkeys. *Physiology & behavior*, *55*(4), 681–684. https://doi.org/10.1016/0031-9384(94)90044-2

138.    Hagstrum J. T. (2013). Atmospheric propagation modeling indicates homing pigeons use loft-specific infrasonic 'map' cues. *The Journal of experimental biology*, 216(Pt 4), 687–699. https://doi.org/10.1242/jeb.072934

139.    Hakeem J. Kadhim, Seong W. Kang & Wayne J. Kuenzel (2021) Possible roles of brain derived neurotrophic factor and corticotropin releasing hormone neurons in the nucleus of hippocampal commissure functioning within the avian neuroendocrine regulation of stress, *Stress*, 24:5, 590-601, DOI: 10.1080/10253890.2021.1929163

140.    Hall, B.K. (2003). Descent with modification: the unity underlying homology and homoplasy as seen through an analysis of development and evolution. *Biological Reviews*, 78: 409-433. https://doi.org/10.1017/S1464793102006097

141.    Hall, B.K. (2013). Homology, homoplasy, novelty, and behaviour. *Developmental psychobiology*, 55(1), 4–12. https://doi.org/10.1002/dev.21039

142.    Hampton, R. R., & Shettleworth, S. J. (1996). Hippocampal lesions impair memory for location but not color in passerine birds. *Behavioral neuroscience*, *110*(4), 831.

143.    Hansson, A. C., Sommer, W., Rimondini, R., Andbjer, B., Strömberg, I., & Fuxe, K. (2003). c-fos reduces corticosterone-mediated effects on neurotrophic factor expression in the rat hippocampal CA1 region. *The Journal of neuroscience: the official journal of the Society for Neuroscience*, *23*(14), 6013–6022. https://doi.org/10.1523/JNEUROSCI.23-14-06013.2003

144.    He, J., & Crews, F. T. (2007). Neurogenesis decreases during brain maturation from adolescence to adulthood. *Pharmacology Biochemistry and Behavior*, 86(2), 327–333.

145.    Henke P. G. (1990). Hippocampal pathway to the amygdala and stress ulcer development. *Brain research bulletin*, 25(5), 691–695. https://doi.org/10.1016/0361-9230(90)90044-z

146.    Herdegen, T., & Leah, J. D. (1998). Inducible and constitutive transcription factors in the mammalian nervous system: control of gene expression by Jun, Fos and Krox, and CREB/ATF proteins. *Brain research. Brain research reviews*, 28(3), 370–490. https://doi.org/10.1016/s0165-0173(98)00018-6

147.    Herman, J. P., & Cullinan, W. E. (1997). Neurocircuitry of stress: central control of the hypothalamo–pituitary–adrenocortical axis. *Trends in neurosciences*, *20*(2), 78-84.

148.    Herman, J. P., Dolgas, C. M., & Carlson, S. L. (1998). Ventral subiculum regulates hypothalamo-pituitary-adrenocortical and behavioural responses to cognitive stressors. *Neuroscience*, 86(2), 449–459. https://doi.org/10.1016/s0306-4522(98)00055-4

149.    Herman, J. P., Figueiredo, H., Mueller, N. K., Ulrich-Lai, Y., Ostrander, M. M., Choi, D. C., & Cullinan, W. E. (2003). Central mechanisms of stress integration: hierarchical circuitry

controlling hypothalamo-pituitary-adrenocortical responsiveness. *Frontiers in neuroendocrinology*, *24*(3), 151–180. https://doi.org/10.1016/j.yfrne.2003.07.001

150. Herman, J. P., McKlveen, J. M., Ghosal, S., Kopp, B., Wulsin, A., Makinson, R., Scheimann, J., & Myers, B. (2016). Regulation of the Hypothalamic-Pituitary-Adrenocortical Stress Response. *Comprehensive Physiology*, 6(2), 603–621. https://doi.org/10.1002/cphy.c150015

151. Herman, J. P., Schäfer, M. K., Young, E. A., Thompson, R., Douglass, J., Akil, H., & Watson, S. J. (1989). Evidence for hippocampal regulation of neuroendocrine neurons of the hypothalamo-pituitary-adrenocortical axis. *The Journal of neuroscience: the official journal of the Society for Neuroscience*, 9(9), 3072–3082.

152. Herman, J. P., Tasker, J. G., Ziegler, D. R., & Cullinan, W. E. (2002). Local circuit regulation of paraventricular nucleus stress integration: glutamate–GABA connections. Pharmacology Biochemistry and Behavior, 71(3), 457-468.

153. Herman, J., & Mueller, N. (2006). Role of the ventral subiculum in stress integration. *Behavioural Brain Research*, 174(2), 215–224.

154. Hermans, E. J., Henckens, M. J., Joëls, M., & Fernández, G. (2014). Dynamic adaptation of large-scale brain networks in response to acute stressors. Trends in neurosciences, 37(6), 304–314. https://doi.org/10.1016/j.tins.2014.03.006

155. Herold, C., Bingman, V. P., Ströckens, F., Letzner, S., Sauvage, M., Palomero-Gallagher, N., Zilles, K., & Güntürkün, O. (2014). Distribution of neurotransmitter receptors and zinc in the pigeon (Columba livia) hippocampal formation: A basis for further comparison with the mammalian hippocampus. *The Journal of comparative neurology*, 522(11), 2553–2575. https://doi.org/10.1002/cne.23549

156. Herold, C., Schlömer, P., Mafoppa-Fomat, I., Mehlhorn, J., Amunts, K., & Axer, M. (2019). The hippocampus of birds in a view of evolutionary connectomics. *Cortex; a journal devoted to the study of the nervous system and behavior*, 118, 165–187. https://doi.org/10.1016/j.cortex.2018.09.025

157. Holland, R. (2014). True navigation in birds: From quantum physics to global migration. *Journal of Zoology*. 293. 10.1111/jzo.12107.

158. Honkaniemi, J. (1992). Colocalization of peptide-and tyrosine hydroxylase-like immunoreactivities with Fos-immunoreactive neurons in rat central amygdaloid nucleus after immobilization stress. *Brain research*, *598*(1-2), 107-113.

159. Hough, G. E., 2nd, Pang, K. C., & Bingman, V. P. (2002). Intrahippocampal connections in the pigeon (Columba livia) as revealed by stimulation evoked field potentials. *The Journal of comparative neurology*, 452(3), 297–309. https://doi.org/10.1002/cne.10409

160. Hunsaker, M. R., & Kesner, R. P. (2008). Dissociations across the dorsal–ventral axis of CA3 and CA1 for encoding and retrieval of contextual and auditory-cued fear. Neurobiology of learning and memory, 89(1), 61-69.

161.    Ismail, S. N., Awad, E. A., Zulkifli, I., Goh, Y. M., & Sazili, A. Q. (2019). Effects of method and duration of restraint on stress hormones and meat quality in broiler chickens with different body weights. *Asian-Australasian journal of animal sciences,* 32(6), 865–873. https://doi.org/10.5713/ajas.18.0354

162.    Jaccoby, S., Koike, T. I., & Cornett, L. E. (1999). c-fos expression in the forebrain and brainstem of White Leghorn hens following osmotic and cardiovascular challenges. *Cell and tissue research*, 297(2), 229–239. https://doi.org/10.1007/s004410051351

163.    Jacobson, l., & Sapolsky, R. (1991). The Role of the Hippocampus in Feedback Regulation of the Hypothalamic-Pituitary-Adrenocortical Axis. *Endocrine Reviews*, 12(2), 118–134. https://doi.org/10.1210/edrv-12-2-118

164.    Jayanthi, S., Kang, S. W., Bingham, D., Tessaro, B. A., Suresh Kumar, T. K., & Kuenzel, W. J. (2014). Identification of antagonists to the vasotocin receptor sub-type 4 (VT4R) involved in stress by molecular modelling and verification using anterior pituitary cells. *Journal of Biomolecular Structure and Dynamics,* 32(4), 648-660.

165.    Jiang, Z., Rajamanickam, S., & Justice, N. J. (2019). CRF signaling between neurons in the paraventricular nucleus of the hypothalamus (PVN) coordinates stress responses. *Neurobiology of stress*, *11*, 100192. https://doi.org/10.1016/j.ynstr.2019.100192

166.    Jimenez, J. C., Su, K., Goldberg, A. R., Luna, V. M., Biane, J. S., Ordek, G., ... & Kheirbek, M. A. (2018). Anxiety cells in a hippocampal-hypothalamic circuit. *Neuron*, *97*(3), 670-683.

167.    Jinno, S. (2011). Topographic differences in adult neurogenesis in the mouse hippocampus: A stereology-based study using endogenous markers. *Hippocampus*, 21(5), 467-480.

168.    Joëls, M., & Baram, T. Z. (2009). The neuro-symphony of stress. Nature reviews. Neuroscience, 10(6), 459–466. https://doi.org/10.1038/nrn2632

169.    Johnson, A. C., Uhlig, F., Einwag, Z., Cataldo, N., & Erdos, B. (2022). The neuroendocrine stress response impairs hippocampal vascular function and memory in male and female rats. *Neurobiology of disease*, 168, 105717. https://doi.org/10.1016/j.nbd.2022.105717

170.    Jung, M. W., Wiener, S. I., & McNaughton, B. L. (1994). Comparison of spatial firing characteristics of units in dorsal and ventral hippocampus of the rat. *Journal of Neuroscience*, 14(12), 7347-7356.

171.    Jung, Min Whan & Wiener, Sidney & Mcnaughton, Bruce. (1995). Comparison of spatial firing characteristics of units in dorsal and ventral hippocampus of the rat. *The Journal of neuroscience: the official journal of the Society for Neuroscience*. 14. 7347-56. 10.1523/JNEUROSCI.14-12-07347.1994.

172.    Kadhim, H. J., & Kuenzel, W. J. (2022). Interaction between the hypothalamo-pituitary-adrenal and thyroid axes during immobilization stress. *Frontiers in physiology*, 13, 972171. https://doi.org/10.3389/fphys.2022.972171

173. Kadhim, H. J., Kang, S. W., & Kuenzel, W. J. (2019). Differential and temporal expression of corticotropin releasing hormone and its receptors in the nucleus of the hippocampal commissure and paraventricular nucleus during the stress response in chickens (*Gallus gallus*). *Brain Research*, *1714*, 1–7. https://doi.org/10.1016/j.brainres.2019.02.018

174. Kadhim, H. J., Kidd Jr, M., Kang, S. W., & Kuenzel, W. J. (2020). Differential delayed responses of arginine vasotocin and its receptors in septo-hypothalamic brain structures and anterior pituitary that sustain hypothalamic–pituitary-adrenal (HPA) axis functions during acute stress. *General and Comparative Endocrinology*, 286, 113302.

175. Kahn, M. C., Hough, G. E., 2nd, Ten Eyck, G. R., & Bingman, V. P. (2003). Internal connectivity of the homing pigeon (*Columba livia*) hippocampal formation: an anterograde and retrograde tracer study. *The Journal of comparative neurology*, 459(2), 127–141. https://doi.org/10.1002/cne.10601

176. Kamil, A. C., Goodyear, A. J., & Cheng, K. (2001). The Use of Landmarks by Clark's Nutcrackers: First Tests of a New Model. *Journal of Navigation*, 54(3), 429–435. doi:10.1017/S0373463301001436

177. Karten, H., & Hodos, W. (1967). A stereotaxic atlas of the brain of the pigeon (*Columba livia*).

178. Kaufman, I. C., & Hinde, R. A. (1961). Factors influencing distress calling in chicks, with special reference to temperature changes and social isolation. *Animal Behaviour, 9*(3-4), 197–204. https://doi.org/10.1016/0003-3472(61)90009-4

179. Kawasaki, M. (1993). Independently evolved jamming avoidance responses employ identical computational algorithms: a behavioral study of the African electric fish, *Gymnarchus niloticus*. *Journal of comparative physiology*, 173(1), 9–22. https://doi.org/10.1007/BF00209614

180. Keller-Wood, M. (2011). Hypothalamic-pituitary-adrenal Axis—feedback control. *Comprehensive Physiology*, 5(3), 1161-1182.

181. Kempermann, G., Kuhn, H. G., & Gage, F. H. (1997). More hippocampal neurons in adult mice living in an enriched environment. *Nature*, 386(6624), 493-495.

182. Kheirbek, M. A., Drew, L. J., Burghardt, N. S., Costantini, D. O., Tannenholz, L., Ahmari, S. E., … & Hen, R. (2013). Differential control of learning and anxiety along the dorsoventral axis of the dentate gyrus. *Neuron*, *77*(5), 955-968.

183. Kikusui, T., Winslow, J. T., & Mori, Y. (2006). Social buffering: relief from stress and anxiety. *Philosophical transactions of the Royal Society of London. Series B, Biological sciences*, *361*(1476), 2215–2228. https://doi.org/10.1098/rstb.2006.1941

184. Kim, E. J., Pellman, B., & Kim, J. J. (2015). Stress effects on the hippocampus: a critical review. *Learning & memory* (Cold Spring Harbor, N.Y.), 22(9), 411–416. https://doi.org/10.1101/lm.037291.114

185.   Kim, J. J., & Diamond, D. M. (2002). The stressed hippocampus, synaptic plasticity and lost memories. *Nature Reviews Neuroscience*, 3(6), 453-462.

186.   Kimball, M. G., Gautreaux, E. B., Couvillion, K. E., Kelly, T. R., Stansberry, K. R., & Lattin, C. R. (2022). Novel objects alter immediate early gene expression globally for ZENK and regionally for c-Fos in neophobic and non-neophobic house sparrows. *Behavioural brain research*, 428, 113863.

187.   Kino, T., & Chrousos, G. P. (2001). Glucocorticoid and mineralocorticoid resistance/hypersensitivity syndromes. *The Journal of endocrinology*, 169(3), 437–445. https://doi.org/10.1677/joe.0.1690437

188.   Kishi, T., Tsumori, T., Yokota, S., & Yasui, Y. (2006). Topographical projection from the hippocampal formation to the amygdala: a combined anterograde and retrograde tracing study in the rat. *The Journal of comparative neurology*, *496*(3), 349–368. https://doi.org/10.1002/cne.20919

189.   Kjelstrup, K. B., Solstad, T., Brun, V. H., Hafting, T., Leutgeb, S., Witter, M. P., Moser, E. I., & Moser, M. B. (2008). Finite scale of spatial representation in the hippocampus. *Science* (New York, N.Y.), 321(5885), 140–143. https://doi.org/10.1126/science.1157086

190.   Kjelstrup, K. G., Tuvnes, F. A., Steffenach, H. A., Murison, R., Moser, E. I., & Moser, M. B. (2002). Reduced fear expression after lesions of the ventral hippocampus. *Proceedings of the National Academy of Sciences*, *99*(16), 10825-10830.

191.   Klur, S., Muller, C., Pereira de Vasconcelos, A., Ballard, T., Lopez, J., Galani, R., ... & Cassel, J. C. (2009). Hippocampal-dependent spatial memory functions might be lateralized in rats: An approach combining gene expression profiling and reversible inactivation. *Hippocampus*, 19(9), 800-816.

192.   Knigge, K. M. (1961). Adrenocortical Response to Stress in Rats with Lesions in Hippocampus and Amygdala. *Experimental Biology and Medicine*, 108(1), 18–21.

193.   Korf H. W. (1984). Neuronal organization of the avian paraventricular nucleus: intrinsic, afferent, and efferent connections. *The Journal of Experimental Zoology*, 232(3), 387–395. https://doi.org/10.1002/jez.1402320303

194.   Krayniak, P. F., & Siegel, A. (1978). Efferent connections of the hippocampus and adjacent regions in the pigeon. *Brain, behavior and evolution*, *15*(5-6), 372–388. https://doi.org/10.1159/000123788

195.   Krebs, J. R., Erichsen, J. T., & Bingman, V. P. (1991). The distribution of neurotransmitters and neurotransmitter-related enzymes in the dorsomedial telencephalon of the pigeon (Columba livia). *The Journal of Comparative Neurology*, 314(3), 467–477. https://doi.org/10.1002/cne.903140305

196.    Krieger D. T. (1975). Rhythms of ACTH and corticosteroid secretion in health and disease, and their experimental modification. *Journal of steroid biochemistry*, 6(5), 785–791. https://doi.org/10.1016/0022-4731(75)90068-0

197.    Kuenzel, & Jurkevich, A. (2022). The avian subpallium and autonomic nervous system. In Sturkie's avian physiology / (Seventh edition., pp. 257–290). Academic Press, an imprint of Elsevier. https://doi.org/10.1016/B978-0-12-819770-7.00031-1

198.    Kuenzel, W. J., & Jurkevich, A. (2010). Molecular neuroendocrine events during stress in poultry. *Poultry science*, 89(4), 832–840. https://doi.org/10.3382/ps.2009-00376

199.    Kuenzel, W. J., Kang, S. W., & Jurkevich, A. (2013). Neuroendocrine regulation of stress in birds with an emphasis on vasotocin receptors (VTRs). *General and comparative endocrinology*, 190, 18–23. https://doi.org/10.1016/j.ygcen.2013.02.029

200.    Kumaran, D., Summerfield, J. J., Hassabis, D., & Maguire, E. A. (2009). Tracking the emergence of conceptual knowledge during human decision making. *Neuron*, 63(6), 889-901.

201.    LaDage, L. D., Roth, T. C., Fox, R. A., & Pravosudov, V. V. (2009). Ecologically relevant spatial memory use modulates hippocampal neurogenesis. *Proceedings of the Royal Society B: Biological Sciences*, 277(1684), 1071–1079.

202.    Lankester, E. R. (1870). On the use of the term homology in modern zoology, and the distinction between homogenetic and homoplastic agreements. *Journal of Natural History*, 6(31), 34–43.

203.    Larsen, P. J., Hay-Schmidt, A., & Mikkelsen, J. D. (1994). Efferent connections from the lateral hypothalamic region and the lateral preoptic area to the hypothalamic paraventricular nucleus of the rat. *The Journal of Comparative Neurology*, 342(2), 299–319. https://doi.org/10.1002/cne.903420211

204.    Lee, I., Hunsaker, M. R., & Kesner, R. P. (2005). The role of hippocampal subregions in detecting spatial novelty. *Behavioral neuroscience*, 119(1), 145–153. https://doi.org/10.1037/0735-7044.119.1.145

205.    Lee, T., Jarome, T., Li, S. J., Kim, J. J., & Helmstetter, F. J. (2009). Chronic stress selectively reduces hippocampal volume in rats: a longitudinal MRI study. Neuroreport, 20(17), 1554.

206.    Lehmann, M. L., Brachman, R. A., Martinowich, K., Schloesser, R. J., & Herkenham, M. (2013). Glucocorticoids orchestrate divergent effects on mood through adult neurogenesis. *Journal of Neuroscience*, 33(7), 2961-2972.

207.    Lever, C., Burton, S., & O'Keefe, J. (2006). Rearing on hind legs, environmental novelty, and the hippocampal formation. *Reviews in the neurosciences*, 17(1-2), 111–133. https://doi.org/10.1515/revneuro.2006.17.1-2.111

208.    Lewis, D. I., & Coote, J. H. (1990). Excitation and inhibition of rat sympathetic preganglionic neurones by catecholamines. *Brain research*, *530*(2), 229–234.

209. Littin, K. E., & Cockrem, J. F. (2001). Individual variation in corticosterone secretion in laying hens. *British poultry science*, 42(4), 536–546.

210. Loconsole, M., & Regolin, L. (2022). Here I am, why don't you answer me? Sensitivity to social responsiveness in domestic chicks. *iScience*, *26*(1), 105863. https://doi.org/10.1016/j.isci.2022.105863

211. Løtvedt, P., Fallahshahroudi, A., Bektic, L., Altimiras, J., & Jensen, P. (2017). Chicken domestication changes expression of stress-related genes in brain, pituitary and adrenals. *Neurobiology of Stress*, 7, 113–121.

212. Lu, S., Wei, F., & Li, G. (2021). The evolution of the concept of stress and the framework of the stress system. *Cell stress*, 5(6), 76–85. https://doi.org/10.15698/cst2021.06.250

213. Luine, V., Villegas, M., Martinez, C., & McEwen, B. S. (1994). Repeated stress causes reversible impairments of spatial memory performance. Brain research, 639(1), 167-170.

214. Madison, F. N., Bingman, V. P., Smulders, T. V., & Lattin, C. R. (2024). A bird's eye view of the hippocampus beyond space: Behavioral, neuroanatomical, and neuroendocrine perspectives. *Hormones and behavior*, *157*, 105451.

215. Magariños, A., Somoza, G., & De Nicola, A. (1987). Glucocorticoid Negative Feedback and Glucocorticoid Receptors After Hippocampectomy in Rats. *Hormone and Metabolic Research*, 19(03), 105–109.

216. Mandell A.J., Chapman L.F., Rand R.W., Walter R.D. (1963) Plasma corticosteroids: changes in concentration after stimulation of hippocampus and amygdala. *Science,* 139:1212

217. Maras, P. M., Molet, J., Chen, Y., Rice, C., Ji, S. G., Solodkin, A., & Baram, T. (2014). Preferential loss of dorsal-hippocampus synapses underlies memory impairments provoked by short, multimodal stress. *Molecular psychiatry*, *19*(7), 811-822.

218. Maren, S., & Fanselow, M. S. (1995). Synaptic plasticity in the basolateral amygdala induced by hippocampal formation stimulation in vivo. *Journal of Neuroscience*, 15(11), 7548-7564.

219. Maren, S., & Holt, W. G. (2004). Hippocampus and Pavlovian fear conditioning in rats: muscimol infusions into the ventral, but not dorsal, hippocampus impair the acquisition of conditional freezing to an auditory conditional stimulus. *Behavioral neuroscience*, 118(1), 97–110. https://doi.org/10.1037/0735-7044.118.1.97

220. Maren, S., Aharonov, G., & Fanselow, M. S. (1997). Neurotoxic lesions of the dorsal hippocampus and Pavlovian fear conditioning in rats. *Behavioural brain research*, 88(2), 261–274. https://doi.org/10.1016/s0166-4328(97)00088-0

221. Martínez-García, F., Novejarque, A., & Lanuza, E. (2008). Two interconnected functional systems in the amygdala of amniote vertebrates. *Brain Research Bulletin*, *75*(2-4), 206-213.

222. Marx, G., Leppelt, J., & Ellendorff, F. (2001). Vocalisation in chicks (Gallus gallus dom.) during stepwise social isolation. *Applied Animal Behaviour Science, 75*, 61-74.

223. Matsui, R., Tanabe, Y., & Watanabe, D. (2012). Avian adeno-associated virus vector efficiently transduces neurons in the embryonic and post-embryonic chicken brain. *PloS one*, 7(11), e48730. https://doi.org/10.1371/journal.pone.0048730

224. Mayer, U., Bhushan, R., Vallortigara, G., & Lee, S. A. (2018). Representation of environmental shape in the hippocampus of domestic chicks (*Gallus gallus*). *Brain structure & function*, 223(2), 941–953. https://doi.org/10.1007/s00429-017-1537-5

225. McEwen, B. S. (1999). Stress and Hippocampal Plasticity. Annual Review of *Neuroscience*, 22(1), 105–122.

226. McEwen, B. S. (2000). Stress, Definitions and Concepts of. In G. Fink (Ed.), Encyclopedia of Stress, 2nd ed., p. 653. Elsevier Inc. 10.1016/B978-012373947-6.00364-0

227. McEwen, B. S. (2005). Stressed or stressed out: what is the difference? *Journal of psychiatry & neuroscience: JPN*, *30*(5), 315–318.

228. McEwen, B. S. (2007). Physiology and neurobiology of stress and adaptation: central role of the brain. Physiological reviews, 87(3), 873-904.

229. McEwen, B. S. (2016). Central role of the brain in stress and adaptation: Allostasis, biological embedding, and cumulative change. In G. Fink (Ed.), *Stress: Concepts, cognition, emotion, and behavior*, p. 39–55. Elsevier Academic Press.

230. McEwen, B. S. (2017). Stress: Homeostasis, Rheostasis, Reactive Scope, Allostasis and Allostatic Load. 10.1016/B978-0-12-809324-5.02867-4.

231. McEwen, B. S., & Wingfield, J. C. (2003). The concept of allostasis in biology and biomedicine. *Hormones and behavior*, 43(1), 2–15. https://doi.org/10.1016/s0018-506x(02)00024-7

232. McEwen, B. S., Weiss, J., & Schwartz, L. (1968). Selective retention of corticosterone by limbic structures in rat brain. *Nature,* 220:911–12

233. McGaugh, J. L., & Roozendaal, B. (2002). Role of adrenal stress hormones in forming lasting memories in the brain. Current opinion in neurobiology, 12(2), 205-210.

234. Medina, L., & Abellán, A. (2009). Development and evolution of the pallium. *Seminars in Cell & Developmental Biology*, 20(6), 698–711.

235. Medina, L., Abellán, A., Vicario, A., Castro-Robles, B., & Desfilis, E. (2017). The amygdala. In J. Kaas (Ed.), Evolution of nervous systems (Vol. 1, 2nded., pp. 427–478). Oxford: Elsevier.

236. Melia, K. R., Ryabinin, A. E., Schroeder, R., Bloom, F. E., & Wilson, M. C. (1994). Induction and habituation of immediate early gene expression in rat brain by acute and repeated restraint stress. *The Journal of Neuroscience*, 14(10), 5929–5938.

237. Mirescu, C., & Gould, E. (2006). Stress and adult neurogenesis. *Hippocampus*, 16(3), 233–238.

238.    Montagnese, C. M., Geneser, F. A., & Krebs, J. R. (1993). Histochemical distribution of zinc in the brain of the zebra finch (*Taenopygia guttata*). *Anatomy and embryology*, 188(2), 173–187. https://doi.org/10.1007/BF00186251

239.    Montagnese, C. M., Krebs, J. R., and Meyer, G. (1996). The dorsomedial and dorsolateral forebrain of the zebra finch, *Taeniopygia guttata*: a Golgi study. *Cell and Tissue Research*. 283, 263–282. doi: 10.1007/s004410050537

240.    Montagnese, C. M., Székely, A. D., Adám, A., & Csillag, A. (2004). Efferent connections of septal nuclei of the domestic chick (*Gallus domesticus*): an anterograde pathway tracing study with a bearing on functional circuits. *The Journal of comparative neurology*, 469(3), 437–456. https://doi.org/10.1002/cne.11018

241.    Montagnese, C. M., Zachar, G., Bálint, E., & Csillag, A. (2008). Afferent connections of septal nuclei of the domestic chick (*Gallus domesticus*): a retrograde pathway tracing study. *The Journal of comparative neurology*, 511(1), 109–150. https://doi.org/10.1002/cne.21837

242.    Montevecchi, W. A., Gallup, G. G., Jr, & Dunlap, W. P. (1973). The peep vocalisation in group reared chicks (Gallus domesticus): its relation to fear. *Animal behaviour*, *21*(1), 116–123. https://doi.org/10.1016/s0003-3472(73)80049-1

243.    Morandi-Raikova, A., & Mayer, U. (2020). The effect of monocular occlusion on hippocampal c-Fos expression in domestic chicks (*Gallus gallus*). *Scientific reports*, 10(1), 7205. https://doi.org/10.1038/s41598-020-64224-9

244.    Morgan, J. I., & Curran, T. (1991). Stimulus-transcription coupling in the nervous system: involvement of the inducible proto-oncogenes fos and jun. *Annual review of neuroscience*, 14, 421–451. https://doi.org/10.1146/annurev.ne.14.030191.002225

245.    Morris, R. G., Garrud, P., Rawlins, J. N., & O'Keefe, J. (1982). Place navigation impaired in rats with hippocampal lesions. *Nature*, 297(5868), 681–683.

246.    Moser, E., Moser, M. B., & Andersen, P. (1993). Spatial learning impairment parallels the magnitude of dorsal hippocampal lesions, but is hardly present following ventral lesions. *Journal of neuroscience*, 13(9), 3916-3925.

247.    Moser, M. B., & Moser, E. I. (1998). Functional differentiation in the hippocampus. *Hippocampus*, 8(6), 608–619.

248.    Moser, M. B., Moser, E. I., Forrest, E., Andersen, P., & Morris, R. G. (1995). Spatial learning with a minislab in the dorsal hippocampus. *Proceedings of the National Academy of Sciences*, 92(21), 9697–9701. doi:10.1073/pnas.92.21.9697

249.    Mueller, N. K., Dolgas, C. M., & Herman, J. P. (2004). Stressor-selective role of the ventral subiculum in regulation of neuroendocrine stress responses. *Endocrinology*, 145(8), 3763-3768.

250. Mueller, N. K., Dolgas, C. M., & Herman, J. P. (2006). Regulation of forebrain GABAergic stress circuits following lesion of the ventral subiculum. *Brain Research*, 1116(1), 132–142. https://doi.org/10.1016/j.brainres.2006.07.101

251. Muzio, R. N., & Bingman, V. P. (2022). Brain and Spatial Cognition in Amphibians: Stem Adaptations in the Evolution of Tetrapod Cognition. In M. A. Krause, K. L. Hollis, & M. R. Papini (Eds.), Evolution of Learning and Memory Mechanisms (pp. 105–124). chapter, Cambridge: Cambridge University Press.

252. Nagarajan, G., Jurkevich, A., Kang, S. W., & Kuenzel, W. J. (2017a). Anatomical and functional implications of corticotrophin-releasing hormone neurons in a septal nucleus of the avian brain: an emphasis on glial-neuronal interaction via V1a receptors in vitro. *Journal of neuroendocrinology*, *29*(7), 10.1111/jne.12494. https://doi.org/10.1111/jne.12494

253. Nagarajan, G., Kang, S. W., & Kuenzel, W. J. (2017b). Functional evidence that the nucleus of the hippocampal commissure shows an earlier activation from a stressor than the paraventricular nucleus: Implication of an additional structural component of the avian hypothalamo-pituitary-adrenal axis. *Neuroscience letters*, *642*, 14–19.

254. Nagarajan, G., Tessaro, B. A., Kang, S. W., & Kuenzel, W. J. (2014). Identification of arginine vasotocin (AVT) neurons activated by acute and chronic restraint stress in the avian septum and anterior diencephalon. *General and comparative endocrinology*, 202, 59–68. https://doi.org/10.1016/j.ygcen.2014.04.012

255. Nakagawa, S., & Waas, J. R. (2004). 'O sibling, where art thou?'-a review of avian sibling recognition with respect to the mammalian literature. *Biological Reviews*, *79*(1), 101-119.

256. Nikbakht, N., & Diamond, M. E. (2021). Conserved visual capacity of rats under red light. *eLife*, 10, e66429. https://doi.org/10.7554/eLife.66429

257. Northcutt, R.G. (1984). Evolution of the Vertebrate Central Nervous System: Patterns and Processes. *Integrative and Comparative Biology*, 24, 701-716.

258. Nostramo, R. & Sabban, E. L. (2015). Stress and Sympathoadrenomedullary Mechanisms. Russell, J. & Shipston, M. (Eds.). *Neuroendocrinology of Stress*, pp. 95-120.

259. O'Keefe, J., & Dostrovsky, J. (1971). The hippocampus as a spatial map: preliminary evidence from unit activity in the freely-moving rat. *Brain research*.

260. Omer, D. B., Maimon, S. R., Las, L., & Ulanovsky, N. (2018). Social place-cells in the bat hippocampus. *Science* (New York, N.Y.), 359(6372), 218–224. https://doi.org/10.1126/science.aao3474

261. Øverli, Ø., Sørensen, C., Pulman, K. G., Pottinger, T. G., Korzan, W., Summers, C. H., & Nilsson, G. E. (2007). Evolutionary background for stress-coping styles: relationships between physiological, behavioral, and cognitive traits in non-mammalian vertebrates. *Neuroscience and biobehavioral reviews*, *31*(3), 396–412.

262. Owen, R. (1843). Lectures on comparative anatomy and physiology of invertebrate animals, delivered at the Royal College of Surgeons in 1843. London: Longman, Brown, Green & Longmans.

263. Pace, T. W., Gaylord, R., Topczewski, F., Girotti, M., Rubin, B., & Spencer, R. L. (2005). Immediate-early gene induction in hippocampus and cortex as a result of novel experience is not directly related to the stressfulness of that experience. *The European journal of neuroscience*, *22*(7), 1679–1690. https://doi.org/10.1111/j.1460-9568.2005.04354.x

264. Panksepp, J., Nelson, E., & Bekkedal, M. (1997). Brain systems for the mediation of social separation-distress and social-reward. Evolutionary antecedents and neuropeptide intermediaries. *Annals of the New York Academy of Sciences*, *807*, 78–100. https://doi.org/10.1111/j.1749-6632.1997.tb51914.x

265. Papp, G., Witter, M. P., & Treves, A. (2007). The CA3 network as a memory store for spatial representations. Learning & memory (Cold Spring Harbor, N.Y.), 14(11), 732–744. https://doi.org/10.1101/lm.687407

266. Parfitt, G. M., Nguyen, R., Bang, J. Y., Aqrabawi, A. J., Tran, M. M., Seo, D. K., Richards, B. A., & Kim, J. C. (2017). Bidirectional Control of Anxiety-Related Behaviors in Mice: Role of Inputs Arising from the Ventral Hippocampus to the Lateral Septum and Medial Prefrontal Cortex. *Neuropsychopharmacology : official publication of the American College of Neuropsychopharmacology*, *42*(8), 1715–1728. https://doi.org/10.1038/npp.2017.56

267. Patel, S. N., Clayton, N. S., & Krebs, J. R. (1997). Hippocampal tissue transplants reverse lesion-induced spatial memory deficits in zebra finches (*Taeniopygia guttata*). Journal of *Neuroscience,* 17(10), 3861-3869.

268. Paxinos G, Watson C. (1998). The rat brain in stereotaxic coordinates. Academic Press , San Diego.

269. Payne, H. L., Lynch, G. F., & Aronov, D. (2021). Neural representations of space in the hippocampus of a food-caching bird. *Science (New York, N.Y.)*, *373*(6552), 343–348. https://doi.org/10.1126/science.abg2009

270. Pereira, E., Nääs, I. A., Ivale, A. H., Garcia, R. G., Lima, N. D. D. S., & Pereira, D. F. (2022). Energy Assessment from Broiler Chicks' Vocalisation Might Help Improve Welfare and Production. *Animals: an open access journal from MDPI*, 13(1), 15. https://doi.org/10.3390/ani13010015

271. Pfeiffer, B. E., & Foster, D. J. (2013). Hippocampal place-cell sequences depict future paths to remembered goals. *Nature*, 497(7447), 74-79.

272. Phelps, E. A., & LeDoux, J. E. (2005). Contributions of the amygdala to emotion processing: from animal models to human behavior. *Neuron*, *48*(2), 175-187.

273. Phillips, J. B., & Jorge, P. E. (2014). Olfactory navigation: failure to attempt replication of critical experiments keeps controversy alive. Reply to Wallraff. *Animal Behaviour*, (90), e7-e9.

274. Pitkänen, A., Pikkarainen, M., Nurminen, N., & Ylinen, A. (2000). Reciprocal connections between the amygdala and the hippocampal formation, perirhinal cortex, and postrhinal cortex in rat. A review. *Annals of the New York Academy of Sciences*, 911, 369–391. https://doi.org/10.1111/j.1749-6632.2000.tb06738.x

275. Pothuizen, H. H., Zhang, W. N., Jongen-Rêlo, A. L., Feldon, J., & Yee, B. K. (2004). Dissociation of function between the dorsal and the ventral hippocampus in spatial learning abilities of the rat: a within-subject, within-task comparison of reference and working spatial memory. *European Journal of Neuroscience*, *19*(3), 705-712.

276. Poulter, S., Hartley, T., & Lever, C. (2018). The Neurobiology of Mammalian Navigation. *Current biology*: CB, 28(17), R1023–R1042. https://doi.org/10.1016/j.cub.2018.05.050

277. Pravosudov, V. V., & Omanska, A. (2004). Dominance-related changes in spatial memory are associated with changes in hippocampal cell proliferation rates in mountain chickadees. *Journal of Neurobiology*, 62(1), 31–41.

278. Pravosudov, V. V., Kitaysky, A. S., & Omanska, A. (2006). The relationship between migratory behaviour, memory and the hippocampus: an intraspecific comparison. *Proceedings. Biological sciences*, 273(1601), 2641–2649.

279. Pross, A., Metwalli, A. H., Desfilis, E., & Medina, L. (2022). Developmental-Based Classification of Enkephalin and Somatostatin Containing Neurons of the Chicken Central Extended Amygdala. *Frontiers in physiology*, 13, 904520. https://doi.org/10.3389/fphys.2022.904520

280. Puelles, L., Martinez-de-la-Torre, M., Martinez, S., Watson, C., & Paxinos, G. (2007). The chick brain in stereotaxic coordinates. An atlas featuring neuromeric subdivisions and mammalian homologies. San Diego: Academic Press.

281. Radley, J. J., & Sawchenko, P. E. (2011). A common substrate for prefrontal and hippocampal inhibition of the neuroendocrine stress response. *The Journal of neuroscience: the official journal of the Society for Neuroscience*, 31(26), 9683–9695. https://doi.org/10.1523/JNEUROSCI.6040-10.2011

282. Ramsay, D. S., & Woods, S. C. (2014). Clarifying the roles of homeostasis and allostasis in physiological regulation. *Psychological review*, *121*(2), 225–247.

283. Rehkämper, G., Haase, E., & Frahm, H. D. (1988). Allometric comparison of brain weight and brain structure volumes in different breeds of the domestic pigeon, *Columba livia* f.d. (fantails, homing pigeons, strassers). *Brain, behavior and evolution*, 31(3), 141–149.

284. Reiner, A., Perkel, D. J., Bruce, L. L., Butler, A. B., Csillag, A., Kuenzel, W., Medina, L., Paxinos, G., Shimizu, T., Striedter, G., Wild, M., Ball, G. F., Durand, S., Güntürkün, O., Lee, D. W., Mello, C. V., Powers, A., White, S. A., Hough, G., Kubikova, L., … Avian Brain Nomenclature Forum (2004). Revised nomenclature for avian telencephalon and some related brainstem nuclei. *The Journal of Comparative Neurology*, 473(3), 377–414. https://doi.org/10.1002/cne.20118

285. Remage-Healey, L., Adkins-Regan, E., & Romero, L. M. (2003). Behavioral and adrenocortical responses to mate separation and reunion in the zebra finch. *Hormones and Behavior*, *43*(1), 108-114.

286. Reul, J. M., & de Kloet, E. R. (1985). Two receptor systems for corticosterone in rat brain: microdistribution and differential occupation. *Endocrinology*, 117(6), 2505–2511. https://doi.org/10.1210/endo-117-6-2505

287. Richard, S., Martínez-García, F., Lanuza, E., & Davies, D. C. (2004). Distribution of corticotropin-releasing factor-immunoreactive neurons in the central nervous system of the domestic chicken and Japanese quail. *Journal of Comparative Neurology*, *469*(4), 559-580.

288. Richmond, M. A., Yee, B. K., Pouzet, B., Veenman, L., Rawlins, J. N., Feldon, J., & Bannerman, D. M. (1999). Dissociating context and space within the hippocampus: effects of complete, dorsal, and ventral excitotoxic hippocampal lesions on conditioned freezing and spatial learning. *Behavioral neuroscience*, 113(6), 1189–1203. https://doi.org/10.1037/0735-7044.113.6.1189

289. Risold, P. Y., & Swanson, L. W. (1996). Structural evidence for functional domains in the rat hippocampus. *Science (New York, N.Y.)*, *272*(5267), 1484–1486. https://doi.org/10.1126/science.272.5267.1484

290. Robertson, B. A., Rathbone, L., Cirillo, G., D'Eath, R. B., Bateson, M., Boswell, T., Wilson, P. W., Dunn, I. C., & Smulders, T. V. (2017). Food restriction reduces neurogenesis in the avian hippocampal formation. *PloS one*, 12(12), e0189158.

291. Rogers, J. L., & Kesner, R. P. (2006). Lesions of the dorsal hippocampus or parietal cortex differentially affect spatial information processing. *Behavioral neuroscience*, 120(4), 852–860. https://doi.org/10.1037/0735-7044.120.4.852

292. Romero, L. M., Dickens, M. J., & Cyr, N. E. (2009). The Reactive Scope Model - a new model integrating homeostasis, allostasis, and stress. *Hormones and behavior*, 55(3), 375–389. https://doi.org/10.1016/j.yhbeh.2008.12.009

293. Rook, N., Stacho, M., Schwarz, A., Bingman, V. P., & Güntürkün, O. (2023). Neuronal circuits within the homing pigeon hippocampal formation. The Journal of comparative neurology, 531(7), 790–813. https://doi.org/10.1002/cne.25462

294. Royer, S., Sirota, A., Patel, J., & Buzsáki, G. (2010). Distinct representations and theta dynamics in dorsal and ventral hippocampus. *The Journal of neuroscience : the official journal of the Society for Neuroscience*, 30(5), 1777–1787. https://doi.org/10.1523/JNEUROSCI.4681-09.2010

295. Ryabinin, A. E., Wang, Y. M., & Finn, D. A. (1999). Different levels of Fos immunoreactivity after repeated handling and injection stress in two inbred strains of mice. *Pharmacology Biochemistry and Behavior*, 63(1), 143-151.

296. Sadananda, M., & Bischof, H. J. (2004). c-fos is induced in the hippocampus during consolidation of sexual imprinting in the zebra finch (*Taeniopygia guttata*). *Hippocampus*, 14(1), 19–27. https://doi.org/10.1002/hipo.10149

297. Salas, C., Broglio, C., & Rodríguez, F. (2003). Evolution of forebrain and spatial cognition in vertebrates: conservation across diversity. *Brain, behavior and evolution*, 62(2), 72–82. https://doi.org/10.1159/000072438

298. Sapolsky, R. M. (2010). Physiological and pathophysiological implications of social stress in mammals. *Comprehensive physiology*, 517-532.

299. Sapolsky, R. M., Krey, L. C., & McEwen, B. S. (1984). Glucocorticoid-sensitive hippocampal neurons are involved in terminating the adrenocortical stress response. *Proceedings of the National Academy of Sciences of the United States of America*, 81(19), 6174–6177.

300. Scharfman H. E. (2007). The CA3 "backprojection" to the dentate gyrus. *Progress in brain research,* 163, 627–637. https://doi.org/10.1016/S0079-6123(07)63034-9

301. Schoenfeld, T. J., & Gould, E. (2012). Stress, stress hormones, and adult neurogenesis. *Experimental neurology*, 233(1), 12-21.

302. Seifert, M., Roberts, P.A., Kafetzis, G., Osorio, D., Baden, T. (2022). Birds multiplex spectral and temporal visual information via retinal On- and Off-channels. *Nature Communications, Nature*, vol. 14(1), 1-19. DOI: 10.1101/2022.10.20.513047.

303. Selvam, R., Jurkevich, A., Kang, S. W., Mikhailova, M. V., Cornett, L. E., & Kuenzel, W. J. (2013). Distribution of the Vasotocin Subtype Four Receptor (VT4R) in the Anterior Pituitary Gland of the Chicken, *Gallus gallus*, and its Possible Role in the Avian Stress Response. *Journal of neuroendocrinology*, 25(1), 56–66. https://doi.org/10.1111/j.1365-2826.2012.02370.x

304. Selye, H. (1946). The general adaptation syndrome and the diseases of adaptation. Journal of Clinical Endocrinology. *Metabolism*. 6, 117–230. doi: 10.1210/jcem-6-2-11

305. Selye, H. (1976a) Stress in Health and Disease. Butterworths, Boston.

306. Selye, H. (1976b). Stress without Distress. In: Serban, G. (eds) Psychopathology of Human Adaptation. Springer, Boston, MA. https://doi.org/10.1007/978-1-4684-2238-2_9

307. Senft, R. A., Meddle, S. L., & Baugh, A. T. (2016). Distribution and Abundance of Glucocorticoid and Mineralocorticoid Receptors throughout the Brain of the Great Tit (*Parus major*). *PLOS ONE*, 11(2), e0148516.

308. Sheng, M., & Greenberg, M. E. (1990). The regulation and function of c-fos and other immediate early genes in the nervous system. *Neuron*, 4(4), 477–485. https://doi.org/10.1016/0896-6273(90)90106-p

309. Sherry, D. F., & Vaccarino, A. L. (1989). Hippocampus and memory for food caches in black-capped chickadees. *Behavioral Neuroscience*, 103(2), 308–318. https://doi.org/10.1037/0735-7044.103.2.308

310.    Siegel, J. J., Nitz, D., & Bingman, V. P. (2005). Spatial-specificity of single-units in the hippocampal formation of freely moving homing pigeons. *Hippocampus*, 15(1), 26-40.

311.    Silverman, A. J., Hoffman, D. L., & Zimmerman, E. A. (1981). The descending afferent connections of the paraventricular nucleus of the hypothalamus (PVN). *Brain Research Bulletin*, 6(1), 47–61. doi:10.1016/s0361-9230(81)80068-8

312.    Singewald, G. M., Rjabokon, A., Singewald, N., & Ebner, K. (2011). The modulatory role of the lateral septum on neuroendocrine and behavioral stress responses. *Neuropsychopharmacology: official publication of the American College of Neuropsychopharmacology*, *36*(4), 793–804. https://doi.org/10.1038/npp.2010.213

313.    Slusher, M. A., & Hyde, J. E. (1961). Effect of Limbic Stimulation on Release of Corticosteroids into the Adrenal Venous Effluent of the Cat. *Endocrinology*, 69(6), 1080–1084.

314.    Smith, S. M., & Vale, W. W. (2006). The role of the hypothalamic-pituitary-adrenal axis in neuroendocrine responses to stress. *Dialogues in Clinical Neuroscience*, 8(4), 383–395.

315.    Smulders T. V. (2021). Telencephalic regulation of the HPA axis in birds. *Neurobiology of stress*, *15*, 100351. https://doi.org/10.1016/j.ynstr.2021.100351

316.    Smulders, T. V. (2017). The Avian Hippocampal Formation and the Stress Response. *Brain, Behavior and Evolution*, 90(1), 81–91.

317.    Smulders, T. V., & DeVoogd, T. J. (2000). Expression of immediate early genes in the hippocampal formation of the black-capped chickadee (*Poecile atricapillus*) during a food-hoarding task. *Behavioural Brain Research*, 114(1-2), 39–49.

318.    Snyder, J. S., Radik, R., Wojtowicz, J. M., & Cameron, H. A. (2009). Anatomical gradients of adult neurogenesis and activity: young neurons in the ventral dentate gyrus are activated by water maze training. *Hippocampus*, 19(4), 360-370.

319.    Sterling, P., & Eyer, J. (1988). Allostasis: A new paradigm to explain arousal pathology. In S. Fisher & J. Reason (Eds.), *Handbook of life stress, cognition, and health* (pp. 629–649). John Wiley & Sons.

320.    Strange, B. A., Witter, M. P., Lein, E. S., & Moser, E. I. (2014). Functional organization of the hippocampal longitudinal axis. *Nature reviews. Neuroscience*, 15(10), 655–669. https://doi.org/10.1038/nrn3785

321.    Striedter, G. F. (2005). Principles of brain evolution. Sunderland, MA, Sinauer Associates.

322.    Striedter, G. F. (2016). Evolution of the hippocampus in reptiles and birds. *Journal of Comparative Neurology*, 524(3), 496–517.

323.    Striedter, G. F., & Northcutt, R. G. (1991). Biological Hierarchies and the Concept of Homology. *Brain, Behavior and Evolution*, 38(4-5), 177–189. doi:10.1159/000114387

324.    Suárez, J., Dávila, J. C., Real, M. A., Guirado, S., & Medina, L. (2006). Calcium-binding proteins, neuronal nitric oxide synthase, and GABA help to distinguish different pallial areas

in the developing and adult chicken. I. Hippocampal formation and hyperpallium. *The Journal of comparative neurology*, 497(5), 751–771. https://doi.org/10.1002/cne.21004

325.　Sufka, K. J., & Weed, N. C. (1994). Construct validation of behavioral indices of isolation stress and inflammatory nociception in young domestic fowl. *Physiology & behavior*, *55*(4), 741–746. https://doi.org/10.1016/0031-9384(94)90054-x

326.　Sufka, K. J., Hughes, R. A., McCormick, T. M., & Borland, J. L. (1994). Opiate effects on isolation stress in domestic fowl. *Pharmacology, biochemistry, and behavior*, 49(4), 1011–1015. https://doi.org/10.1016/0091-3057(94)90257-7

327.　Susman, E. J., Schmeelk, K. H., Worrall, B. K., Granger, D. A., Ponirakis, A., & Chrousos, G. P. (1999). Corticotropin-releasing hormone and cortisol: Longitudinal associations with depression and antisocial behavior in pregnant adolescents. *Journal of the American Academy of Child & Adolescent Psychiatry*, *38*(4), 460-467.

328.　Swanson, L. W., & Cowan, W. M. (1977). An autoradiographic study of the organization of the efferent connections of the hippocampal formation in the rat. *The Journal of comparative neurology*, *172*(1), 49–84. https://doi.org/10.1002/cne.901720104

329.　Székely, A. D. (1999). The avian hippocampal formation: Subdivisions and connectivity. *Behavioural Brain Research*, 98(2), 219–225. https://doi.org/10.1016/S0166-4328(98)00087-4

330.　Székely, A. D., and Krebs, J. R. (1996). Efferent connectivity of the hippocampal formation of the zebra finch (*Taenopygia guttata*): an anterograde pathway tracing study using Phaseolus vulgaris leucoagglutinin. *Journal of Comparative Neurology,* 368, 198–214. doi: 10.1002/(SICI)1096-9861(19960429)368:2<198::AID-CNE3>3.0.CO;2-Z

331.　Takahashi S. (2018). The Hippocampal Ensemble Code for Spatial Navigation and Episodic Memory. *Advances in neurobiology*, 21, 49–70. https://doi.org/10.1007/978-3-319-94593-4_3

332.　Takeuchi, H., Yazaki, Y., Matsushima, T., & Aoki, K. (1996). Expression of Fos-like immunoreactivity in the brain of quail chick emitting the isolation-induced distress calls. *Neuroscience letters*, *220*(3), 191–194. https://doi.org/10.1016/s0304-3940(96)13256-0

333.　Tanti, A., Rainer, Q., Minier, F., Surget, A., & Belzung, C. (2012). Differential environmental regulation of neurogenesis along the septo-temporal axis of the hippocampus. *Neuropharmacology*, 63(3), 374-384.

334.　Tanti, A., Westphal, W. P., Girault, V., Brizard, B., Devers, S., Leguisquet, A. M., ... & Belzung, C. (2013). Region-dependent and stage-specific effects of stress, environmental enrichment, and antidepressant treatment on hippocampal neurogenesis. *Hippocampus*, 23(9), 797-811.

335. Tarr, B. A., Rabinowitz, J. S., Ali Imtiaz, M., & DeVoogd, T. J. (2009). Captivity reduces hippocampal volume but not survival of new cells in a food-storing bird. *Developmental neurobiology*, 69(14), 972–981.

336. Thompson, C. L., Pathak, S. D., Jeromin, A., Ng, L. L., MacPherson, C. R., Mortrud, M. T., ... & Lein, E. S. (2008). Genomic anatomy of the hippocampus. *Neuron*, 60(6), 1010-1021.

337. Tömböl, T., Davies, D. C., Németh, A., Sebestény, T., & Alpár, A. (2000). A comparative Golgi study of chicken (*Gallus domesticus*) and homing pigeon (*Columba livia*) hippocampus. *Anatomy and embryology*, 201(2), 85–101. https://doi.org/10.1007/pl00008235

338. Tsigos, C., & Chrousos, G. P. (2002). Hypothalamic–pituitary–adrenal axis, neuroendocrine factors and stress. *Journal of Psychosomatic Research*, 53(4), 865–871.

339. Tsigos, C., Kyrou, I., Kassi, E., & Chrousos, G. P. (2020). Stress: Endocrine Physiology and Pathophysiology. In K. R. Feingold (Eds.) et. al., Endotext. MDText.com, Inc.

340. Uchoa, E.T., Aguilera, G., Herman, J.P., Fiedler, J.L., Deak, T. and de Sousa, M.B.C. (2014), Novel Aspects of Glucocorticoid Actions. *Journal of Neuroendocrinology*, 26: 557-572.

341. Ulrich-Lai, Y. M., & Herman, J. P. (2009). Neural regulation of endocrine and autonomic stress responses. *Nature reviews neuroscience*, *10*(6), 397-409.

342. Ulrich-Lai, Y. M., & Ryan, K. K. (2014). Neuroendocrine circuits governing energy balance and stress regulation: functional overlap and therapeutic implications. *Cell metabolism*, 19(6), 910–925. https://doi.org/10.1016/j.cmet.2014.01.020

343. Unnerstall, J. R., Kopajtic, T. A., & Kuhar, M. J. (1984). Distribution of alpha 2 agonist binding sites in the rat and human central nervous system: analysis of some functional, anatomic correlates of the pharmacologic effects of clonidine and related adrenergic agents. *Brain research*, *319*(1), 69–101. https://doi.org/10.1016/0165-0173(84)90030-4

344. Vale, W., Spiess, J., Rivier, C., & Rivier, J. (1981). Characterization of a 41-residue ovine hypothalamic peptide that stimulates secretion of corticotropin and beta-endorphin. *Science*, 213(4514), 1394–1397.

345. Van Reeth, O., Hinch, D., Tecco, J. M., & Turek, F. W. (1991). The effects of short periods of immobilization on the hamster circadian clock. *Brain research*, 545(1-2), 208-214.

346. Vandenborne, K., De Groef, B., Geelissen, S. M., Boorse, G. C., Denver, R. J., Kühn, E. R., Darras, V. M., & Van der Geyten, S. (2005). Molecular cloning and developmental expression of corticotropin-releasing factor in the chicken. *Endocrinology*, 146(1), 301–308. https://doi.org/10.1210/en.2004-0608

347. Vann, S. D., Brown, M. W., Erichsen, J. T., & Aggleton, J. P. (2000). Fos imaging reveals differential patterns of hippocampal and parahippocampal subfield activation in rats in response to different spatial memory tests. *The Journal of neuroscience : the official journal of the Society for Neuroscience*, 20(7), 2711–2718. https://doi.org/10.1523/JNEUROSCI.20-07-02711.2000

348. Vogel, J. W., La Joie, R., Grothe, M. J., Diaz-Papkovich, A., Doyle, A., Vachon-Presseau, E., Lepage, C., Vos de Wael, R., Iturria, Y., Bernhardt, B., Rabinovici, G., & Evans, A. (2019). A molecular gradient along the longitudinal axis of the human hippocampus informs large-scale behavioral systems. *Nature Communications* 11, 960 (2020). https://doi.org/10.1038/s41467-020-14518-3

349. Vyas, A., Mitra, R., Shankaranarayana Rao, B. S., & Chattarji, S. (2002). Chronic stress induces contrasting patterns of dendritic remodeling in hippocampal and amygdaloid neurons. *The Journal of neuroscience* : the official journal of the Society for Neuroscience, 22(15), 6810–6818. https://doi.org/10.1523/JNEUROSCI.22-15-06810.2002

350. Wallraff, H. G. (2014). Do olfactory stimuli provide positional information for home-oriented avian navigation?. Animal Behaviour, (90), e1-e6.

351. Wilby, D., & Roberts, N. W. (2017). Optical influence of oil droplets on cone photoreceptor sensitivity. *The Journal of experimental biology*, 220(Pt 11), 1997–2004. https://doi.org/10.1242/jeb.152918

352. Wiley, E.O. (1981). Phylogenetics. New York, Wiley & Sons.

353. Wilson, D. S., Clark, A. B., Coleman, K., & Dearstyne, T. (1994). Shyness and boldness in humans and other animals. Trends in ecology & evolution, 9(11), 442-446.

354. Witter, M. (2012). Hippocampus. The Mouse Nervous System, 112–139.

355. Witter, M. P., & Amaral, D. G. (2004). Hippocampal Formation. *The Rat Nervous System*, 635–704.

356. Won, E., & Kim, Y. K. (2016). Stress, the Autonomic Nervous System, and the Immune-kynurenine Pathway in the Etiology of Depression. Current neuropharmacology, 14(7), 665–673. https://doi.org/10.2174/1570159x14666151208113006

357. Wu, M. V., & Hen, R. (2014). Functional dissociation of adult-born neurons along the dorsoventral axis of the dentate gyrus. *Hippocampus*, 24(7), 751-761.

358. Yu, J. Y., Fang, P., Wang, C., Wang, X. X., Li, K., Gong, Q., Luo, B. Y., & Wang, X. D. (2018). Dorsal CA1 interneurons contribute to acute stress-induced spatial memory deficits. *Neuropharmacology*, 135, 474–486. https://doi.org/10.1016/j.neuropharm.2018.04.002

359. Zanette, L. Y., Hobbs, E. C., Witterick, L. E., MacDougall-Shackleton, S. A., & Clinchy, M. (2019). Predator-induced fear causes PTSD-like changes in the brains and behaviour of wild animals. *Scientific reports*, 9(1), 11474. https://doi.org/10.1038/s41598-019-47684-6

360. Zhang, H., Cui, M., Cao, J. L., & Han, M. H. (2022). The Role of Beta-Adrenergic Receptors in Depression and Resilience. *Biomedicines*, 10(10), 2378. https://doi.org/10.3390/biomedicines10102378

361. Zhang, W.N., Pothuizen, H. H., Feldon, J., & Rawlins, J. N. (2004). Dissociation of function within the hippocampus: effects of dorsal, ventral, and complete excitotoxic hippocampal lesions on spatial navigation. *Neuroscience*, 127(2), 289–300.